56/1/2024
ISSN 1338-3523
ISSN 0369-2086

Mineralia Slovaca

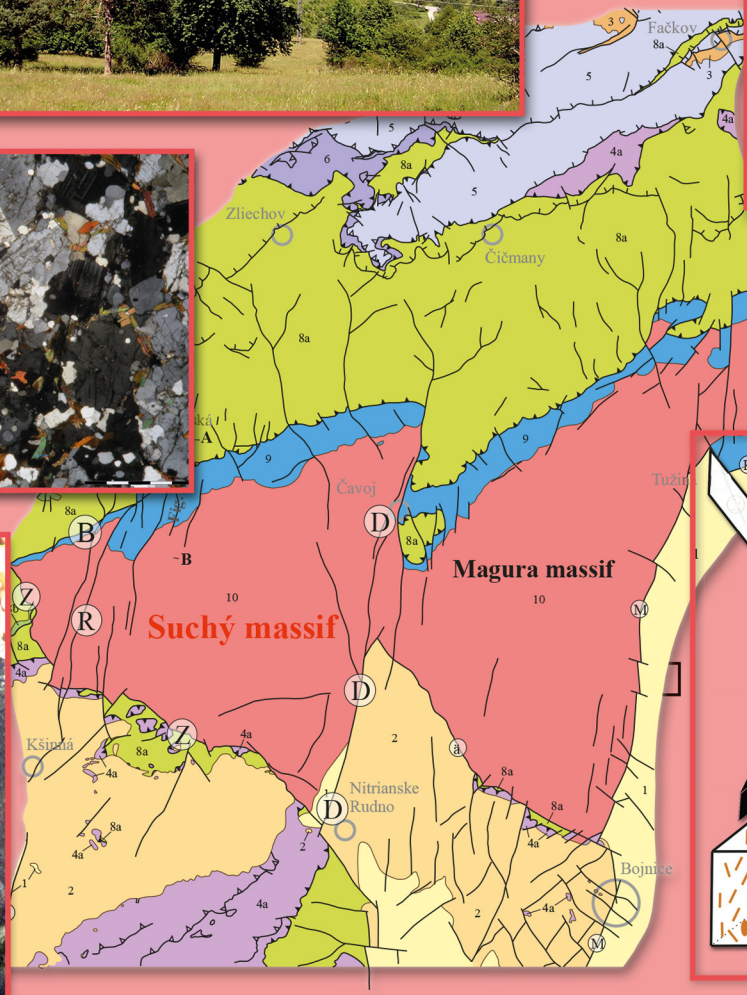

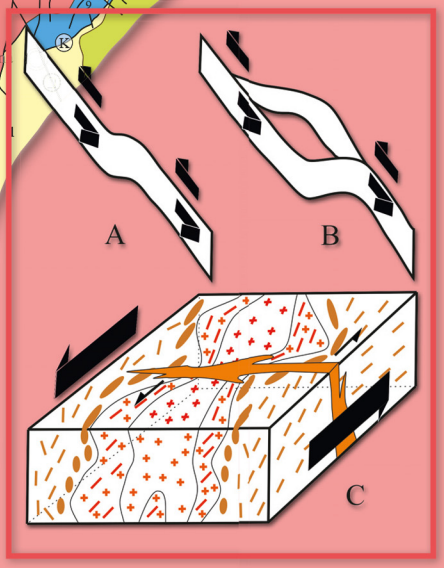

Štátny geologický ústav Dionýza Štúra Bratislava

Mineralia Slovaca

Časopis pre regionálnu a environmentálnu geológiu
a aktivity Slovenskej geologickej spoločnosti a geologických asociácií

Mineralia Slovaca (Web ISSN 1338-3523, ISSN 0369-2086), EV 3534/09, vychádza dvakrát ročne. Vydavateľ a tlač: Štátny geologický ústav Dionýza Štúra, Mlynská dolina 1, 817 04 Bratislava, IČO 31 753 604. Dátum vydania čísla 56/1/2024: júl 2024. Predplatné v roku 2024 vrátane DPH, poštovného a balného pre jednotlivcov 22,00 €, pre členov SGS a geologických asociácií 20,90 €, pre organizácie v SR 31,90 €, pre organizácie v ČR 55,00 €. Cena jednotlivého čísla pri osobnom nákupe v predajniach ŠGÚDŠ v Bratislave a v Košiciach je 6,05 € vrátane DPH. Časopis možno objednať v redakcii a v knižnici regionálneho centra v Košiciach. Adresa redakcie: Štátny geologický ústav D. Štúra – RC Košice (Mineralia Slovaca), Jesenského 8, 040 01 Košice. Telefón: 055/625 00 43; fax: 055/625 00 44, e-mail: mineralia.slovaca@geology.sk, e-mail knižnica: secretary.ke@geology.sk

Mineralia Slovaca (Web ISSN 1338-3523, ISSN 0369-2086) is published twice a year by the State Geological Institute of Dionýz Štúr Bratislava, Slovak Republic. The date of issuing of the number 56/1/2024: July 2024.
Subscription for the whole 2024 calendar year (two numbers of the journal): 66.00 € (Europe), 77.00 € (besides Europe), including VAT, postage and packing cost. Claims for nonreceipt of any issue will be filled gratis.
Order of the Editorial Office: Štátny geologický ústav D. Štúra – RC Košice (Library), Jesenského 8, SK-040 01 Košice, Slovak Republic. Phone: +421/55/625 00 43; fax: +421/55/625 00 44, e-mail: mineralia.slovaca@geology.sk, library: secretary.ke@geology.sk

www.geology.sk/mineralia

PÔVODNÉ ČLÁNKY – ORIGINAL PAPERS

COVER: Tectonic scheme in the center of composition visualizes two blocks of triangular shape, built of crystalline basement of the Strážovské vrchy Mts. Lithotectonic units, tectonometamorphic and granitization processes in the western block of the Suchý massif (left; red-coloured) are presented in the article by **Hraško et al. on pp. XX–XX in this issue of the journal**. **Picture on the top left side** provides a view from the settlement of Pánisovci (E of Valaská Belá village) towards the north, through the valley of Nitrica river. Foreground of this picture shows the western slopes of the elevation Klin (769) built of crystalline rock. In the saddle with the settlement of Studenec the Mesozoic cover sequences of Tatricum occur, on the left side of this picture the terrain is formed by the sediments of the Fatric nappe and in the background – the Strážov elevation (1213) with sequences of Hronic nappe occurs.
The upper right picture: Vein of leucogranite steeply penetrates the paragneiss complex in the valley of the Radiša stream. **Middle left picture** shows microstructure of I-type granodiorite / tonalite in polarizing microscope (N*X*). **Lower left picture** presents different stages of deformation of leucogranite material in migmatitized paragneiss. **Scheme on the bottom right** visualizes the opening of the space in the metamorphic complex during the simultaneous emplacement of leucogranites and at the end of pegmatites. Author of photographs is Ľubomír Hraško.

OBÁLKA: Tektonická schéma v strede kompozície znázorňuje dva bloky trojuholníkového tvaru, budované kryštalinikom Strážovských vrchov. Litotektonické jednotky a tektonometamorfné a granitizačné procesy v západnom bloku masívu Suchého (vľavo; červenej farby) sú charakterizované v článku **Hraška et al. na str. XX – XX v tomto čísle časopisu**. **Obrázok vľavo hore** zobrazuje pohľad z osady Pánisovci (na V od Valaskej Belej) smerom na S cez údolie rieky Nitrica. V popredí tejto fotografie sú západné svahy kóty Klin (769), budované kryštalinickými sekvenciami. V sedle s osadou Studenec sa nachádzajú mezozoické sekvencie tatrika, na ľavej strane tejto fotografie sú sedimenty fatrika a v pozadí vystupuje kóta Strážov (1 213) so sekvenciami hronika. **Fotografia vpravo hore** znázorňuje žilu leukogranitu, strmo prenikajúcu komplexom pararúl v doline potoka Radiša. **V strede vľavo** je fotografia z polarizačného mikroskopu (N*X*) znázorňujúca mikroštruktúru granodioritu typu I/tonalitu. **Fotografia vľavo dole** znázorňuje rôzne štádiá deformácie leukogranitového materiálu v migmatitizovaných pararulách. **Schéma vpravo dole** znázorňuje syndeformačné otváranie priestoru v metamorfnom komplexe za súčasného umiestňovania leukogranitov a v závere pegmatitov. Autor fotografií je Ľubomír Hraško.

Mineralia Slovaca, Web ISSN 1338-3523, ISSN 0369-2086, https://doi.org/10.56623/ms.2024.56.1.1
56, 1 (2024), 3 – 50, © Authors 2024. CC BY 4.0

Variscan lithotectonic units in the Suchý massif of the Strážovské vrchy Mts., Western Carpathians – products of sedimentary, tectonometamorphic and granite forming processes

ĽUBOMÍR HRAŠKO, ZOLTÁN NÉMETH and PATRIK KONEČNÝ

State Geological Institute of Dionýz Štúr, Mlynská dolina 1, SK–817 04 Bratislava, Slovakia;
lubomir.hrasko@geology.sk

Abstract: The present geological investigation of the Pre-Alpine structure of the western part of Strážovské vrchy Mts (the Suchý massif; Western Carpathians) has distinguished three lithologically distinct Variscan lithotectonic units, which originated (1) in the deeper parts of oceanic basin (prevailingly metapelites with different content of organic matter, metabasalts, metacarbonates); (2) sediments of the continental slope (flyschoid sediments with a predominance of greiwacke sediments; both VmD0); (3) a unit of continent basement primarily of pre-VmD0 granitic composition (orthogneiss). These rock sequences of differing geotectonic provenances were amalgamated and metamorphosed in the pre-intrusive (Pre-Mississipian) stage; pre-VmD2). Regarding the Variscan polyorogenic evolution, Variscan processes in Tatricum represent the Meso-Variscan evolution (VmD).

The maximum P-T conditions of orogenic (regional) metamorphism (up to 610 °C and 7.5–8.5 kbar) were not sufficient for more extensive anatexis. Field observations indicated that the production of a limited volume of granitoid melts occurred mainly at the contacts of amalgamated lithotectonic units. Probably due to the heat, produced by the hot line below the collisional orogen and contributing also to unroofing processes (in orogenic phase VmD2) there started new granitization. This stage of Mississipian VmD2 granite formation is associated with the emplacement of various types of granitoid magma, encompassing the oldest granodiorites with frequent schliers, representing a poorly differentiated and poorly mobile crystal slurry (present in the SE part of the territory). In the highly evolved post-collision phase (post-VmD1 phase), masses of leucogranites intruded comformably with the deformation plan in the metamorphic complexes, interacting with surrounding metamorphic rocks in higher crustal conditions and causing their contact metamorphic overprint (up to 590 °C and 3–4 kbar). The syn-deformation character of leucocratic granites is proved by the orientation of biotite flakes parallel to the deformation plane of surrounding metamorphites. Part of leucogranites, especially in the central parts of the bodies, is omnidirectional. The stress field acted not only during the intrusion of the leucogranite magma, but also in the subsolidus stage. The final stage of this process is the formation of large bodies of pegmatites in extensional VmD2 fractures oriented at a large angle to the main stress component. The texture of the grey blocky K-feldspar pegmatites and the lack of H_2O-bearing minerals point to hydrothermal-pneumatolytic fracturing in a subsequently opened environment in VmD2. The final stage of VmD2 is represented by intrusions of I-type granodiorites with indications of magma mixing, or mingling. The chemical dating of monazites in granitoids allowed to date individual phases of granitization process in the range of 360–345 Ma, which youngest ages corresponded with the formation of pegmatites. Dating of monazite in metamorphic rocks points to their thermal overprint during granitization process (360–350 Ma), having already earlier metamorphic overprint (380–370 Ma). The scenario of placement of granitoid intrusions is consistent with the decompression regime (in VmD2) after the end of VmD1c crustal thickening until the fracturing of the crustal block with of I-type magma intrusions of deeper origin. After this period, the exhumation of crystalline blocks, partial diaphtoresis and later surface erosion continue until the Lower Triassic. Re-submergence of the crystalline complexes is associated with a low degree of Alpine metamorphic reworking.

Graphical abstract

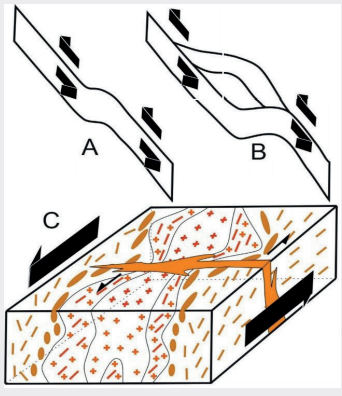

Highlights

- Three types of Meso-Variscan sequences (lithotectonic units; LTUs) were distinguished in the Tatric crystalline basement of the western part of Strážovské vrchy Mts (the Suchý massif), documenting its complicated Paleozoic geological evolution: (1) LTUs of the Lower Paleozoic riftogenic oceanic sedimentation, (2) flyschoid sediments (Paleozoic continental slope sediments; both VmD0) and (3) their basement crustal rocks – orthogneisses (originally pre-VmD0 granitoids). These complexes were amalgamated in a collisional event VmD1c and later at granite forming processes VmD2. The VmD2 metamorphism has produced an initial melting. The formation of granitoids in decompression phase produced thermal overprint of the amalgamated complexes at the granite front. In the first stage, less mobile crystal slurries were formed, which inherit the structural characteristics of the surrounding metamorphites. In the second phase, the complexes were sheared and two-mica granites and pegmatites were formed; this additional thermal metamorphism overprinted also earlier metamorphosed complexes. In the last stage of VmD2 evolution, I-type granodiorites, tonalites and diorites indicating magmatic mixing have intruded. CHIME monazite dating indicates the age of granite formation of 360–345 Ma.

Introduction

In 2015–2020 the State Geological Institute of Dionýz Štúr in Bratislava (Slovakia) carried out new geological mapping and regional geological research in eastern part of the Strážovské vrchy Mts, resulting in compilation of a new regional *Geological map of the Strážovské vrchy Mts (eastern part) at a scale of 1 : 50 000* in 2021 and explanatory notes to this map (currently edited). New map represents an update of a part of earlier geological map compiled by Maheľ et al. (1981). New research focused on Alpine tectonic units: Tatricum, Fatricum, Hronicum and younger geological formations (Paleogene, Neogene and Quaternary). This article is devoted to Variscan evolution and geological structure of the Tatricum crystalline basement of the western segment of mapped region, geographically belonging to the Suchý massif. Despite defining Meso-Variscan lithotectonic units (LTUs) in the Suchý massif, we briefly classify in studied area also those of Cadomian, Paleo-Alpine and Neo-Alpine orogenic cycles.

General characteristics of crystalline basement and its previous researches in the Strážovské vrchy Mts

First and the most comprehensive research of the Strážovské vrchy Mts crystalline basement by A. Klinec, I. Lehotský and M. Ivanov (Klinec, 1956, 1958; Ivanov,

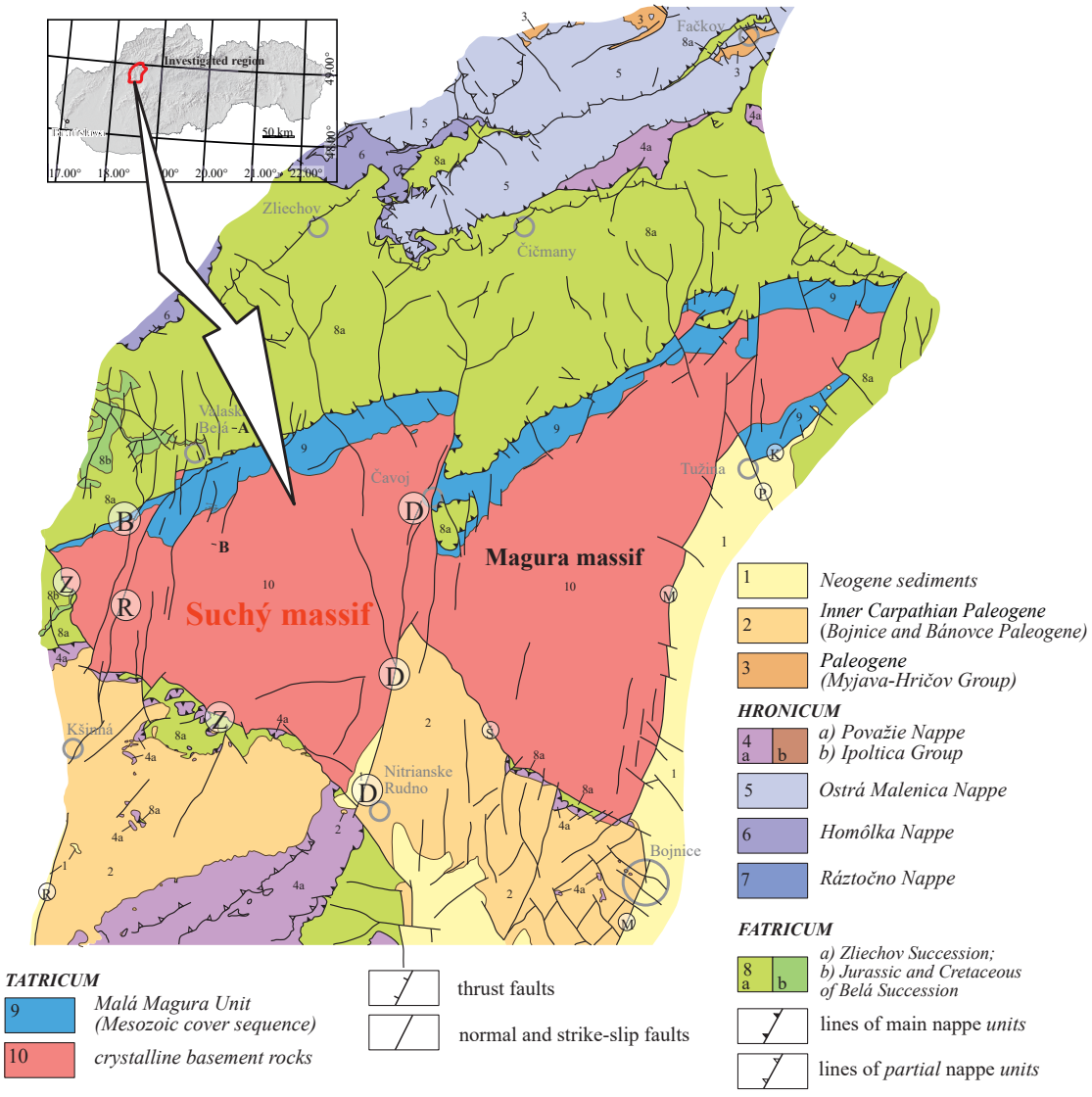

Fig. 1. Tectonic scheme of the Strážovské vrchy Mts, with tectonic blocks of Tatricum (crystalline basement and tectonicallly reduced Mezozoic sequences of the Malá Magura Unit), nappes of Fatricum and Hronicum, as well as Cenozoic sediments. Variscan crystalline basement (VmD) is divided by N-S trending Neo-Alpine (AnD4) Diviaky fault (D) to Suchý and Magura massifs. The Suchý massif is tectonically rimmed by AnD34 Zdychava fault (Z) and Brekovský potok fault (B) and further segmented by intracrystalline Radiša fault system (R) with more pronounced Neo-Alpine deformation of crystalline formations.

1957) included mapping of this region in the 1950s for the sake of compiling its first general geological map at a scale 1 : 200 000.

Ivanov (1957) parallelized the crystalline basement of Suchý and Malá Magura massifs with SW continuation of the Malá Fatra crystalline basement, formed of inhomogeneous sequence of crystalline schists and granitoids. Author correctly recognized the protoliths of metamorphites, as well as multi-stage magmatic granite genesis. The genesis of granitoid rocks he affiliated with Variscan (earlier used synonym used by some authors Hercynian) late- to post-orogenic magmatic cycle. He considered the migmatites, present in paragneisses, mainly as thermodynamic product of granitoid intrusions.

Detail mapping and petrographic research of crystalline basement in the 1970s by Kahan et al. (1978) and Kahan (1979) distinguished several types of metamorphic and granitoid rocks, encompassing also their structural research.

Petrography and geochemistry of amphibolites and associated black schists (graphite gneisses) in Malá Magura and Suchý massifs were investigated by Ivan and Méres (2015). They equate them with effusive basalts, dolerites and gabbros as well as deep water sediments, rich in silica and carbon, being hydrothermally altered before orogenic metamorphism. These rocks represent upper part of ofiolite suite, equal with that, present in Upper Devonian Pernek Group of the Malé Karpaty Mts. The finding of distinctive Cr, V and Mn rich metamorphic rocks and Ca garnets in black schists in the Čierna Lehota area supports this opinion (Bačík et al., 2018). In the area of the Závada valley north of the Závada pod Čiernym vrchom village, the exploration activities were carried out in black schists for graphite raw material (Mikoláš et al., 1995).

Hovorka and Méres (1991) geochemically investigated paragneisses in both crystalline cores of the Strážovské vrchy Mts and also in the Malá Fatra Mts. They interpreted low K/Na lithologies of the continental crust as their source material (especially intermediate to acid magmatites of granodiorite-tonalite composition). The sedimentary maturity of the original material is the highest in the Suchý massif and is manifested by a higher content of the clay component.

Putiš (1976) and Kahan et al. (1978) comprehensively evaluated the structural elements of the crystalline basement (Malá Magura and Suchý massifs) of the Strážovské vrchy Mts, including microstructural analysis. They distinguisheed secondary foliation planes s1 of metamorphic origin (crystallization schistosity), present in paragneisses and simultaneously forming biotite schliers in granitoids. The younger s2 planes, bearing retrograde facies minerals (sericite, chlorite, bauerite, albite, quartz), penetrated s1 planes. Planes s3 of retrograde metamorphism (according to Kahan et al., l.c.) were formed at arching of crystalline cores near the contact with Mesozoic and Cenozoic complexes. Work evaluates also fold structures in crystalline basement, mineral lineations and joints, identifying directional block displacements.

Based on microstructural research of preferred quartz orientation, P. Kováč (1986) demonstrated that in the Suchý massif granitoids quartz elongations are trending NNE–SSW, correspondingly with the course of granitoids, as well as foliation in metamorphites, described by Kahan (1978). P. Kováč (l.c.) supposed that preferred orientation of granitoids, investigated in quartz and micas, represent a one-act process, manifested by recrystallizationa and rotation of quartz and mica minerals.

Based on drilling works and surface exploration trenches in the Čavoj area (Mikoláš et al., 1995), the synform and antiform geological setting of paragneisses was revealed with relatively steeply dipping fold planes and intensive mylonitization of the crystalline basement in the wells increased N-ward, i.e. towards the contact of crystalline complexes with the Mesozoic cover (Malá Magura Unit), formed by quartzite at their contact. Stronger Alpine overprint along the margin of crystalline massif was proved by this way.

Based on relationship of metamorphic rocks, their metamorphic grade, granitization and migmatization, Kahan (1979, 1980) states two alternatives of thermal overprint – either by anatectic process, i.e. orogenic metamorphism producing anatexis, or overheating of "supracrustal" metasedimentary series.

Investigating metamorphic zonality in Suchý massif, Korikovski et al. (1987) distinguished two metamorpic zones: staurolite-andalusite-biotite at the margin and sillimanite-biotite-muscovite in remaining part of crystalline basement. The petrogenetic grid revealed PT conditions of metamorphism 3 kbar (300 MPa) and 540–590 °C. Muscovite-sillimanite aggregates in peraluminous granites indicate their origin at the expense of magmatic feldspars and biotites through the loss of Mg, Fe, Na, partly K, which, according to authors, points to the process of high-temperature acid leaching. Simultaneously they separated this process from pervasive muscovitization in connection with granites. Authors (l.c.) consider this process to be a deeper analogue of greisenization with metasomatic origin of muscovite and andalusite.

The presence of the staurolite–sillimanite and garnet mineral association especially at the W margin of the Suchý massif Dyda (1988) explains by the pre-metamorphic protolith rich in clay schists. According to Dyda (1990), mineral balances indicate different metamorphic conditions in the Mala Magura and Suchý crystalline basements: In the first case their culmination reached 640 °C with pressure of 5 kbar and in the case of the Suchý paragneisses it was 560 °C and pressure of 4.5 kbar.

Hovorka and Méres (1991) distinguished two events in metamorphic overprint of the paragneisses of the Strážovské vrchy and Mala Fatra crystalline basements. The first event –found only in the Malá Fatra basement (garnets with pyrope content above 30 %) – took place in higher temperature amphibolite facies (sillimanite zone), second event – under lower conditions (staurolite and sillimanite zone) – was revealed in both basements.

High-temperature metamorphic conditions were determined by TERMOCALC software (Čík & Petrík, 2014) from migmatite and paragneiss of the Magura massif (Poruba valley). The peak conditions for migmatite – 782 ± 53 °C (resp. 670–760 °C), pressure 7.4 ± 1.7 kbar (resp. 6.9–7.4 kbar). For paragneiss it was - 668 ± 53 °C (resp. 700–770 °C) at pressure 5.5 ± 1.2 kbar (resp. 6.7–8.2 kbar). Younger low-temperature metamorphism was defined in the Magura massif (l.c.) by the presence of margarite and pumpellyite. Calculations of retrograde conditions in migmatite gave values of 480 °C and pressure of 4.6 kbar and in paragneiss 300 °C and a pressure of 2.9 kbar.

The composition and ages of granitoids and paragneisses from the Strážovské vrchy Mts. were studied by Vilinovičová (1988, 1990). She divided tonalities, granodiorites and granites based on their petrochemical and mineral characteristics. Rocks of granodiorite composition dominate in the Suchý massif, less often are tonalities and granites. In the gneiss complex she (l.c.) investigated the fine-grained gneisses, banded gneisses and augen gneisses [in present geological map by Hraško & Kováčik (eds.) et al., 2021, being redefined to orthogneisses]. Vilinovičová (l.c.) investigated also chemical composition of the trace elements in feldspars and stated their structural arrangement. Fe^{2+} biotites in all granitoid types with a relatively small compositional range, correspond by composition with biotites from gneisses. In garnets of granitoids, which are relatively non-zonal, the content of the spressartite molecule increases from leucogranites to granodiorites and tonalites. The normalized REE curves show the absence of Eu minimum in tonalites and enrichment of light REEs. The application of feldspar Plg-Kfs thermometry points to subsolidus equilibrium temperatures in granitoids (up to 550 °C). Leucogranites of the Strážovské vrchy Mts are frequently bearing garnets of several mm up to a few cm in size, which occur together with sillimanite, biotite, muscovite in the prevailing quartz–K-feldspar–plagioclase granite composition. Hovorka and Fejdi (1983) distinguished two types of garnets with very close composition. Garnets have prevailing almandíne component (1. Alm_{71}, $Py_{9.5}$, $Spess_{18}$, $Gross_{1}$, $Andr_{0.5}$ and 2. Alm_{75}, Py_{12}, $Spess_{10}$, $Gross_{0.5}$, $Andr_{2.5}$). Authors interpret this differentce in composition to be the result of melt crystallization under different thermodynamic conditions – they crystallized before the emplacement of magma into higher crustal conditions.

Kráľ et al. (1987) investigated izotopic composition and age of granitoids based on $^{87}Rb/^{86}Sr$ izotopic system, including more types of granitoid samples and aiming to calculate the isochrone Rb/Sr age form the Suchý and Malá Magura massifs. Izochrone age was calcualted to 393 ± 6 Ma, with inicial $^{87}Sr/^{86}Sr$ ratio 0.7060 ± 0.0002. According our opinion these samples were not genetically related. The dating of S-type granite sample (V-94) by Kráľ et al. (1997) using TIMS analysis provided the age of 356 ± 9 Ma.

More recent zircon dating based on SHRIMP analysis (concordia age) from sample of S-type muscovite-biotite granite with garnet (sample MM-29) performed by Kohút & Larionov (2021) from the Magura part of the Strážovské vrchy Mts and from the Porubský potok stream provided the age 360.9 ± 2.7 Ma.

The geological structure of the territory was comprehensively described in the monographs of Maheľ (1983, 1985).

Used methodology

The field geological research was supported by detail petrography of mapped rock types. Chemical composition and BSEI images of rock-forming minerals were obtained by electron microprobe CAMECA SX 100, housed in the State Geological Institute of Dionýz Štúr (P. Konečný, V. Kollárová). In the laboratory, monazite dating methodology MARC (monazite age reference calibration) developed over past years by P. Konečný (2018 including further improvements) was applied to granitic rocks.

Monazites suitable for dating have to meet several conditions. A low concentration of Pb in the order of tenths of ppm can only be detected with the application of a strong analytical conditions (e.g long counting times and high beam current). Pb was acquired with accelerating voltage of 15 kV, long counting times of 300 s for peak and 150 s for two background points were applied and the high sample current of 180 nA was used. The electron beam diameter was adjusted to 3 μm. Under such conditions, the PbMα line is effectively excited and offers acceptable compromise between beam damage and counting efficiency. Th, U included in the age calculation and Y overlapping the PbMα were also precisely measured with an extended measurement time of 35 s, 90 s and 45 s, respectively. The following calibration standards (natural minerals or synthetic components) were used to calibrate the electron microprobe: apatite (P-Kα), wollastonite (Si-Kα, Ca-Kα), GaAs (As-Lα), baryte (S-Kα, Ba-Lα), Al_2O_3 (Al-Kα), ThO_2 (Th-Mα), UO_2 (U-Mβ), cerussite (Pb-Mα), YPO_4 (Y-Lα), $LaPO_4$ (La-Lα), $CePO_4$ (Ce-Lα), $PrPO_4$ (Pr-Lβ), $NdPO_4$ (NdLα), $SmPO_4$ (Sm-Lα), $EuPO_4$ (Eu-Lβ), $GdPO_4$ (Gd-Lα), $TbPO_4$ (Tb-Lα), $DyPO_4$ (Dy-Lβ), $HoPO_4$ (Ho-Lβ), $ErPO_4$ (Er-Lβ), $TmPO_4$ (Tm-Lα), $YbPO_4$ (Yb-Lα), $LuPO_4$ (Lu-Lβ), fayalite (Fe-Kα) and $SrTiO_3$ (Sr-Lα). UMβ overlapped by ThMζ, ThM3-N4, ThM5-P3 and PbMα overlapped by ThMζ1, ThMζ2 and PbMα overlapped

also by YLγ2,3 as well as numerous other interferences among REE were corrected by correction coefficients obtained by measurement on calibration standards. Each analysis of monazite includes the complete set of elements of which it is composed. We are avoiding the methodology where only Th, U, Pb and Y are measured and the other elements are measured elsewhere in the same monazite zone. Such method creates inaccuracies depending on the homogeneity of the monazite and also on the matrix effect, where all elements are required for the ZAF correction. The age determined from the given analysis is only the apparent age. To find out the real age, it is necessary to combine measurements at several points (10-50). The age group plotted on the histogram can indicate whether it represents one or several age populations. The resulting age from the age of population is then calculated using the weighted average of the apparent ages. On the isochron (Pb vs. Th – including the contribution from U) the age population is spread around a linear relationship. The linear regression should ideally intersect the zero coordinate and thus represents an additional test of the correctness of the dating. The method of age calculating based on statistical evaluation was described by Montel et al. (1996). The methodology developed in the Electron Microanalysis Laboratory (ŠGÚDŠ) represents an improved methodology that is practiced only in this laboratory. It is based on a final correction using 7-9 monazite age standards, where the age is determined by more accurate isotopic dating methods – Th-U-Pb: SHRIMP, LA-ICPMS, ID-TIMS, etc. Methodology named as MARC (Monazite Age Reference Correction, P. Konečný et. al., 2018) includes corrections for interferences, corrections for exponential background, an innovative method of determining the dependence between the composition of monazite (average atomic number) and the difference between the linear and exponential background for the PbMα line, determining the dependence between the measured Pb and the theoretically required (ΔPb) to reach the age of the monazite standard, determination of MARC coefficients, which will be used for final fine-tuning of the age calculation and others.

The pressure–temperature conditions of metamorphic overprint were determined by R. Demko (SGUDS), using methodology of garnet-biotite-plagioclase-quartz (GBPQ) geobarometry in medium- to high-grade metapelites (Wu et al., 2004).

Cassification of lithotectonic units – **LTUs** – is based on orogenic (Wilson) cycles, being indicated by the **XD labelling method** in polyorogenic terrains in the prefix X (cf. Németh, 2021; Fig. 2 ibid), as well as by affiliation of individual orogenic phases of these cycles by a **number after D**: **XD0** – divergent process of riftogenesis; **XD1** – convergent processes of subduction (XD1s), obduction (XD1o) and closure of elongated oceanic space by collision (XD1c); **XD2** – post-collisional thermal / deformation processes, unroofing and metamorphic core complex evolution; **XD3** – intraplate consolidation – strike-slip faults preferably of NW–SE and NE–SW trends (cf. Németh et al., 2023), transpression, transtension, rotation of blocks, *etc*.; and **XD4** – regional extension (pure shear-type regional faults, dominantly of E–W and N–S courses, cf. l.c.). From **X prefixes** for orogenic cycles within Europe suggested by Németh (2021) in this paper we use: Cd – Cadomian, V – Variscan, Ap – Paleo-Alpine (Mesozoic Alpine orogenic cycle) and An – Neo-Alpine (Cenozoic Alpine orogenic cycle; both represent complete orogenic cycles).

Similar principle of designation is used at metamorphic overprints – the **MX labelling** (e.g. MV0, MV1sc, MAp2, etc., l.c.)

New characteristic of lithotectonic units of the pre-granite crystalline basement in tee Suchý massif

Published geological map by Hraško & Kováčik (eds., 2021) for the reader of this paper is available on:

https://www.geology.sk/wp-content/uploads/documents/foto/geol_mapy_50k/58_StrazovskeVrchy_final.jpg.

Detail geological mapping of crystalline basement in the western part of Tatric occurrences in the Strážovské vrchy Mts (Suchý massif), research of structural and spatial relations acting before the granite-forming process and lithological pecularities, allowed to define three below stated main lithotectonic units (LTUs) of differing geotectonic provenience. Rock sequences of these LTUs were amalgamated during Variscan collision and later partial melting.

1. **LTU of deep-water euxinic facies (VmD01s)**, in pre-metamorphic state consisting mainly of fine-grained pelitic and quartzy sedimentary facies rich in organic matter, with preserved fragments of accompanying oceanic mafic volcanites;
2. **LTU of proximal sedimentay facies of continental slope (VmD01s)** of Paleozoic basin, built mainly of flyschoid sediments of sandy-greiwacke composition. In the field, these can be distinguished by alternating of metamorphosed sandy vs. clayey-sandy beds (less Al-rich sediments), having lower content of organic matter and rare occurrence of small metabasite bodies;
3. **LTU of orthogneisses** is common in the Suchý massif. In smaller scale orthogneisses occur also in the W part of the Magura massif. They represent a crustal granitoid segment thrust at Meso-Variscan collision (**VmD1c**) on previously described **VmD01s** LTUs. Later the originating thick skinned sequence was metamorposed in **VmD2 / MVm2**. This LTU of orthogneisses crops out in upper structural position of fan structure with fan axis

trending ENE–WSW (shown in geological profile 1–2 in published geological map by Hraško & Kováčik, eds., 2021, l.c.).

These originally separated complexes were interconnected and submerged owing to convergence in zone of elongated Variscan basin. In the area of the lower part of the metamorphic packet and along shear faults, a partial melting of the protolith with an appropriate lithological composition took place in **VmD2**.

General lithological and metamorphic characteristic of new lithotectonic units

Lithotectonic unit built of deep-water euxinic facies (VmD01s)

It is originally formed mainly of the fine-grained pelitic and quartzy sedimentary facies rich in organic matter, with preserved fragments of accompanying oceanic mafic volcanites;

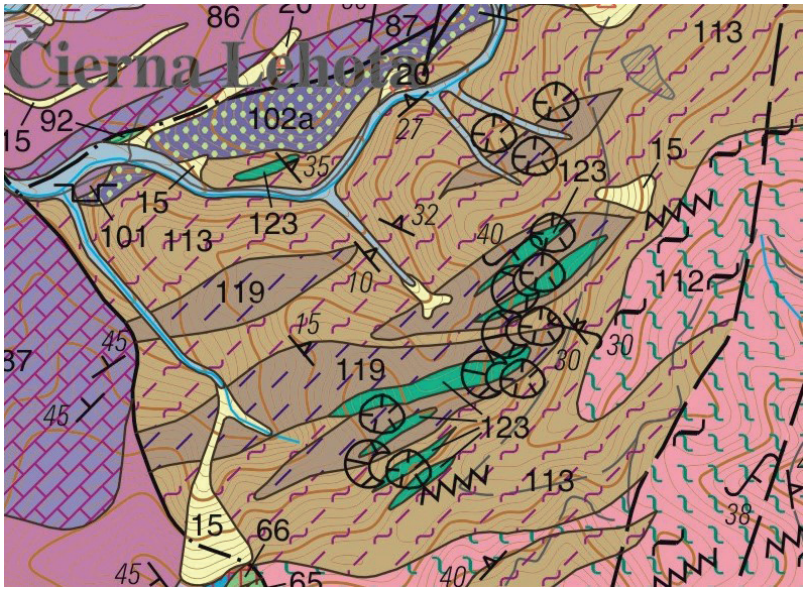

Fig. 2. Association of amphibolites (123) and black schists (119) SE of the Čierna Lehota village. Numerous mining works exploring possible sulphide mineralization are typical for this area.

Fig. 3. Amphibolite bodies (123) and small bodies of tremolite-plagioclase amphibolites (124b), black graphitic schists, black paragneisses and black metaquarzites (119), lying on the complex of schistose or massive biotite and two-mica paragneisses (113) (continental slope sediments). Orthogneisses (111) occur in upper structural position. Geological situation near the Závada stream.

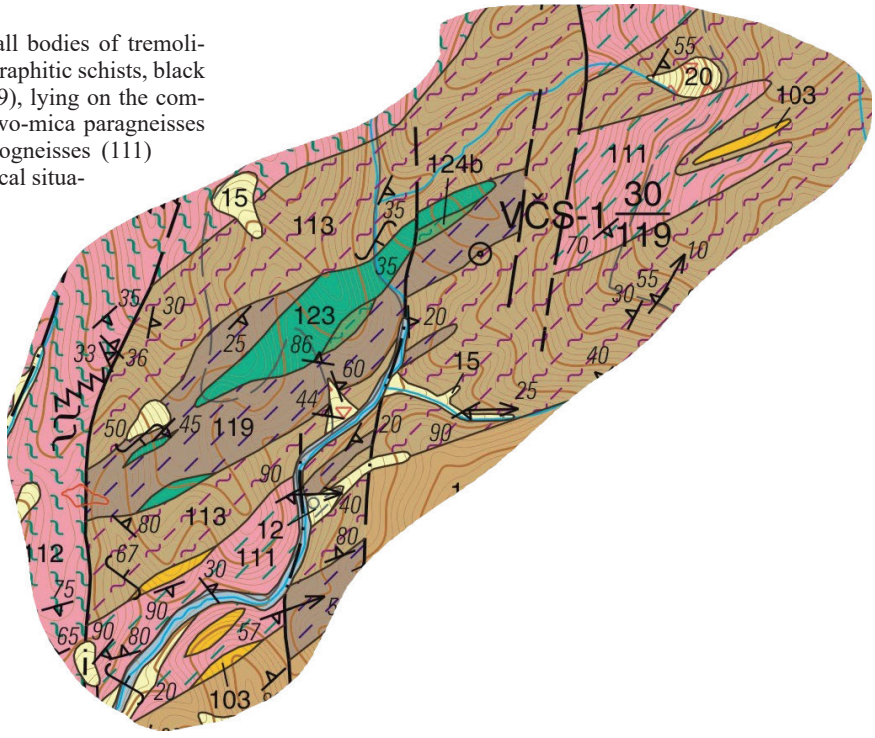

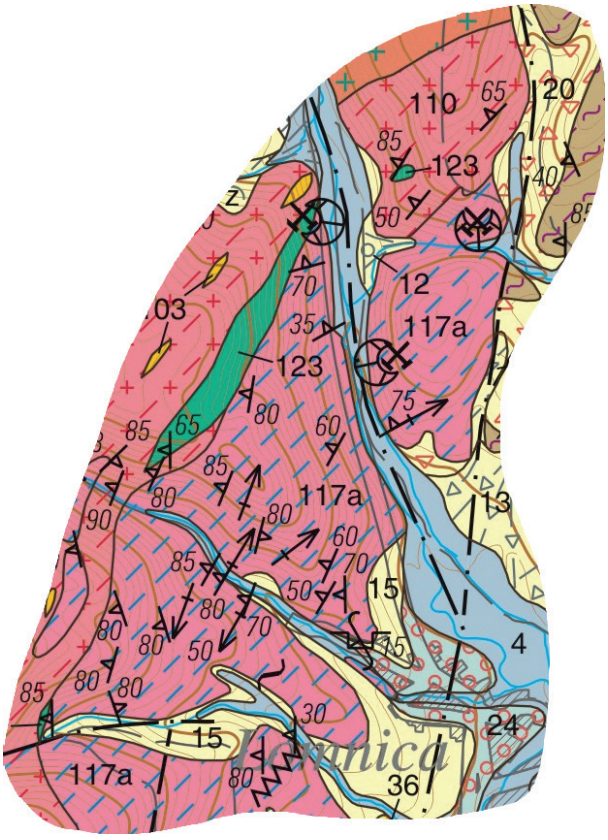

Fig. 4. The position of the largest amphibolite body (123), concordantly with the subvertical deformation structure, at the contact between migmatites with prevalence of stromatitic to ptygmatitic textures (117a) and massive to weakly oriented hybridic (schliered) granodiorite with frequent biotite schliers and xenoliths of paragneisses (110). No black schists were found, but according to presence of remnants of old mining in the northern part of body, their presence is probable. Amphibolite has signs of partial melting and intrusion of later leucogranites. Situation between Krstenica a Nitrica valleys.

Amphibolites and associated rocks (amphibolic and amphibole-biotite gneisses, quartzy massive paragneisses, graphitic metaquartzites, pyroxene amphibolites, amphibolites with garnet and tremolite-plagioclase amphibolites) are in earlier geological maps from this area (Kahan in Maheľ et al., 1982; Ivanov, 1957) shown in summary as amphibolites. Visualized are mainly large bodies at the Chvojnica area (Magura part), Liešťany (S part of the Krstenica valley) and in area north of the Závada pod Čiernym vrchom village (Závada valley, area of its right tributary – the Železná dolina valley). Amphibole-bearing rocks and associated sediments with prevailing pelitic / resp. quartzy composition represent common source of disseminated sulphidic mineralization, which is demonstrated also by numerous old mining works in their space. Also based on the remnants of old mining we have identified such lithologies also in the westernmost termination of crystalline basement in the Suchý massif (SE of Čierna Lehota village, area of Závadská poľana hill).

Due to metamorphic overprint, it was not possible to express quite well the facies differences between the metapelitic and quartzy-pelitic, siliciclastic metasediments in cartographic visualization. Despite, in wider context in areas with higher representation of amphobolitic rocks, there was observable the presence of metasediments with higher content of Al-rich minerals –sillimanite and staurolite, as a reflection of more pelitic composition of metasediments. In the surrounding of smaller mafic bodies in area located SW and NW of Suchý vrch hill (altitude point 1028), there occur also metapelitic metamorphites with common macroscopic staurolite, representing an indicator of Al-rich protolith. At the contact zone of stromatitic migmatites (117a) and massive to weakly oriented schlier granodiorites (110) in the area of Nitrica river and Krstenica valley there were found two smaller and one big bodies of metamafites (123), which underwent interaction with leucogranitic melt (Fig. 4).

Amphibole occassionally occurs also in paragneisses, which can be in this case named as “amphibole-biotitite gneisses”. These thin lithological intercallations we do not describe here, but in geological map some their occurrences are visualized with a special hatch (122).

The amphibolite bodies occur in the Suchý massif concordantly with the structural elements of the surrounding metamorphites.

Present types of amphibolic rocks

Amphibolitic rocks with calcareous-silicate component, loccally with garnet and clinopyroxene (124a)

They are usually heterogeneous, often complexly deformed rocks, appearing in various green, greenish-grey shades in the area of larger amphibolite bodies of Suchý hill.

Fig. 5. Dark-grey amphibolic rock with thin light-grey interbed of diopside pyroxene (area of Železná dolina valley, sample SZN-32a).

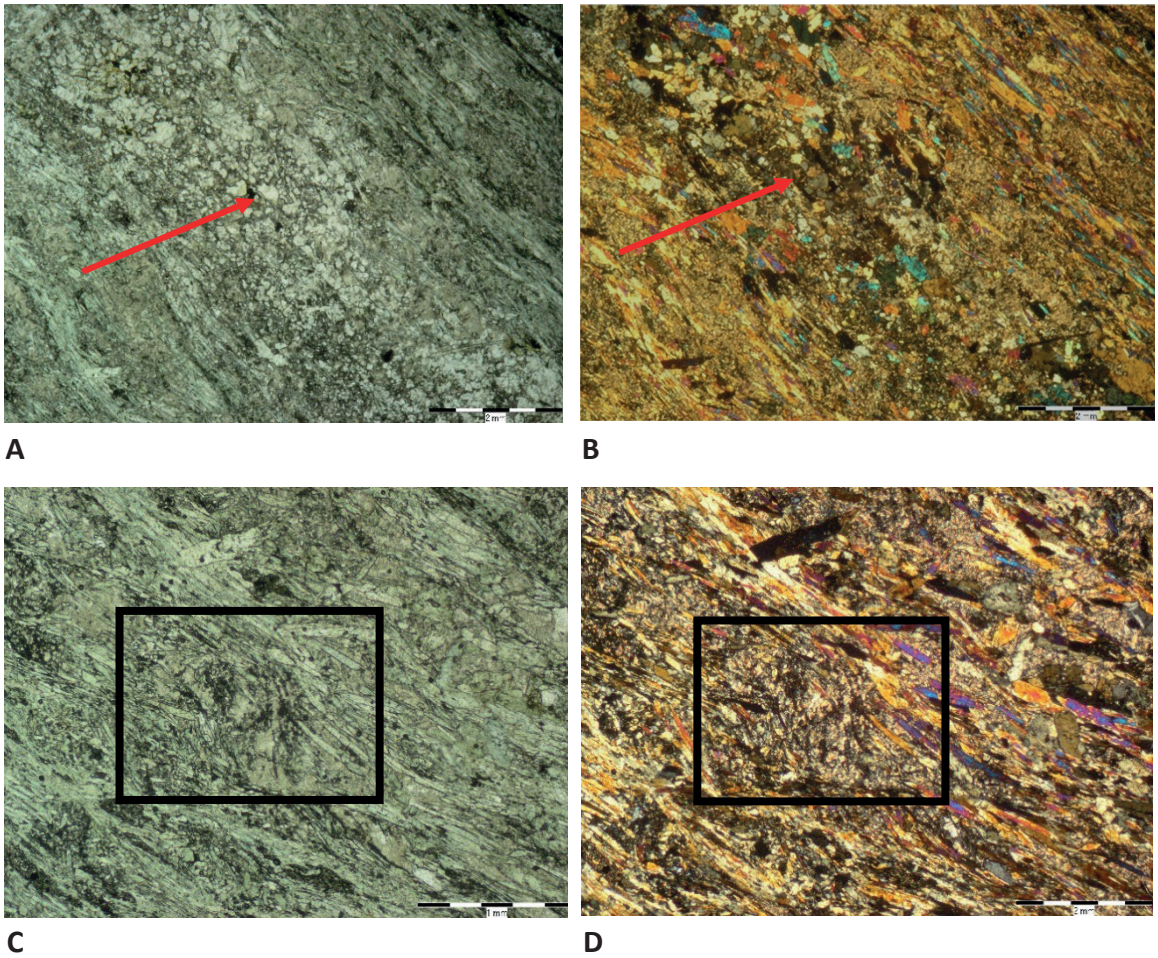

Fig. 6. Microphotographs of polymetamorpic clinopyroxene-amphibole amphibolite (sample SZN -32a, area of the **Železná** dolina valley, being **a** tributary to the Závada valley). A–B – granoblastic diopside (highlighted by red arrow) from Ca-rich, originally carbonate interbed in tuffitic sequence; C–D – dynamic deformation of older plagioclase (highlighted by black rectangle) with S-C setting represents younger deformation phase in the epidotic amphibolite facies.

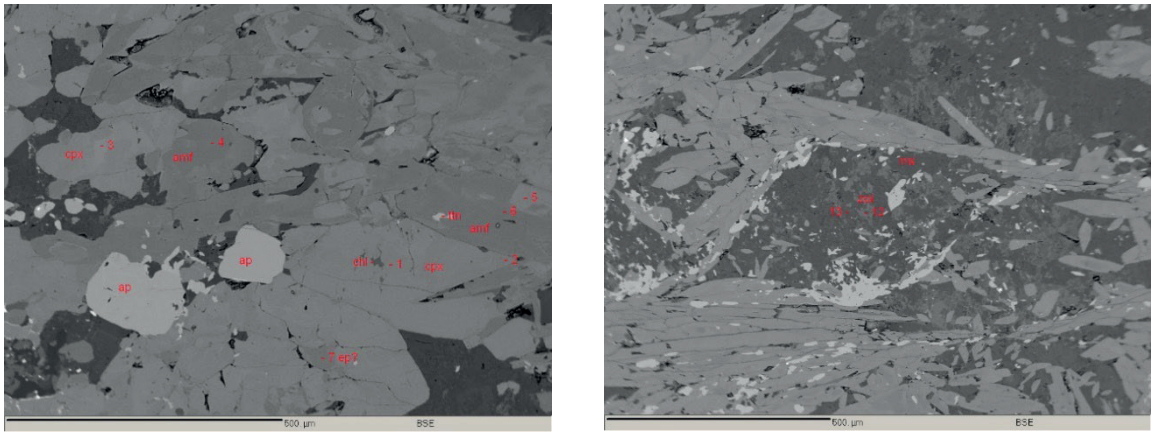

Fig. 7. BSEI of clinopyroxene-amphibole amphibolite, sample SZN-32a, the Železná dolina area. A – Assemblage of diopside (cpx) with amphibole (tschermakite and younger actinolite), accessoric apatite and chalcopyrite. B – Rotation of older plagioklase due to the decomposition of former plagioclase to Pl X_{An} 40 –48 %, muscovite, zoisite and rim consisting of grey actinolite. Light phases represent titanite. Assemblage in part of this rock, consisting of prehnite, albite and actinolite belongs to the lowest thermal part of polymetamorphism.

Their affiliation to metamorphosed calcium-silicate rocks is evidenced by the increased proportion of epidote (clinozoisite), the common presence of clinopyroxene phenocrysts and garnet rich in grossularite component. The plagioclase-amphibole-dominated composition of the rocks and the loose spatial association with amphibolites indicate that the primary lithology consisted of pyroclastic (?) products of basic volcanism enriched with a calcareous admixture. Microscopically present bright positions parallel to the metamorphic foliation are formed by diopside (Figs. 5 and 6).

The composition of clinopyroxenes corresponds to diopside with a content of 1.3 % jadeite component, older amphiboles correspond to tschermakite, while younger recrystallized amphiboles are of actinolite composition.

Plagioclase is usually recrystallized to form a new generation XAn = 41–48 %. Based on the presence of clinozoisite, which was formed at the expense of plagioclase, the original plagioclases were more basic. The lowest thermal part includes the albite-prehnite association, which is probably of Alpine age.

Tremolite-plagioclase fine-grained pale amhibolites (124b)

Rarely present light fine-grained rocks are part of the complex of amphibolites (metabasalts) and appear at the contact with black metaquartzites, irregularly rimming the southeastern part of the elongated body of amphibolite in the area of the Železné and Závada valleys north of the village of Závada pod Čierny vrchom.

Considering the mineral composition, they probably represented mica-carbonate (dolomite) sedimentary inlays in black metaquartzites in contact with metabasalts. The alternative of altered ultramafite due to the lack of sedimentary textures is also possible (this would also be indicated by the position in the lower part of the amphibolite body, which could represent a fragment of the ophiolite suite). Another alternative is that the rock represented the acidic part of the ophiolite suite (keratophyre).

Fig. 8. Sample of tremolitic-plagioclase rock with deficiency of dark minerals. In the field this rock resembles the fine-grained quartzitic rock (sample SZN-24).

The samples represent a light omnidirectional fine-grained rock (Figs. 8 and 9), without dark minerals. The microscopically visible metamorphic structure of the rock is formed by omnidirectional colorless strips of amphibole of tremolite composition. The basic material is composed of plagioclase ($An_{41–43}$). Younger metamorphic overprint is

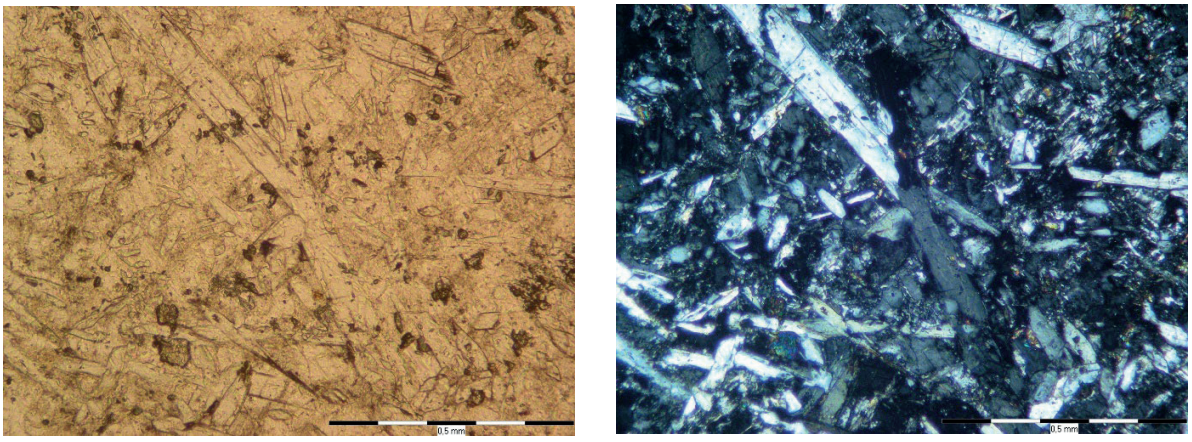

Fig. 9. A, B – Microphotographs of sample SZN 24 from the area between the Závada and its righ-side tributary from Železná dolina in western part of the Suchý massif. A rarely occurring amphibolic (tremolitic)-plagioclase fine-grained rock at first glance resembles metaquartzite. It contains a ground mass formed by plagioclase and phenocrysts of light amphibole of tremolite composition. The interstices between amphiboles of tremolite composition are formed by plagioclase. This rock occurs in marginal parts of large amphibolite bodies. A – parallel (N*II*) and B – crossed nicols (N*X*) of polarizing microskope.

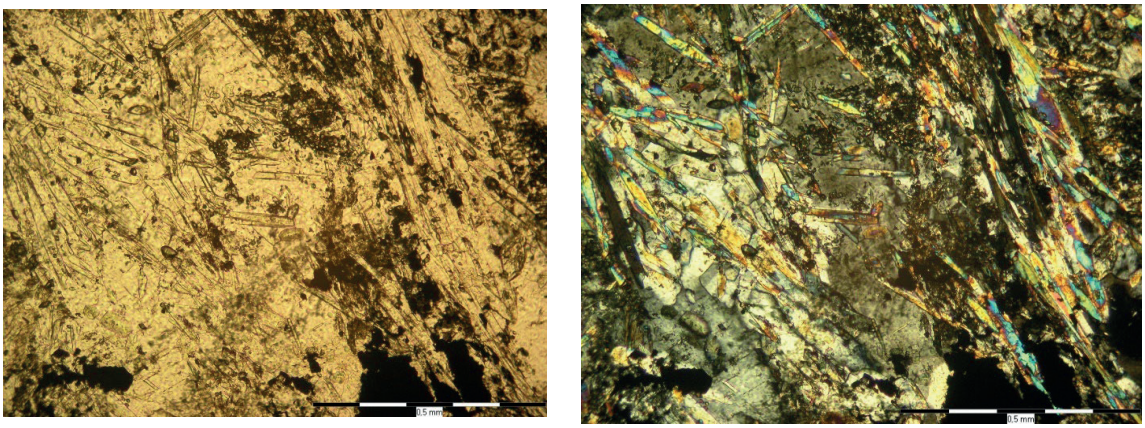

Fig. 10. Microphoto of the sample LHS 261: A, B – nematoblastic structure of rock bormed by tremolitic to Mg-hornblende amphibole and plagioclase, N//, NX. C – BSEI – besides tremolitic to Mg-hornblende amphibole and plagioclase (An – 32, 46, 61 %) rock contains a great number of sulphides – pyrite, pyrhotite, chalcopytite. Younger, lower temperature metamorphic association is formed by albite, chlorite and pumpellyite.

associated with formation of chlorite, barite, pumpelleyite and oligoclase (An_{28}).

A similar sample LHS-261 from the Suchý massif taken from Závada and Železná dolina valleys area at the junction of paragneisses and black-graphitic schists in continuation of the amphibolite body above E side of the Závada valley. The rock resembling fine–grained light quartzite contains tremolitic-Mg-hornblende amphiboles, basic plagioclase of andesine-labradorite composition (max. An 61 %). The presence of sulphides is common.

Amphibolites – olive-green-grey fine-grained foliated types (123)

Amphibolite bodies were already considered by Ivanov (1957) to be part of the ophiolite (oceanic) suite of basic magmatites, which was confirmed by later geochemical research.

Amphibolites usually form several meters, max. the first 10 m thick bodies of dark green to grey fine-grained, detailed foliated rocks, mostly conformal with the surrounding paragneiss substrate. Tiny lenses of amphibolites are irregularly dispersed in the metamorphic substrate.

In the Suchý massif there are two to three more distinct bodies, or groups of bodies. The easternmost of them is located in the Liešťanská dolina valley (Krstenica valley), and like the body in the Chvojnica valley in the Magura part of the crystalline basement, it occurs at the junction of migmatites and granitoids, with exceptionally preserved higher-temperature paragneisses in the vicinity. From the point of view of the Variscan setting, this body occurs in the lower tectonic position at the contact of the lower part of the schist-like granodiorites near their contact with the migmatites (Fig. 4). These bodies are probably the relics of a larger set of metapelites, metapsammites, which, however, are found only rudimentarily in this position in the form of paragneisses. Only rarely is it possible, e.g. E from Nitrica to find amphibolite relics in association with paragneisses in hybrid granitoids. Such a lack of metasedimentary associating lithologies is very likely a consequence of the tectonic reduction of a significant part of the volcanic-sedimentary complex during the granitizing Devonian-Lower Carboniferous event. The second position of the amphibolites in the Suchý massif is the upper structural position of the amphibolites, which emerges both in the area of the Závada valley and its tributary Železná dolina valley, and on the other hand from the ridge of Závadská poľana towards the Čierna Lehota village, where the amphibolites are part of a complex of black schists (graphitic metaquartzites), graphitic and graphite-amphibole paragneisses. The association of amphibolic rocks with metapelitic rocks,

which are characterized by Al-rich metamorphic minerals – sillimanite and staurolite, is striking in the western part of the territory. This structural position is spatially more remote from granitization processes.

Fig. 11. Banded amphibolite from the zone of granitization (sample LHS-153) above left side of the Krstenica valley (Liešťanská dolina valley) under this high voltage line. Rock in brittle regime is intruded by aplitic leucogranite without mutual interactions, which proves intrusion of leucogranite in higher crustal level with more rapid crystallization of leucogranite magma.

The mineral content of amphibolites is usually characterized by a significant predominance of common amphibole with green pleochroism prevailing over plagioclase. In minor quantities, but characteristically represented minerals are titanite, epidote, or clinozoisite and opaque ore phases. As a rule, amphibolites are fine-grained (the average grain size reaches around 0.2 mm), amphibole in some places makes up to 90 vol. % of the mineral composition of the rock.

Amphibole-biotite and amphibole-plagioclase gneisses (122)

Due to the problematic differentiation of amphibolic gneisses and amphibolites at field mapping, these are usually cartographically included under the group of amphibolites (123). Only in some places do we highlight in the geological map with a special symbol the areas with a greater occurrence of paragneisses with amphibole, in which biotite and amphibole gneisses alternate, which often contain several cm thick positions richer in biotite and positions richer in amphibole. The marginal member is represented by amphibole–plagioclase gneisses, which originally probably represented intercalations of basic tuffites in the marine sediment. Plagioclases (from the

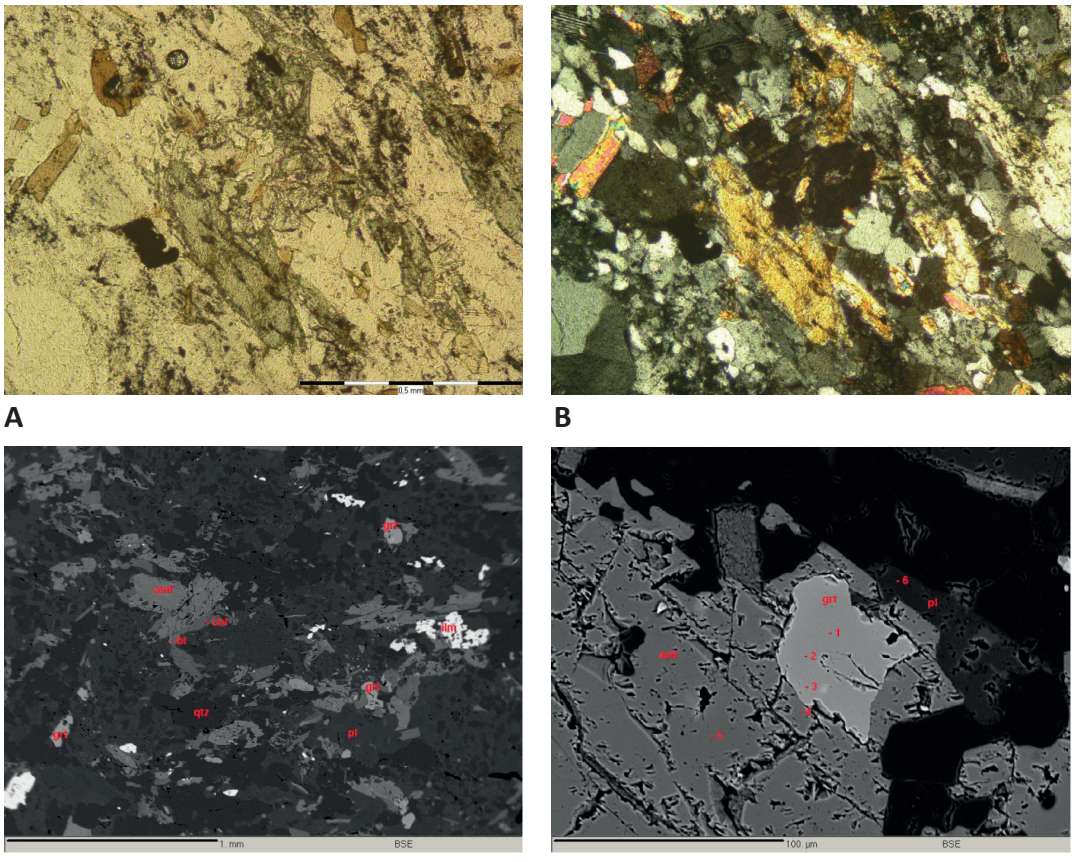

Fig. 12. Transitional type of paragneiss. Qtz–Plg–Hbl–Bt–Grt–Chl paragneiss in the vicinity of amphibolite bodies (sample SZN-57) contains often graphitic pigment. A – N//, B – N*X*: microphoto of lepidogranoblastic structure of paragneiss with often graphitic pigment. C, D – BSEI. D – Hornblend (Hbl) closes irregular garnet (Grt).

sample SZN-85 from the Závada valley area) correspond in composition to the oligoclase / andesine interface (X_{An} = 31 %). Amphibole corresponds to chermakite to magnesiohornblende, and the younger generation corresponds to actinolite.

Graphitic schists, graphitic paragneisses and black graphitic metaquarzites in association with amphibolites (119)

Dark grey schists with an organic, graphite substance are sporadically scattered within the metamorphic substrate, conformly with its metamorphic schistosity. Distinctive beds of black schists have been identified near several amphibolite bodies, suggesting a genetic link between basic volcanism and euxinic facies sedimentation in deep-water conditions. Such rocks are also present in the SE region from the elevation Klin (769 m) towards the Jasenina stream, or, according to the drilling works, they are also part of the paragneiss complex, where amphibolites occur only rarely (area SW from the settlement of Gápel towards the settlement of Petriská). The spred of graphite-rich lithologies in the paragneiss complex is relatively frequent, but without detailed surface petrographic or geophysical research, it is difficult to visualize it spatially. Graphitic rocks are finer-grained, contain more quartz and muscovite, which are otherwise insignificantly represented in the metamorphic substrate in the primary metamorphic form. These rocks are generally poorer in plagioclase and biotite and primarily represented black schists. They can also be considered to be suitable carriers of disseminated sulphide mineralization, as indicated by remnants of old exploration activity in graphitic or silicified rock environments. At the scale of the geological map, identifiable occurrences of these lithological variations, similar to the gneisses with amphibole mentioned below, are marked with a special hatch. Dark grey biotite paragneisses are also an example (sample LHS-350 – Fig. 13) with an organic admixture in association with black graphitic schísts and amphibolic schists in the area of the westernmost termination of the crystallinics above the right side of Brekovský potok valley (south from the Čierna Lehota village). Paragneisses have a lepidogranoblastic structure with a predominance of Qtz-Pl matter, Bt has metamorphic preferred orientation, associated in places with zonal Grt, which has cloudy edges (the poikilitic edge part is a consequence of new thermal metamorphism). Very fine organic matter is

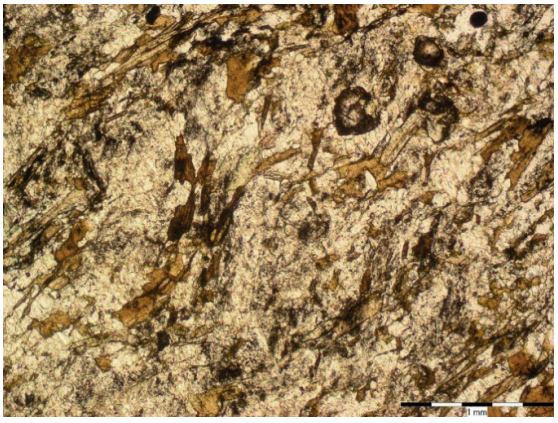

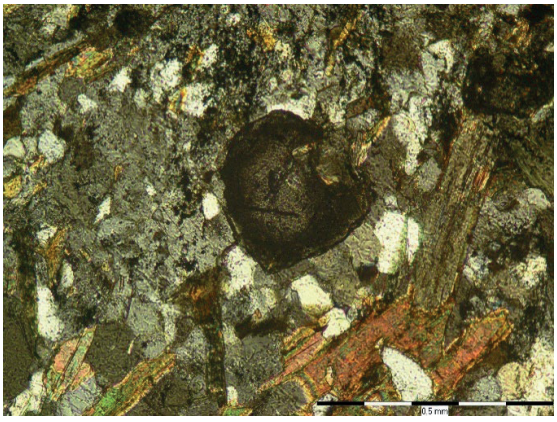

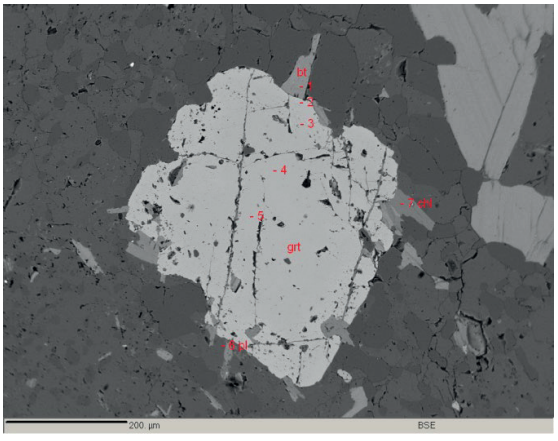

Fig. 13. A, B – Microphotograph at various magnifications (massif N, SSE from the Čierna Lehota village, sample LHS-350): A – view on structure of Bt paragneiss with fine disseminated graphite bound mainly on plagioclase, N//; B – detail of association Qtz–Plg–Bt–Grt; C – BSEI of garnet in assemblage with Bt and Chl in plagioclase. Garnet closing poikilitically fine Qtz–Pl–Chl, inclusions are richer present in marginal part of garnet, which causes the cloudy character of the Grt edges.

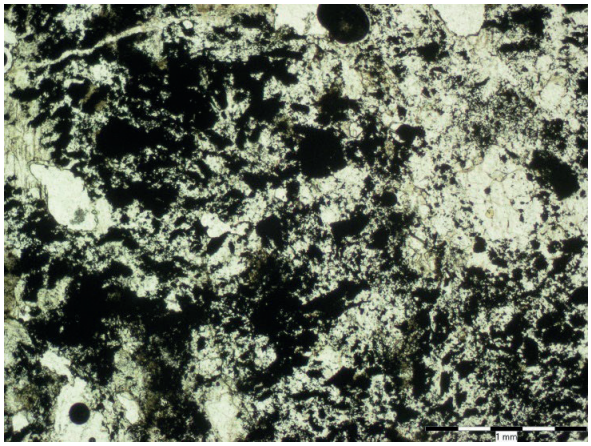

A

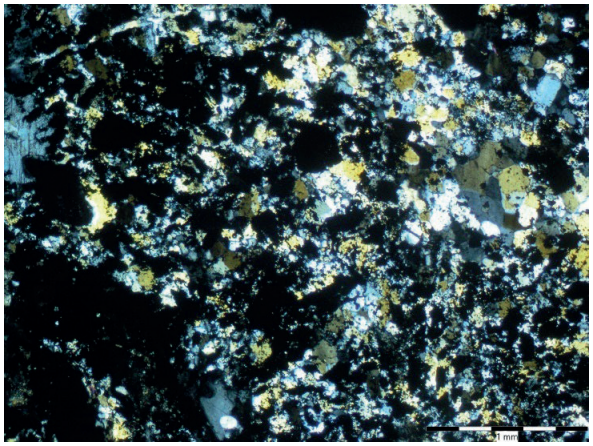

B

Fig. 14. A, B, – Sample SZN-25 from the area of Železná dolina valley; A – greyblack fine-grained cevernous metaquartzite rich in graphite, porous after the weathering of sulphidic impregnation; B – N//, **C–NX** Thin section of the rocks composed of from a substantial proportion of organic matter and quartz.

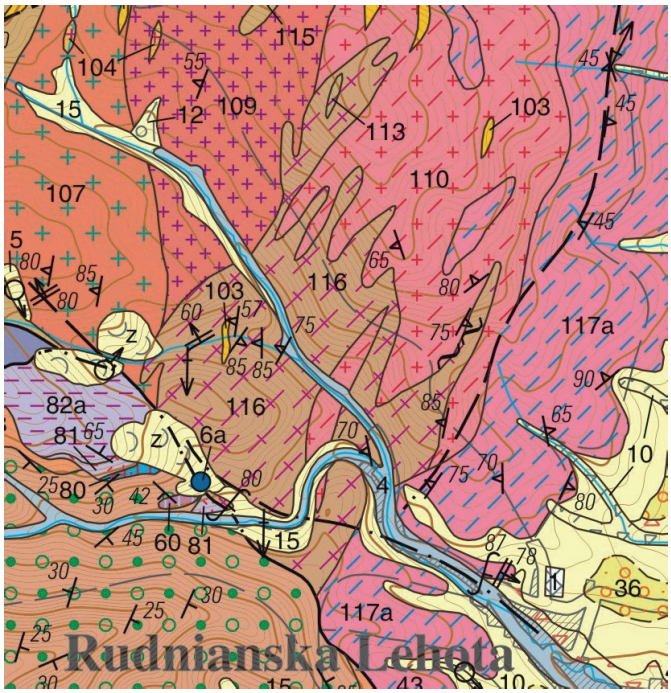

Fig. 15. Position of migmatitized paragneisses (116) with small content of ductile folded leucosoms, neighbouring with migmatites (117a) and schlier granodiorites (110).

Fig. 16. Migmatitized paragneiss with distinct primary "bedding of metasediment" s0 = s1, which demonstrated with alternation of X cm thick light greiwacke-rich interbeds with more pelitic (rich in mica) beds. The multi-stage of granitization process is distinct. Larger beds were formed in ductile stage of the thermal metamorphism of the rock, while thin veinlet (above hammer) is tied to semiductile flexure, originating in higher part of the crust (sample LHS-42).

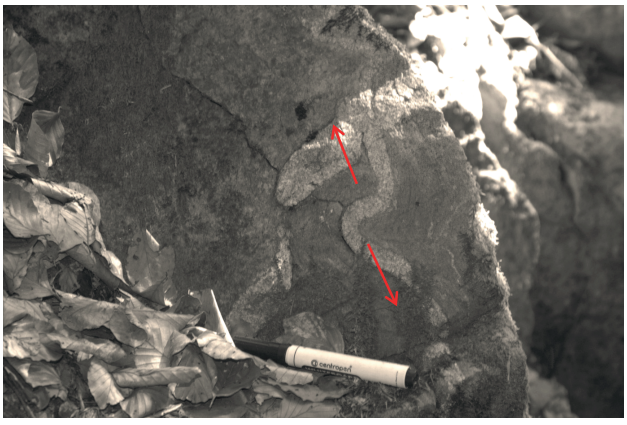

Fig. 17. Crossing off the older granite position during ductile deformation, resulting in origin of oblique ptygmatitic vein of granite (sample LHS-57)

irregularly dispersed in thin section. Rare there is present Chl in association with Grt. Pl has intermediate oligoclase composition (An_{23}), biotite and chlorite are probable coexisting minerals with roughly similar share of Fe/Mg. Grt is prograde zonal in the center with a predominance of the spessartite component over the almandine component, towards the edge with a predominance of the almandine molecule, a decrease in the grossulare component and an increase in the pyrope molecule.

Chemical dating of monazite

Chemical dating of monazite from the sample LHS-350 (Plt. 1-1) provided identical result as Mnz dating from samples of further paragneisses. Distribution and age diagram of chemically dated monazites (Plt. 1-1) and isochrone with the age of **366 ± 6.8 Ma** are typical for metamorphites of the Suchý hill. The data can be understood as a bimodal distribution corresponding to the

A

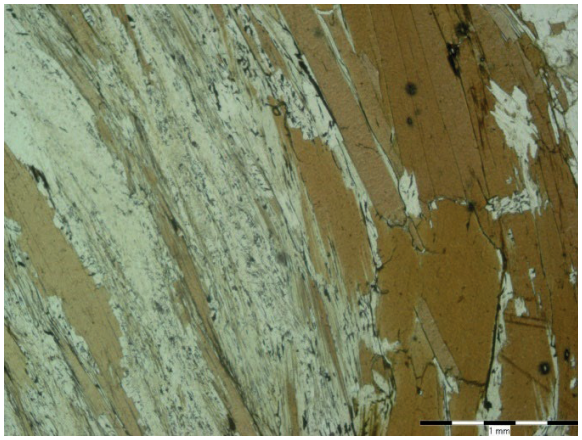

B

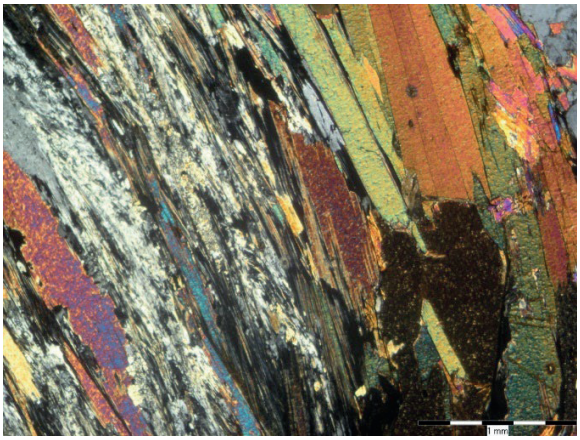

C

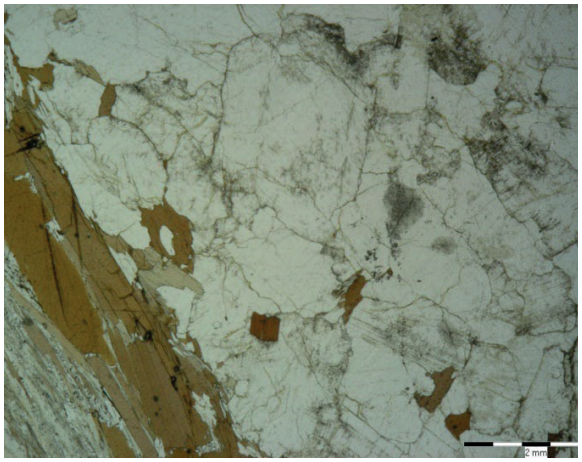

D

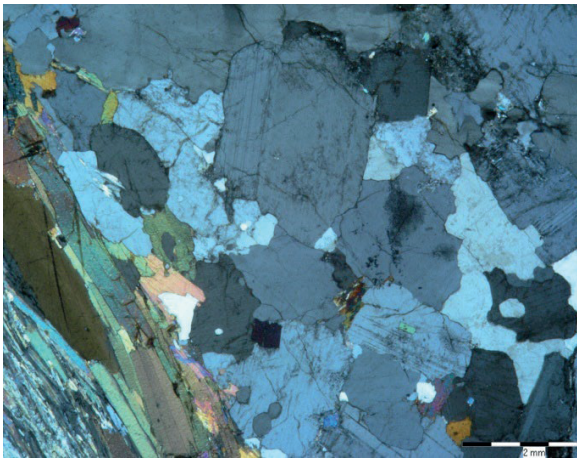

E

Fig. 18. A – Leucocratic melt at the boundary of granitoid part formed by hypidiomorphic plagioclase and quartz, containing relic biotite. Microphoto: melanosome composed of biotite and muscovite (after sillimanite) and chlorite. B–C – Detail melanosome formed of biotite and sillimanite N//, NX. D–E – Granite part formed of hypidiomorphic Plg and quartz. N//, NX (sample LHS-114A).

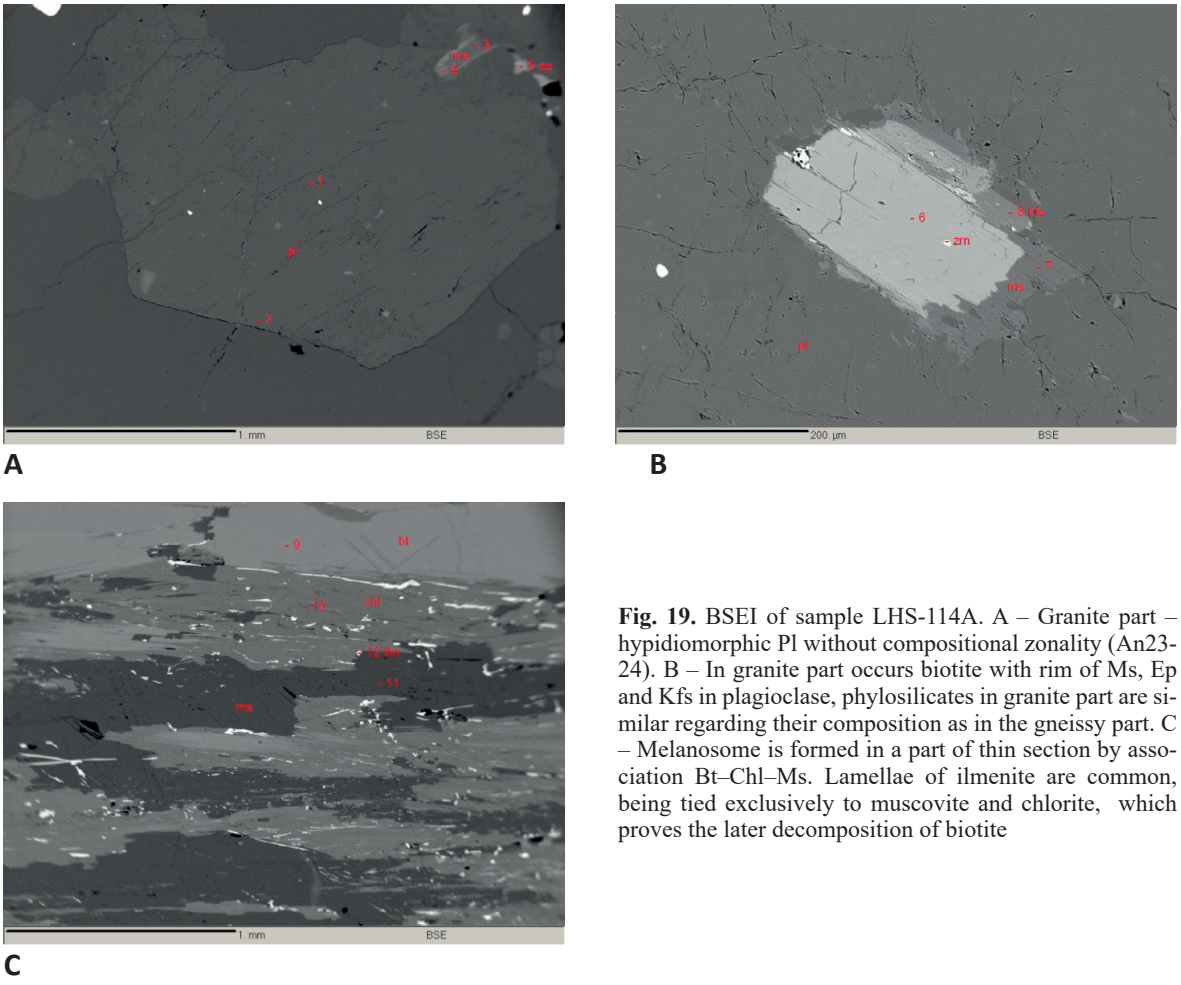

Fig. 19. BSEI of sample LHS-114A. A – Granite part – hypidiomorphic Pl without compositional zonality (An23-24). B – In granite part occurs biotite with rim of Ms, Ep and Kfs in plagioclase, phylosilicates in granite part are similar regarding their composition as in the gneissy part. C – Melanosome is formed in a part of thin section by association Bt–Chl–Ms. Lamellae of ilmenite are common, being tied exclusively to muscovite and chlorite, which proves the later decomposition of biotite

peak of metamorphism around **380–370 Ma** and thermal reworking by granitization event **360–350 Ma**.

We have shown more significant beds of black graphitic paragneisses, black metaquartzites, which are in clear association with amphibolite bodies, in the area of Závada and Železna dolina valleys and in the area of Závadská poľana towards the Čierna Lehota village. Impregnations of sulfidic minerals are typical for this group of rocks, which create light, graphite-rich cavernous rock during weathering. In the environment of graphitic paragneisses and black metaquartzites, there are frequent traces of field exploration works. In the past in the area of the Závada valley, a forecast area was set aside for graphite raw material.

Lithotectonic unit consisting of a complex of proximal sedimentary facies of the continental slope of the Paleozoic sedimentary basin

This complex is built mainly by metamorphosed, flyschoid sediments of a sandy-loamy composition with a very small proportion of clayey-sandy facies and a very small representation of basic metavolcanites, or even their absence. Depending on the depth of the erosional cut, these lithologies are strongly metamorphosed.

Migmatitized paragneisses locally with stromatitic and ptygmatitic bodies of leucogranites (116)

The migmatitized paragneisses represent a part of the lower tectonic unit (it contains mainly metasediments of greywacke nature, which we affiliate with flyshoid sediments of the continental slope with the absence of amphibolite lithologies. They occur mainly in contact with hybrid granodiorites, with which they finger-like alternate and occur in a tight overburden of migmatites. They typically occur in the Suchý massif in the area of the Bystrica valley closer to Rudnianska Lehota municipality, or in the area of the Krstenica stream (Liešťanská dolina valley) W of Liešťany village. These underwent initial partial melting and are a suitable lithology for tracing deformation structures in relation to granitoid formation.

Within this rock assemblage, the gneiss component significantly predominates over the leucogranite compo-

nent, which is characterized by ductile granite structures manifested by bulging of granitoid material, which undoubtedly originated at different crustal levels (e.g. Figs. 16 and 17). Also from this example, it is possible to deduce the assumption that the main granitization process was more related to the contribution of heat from the intruding large granitoid masses, which is manifested by the different intensity of the migmatization process, than to deep crustal partial anatexis. At the same time, it is possible to state that the crustal thickening and melting in the deeper parts of the crust was followed by gradual decompression, the subsequent ascent of granitoid magmas into the metamorphic assemblage during the syntectonic regime and a change in the rheology of the metasediments from a ductile to a semi-ductile regime, and finally to a regime with signs

As is evident from the presence of leucogranite positions with melanosome rims, deeper crustal conditions of partial melting can be assumed through leucogranite ptygmatitic structures, without significant interaction with the gneiss substrate, to semiductile structures with transversal tabular veins. The mentioned structures are a consequence of the decompression of the metamorphic complex. Larger bodies of hybrid (schlier) granodiorites that are associated with this complex could have formed as a product of segregation of granitoid material into suitable structures, but more likely represent independent pulses of granitoid magma into the metamorphic substrate.

Monazite dating from leucocratic melts, associating with migmatitized paragneisses and hybridic granitoids

Chemical dating of monazite indicates in high–metamorphic migmatitized paragneisses to presence of Mnz population, coresonding by age with pre-granite regional metamorphism, while all metamorphosed lithological members of the Suchý crystalline basement contain the Mnz population corresponding by age, where the chemical age approaches approximately **370–380 Ma**, which correstponds with Upper Devonian. Origin of first melts relates with later thermal overprint with the age around **350–360 Ma**, which correpsonds with the boundary of Upper Devonian / Mississipian.
First leucocratic melts contain mixed population of monazites from older metamorphic phase as well as younger granitization stage. Following bigger volumes of hybridic tonalites and granodiorites contain only population of granitic stage.

Higher metamorphosed biotite to muscovite-biotite paragneisses with garnet, medium- grained, often with oriented secondary biotite (locally with sillimanite and staurolite) –distinctly injected with leucocratic granite (115)

In geological map we separate complex of biotitic and two-mica paragneisses, very intensively injected by leucogranites, aplites and pegmatites. At the same time – in profiles the paragneisses are alternating with paragneisses and granitoid injections in distances of several meters and dekameters.

Part of these rocks do not contain such leucocratic injection, but the presence of larger oriented and thermally induced biotite blasts, usually associates with nearby bodies of leucogranites in the footwall. The distinguishing of a zone of paragneisses with blastesis of secondary, thermally induced biotite in conditions of dynamic emplacement of leucogranite magmas indicated the vicinity of larger bodies of leucogranites and pegmatites–aplites in nearby footwall. Locally paragneisses form larger xenoliths in leucogranites. The presence of ptygmatitic structures of leucogranites is absent, or is very rare, which indicates the higher crustal level of these lithologies during intrusion of leucogranite melt.

Thermal effect of granitoid intrusions produces larger flakes of biotite of 2nd generation, either in foliation planes of metamorphites, or growth of biotite II is characteristic for the whole rock. Blasts of biotite II have linear orientation and their arrangement corresponds with orientation of larger biotite flakes in leucogranites. Porphyroblasts of biotive II (Bt II) with flakes large up to 2–4 mm are characteristic for this type of gneisses (Fig. 21). They usually contain secondary garnet of contact thermic origin, reaching dimenskons up to ca 0.1–0.2 mm (Fig. 25)

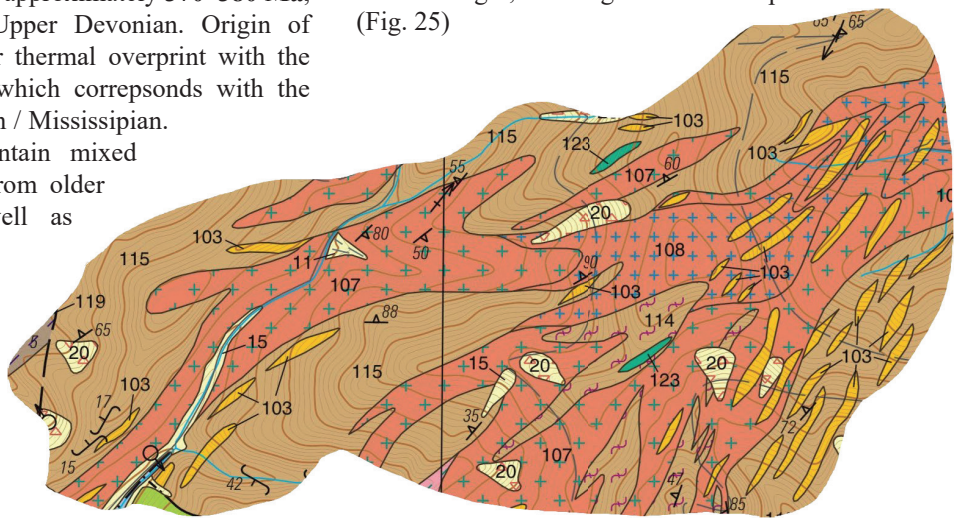

Fig. 20. Position of higher thermally affected parageisses with thermally induced biotite II (115).

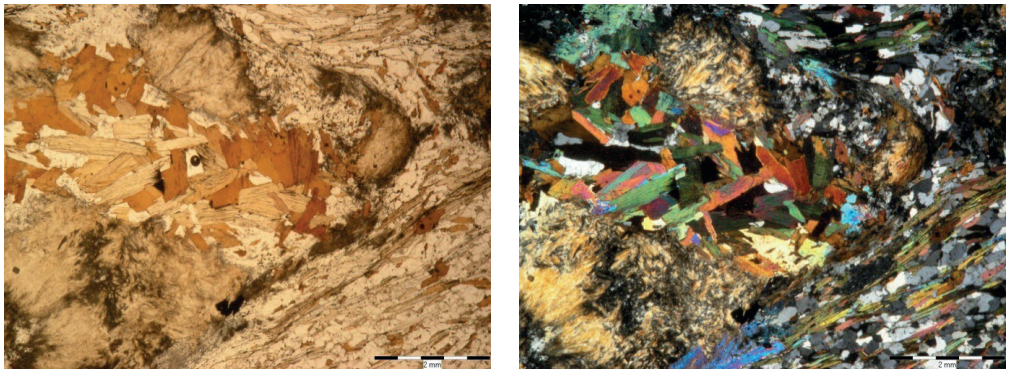

Fig. 21. Qtz–Pl–Bt–Ms paragneiss with older sillimanite–fibrolite (prevalence of Qtz over Pl). Sillimanite phenocrysts overreach 2 mm. At marging the fibrolite is replaced by Ms. The graphite pigment is abundant. Large blast of rotated sillimanite from regionally metamorphic phase is in later stage in connection with intrusive leucogranitic thermic stage cataclased and fracture is filled with red-brown Bt, which has different position concerning the older Bt of subparallel metamorphic setting of two-mica paragness. A – N//, B – N*X* (sample LHS-197). Grey fine-grained paragneiss, overheated by thermic metamorphism in connection with deformation related to ingress of leucogranites. Synintrusive deformation is manifested by the formation of microfolds and formation of larger flakes of phyllosilicates. Metamorphic schistosity is subvertical of E–W direction.

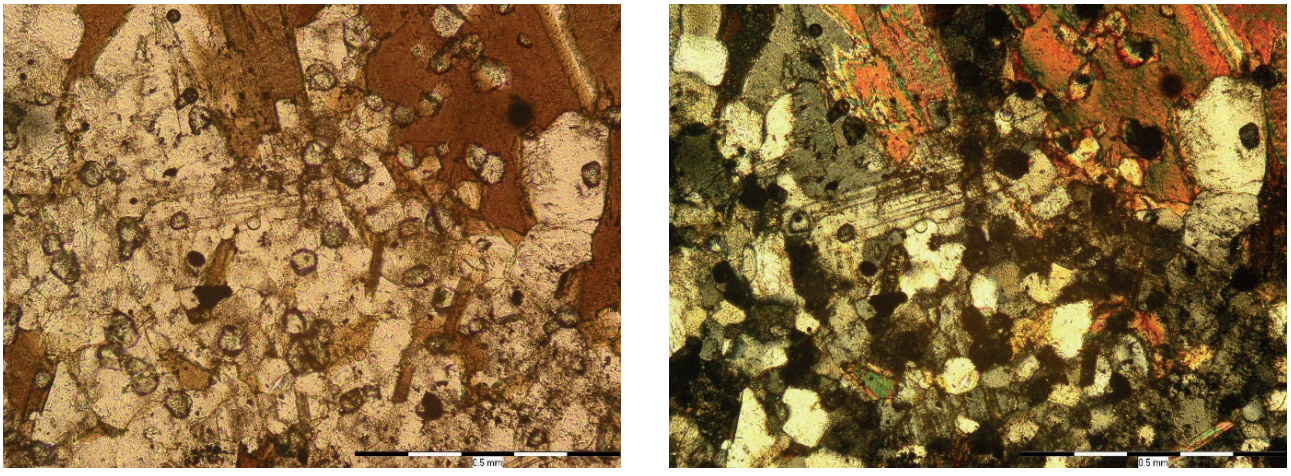

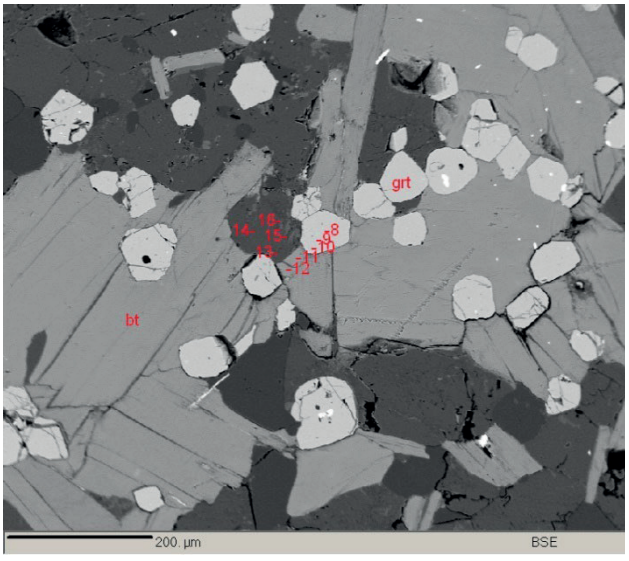

Fig. 22. Sample of biotite paragneiss with thermal overprint (LHS-255) and origin of redbrown biotites and tiny garnet. A – N//, B – NX, C – BSEI of disseminated tiny Grt in feldspars and Bt. Tiny Grt (below 0.1 mm) associate with Bt. Bt has intermediáry ration Mg/(Fet + Mg) = 0.45–0.44. Grt has trong prevalence of almandine component. Composition of Pl is in this association in the range XAn 29.5–32 %. Regardins very small dimensions of Grt we can state their relatively homogeneous composition in the profile. Typical average compositon of non-zonal Grt is Alm – 71 %, Spess – 16, Pyr – 8, Gross – 4.6 %. Sample by taken from the contact of paragneisses with aplite veins and granite.

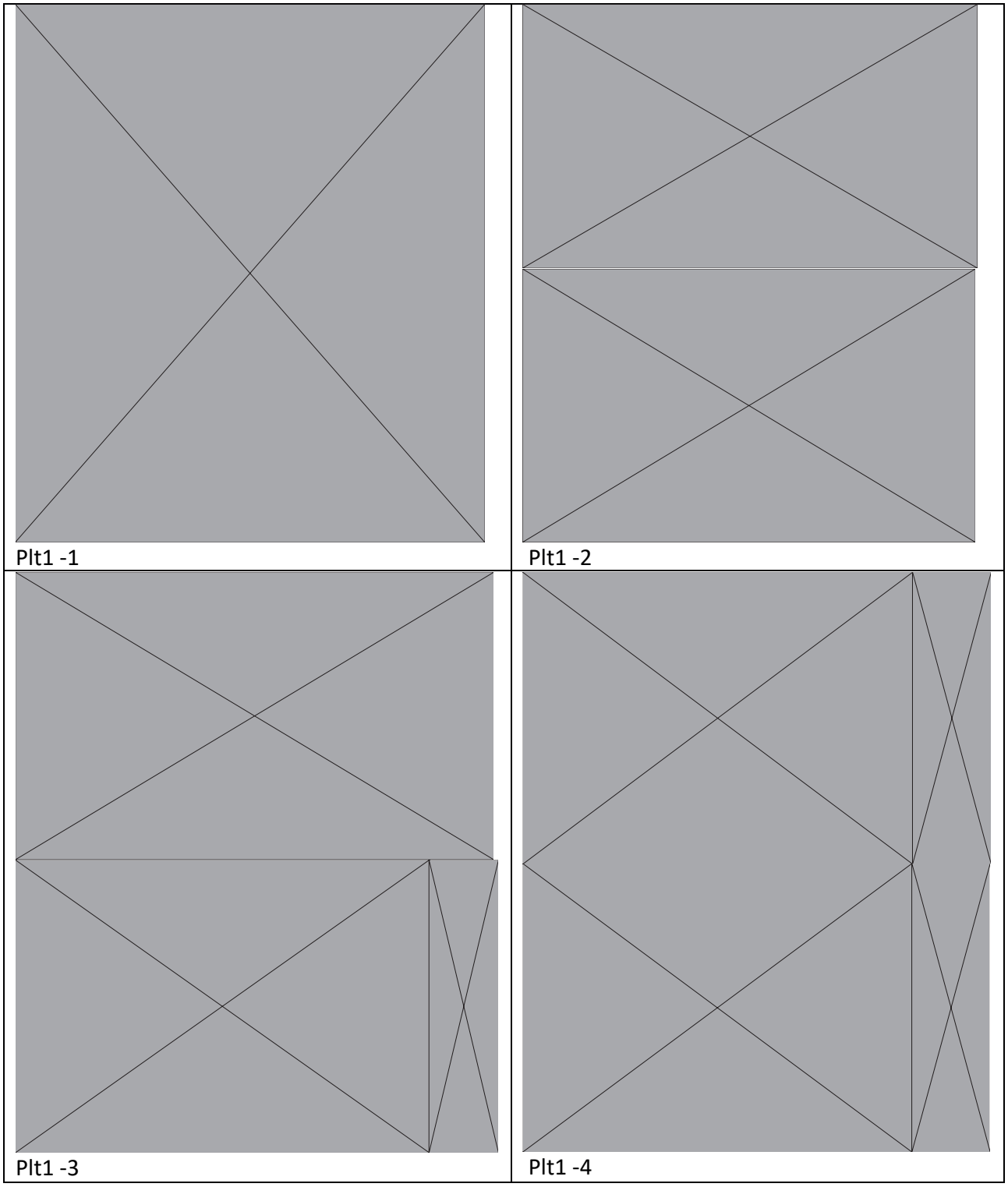

Plate 1. Mnz dating from granite part (sample LHS-114AG – Plt 1-2) is formed by Mnz, crystallizing from the melt and relict, being a part of relict minerals, mainly micas and monazite enclosed in them. The file can be divided to two age groups with the ages **350 and 390 Ma.**

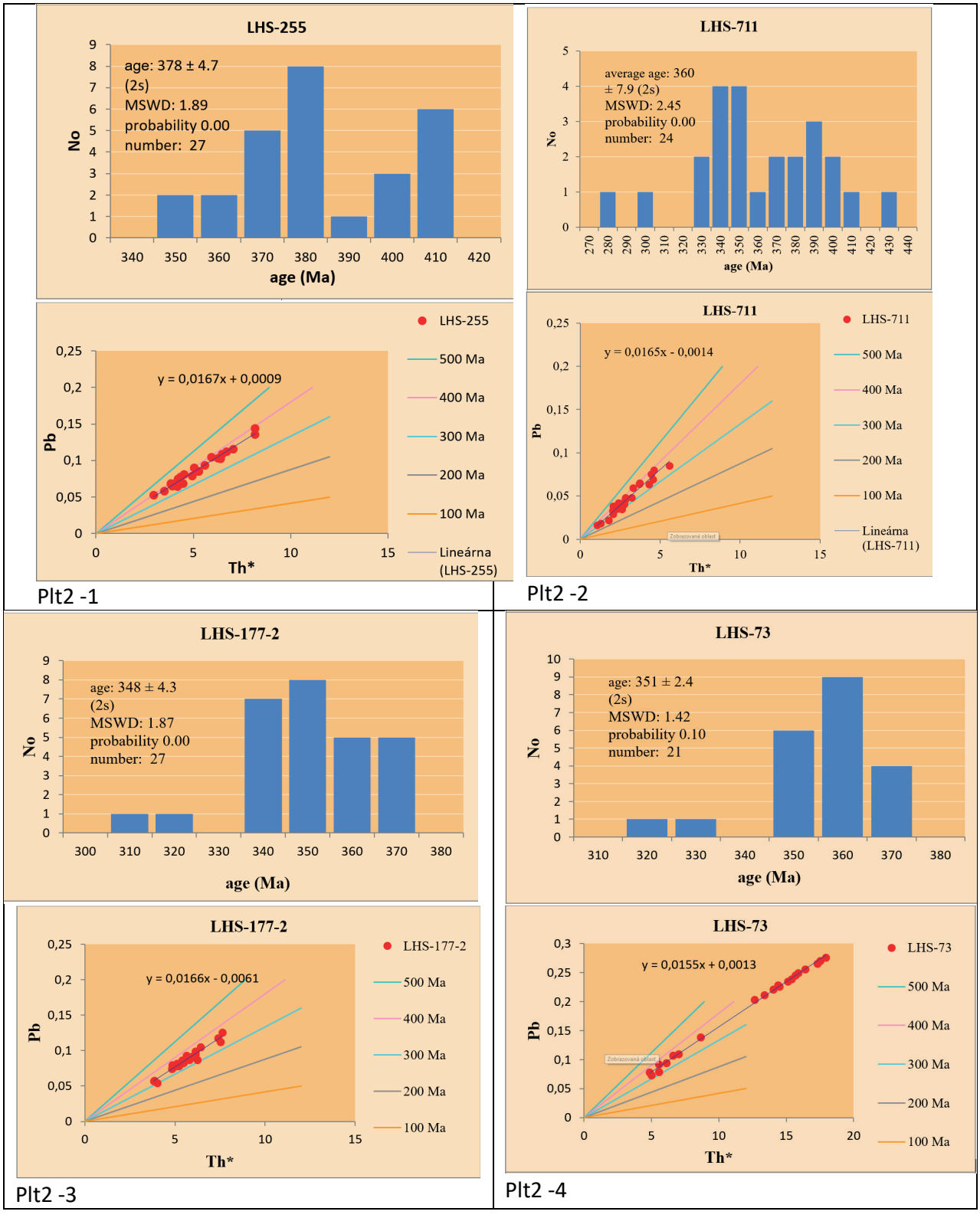

Plate 2. Mnz dating from gneissy part (Plt 1-3) contains exclusively older generation of Mnz (**368 ± 5.7 Ma**). This age is characteristic for all distinguished types of metamorphites and most likely represents peak of regional metamorphism around **380–370 Ma**.

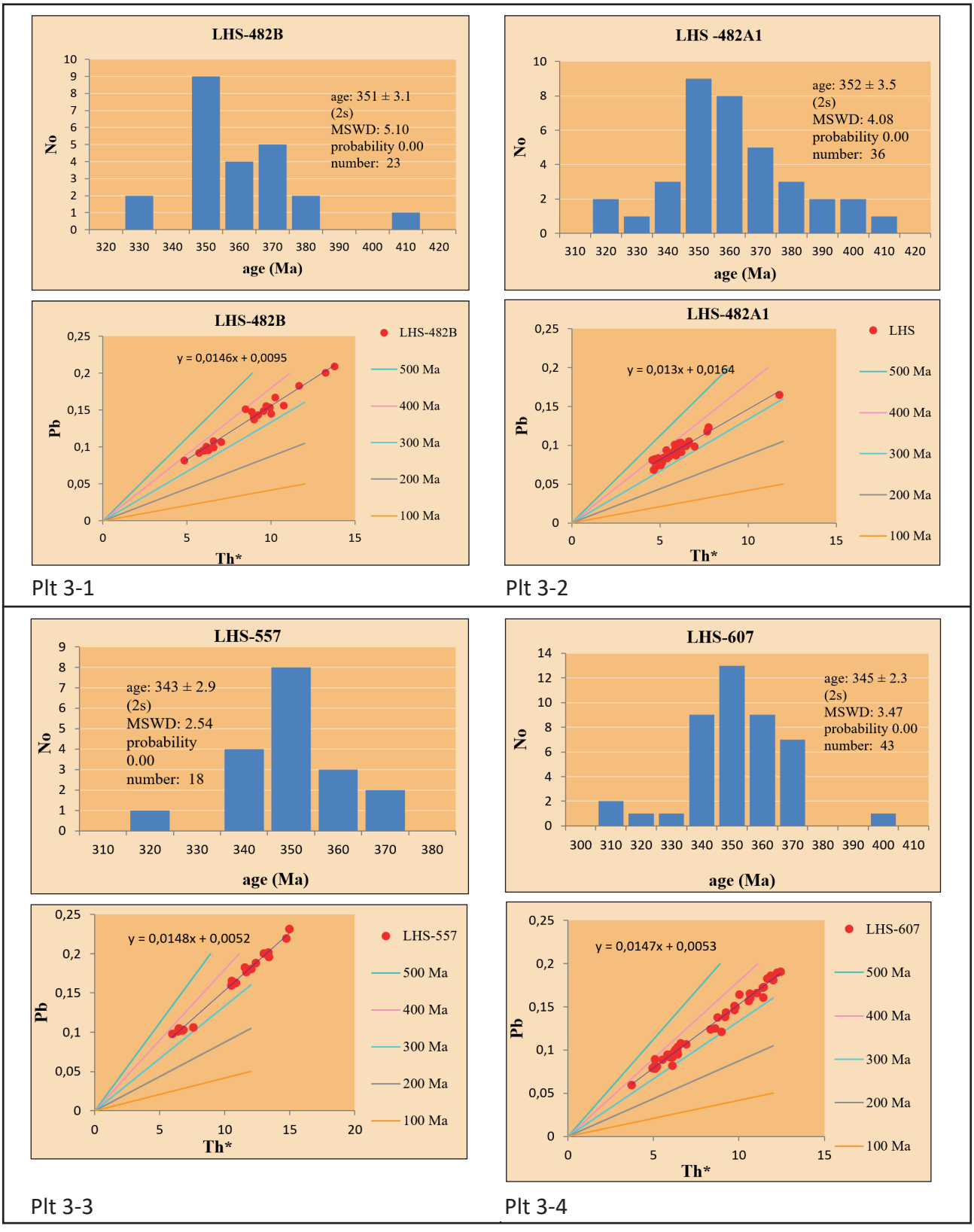

Plate 3: Mnz dating from hybridic homogenous leucotonalite-leucotrondhjemite (sample LHS-114B) (Plt 1-4), as ductile melt from the environment of migmatitized paragneisses, indicating the prevalence of Mnz age generation **350 ± 4.8** Ma.

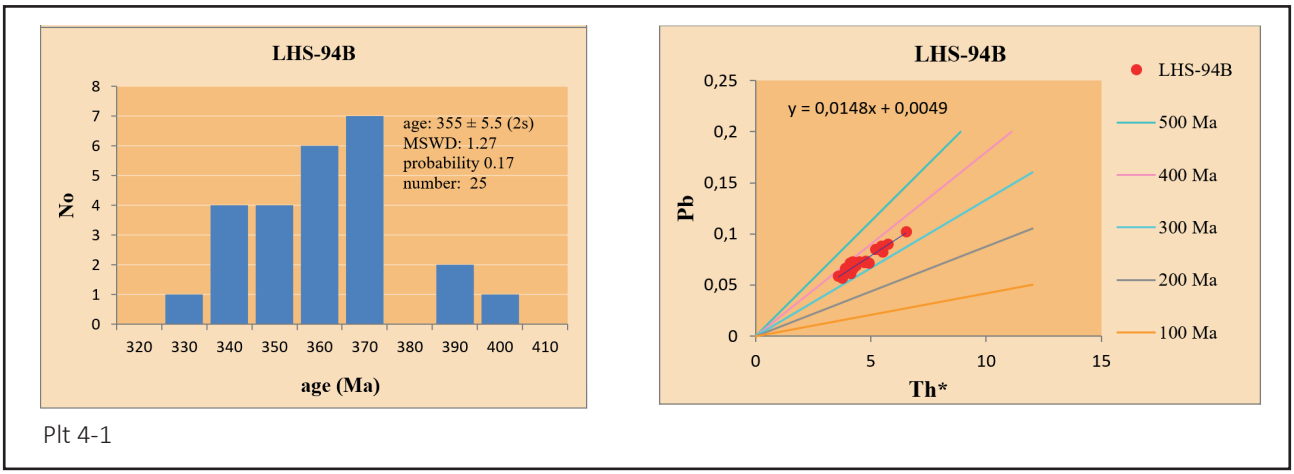

Plate 4. Mnz dating from the sample of omnidirectional granodiorite LHS-94B providing the age **355 ± 5.5 Ma**

It is proved by concordance of the main component of the stress field of synintrusive deformation regime with emplacement of leucogranite veins. These simultaneously with emplacement and decompresion of the whole crystalline block rapidly solidified and behaved as dense crystal slurry.

They have corresponding mineral composition as following type of paragneisses, but slightly larger grain. In prevailing lepidogranoblastic structúre the bands of biotite-plagioclase material alternate with cleaner quartz-rich lamina. Plagioclase grains usually connect by polygonal way and obtain hornfels structure. In comparison with the standard biotite gneisses, gneisses of this type were to some extend injected by leucocratic material. In the process of "thermic" metamorphic crystallization they acquired larger grain size, and probable there rarely crystallized also transversal muscovite.

Chemical dating of monazite in metapsammitic paragneisses

Monazite in biotitic paragneisses is relatively abundant mineral, often containing according the results of dating at least two separate populations. In paragneiss sample LHS-255 two temporal groups of monazite occur. Older group correpsonds to boundary of Silurian / Devonian (410 Ma) and probable can be correlated with the period of filling sedimentary basin with clastic material? Age 380–370 Ma is significantly more distinct and probable relates with collision and metamorphic overprint in Upper Devonian. Following thermal metamorphism of Lower Carboniferous age was only indistinctly reflected by the origin of new generation of monazite (Plt 2-1).

Lithotectonic unit consisting of orthogneisses complex (granite protolith CdD2, tectonometamorphic overpring VmD2)

Biotite, quartz-plagioclase (± K-feldspar ± mucovite), foliated and lineated orthogneisses (111)

Quartz-, plagioclase-biotite orthogneisses with variable content of interstitial K-felddspar and muscovite crops out mainly in separate, distinctly limited zone with sharp contact with neihbouring biotite paragneisses. Main body

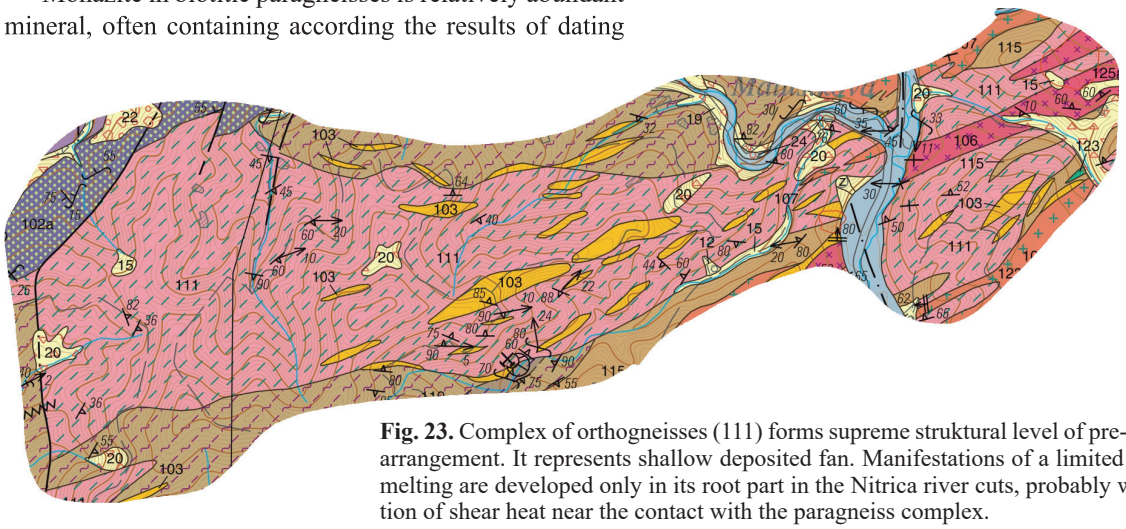

Fig. 23. Complex of orthogneisses (111) forms supreme struktural level of pre-granite structural arrangement. It represents shallow deposited fan. Manifestations of a limited degree of partial melting are developed only in its root part in the Nitrica river cuts, probably with the contribution of shear heat near the contact with the paragneiss complex.

of E–W direction is situated south of Valaská Belá village approximately W of the elevation point Capárka (924 m) through Okrúhly vrch (914 m) towards the confluence of the streams Jasenina and Nitrica (area at the crossing at the Motorest Klin). In this area the body of orthogneisses is areally reduced, which is caused by deeper erosion cut with higher degree of granitization, connected probable with the contribution of shear heat. This fact indicates the upper structural position of the body within Variscan tectonic setting (profile 1–2 in published geological map) in the footwall with the paragneiss complex. In this zone we interpret this position as fan structure, wedging into the deeper parts. Further this body follows in E–W to ENE direction towards the area of fault east of Temešská

Fig. 24. A – Banded orthogneiss with transversal vein of leucocratic granite (sample LHS-207); B – ductile deformed relics of plagioclases in orthogneis (sample LHS-273).

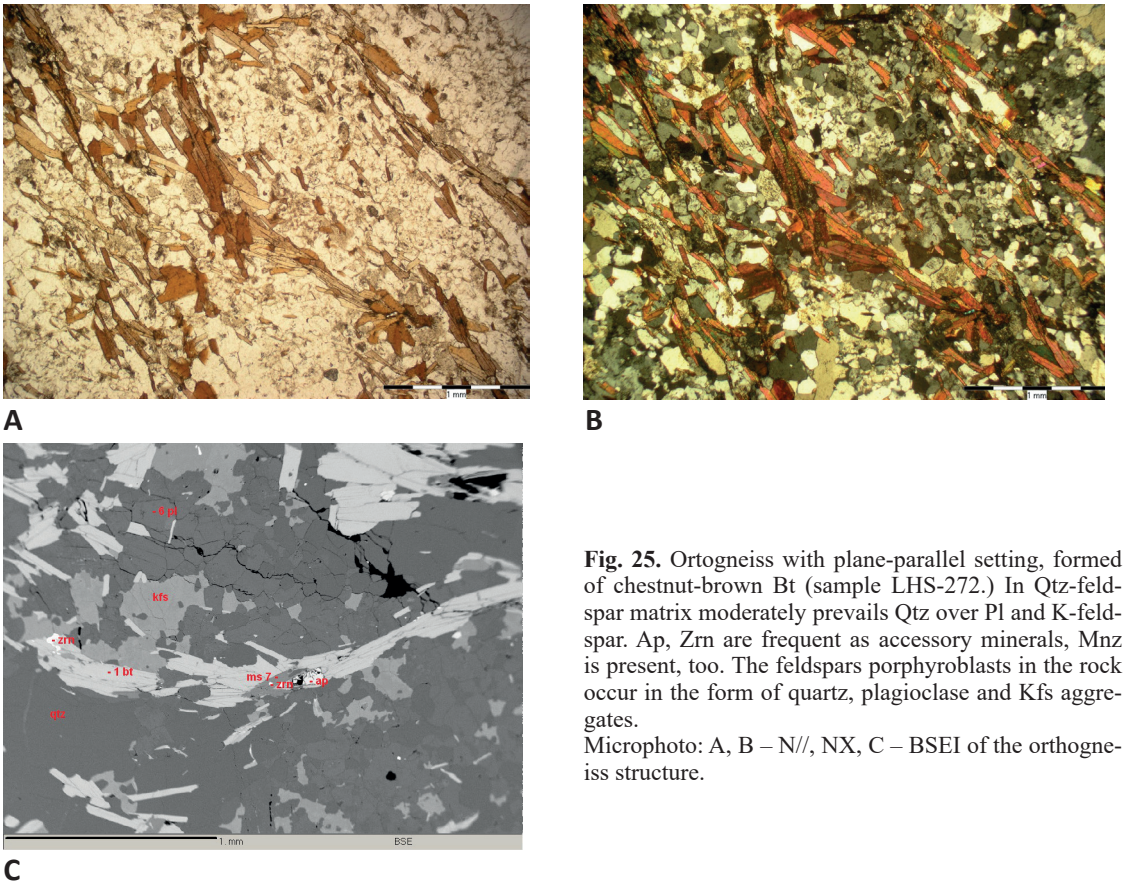

Fig. 25. Ortogneiss with plane-parallel setting, formed of chestnut-brown Bt (sample LHS-272.) In Qtz-feldspar matrix moderately prevails Qtz over Pl and K-feldspar. Ap, Zrn are frequent as accessory minerals, Mnz is present, too. The feldspars porphyroblasts in the rock occur in the form of quartz, plagioclase and Kfs aggregates.
Microphoto: A, B – N//, NX, C – BSEI of the orthogneiss structure.

skala hill. Here it is intruded by younger leucogranites and biotite I-type granodiorites (106).

In the past, this lithology was considered as migmatites. However, the processes of migmatization in the rock are completely absent and are limited only to narrow zones, even in the deeper parts of the fan-shaped structure.

These are monotonous banded rocks, where quartz-feldspar bands alternate with biotite bands a few mm thick. The content of biotite and plagioclase slightly varies. The presence of spindle-shaped plagioclase is typical. The metamorphic foliations are steep, mainly in the E–W direction, with lineations mainly of biotite glomeroblasts of a subhorizontal direction, which contrast with the light quartz-feldspar mass. The position of orthogneisses during granitization processes was more external (higher), which is indicated by only very rare ductile deformations of orthogneisses associated with the presence of leucocratic melts. The aplite and pegmatite veins present in them are usually oriented at a high angle to the foliation of the orthogneisses.

The dominating foliation features indicate the presence of ductile shear folds with steep fold planes, shallow fold axes, and shallow lineations accentuated by elongation of biotite glomeroblasts. The pre-deformation origin of orthogneisses is not clear. Unlike the lighter, fine-grained paragneisses, the rock lacks graphitic pigment, which shifts our opinion to the assumption that it is an acidic, originally magmatic rock of granitic to granodiorite composition.

Monazite chemical dating

Chemical dating of monazite from orthogneiss (sample LHS-711) indicates an average age of 360 Ma, which, however, does not correspond to a real geological event. Dividing the data into two distinct peaks – into two separate events, where we interpret the older event (400–380 Ma) as the age of metamorphic event. The second significant maximum is the age of 355–345 Ma, which corresponds to a younger thermal event associated with the formation of granitoids in the Strážovské vrchy area (Plt 2-2).

Migmatites with prevalence stromatitic, loc. ptygmatitic textures (117a)

Migmatites form the lowest structural level of the crystalline massif from the point of view of the Variscan (pre-granite) setting. They emerge in the SE edge of the Suchý massif (so-called Liešť migmatites). Pre-granitization, or syngranitizing fold planes and elements of metamorphic foliation have a steep to subvertical course in the NNE–SSW to NE-SW direction. The axes of the folds are predominantly subhorizontal.

In *stromatitic migmatites* there varies the content of the light quartz-feldspar component representing the neosome relative to the relict part, locally enriched with minerals rich in Fe and Mg (melanosome). The content of light and dark components varies from types with a predominance of the light component to the dark component in a ratio of approximately 70 : 30, to types with a slight predominance of the dark component over quartz-feldspar component. It points more to the variability of the composition of the substrate than to the intensity of the anatectic process. The process of anatexis led to a maximum of the first few tens of percent of the share of the original volume of the rock. Smaller volumes of migmatized pararules are also present, where, in addition to granitoid injections, more or less numerous ptygmatitic granitoid melts appear.

In the Suchý massif, a strip of migmatites is adjacent from the western side to lighter schist-like (hybrid) granodiorites (110), which represent an overlying complex to the migmatites. Although the contact is relatively sharp, larger migmatite septa are found parallel to the foliation elements in the migmatites and parallel to the inhomogeneities – schliers in granodiorite. Among the migmatites and hybrid granodiorites, amphibolite bodies that have undergone granitization occur. From a lithological point of view, this type of migmatites may correspond to the original composition of the orthogneiss material.

The composition of large flakes of biotite, characterized by a stable composition with Mg# = 0.38–0.40, is close to the composition of muscovite with Mg# = 0.43, which points to equilibrium conditions of association. Ms is often very intensively replaced by sillimanite by the reaction Ms + Qtz to form a melt, resp. Bt + Qtz to form a K-feldspar-rich melt (outside of the presented thin sections). Putiš (1976) reports the volume composition of mineral components from the more isotropic type of migmatite SW from Temeš village – quartz (19.2 vol. %), plagioclase-oligoclase (27.9 %), orthoclase-microcline (19.4 %), biotite (18.1 %), muscovite (2.5 %) and sillimanite (12.4 %).

Fig. 26. Ductile deformed migmatites with equal representation of light and dark component. Right beneath the hammer the boudins of quartz-feldspar pegmatite-type melt are visible (sample LHS-131 – the Krstenica valley).
Structure of the rock is grano-lepidoblastic to lepidoblastic with dominating plagioclase, biotite, K-feldspar, muscovite, sillimanite.

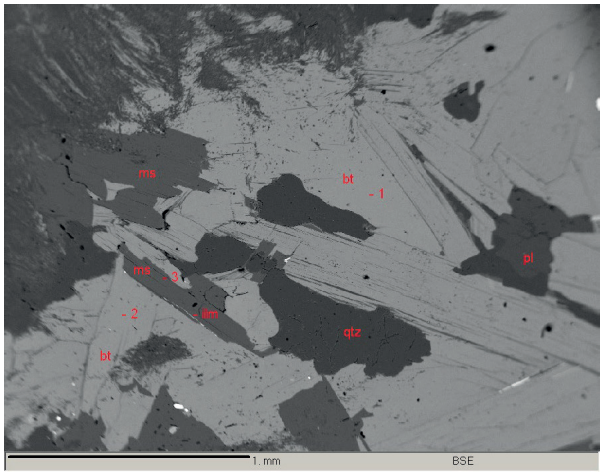

Fig. 27. Mineral association of melanosome from migmatite is formed in prevalence of biotite associated with Ms, Qtz and Pl replacement by Bt and Ms by sillimanite left part of the picture (sample LHS-137), BSEI.

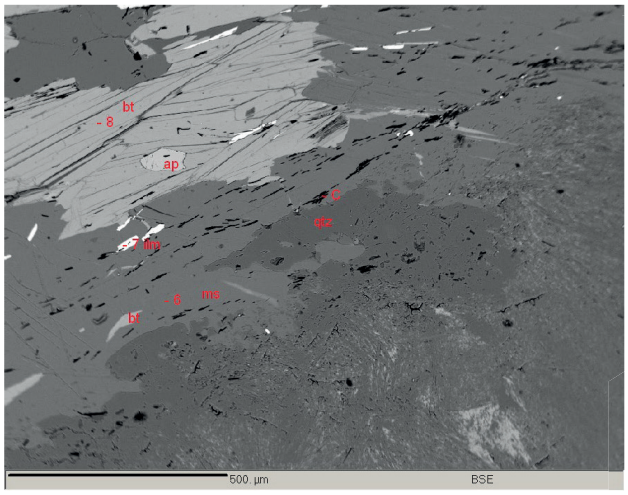

Fig. 28. Association Ms + Bt melanosome (apatite incusion). Black subparallel tables of graphite enclosed mainly in Ms. Subparalel arrangement of grafite strips shows that this part represents former metamorfic assemblage. Chaotic arrangement of graphite right down points on flow arrangement due to melting of former conzumed Bt (light relic right down). Ilmenite with content up to 5.61 wt.% of MnO crops as akcesoric mineral together with plagioclase with An_{18}. Ilmenite and graphite are oriented according to metamorphic foliation surfaces (sample LHS-137). BSEI.

Late Devonian – Mississippian granitoids (VmD2)

In the Suchý massif there is possible to distinguish several granitoid portions, which are close in time, but intruded at specific crustal conditions in decompression regime. In lower part of metamorphic packet there intruded the schlier granodiorites with less mobile magma, which is proved by inhomogenities parallel with those developed in migmatites. In schliered shallower crustal conditions the transtension shearing applied with intrusions of S-type prevailingly two-mica granites (connected with distinct presence of transtension pegmatite intrusions), up to intrusions of I-type granodiorites, or even small diorite bodies.

Massive to weakly oriented hybridic granodiorites with common schliers and xenoliths of paragneisses and migmatites (110)

Schliered granodorites emerge to the west of the migmatite zone, while their mutual relationship is relatively sharp, but blocks of underlying migmatites can be found quite commonly, especially in the contact zone, about a few more 100 m from the mapped border with migmatites. The contact is highlighted in places by smaller or larger bodies of amphibolites. The higher part of the complex is dominated by bodies of migmatized paragneisses and biotitic to two-mica paragneisses. These granitoids crop out in the zone of NNW direction from the Bystrica valley W of Rudnianska Lehota, where they alternate with migmaritized paragneisses (116), through the localities Háj – Predné lazy – Prostredná dolina – Obory nad dolinou Krstenica

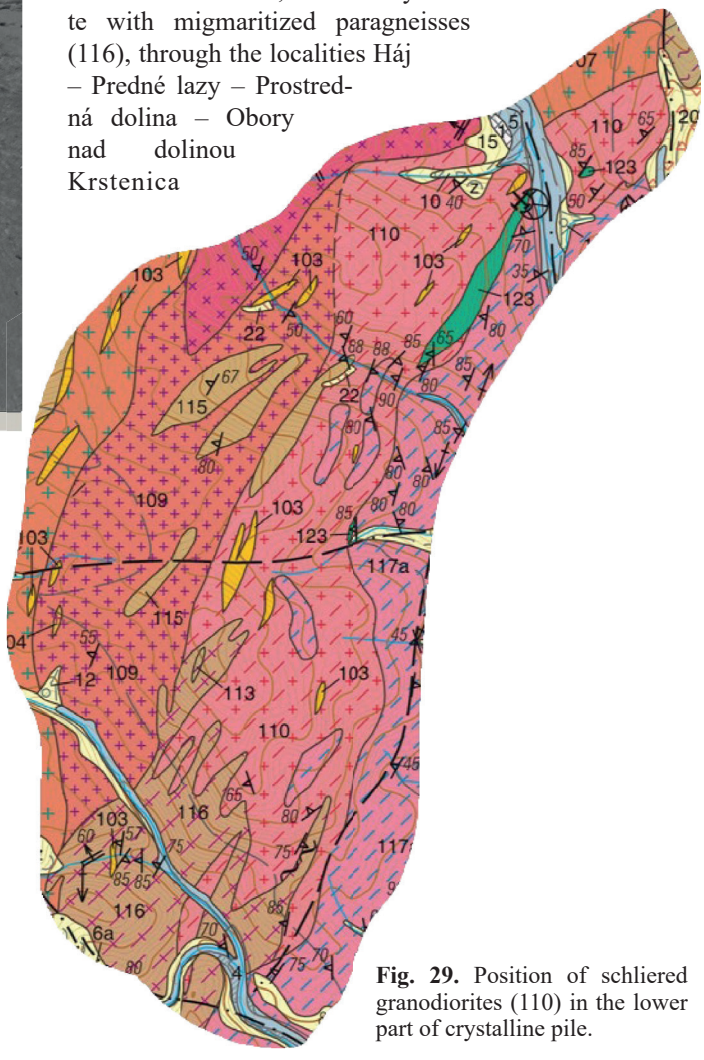

Fig. 29. Position of schliered granodiorites (110) in the lower part of crystalline pile.

(Liešťanská dolina valley) – Mihálová (where they are in contact with omnudirecional younger biotite granodiorite) – towards Nitrica and in the E this zone ends on fault zone of N–S direction.

The preferred orientation of foliation structural elements of NNE–SSW direction in migmatite and paragneisses blocks is identical and corresponds with preferred orientation of dark biotite schliers in granodiorites.

Granodiorites represent medium-grained granitoids, where the quartz-feldspar component is more or less omnidirectional and the inhomogeneities are formed by biotite schliers, gneiss and migmatites xenolits, which setting indicates preferred orientation. However, there are also present varieties with a low content of inhomogeneities and omnidirectional biotite.

Xenoliths of pararules and migmatites range in size from a few cm to hundreds of meters in places. The composition of granitoid rocks varies from tonalite to granodiorite.

Schliered biotite granodiorite–tonalite (sample LHS-177-2) contains moderately zonal plagioclases of composition $An_{24–28}$ and biotite with Mg # = 0.41–0.44. Rare Ms appears in the structure as later, which is indicated by different Mg # = 0.52. Zircon, monazite, apatite and ilmenite are rare present as accessoric minerals.

Mnz dating based on 27 values gave a fairly uniform distribution, where the age **348 ± 4,3 Ma** (sample LHS-177-2, Plt 2-3) can be considered as an age close to the thermal event that led to the emergence of melting processes and subsequent crystallization.

Schliered granodiores represented the less mobile crystal slurry, which is associated with the underlying migmatites and was generated by ongoing thermal reworking of the metasediments. The rock is essentially a diatexite, i.e. a rock that has passed through the initial magmatic stage, which is evidenced by the zonality

Fig. 30. A – Schliered granodiorite with xenoliths of migmatized paragneisses and oriented biotite.

Fig. 30. B – A schliered granodiorite with a substantial representation of an inhomogenously distributed components, subparallel, unevenly distributed laths and accumulations of biotite, which represent a redistributed melanosome. In some places, the biotite melanosome forms separate areas of biotite, separated by fuzzy pale stripes: The rock represents a higher degree of melting and mixing of granodiorite leucosome with melanosome in the form of a dense crystal slurry (sample LHS-185).

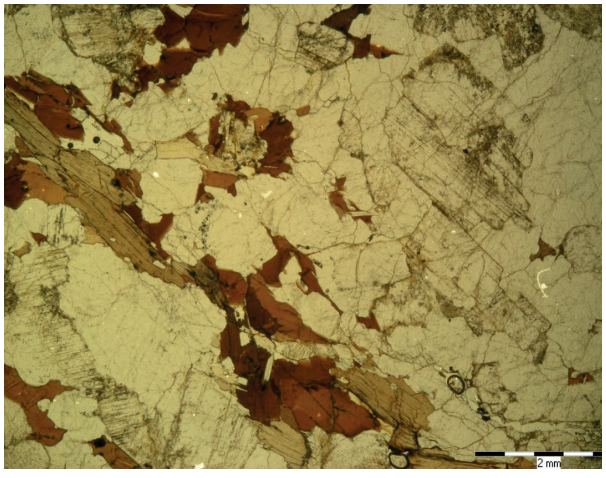

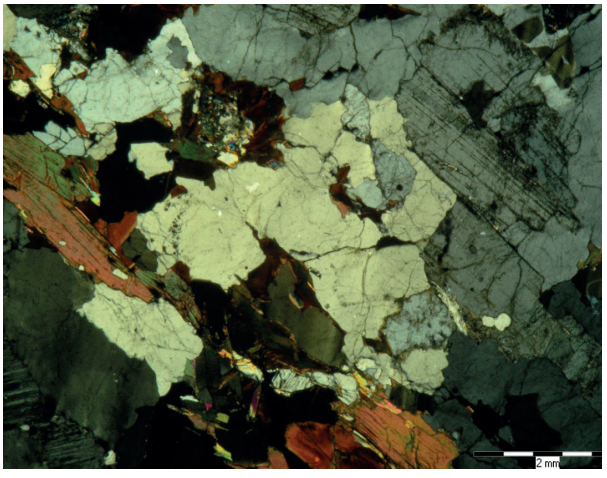

Fig. 31. Stucture of the schliered granodiorite with oriented Bt laths, xenomorphic to hypidiomorphic weakly zona Plg. Ms is rare and appears in the structure as late in origin (sample LHS-177-2).

of plagioclase and biotite orientation, the presence of numerous schists, migmatite xenoliths and migmatized paragneisses. The separation of the K-feldspar component is only very limited and manifests itself in isolated positions parallel to the inhomogeneities in K-feldspar rich grey parts. Despite the rheological properties, the mobility of the crystal slurry can be observed in places, which is manifested by sharp contacts with the migmatites, which appear as septa in this granitoid.

Biotite or muscovite-biotite granites, loccally leucocratic (109)

They form a strip emerging west of the rock type No. 110 and are spatially and genetically connected to it. They represent a band of granitoids dominated by more leucocratic types of granodiorites. They have a lower content of dark components.

The rocks have a slightly oriented biotite, which is generally inhomogeneous and size-distributed. But

Fig. 32. The character of medium-coarse-grained, more leucocratic types of granodiorite rocks with irregular spatially and size-distributed biotite.

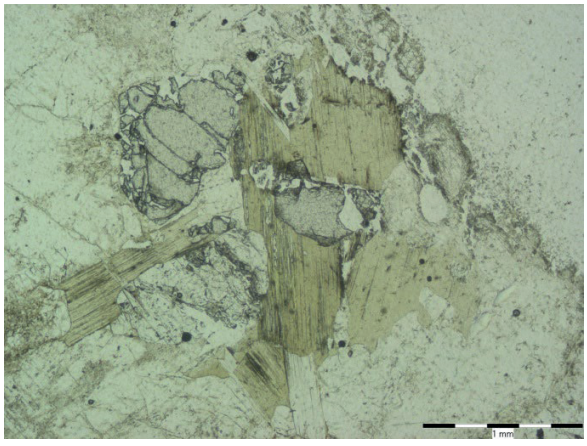

A

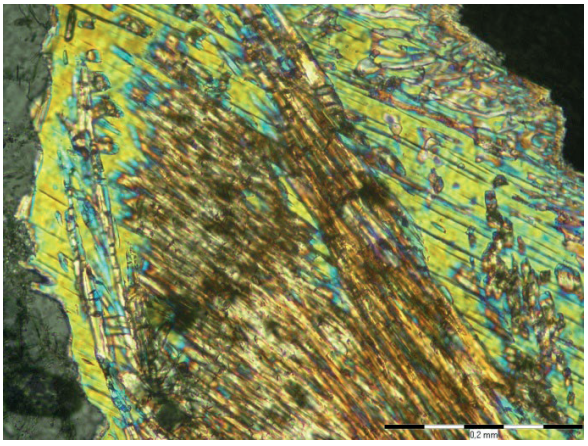

B

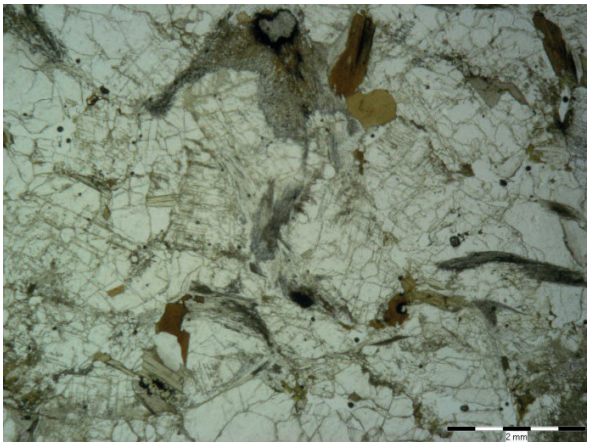

C

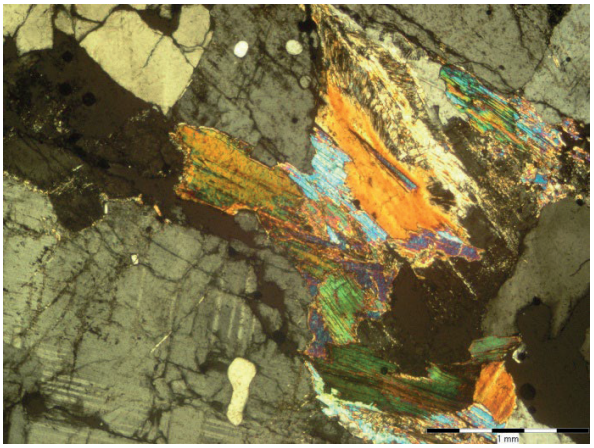

D

Fig. 33. Microphoto of the rock type in Fig. 32 – association Bt–Grt–Ms from the schlier, B – muscovitization of sillimanite, C – association quartz–plagioclase–Bt–Sill (gray tufty objects), D – replacement of Bt in association with sillimanite into the quartz-feldspar matrix by fan-shaped Ms. A, C = N//, B, D = N*X* (sample LHS-94 A).

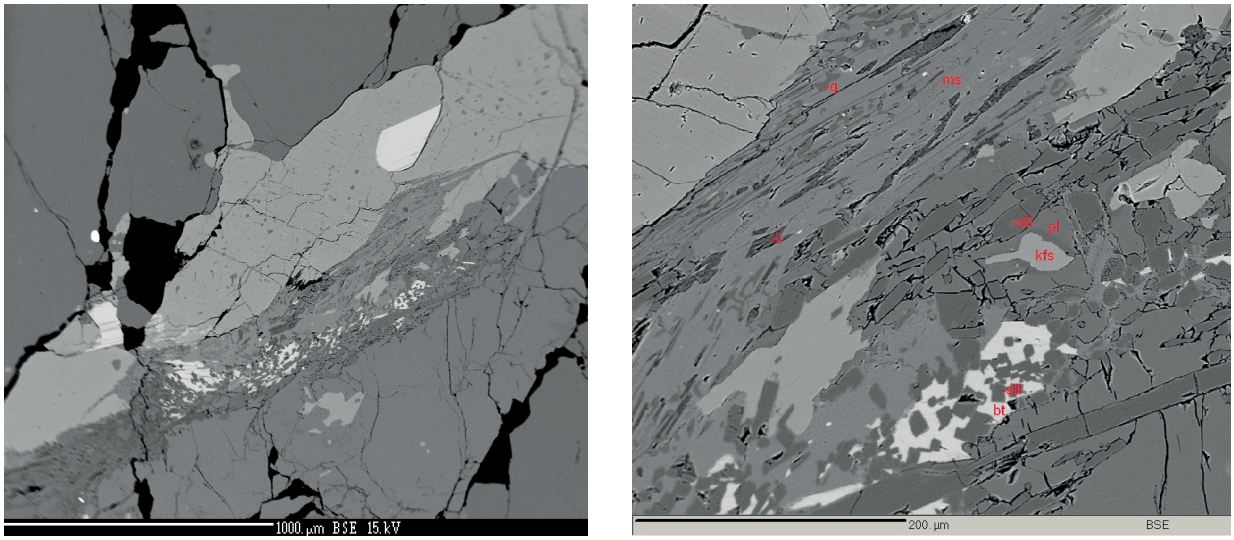

Fig 34. BSEI of biotite schlier (A – general view, B – detail). Kfs (light grey phase in Fig. B upper left) due to its morphology, it is a product of the melting reaction of biotite to form sillimanite + K-feldspar and garnet. The lightest phase represents a relict of decaying biotite with overgrown sillimanite, and the slightly grey phase is decaying muscovite with inclusions of euhedral sillimanite. The second stage, in subsolid conditions, is the replacement of the original association by muscovite, in which relics of sillimanite are still preserved (upper left under Kfs).

there are also varieties with omnidirectional Bt. The Bt dimensions sometimes exceed 1 cm. The different size and spatial characteristics of Bt indicate that only a small amount of the biotite crystallized from the magmas. They contain significantly fewer xenoliths of paragneisses as well as biotite schists compared to lithotype No. 110.

The structure is dominated by plagioclase (up to 7–8 mm in size), which is hypidiomorphic to xenomorphic, usually oriented in the direction of magmatic flow (or flow of crystal slurry), which is simultaneously parallel to the course of isolated schliers. Interstitial Kfs has a relatively small presence. Rarely, Grt is macroscopically observable together with Bt. Sillimanite was observable only in thin sections. Grt is moderately zonal with with a retrograde type of zonality from the center (Alm 74 – Pyr 12.3 – Spess 10.7 – Gross 3.0) towards the margin (Alm 73.1 – Pyr 8.5 – Spess. 15.2 – Gross 3.2). Biotite has a prevalence of Fe – Mg# = 0.38–0.40.

Leucocratic two-mica granites (107, 108)

This type of granite is dominantly developed in the central zone of the Suchý massif. These subvertical intrusions are associated with a process of shear deformation with a NE–SW direction. The importance of this deformation is manifested in the surrounding metasediments by opening of spaces for linear types of intrusions, in connection with their thermal effect. Shear deformation occurred continuously from the suprasolidus to the subsolidus stage, which is consistent with the scenario of decompression emplacement of granitoid intrusions.

Leucocratic syn-intrusive oriented two-mica granites (108)

Leucocratic two-mica granites are the most widespread petrographic type in the Suchý massif, building mainly its central part. They are spatially connected mainly with paragneisses (115), into which they intensively penetrate. However, they also form separate sttocks and linearly oriented strips, preferably trending NE–SW. From the point of view of the Variscan setting, they represent the upper part of a complex intrusive body, while the content of muscovite in the granitoids increases in the direction towards the overburden, i.e. to the NW. From the point of view of the genesis of pegmatites, it can be stated that only in these leucocratic granites can one observe gradual transitions from zonal bodies formed on the edge by aplite and in the central part by pegmatites with an albite fine-grained zone and the central part formed by blocky grey K-feldspar, quartz with occasional muscovite and biotite. Ms appears in the texture as primary, but also as later one, which is evidenced by the growth of Ms at the expense of sillimanite.

It follows from the above stated that the majority of pegmatites can be associated with leucogranites of this type, where in the contraction zones formed at a steep angle to the linear flow of leucogranite magma, cracks were formed in the high-temperature regime, being filled with pegmatite melt together with enrichment with a fluid component. The course of the pegmatite veins is dominantly N–S with variations the NNW or NNE direction.

A B

Fig. 35. Different types of planar oriented leucogranites: A – Planar oriented two-mica granite in the subsolid stage, with a pegmatite vein without deformation (sample LHS-626). B – Planar oriented two-mica granite up to developed the subsolid quartz bands (sample LHS-623).

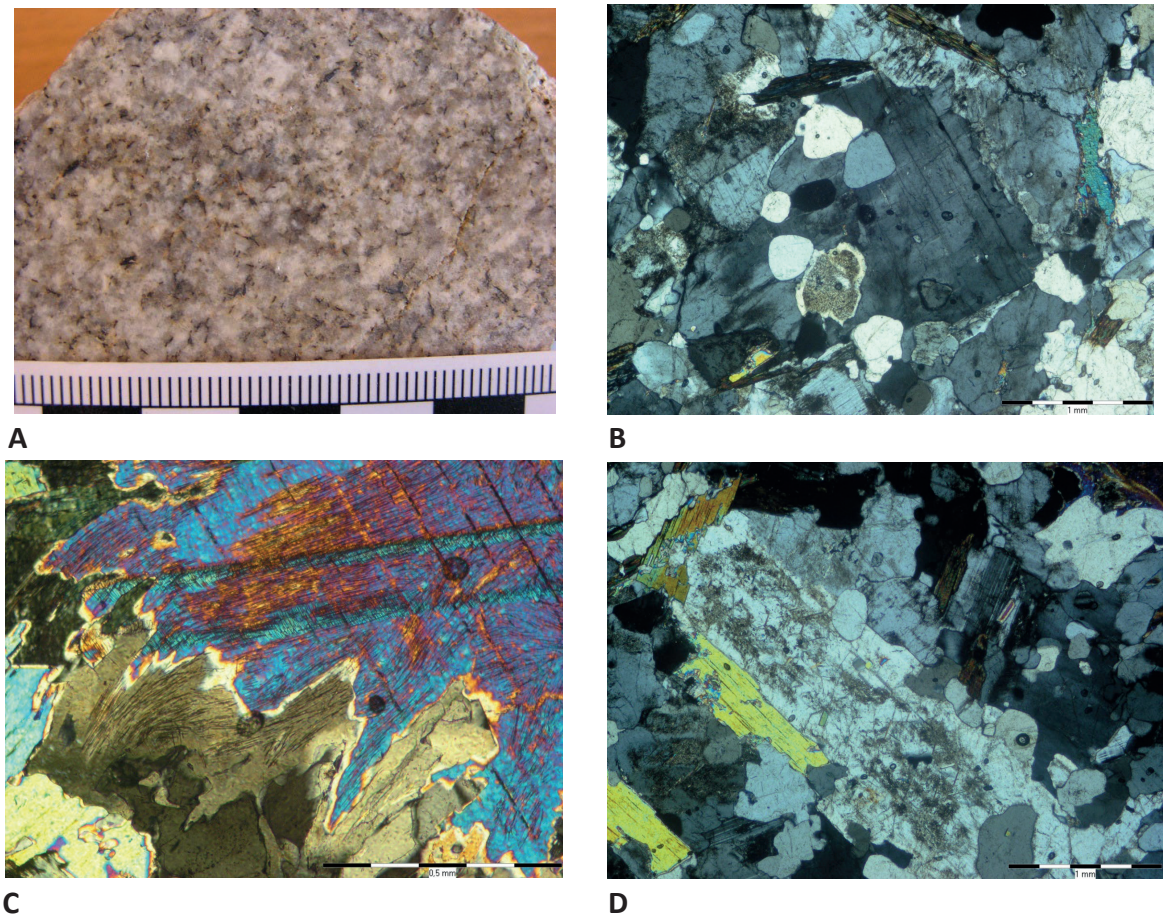

A B C D

Fig. 36. A stock of muscovite-biotite granite that intrudes into biotite paragneisses (about 100 m from the contact with them). The granites are fine- / coarse-grained leucocratic, sometimes containing Grt. Pegmatitoid granites with Grt are also common. Omnidirectional leucogranite with a predominance of Ms over Bt. It contains a microcline that poikilitically encloses oval Qtz and Pl I (up to 0.2 mm in size; Fig. B). Fibrolitic sillimanites are present, being replaced by large flakes of Ms. But there is also present longer prismatic Na-richer Pl, which has a Ms shell in the vicinity without fibrolite. Pl encloses the oval Qtz I, which, due to the high content of Si in the melt, crystallized among the first minerals. Pl is composed of albite to Na-oligoclase (X_{An} 3–16) and is only indistinctly zonal, Kfs contains 7.6–10.9 vol. % of albite molecule. Bt is slightly directional and is probably relict. Grt was not revealed in the thin section, tiny pink Grt is macroscopically is rarely present. The average grain size of the rock is 1–2 mm. A – texture of two-mica granite, where K-feldspar encloses Pl and Qtz of the 1st generation; B – An omnidirectional microcline closing Qtz I and Pl I; C – Fibrolitic sillimanite replaced by muscovite. D – Long-prismatic Pl, rimmed with Ms flakes, partially closing Otz I. *NX* (sample LHS-73).

The flow structure resulting from the magmatic flow direction is finally reflected from the early stages of crystallization up to the subsolid stage. It corresponds to the decompression stage of magma emplacement as well as the entire crystalline complex. The emplacement of these leucogranites took place partly even in the subsolid regime, while the foliated types of leucogranitoids were formed, which can be found in the footwall of injected gneiss complex (115) in the source area of the Krstenica stream (Liešťanská dolina valley). At the same time, the dynamic placement of leucogranites leads in the adjacent gneiss lithologies to the origin of preferred orientation, rotation of the former blasts of regional-metamorphic minerals (e.g. sillimanite, staurolite), the formation of larger lineated blasts of biotite of the second generation (Bt2).

The leucogranites are mostly medium-grained, with a small representation of Bt. Their texture varies from omnidirectional to that wich preferred orientation of newly formed minerals (lineated Bt) but also planar foliated. The structure is hypidiomophically granular. Rocks have a multi-stage crystallization history of rock-forming components.

Based on microprobe analyses, the plagioclase composition ranges from An_2 to An_{17}, K-feldspar – with max. content of albite component – 10 vol. %. Muscovite has content TiO_2 0.15–0.75, which points to the fact that it probably did not crystallize within the magmatic stage, but

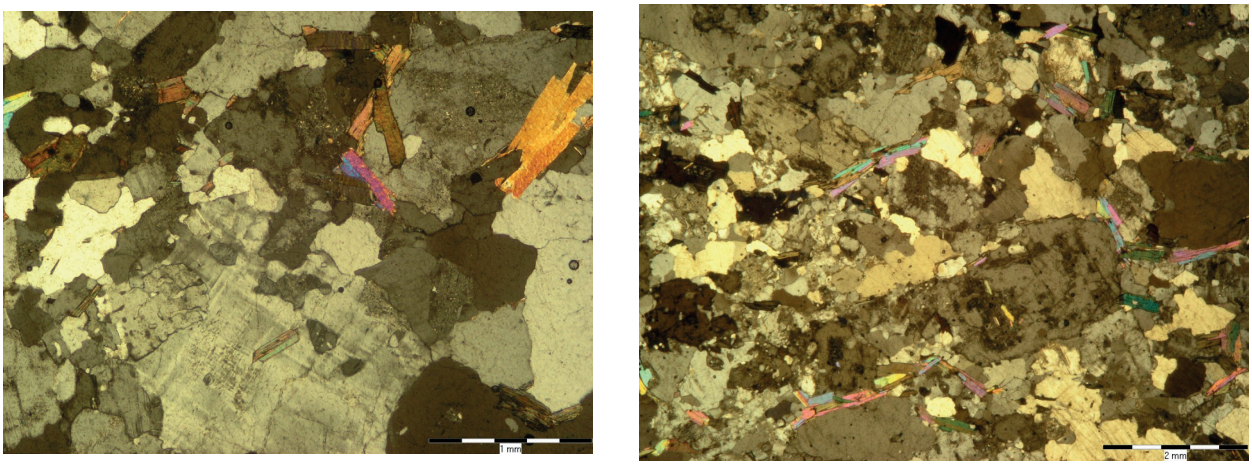

Fig. 37. Muscovite-biotitic (Ms : Bt ratio about 1 : 3) equigranular omnidirectional granite. Bt and Ms, as well as Pl ± Qtz are moderately oriented, while the small Qtz and Kfs are without preferred orientation – omnidirectional. The myrmekites are developed in places among Kfs and acidic Pl This indicates synintrusive deformation due to flow direction. The average grain size of the Qtz-feldspar material is 1–2 mm, the average size of flakes of Ms up to 0.5 mm and Bt up to 0.1x0.4 mm (sample LHS-200).

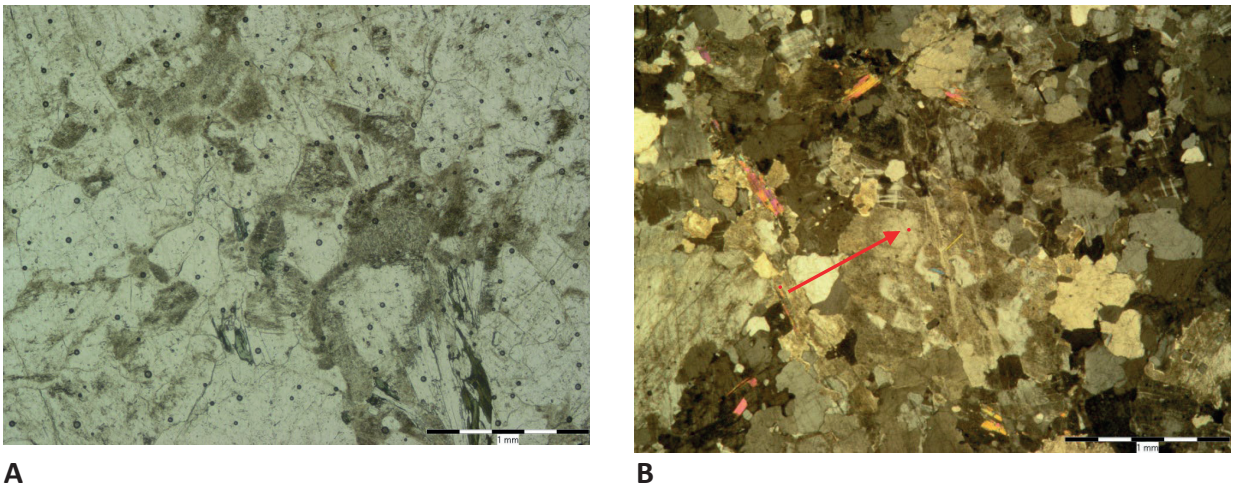

Fig. 38. Leucogranite. A – Sillimanite with Bt relicts is replaced by muscovite, N//. B – Manifestation of subsolid de formation in the solid state (zone in the middle of the image - red arrow), which is nearly parallel to the earlier crystallizing Pl (sample LHS-206).

is younger and partly formed at the expense of sillimanite and biotite. The rarely present garnet is rich in almandine component (Alm – 78, Pyr – 8.7–10.3, Spess – 9.2–11.5, Gross – 2.3–2.4). The Hg content of biotite is low – M # = 0.31–0.39, muscovite – 0.40–0.47. Content of TiO_2 in biotite varies from 2.2 to 3 wt. %.

Leucocratic omnidirectional to weakly oriented two-mica granites (107)

They occur together with the previous type of more syndeformation oriented granitoids. Similar to the previous type of leucogranites, the deformation is caused by the magmatic flow, concordantly with the shear deformation in the surrounding metamorphites.

Dating of monazite from two-mica granites indicates a relatively narrow intrusive age range of **352–351 Ma** (sample LHS-73, Plt 2-4; sample LHS-482B, Plt 3-1 and sample LHS-482A1, Plt 3-2), which can be considered as the age of maximum granite forming process (intrusive phase in the shear regime). At the same time, the mentioned granites are characterized by the rapid dynamics of crystallization of mineral components. If the initial phases (crystallization of mainly plagioclase and coexisting micas) are oriented in the magmatic flow, the final phases are already more or less omnidirectional. However, already rheologically solidified rocks are still further deformed with the origin of planar structures in places (Fig. 35).

The whole process is thus related with the ongoing deformation of the rock complex and at the same time the decompression of the entire set of metamorphic and igneous rocks (rapid ascent to higher levels of the crust). Residual melts of aplites and pegmatites, associated with this complex, are bound to ongoing deformation in the semiductile to brittle stage of magma solidification and are placed in extensional structures that arise at a large angle to the main component of tectonic stress.

Pegmatitic and aplitic veins (103)

Pegmatites and aplites are genetically related to the development of the shear system and intrusions of two-mica leucogranites. As a rule, they fill transversally oriented brittle structures, oriented at a large angle to the main stress component. In the Suchý massif, their course is usually oriented N–S (varying within NNE–NNW).

Pegmatites and aplites are genetically related, with aplites forming the external part of a complex pegmatite-aplite system. The marginal, aplite part is made up of fine-grained "sugary" aplite, whose mineral components, especially quartz and feldspar, are oriented omnidirectional, unlike it is in leucogranites. The macroscopic pink garnet that is often present in the aplite structure is striking, and can range from mm to several cm in size. Although the aplites crystallized together with the pegmatites as a final stage, some orientation caused by magmatic flow in a dynamic environment is evident from the occasional linear arrangement of garnet phenocrysts (Fig. 39D). Pegmatites are coarse-grained and formed from the edge by a less coarse-grained zone with a predominance of albite feldspar, while inside they are formed by blocky quartz and grey K-feldspar, which sometimes reaches several dm to m in size. As a rule, pegmatites contain little mica, but there are varieties with large-scale Ms and, in places, Bt, which is preferably bound to the marginal part of the pegmatite bodies. The relation to the metamorphic rocks and older granitoids is sharp, and the aplite and pegmatite bodies occur in the form of sharply bounded tabular bodies. The only exception is the relationship to two-mica leucogranites, where in some places indistinct transitions from leucogranite and aplite to pegmatite are observable. This fact points to the genetic relationship of these lithologies.

The abundance of aplite and pegmatite veins is highest in the central part of the territory SE, ENE of Suchý vrch hill, while it is mainly linked to leucogranites and the overlying paragneiss complex, which is in contact with leucogranites. Injections of leucogranites and pegmatites – aplites often alternate in the paragneiss complex (115). In the direction to the SE – into the underlying formations, the number of pegmatite and aplite veins decreases, and the same occurs in the direction to the NW and to marginal (upper) parts of the crystalline basement. Pegmatite and aplite bodies are not always complexly developed in the zonality described above. In places, only separate swarms of aplites are present, or only swarms of pegmatites.

Regarding the cartographic visualization in the published geological map (Hraško & Kováčik, eds., 2021; web link available), from the genetic point of view we do not differentiate between pegmatites and aplites. The course of the bodies in the geological map does not always correspond to the actual course of the veins, but represents the concentration of vein swarms in the given area.

According to the chemical dating of the monazite, as well as according to the geological position, these bodies represent younger magmatic stage of the shear emplacement of the granitoid magma – **345–343 Ma** (sample LHS-557, Plt 3-3; sample LHS-607, Plt 3-4).

Aplite garnets are almost non-zonal with high almandine content, in association with Fe-rich Bt with M/MF = 0.35–0.36.

Chemical dating of monazite from two selected aplite samples indicates consistently low ages in the given range of Lower Carboniferous ages. Age **345 ± 2.9 Ma** Ma up to **343 ± 2.9** can be reliably considered as the conclusion of magmatic processes associated with the shear emplacement of leucogranites and aplite-pegmatites.

A – Up to 3 cm thick transversal pegmatite veinlet with grey Kfs, forming tabular body with oblique orientation of ca 75° to course of lineation of biotite glomeroblasts biotitu in biotitic orthogneiss (sample LHS-415).

B – Wedging of the Ms pegmatite vein in Al-rich (metapelitic) paragneiss (Stau-Sill), at the time of intrusion the paragneiss was partially plastic (sample LHS-555).

C – Several cm large garnet in coarse-grained quartz-albite part of pegmatite (sample LHS.599).

D – Omnidirectional "sugar" aplite with small pink Grt on the edge of the Ms pegmatite (sample LHS-572).

E – Partially weathered pegmatite, where prominent blocks of grey K-feldspars are chaotically arranged in quartz-albite fine-grained mass. The texture is a result of subsolid (pneumatolytic?) fracturing (sample LHS-611).

Fig. 39. Typical present surface position of pegmatite and aplite bodies:

From the S-type highly orogenic granitoid stage to the I-type late-kinematic granitoids

A special type of I-type granitoids mainly builds up the NW edge of the crystalline area, to a limited extent in the Suchý massif, but especially the eastern area of the Magura part chemical basement. From the point of view of using dating of monazite, it was not possible to decide on the temporal relationship of the leucogranite and aplite-pegmatite intrusive stage (**350–345 Ma**) associated with the shear-deformation regime and the intrusion stage of I-type magmas. However, from the point of view of spatial relations, it is clear that I-type intrusions have a late kinematic character in relation to the shear deformation of the complexes.

Biotitic granodiorites — tonalites, omnidirectional, only locally weakly oriented (106)

Biotite granodiorites form several separate bodies of predominantly isometric shape, which points to their later age compared to the shear-deformation events of the Lower Mississipian. They mainly penetrate these structures. Smaller bodies emerge on the E-oriented slope of the Suchý massif, W from Nitrica, and the larger body emerges in the area of Čavoj locality.

Granodiorites are conspicuous by their omnidirectional structure, fresh appearance and the lack, or the complete absence of pegmatite veins. This fact also points to their younger and deeper magnatic portion in the Variscan geological structure of the crystalline basement. In some places, several more mafic "globules" of omnidirectional granodiorites to tonalites can be observed, which interpenetrate each other in the form of loaf-like bodies of different grain sizes (Fig. 41). This indicates a good viscosity and a higher temperature of the magma.

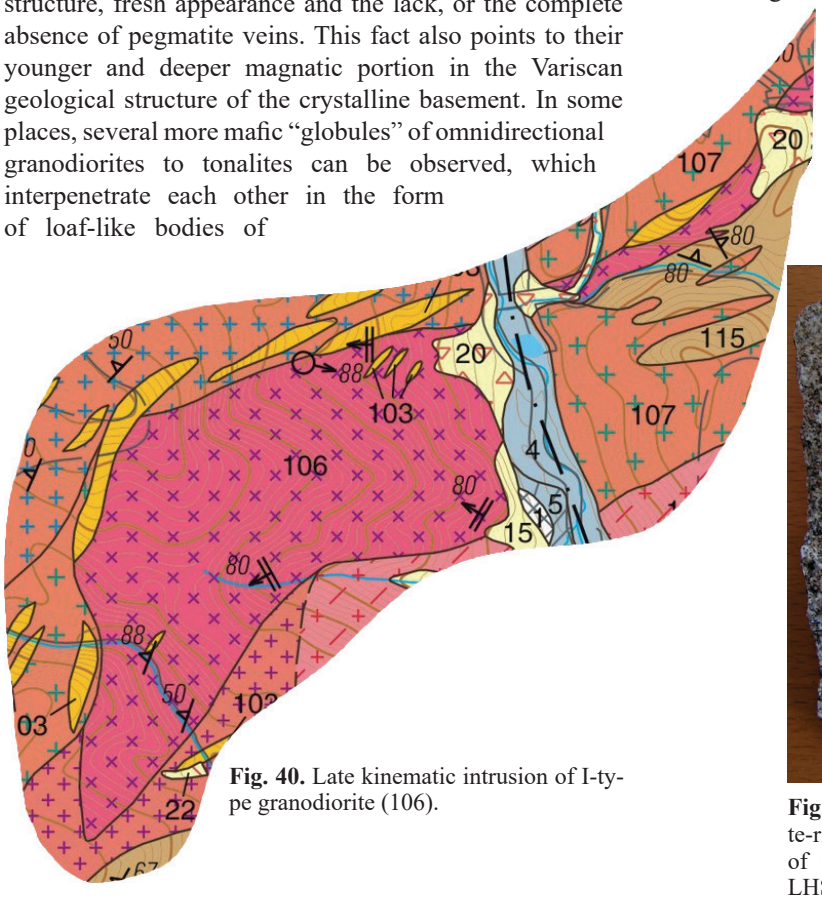

Fig. 40. Late kinematic intrusion of I-type granodiorite (106).

Fig. 41. Biotitic granodiorites – tonalites – mixing of two types – block of more mafic part rich in plagioclase and the biotite rich part (above hammer) in more quartzy coarser-grained rock.

From a petrographic point of view, rocks represent biotitic granodiorites to tonalites. The Pl (up to about 50 %) rich granodiorite, which is also rich in Bt (up to 20 %), while in some places it may represent portions of mafic magma in a lighter type (Fig. 41). Pl usually 1 mm (rarely 2 mm) large are idiomorphic to hypidiomorphic, the intergranular spaces are filled mainly with Bt and Qtz.

Hypidiomorphic plagioclase is zonal, oriented in all directions, without inclusions, only in the final phase it crystallized together with quartz. Biotite with a

Fig. 42. Fine-grained omnidirectional, grey biotite-rich microgranodiorite-microtonalite, as one part of the biotite granodiorite-tonalite body (sample LHS-122 – Krstenica valley).

content of 15 to 20 vol. % is reddish-brown in colour and appears usually along the edge of plagioclase, from the point of view of succession it is later than Pl. As a rule, quartz and quartz are interstitial and crystallized last in the succession. Of the accessory minerals, apatite (Ap) and also monazite (Mnz) are commonly present, which were chemically dated here. Magnetite is also present, which indicates a higher activity of water in the magma, as it points to an oxidation regime in the magma, which was a consequence of the dissociation of water vapor in the magmatic reservoir.

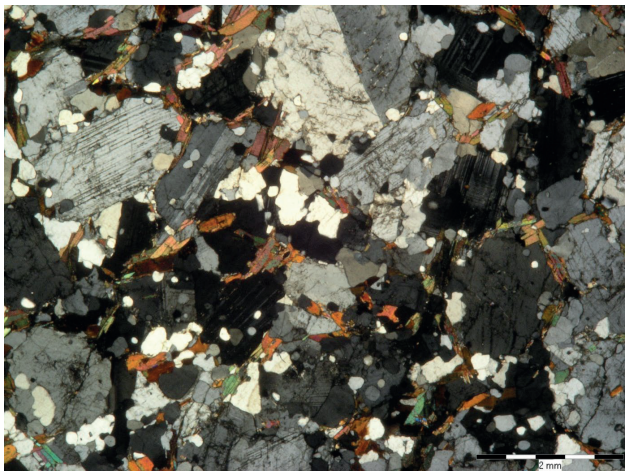

Fig. 43. Granite sample LHS-94B. Hypidomorphic plagioclases are zonal, crystallizing first in crystallization succession. Only rarely in their final phase of crystallization the interstitial K-feldspar crystallized. N*X*.

Mineralogy: Plagioclase, K-feldspar, biotite and rare muscovite were measured in the granite in association with Bt. The composition of plagioclase measured by microprobe analyser is An26 to An36. The content of the albite component in K-feldspar reaches 10 vol. %. the BaO content is around 2.5 wt. %. The magnesium content of biotite (Mg#) varies in a narrow range of 0.51–0.52 and the TiO_2 content – 3.4–3.65 wt. %. The Mg content of Ms is around 0.57.

Chemical dating of monazite (Mnz) from a sample of omnidirectional granodiorite (sample LHS-94B, Plt 4-1) provided an age of **355 ± 5.5 Ma**, while the statistical distribution of the set points to one, homogeneous population of monazite.

Coarse-grained amphibole diorite (125a)

Such coarse-grained, to medium-grained omnidirectional, to weakly oriented amphibole-plagioclase rock was found in the environment of the previous type of omnidirectional granodiorites-tonalites of the I-type (sample only in scree).

The amphiboles correspond to the composition of magnesiohornblende, the plagioclase that fills the spaces between the amphiboles is of andesine composition. The association of ilmenite and titanomagnetite and then rutile and titanite is common, which indicates the oxidation regime in the magma and sulphide minerals (pyrite, chalcopyrite?) are present. The stated oxidation conditions correspond to the conditions of magmatic crystallization of the intermediate magma. Therefore, we consider this lithology to be a part of the previous type of granodiorites to tonalites with features close to I-type granitoids, with higher temperature and water-rich magma.

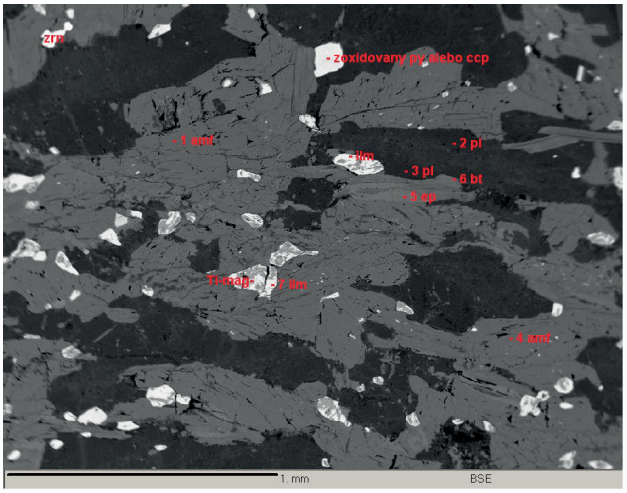

Fig. 44. BSEI of sample SZN-304 consisting of phenocrysts of magnesiohornblende and interstitial andesine. Former ilmenite is replaced by rutile and titanite aggregate due to postmagmatic oxidation.

Discussion and Conclusion

Character of pre-granite lithotectonic units present in crystalline basement of the Suchý massif

Pre-Alpine crystalline basement is built of variegated Paleozoic rock sequences regarding their position and depth in sedimentary basin, where they originated before they were amalgamated by Variscan tectonometamorphism process:

- Paleozoic deep water euxinic facies, formed originally mainly by fine-grained pelitic and quartzitic sedimentary facies rich in organic matter, with preserved fragments of accompanying oceanic basic volcanites. At field research these associations are relatively well detectable;
- Proximal sedimentary facies of continental slope of Paleozoic sedimentary basin, represented mainly by flyschoid sandy-greywacke sediments. They they contain almost no bodies of basic rocks and pelitic lithologies are very rare;

– The upper part of present Variscan setting is built of orthogneiss complex (less in W part of Magura massif and more extensive in the Suchý massif). In Variscan collision the orthogneiss complex as crustal granitoid segment was thrust on two above described rock sequences and later metamorphosed together with them.

Relations of metamorphic complexes and granitoid intrusions

Due to the Alpine tectonic rotation of the blocks of crystalline basement and cover Mesozoic sequences, the Suchý massif provides a more comprehensive profile through the basement, indicating an increase of regional overprint from NW to SE. The highest degree of ductile deformation reworking is present in stromatitic migmatites, which typically crop out in the valley of the Krstenica stream (NW from Liešťany municipality), up to the area of Rudnianska Lehota. Biotite dehydration melting processes were also observed here. At the same time, intense granitization processes are present in this SE part, which are getting weaker towards the W–NW. For this reason, there were analysed the p-T metamorphic conditions from the W part of the crystalline basement, with minimal presence of granitization processes. On the other hand, to determine the pressure-temperature conditions due to the influence of intruding granitoids, samples were selected from the area of intense manifestations of granitizing activity.

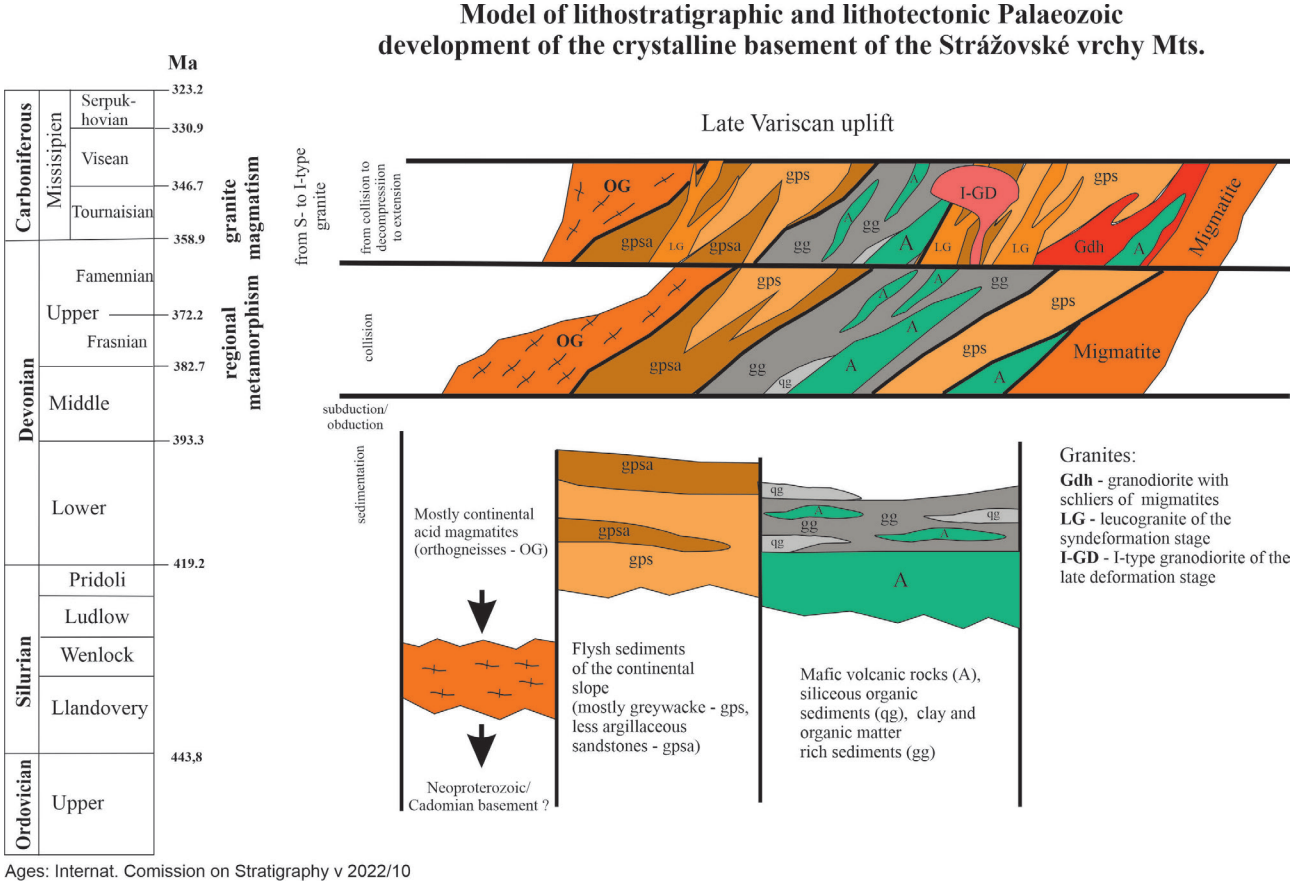

Fig. 45. Lithostratigraphic and lithotectonic column with indicated position of protolith in sedimentary basins of various crustal provenience, their following amalgamation at collision, metamorphic overprint and syn-kinematic up to late-kinematic granite forming phase. Subsequent post-kinematic unroofing relates with orogic collapse and ascent of crystalline basement to higher crustal levels (used ages are from actual International chronostratigraphic chart). OG – granitoid orthogneisses, gpe – sediments with predominance of pelitic component, gps – sediments with predominance of psammitic component, A – amphibolites-metabasalts, U – utramafites, qg – quartzy sediments with organic matter (black metaquartzites), C – metamorphosed carbonates, sM – stromatitic migmatites, GDh – hybridic granodiorites, lG – leucogranites, GD – biotitic omnidirectional granodiorites, P – pegmatites.

Regional metamorphic conditions correspond to temperatures of about 570–620 °C at pressures of about 6–8 kbar. Conversely, mineral associations of younger, contrasting thermal metamorphism correspond to approximately temperatures of 550–600 °C and pressure of 3–4 kbar (p-T calculations of metamorphic events were carried out by R. Demko, ŠGÚDŠ, Slovakia).

These different p-T conditions indicate a rapid uplift of the complex at the simultaneous intrusion of leucocratic granites in a shear regime. Due to the consistent directional relationship of deformation structures in leucocratic granitoids and surrounding metamorphites (concordant lineations of biotite schliers in leucogranites and thermally induced flakes of biotite II in the surrounding metamorphites), it is obvious that the leucocratic granites were emplaced simultaneously with the deformation of the metamorphites.

At the same time, it is obvious that the emplacement of leucocratic granites also took place in the subsolid stage, which is manifested in field conditions by the plate disintegration of leucogranites and deformation microstructures. In the subsolid stage, pegmatite bodies were also placed in the same deformation regime. Their composition (lack of water-bearing minerals) as well as textures indicate open structures and leakage of fluids into the higher parts of the metamorphic packet.

The temperature of regional metamorphism in the western part of the territory (the Suchý massif) did not generally reach the temperature of partial melting, but the granitization manifestations were mainly caused by the combination of the heat supply of granitoid masses in the peak stage of the syncollision event with simultaneous deformation. In the eastern part of the Strážovské vrchy Mts (Magura massif) crystalline basement, the processes of migmatitization were more distinct, because this part represented a deeper structural segment.

Tab. 1

Determination of petrogenetic parameters according White et al. (2014) and applying garnet-biotite-plagioclase-quartz thermobarometry (GBPG) after Wu, Chun-Ming et al. (2004)

Sample	Temperature (°C)	Pressure (kbar)	Comment
M2 granite induced thermal overprint			
LHS-204	593 ± 10	2.9 ± 0.2	thermal decomposition of muscovite to Kfs
LHS-356a	571 ± 13	3.4 ± 0.3	Bt, Ms, St, Grt (inclusion in St), Pl, Qtz
LHS-356b	578 ± 4	3.4 ± 0.1	
SZN-34a	580 ± 9	3.6 ± 0.3	Grt as inclusion in St, Sill and Kfs (product of high thermal decomposition)
LHS-329	561 ± 14	3.7 ± 0.7	cellular, poikilitic garnet, towards rim
LHS-255	585 ± 6	4.0 ± 0.2	enormous thermal blastesis o small Grt crystals
SZN-34c	591 ± 8	4.2 ± 0.2	
M 1 regional metamorphism preceeding granitic intrusions			
LHS-350	561	5.4	
LHS-329	581 ± 5	5.6 ± 0.5 ?	cellular, poikilitic garnet, central part
SZN-34b	582 ± 2	6.7 ± 0.1 ?	
SZN-66	608 ± 15	7.5 ± 0.8 ?	garnet I, in the centre of garnet II
LHS-350	569	8.5	

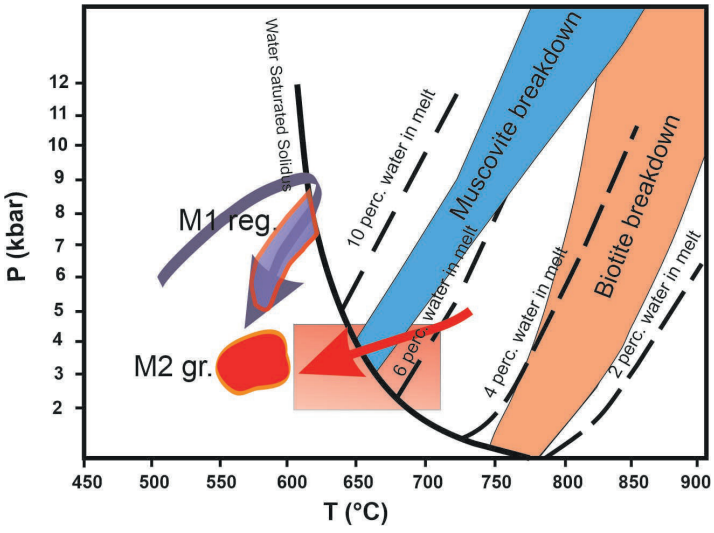

Fig. 46. Presentation of conditions of Variscan regional metamorphism (M1 reg.) in the upper part of the metamorphic pile (blue arrow). Melting reactions must have taken place mainly with the participation of muscovite melting. However, the speed of the process was not sufficient for more extensive melting and segregation of granitic magma. Granitic magma was generated from deeper parts under the influence of new thermal input (red arrow) and caused (M2 gr.) thermal metamorphism in higher crustal levels. The pink rectangle shows the near solid placement of the leucocratic magmas. (field of water-saturated granitic solid, mica melting fields and amounts of water provided during melting processes in metasediments according to Vielzeuf & Montel, 1994).

Deformation and magmatic structures in granitoids and surrounding metamorphites

The oldest Variscan structures are observable only in a microscale as oriented blasts of quartz within younger and larger blasts, especially staurolite. This oldest foliation is designated as sV1. The blastesis of staurolite originated in metapelitic assemblages at the peak stage of orogenic (regional) metamorphism, before the beginning of a younger deformation event, which caused the origin of the most prominent metamorphic foliation sV2 connected with shear deformation, thermal metamorphism under lower pressure conditions, being a reflection of granitoid intrusion in the shear-deformation event.

This younger deformation (sV2), which led to the rotation of older blasts together with their inclusions, is macroscopically and microscopically the best structurally defined phenomenon. It led to the formation of steeply (up to subvertically) built structures of metamorphic schist, which were used in parallel syntectonic leucogranite intrusions in extensional regime of unroofing kinematics (VD2) in the time range of **355–345 Ma**. It is supposed that primary foliation was not so steep and their present spatial position was completed by Alpine (Cenozoic) AnD3 shearing. Dominant structural elements represent metamorphic foliations generally trending NE–SW (with variability in the NNE–SSW to ENE–WSW trend; Fig. 47) with rarely identified fold axes of the same direction and mineral lineations of metamorphic minerals with a shallow orientation on foliation surfaces (Fig. 48). From this, it is possible to infer the shear origin of the fold structures, or to the maximum component of the deformation stress, close to the direction of the fold axes. Based on the dating of monazites in paragneites and orthogneites, it can be

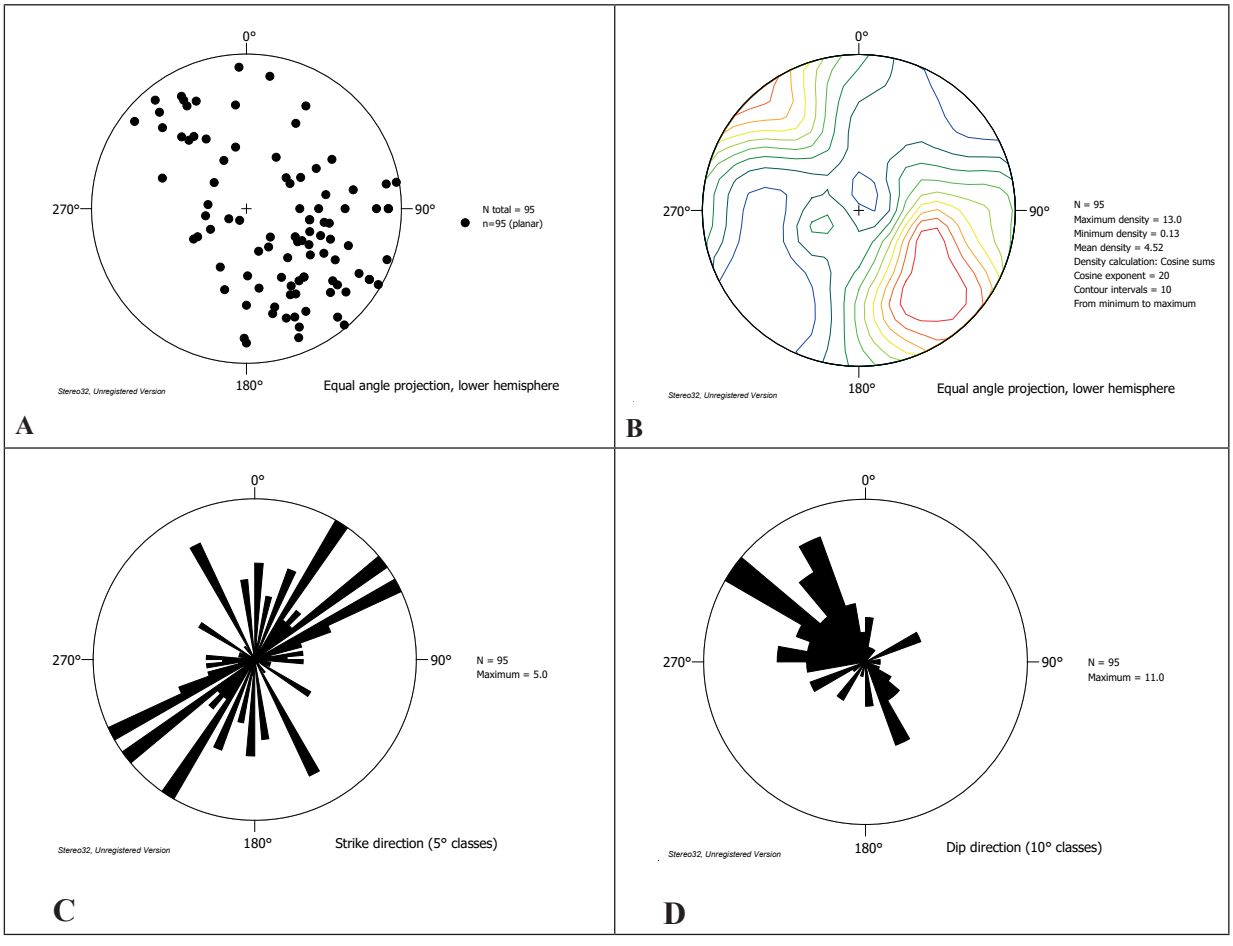

Fig. 47. Courses of metamorphic foliation in paragneisses (prevailingly the Suchý massif – 96 measurements): A – poles of planes, B – contourogram of the poles of the planes, C – prevailing trends of planes, D – dips of planes in paragneisses. Dominating foliations have NE–SW trend with steep dip to NW.

concluded that the maximum metamorphic overprint of rock complexes was around **380 Ma**, which corresponds to the Middle to Upper Devonian boundary and process over the subduction zone (**VD1s**).

Shear deformation in the ductile conditions of the amphibolite facies led, depending on the position of the rock complex in the continental crust, to the tectonic separtion of leucogranite melt located in fold closures of migmatized pararules (Figs. 16 and 17), through the boudinage of leucograne bodies situated in fold limbs still in supersolid to subsolid state up to the placement of thin leucogranite interbeds in semiductile flexures (Fig. 16). This indicates the decompresion of the whole complex and gradual change of rheological conditions from ductile, to semiductile up to brittle conditions. Orogenic metamorphism, leading maximally to first manifestations of local melting of metamorphic complexes, it was followed by decompression and intrusion of thicker leucogranite volumes in shear regime. Granitoid melts were placed to higher crustal levels in ductile state, which is indicated by structures of magmatic flow, defined by position of dark minerals, but also feldspars. In more extreme cases podmienkach along the contact of leucogranite intrusionns with metamorhic mantle there occurred also synintrusive deformations of leucogranite, being nanifested by origin of higher temperature foliation in conditions close to solidus, but also in subsolidus stage (this phenomenon was observed mainly NE of the Suchý vrch peak). These tectonites were distinguished also in geological map as syntectonic leucogranites with preferred orientation.

The structural analysis indicates that only part of inhomogeneíties in granitoids can be derived from relic "pre-granitoid" setting of metamorphites and bigger part corresponds to own dynamics of magmatic flow of leucogranites, which is moderately counter-clockwise rotated with respect to older metamorphic foliation (Figs. 48 and 49).

Regional metamorphic structures (**VD1s, VD1c**) were overprinted by the heat of intruding granite masses (**VD2, MV2**). This overprint produced large macroscopically decipherable biotite II porphyroblasts (Bt of 2nd generation), though also these crystallized with preferred orientation due to acting stress field. Thermal effect of close leucogranite intrusions manifests in microscale by the origin of red-brown biotite and formation of numerous small garnets.

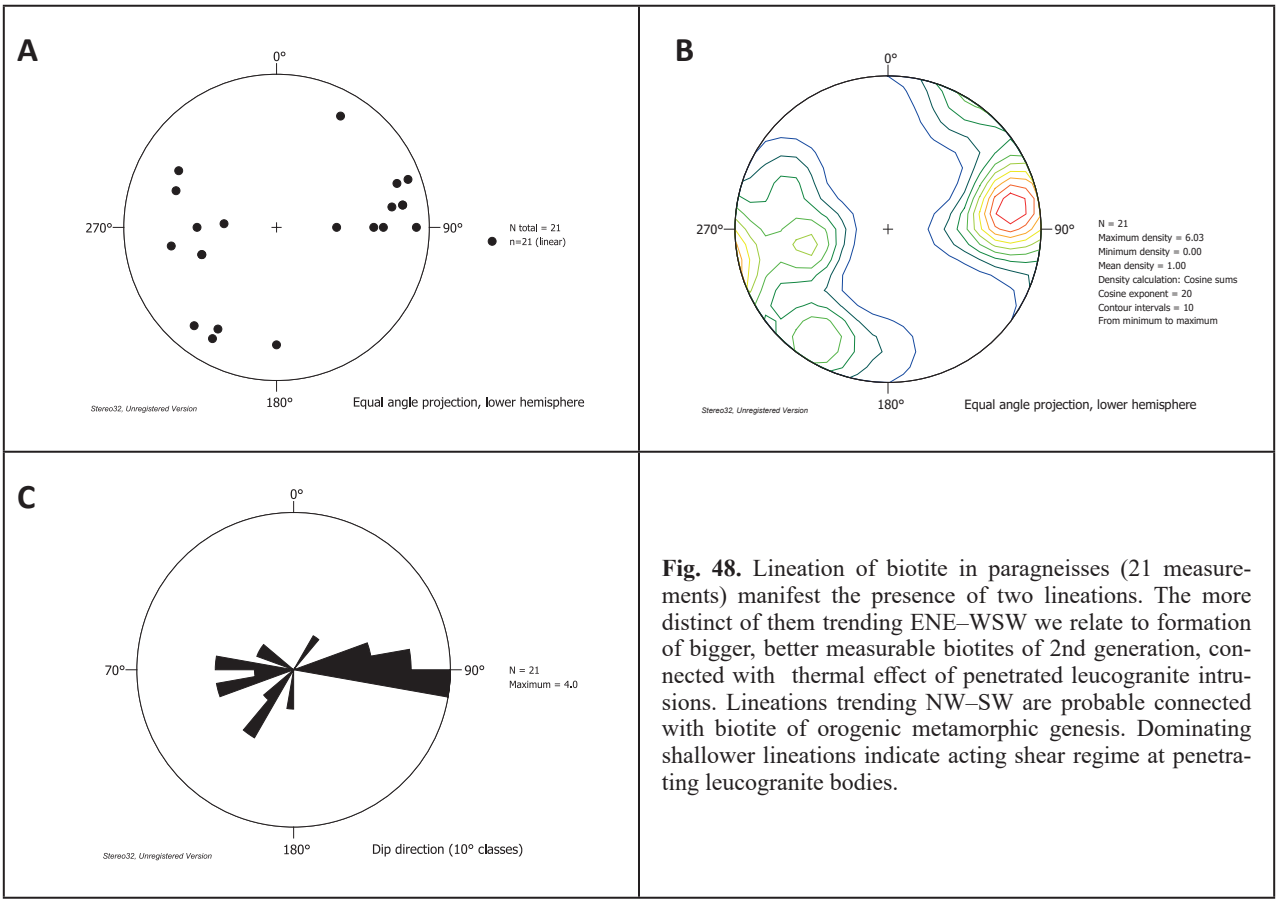

Fig. 48. Lineation of biotite in paragneisses (21 measurements) manifest the presence of two lineations. The more distinct of them trending ENE–WSW we relate to formation of bigger, better measurable biotites of 2nd generation, connected with thermal effect of penetrated leucogranite intrusions. Lineations trending NW–SW are probable connected with biotite of orogenic metamorphic genesis. Dominating shallower lineations indicate acting shear regime at penetrating leucogranite bodies.

Chemical dating of monazite revealed the age **355–345 Ma** of maximum intrusive activity and calculation of its PT conditions indicates pressure 3-4 kbar (for the stage of syntektonic S-type leucogranites **352–351 Ma**).

The shear emplacement of S-type leucogranite intrusions under decompression regime conditions (**VD2**) was followed with later opening of deeper crustal structures used by the intrusion of I-type omnidirectional biotitic granodiorites. They contain fine-grained mafic globules (currently not examined further; Fig. 41), corresponding with mafic portions of the magma, as well as rare rocks of (gabro-)dioritic composition. This type of intrusion has a linear course (**VD4?**) and crops out oblique to older structures in NE part of Suchý massif. By this way the transition from S-type granite intrusions of exclusively crustal origin to more mafic intrusions of I-type reflects **the increase of thermality of granite melt towards the end of granite magmatism**. It indicates the deeper crustal, resp. subcrustal genesis of later magmatic melts. Such time succession, where the I-type granitoid intrusions in short time sequence followed after S-type granices was demonstrated in granitoids of the Malé Karpaty Mts (Kohút et al., 2009).

In our work we used U-Th-Pb chemical dating of monazite, applying methodology by Konečný et al. (2018), whiích after statistic processing of its results can provide results close to zircon dating. It is valie especially at rapidly cooling magmatic systems without additional influence of the Mnz crystals by the fluid regime. With respect to proved Variscan decompression in the crystalline basement of the Suchý massif it is probable that Mnz dating provided data close to real intruiíve age of granites. It is valit mainly for leucogranites, connected with the phase of their rapid shear emplacement (**352–351 Ma**) and formation of pegmatite veins, finishing magmatic regime (**343–345 Ma**; Tournaisian / Visean boundary).

At I-type granodiorites, which finish magmatic process from geological and structural viewpoint, this age is probable influenced by the presence of older monazites, reflecting the mixed origin of the monazite crystals.

The group of S-type granitoids, indicating the contamination with surrounding paragneisses, the mixed

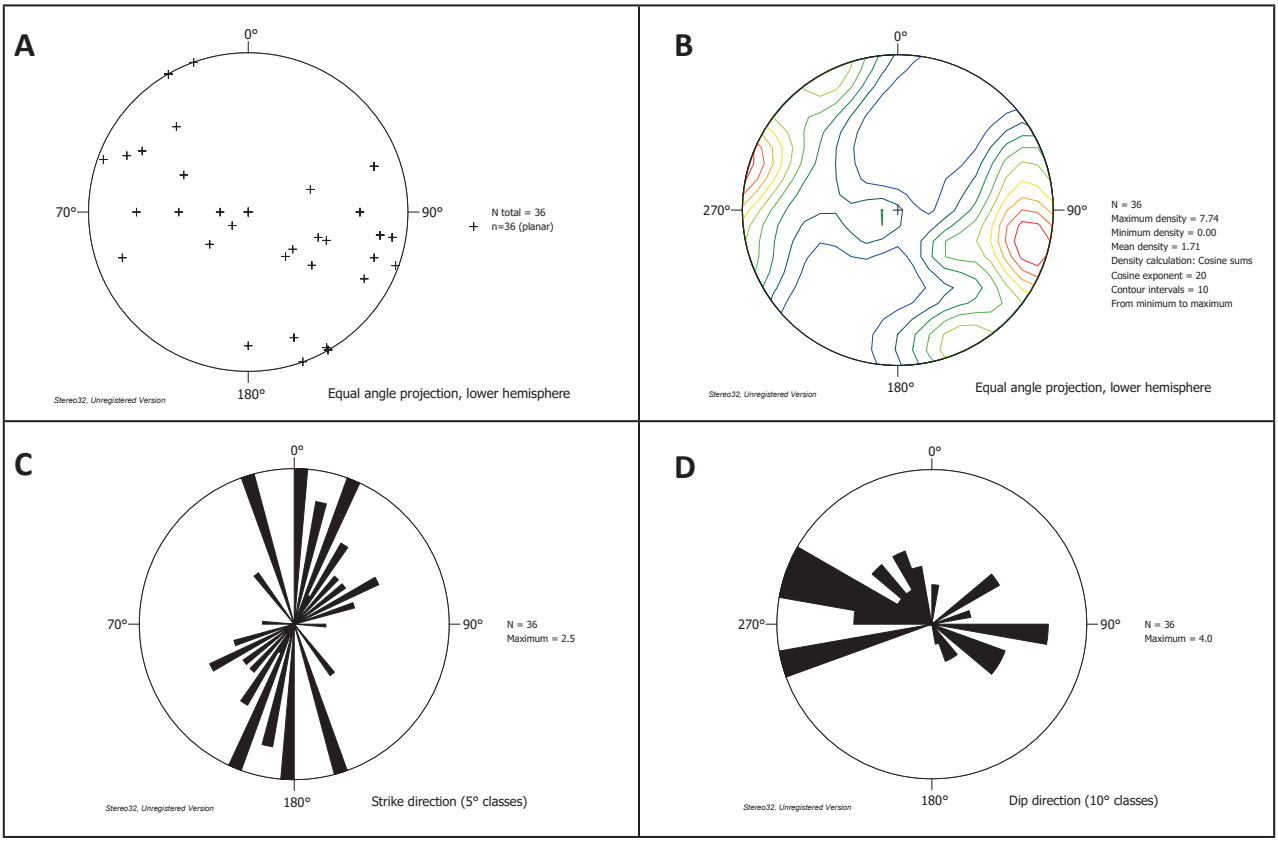

Fig. 49. Foliations (schliers – planar orientation of biotite, eventually feldspars) in granitoids (36 measurements): A – poles of planes, B – contourogram of the poles of planes, C – prevailing trends of planes, D – dips of inhomogeneíties in granitoids. The contour diagram of planes poles (B) shows two distinct maxima, more often corresponding to planes trending NNE–SSW with steep dip to WNW, resp. ESE. Second, less distinct maximum corresponds to planes trending ENE–WSW with steep dip to SSE resp. NNW. While second, less distinct maximum probable represents relict structures connected with metamorphic rim of intrusion, first – very distinct maximum reflects the penetration dynamics of leucogranite magma.

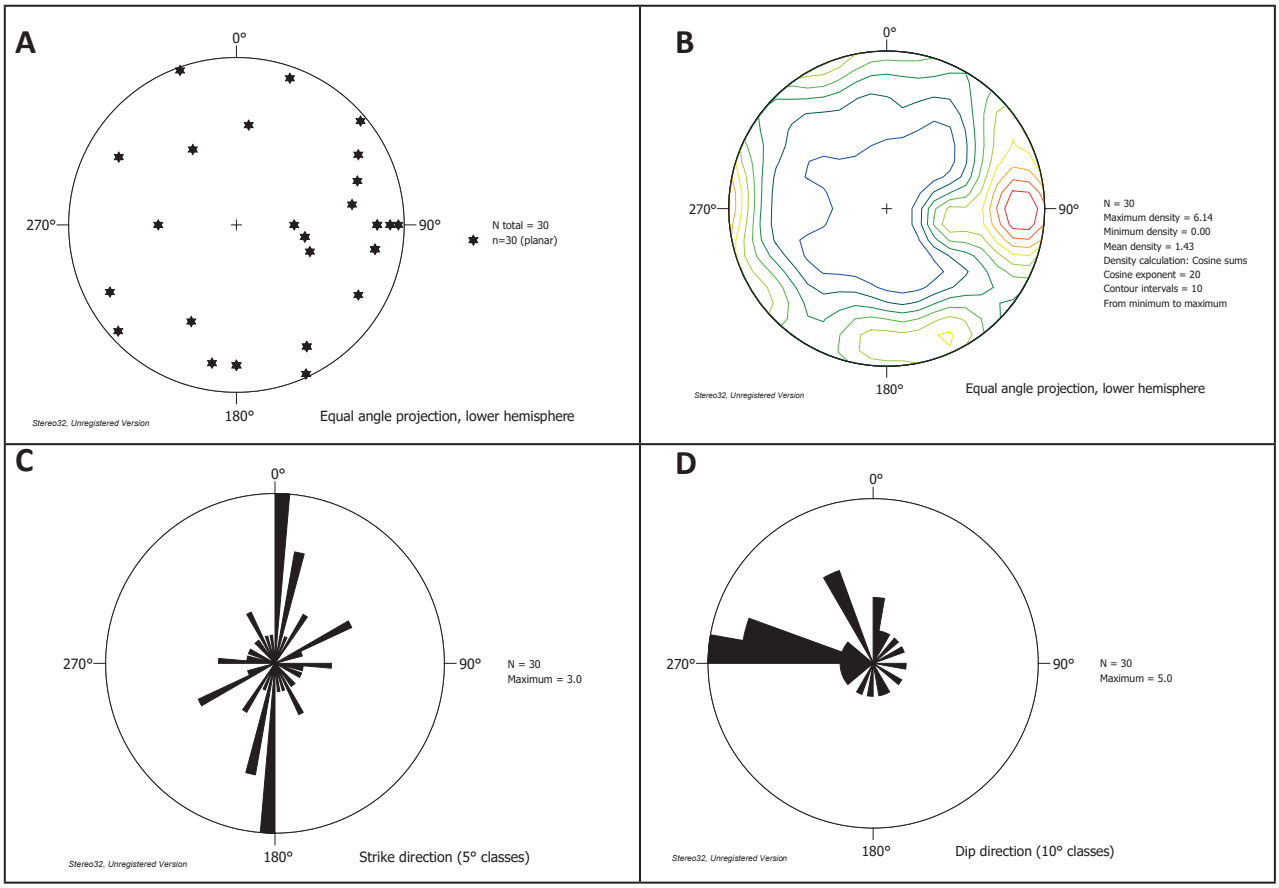

Fig. 50. Prevailing courses of planar structures, filled with pegmatite and aplite-pegmatite melt (30 measurements), representing the last stage of leucogranite intrusions. They have prevailing N–S course with steep dip to W, less NE–SW and E–W. Relatively steep disjunctive structures formed in the final extension phase of the generating of granitoids. A – poles of planes, B – contourogram of the poles of the planes, C – prevailing trends of planes, D – dips of pegmatite and aplite veins.

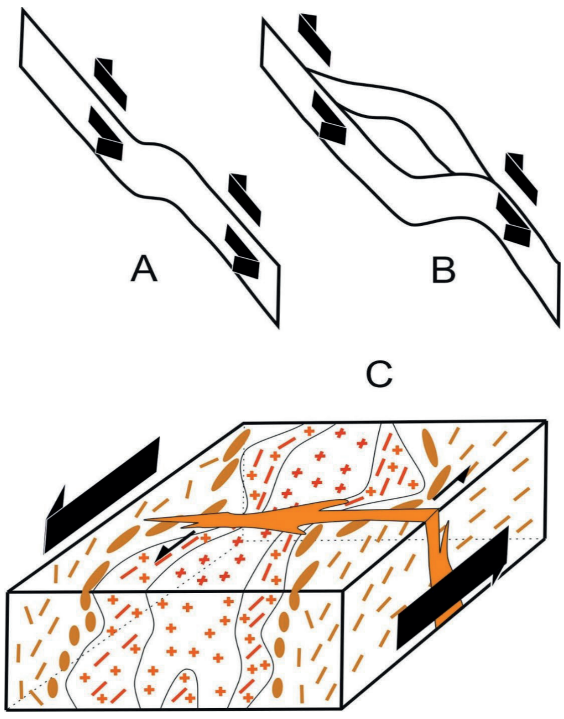

Fig. 51. Diagram of the opening of space for leucogranite intrusions. A – the beginning of the shear regime with the deformation of the metamorphic complex; B – diagram of space opening in a more advanced stage of the shear deformation; C – block diagram of syn-deformation leucogranite intrusions (omnidirectional up to indistinct preferential orientation of minerals – red crosses; and syn-intrusively oriented marginal parts of intrusions – red crosses and dashes). Formation of thermally induced biotite II (brown ellipses). Thermally (granite thermal effects) slightly, or no affected complex of paragneiss. Transversely steep structures filled with aplites and zonal pegmatites, formed from leucogranite magma (orange). Black arrows show the sense of tectonic shear transport.

origin of monazites, reflects the age of intrusion as well as the age of formation of older monazites, analogical with those in paragneisses (which probable reflect the age of orogenic (regional) metamorfic process and in smaller scale also the age of protolith).

SHRIMP dating of zircon of S-type two-mica granite from Magura part of the Strážovské vrchy Mts (Kohút & Larionov, 2021) has shown two age modal groups of zircons (sample MM-29), older, with Neoproterozoic (Cadomian) age **568–551 Ma** and younger **365–361 Ma** (Devonian / Lower Mississipian) with Concordia age **360,9 ± 2,7 Ma**.

Older assumptions and measurements, indicating that I-types granitoids are significantly younger (**310–303 Ma**; Bibikova et al., 1990; Broska et al., 1990) than S-types, in the W. Carpathians were not confirmed by subsequent zircon dating. The LA-ICP-MS zircon dating from Kriváňska Malá Fatra (Broska & Svojtka, 2020) indicated only a small age difference among zircons from S-type granites (**342 ± 3 Ma**) and zircons from I-type granitoids (cores with magmatic age of **353 ± 3 Ma** and rims **342 ± 3 Ma** – this age was probably influenced by fluid regime?), so the I-type granitoids should be slightly older.

On the contrary, the SHRIMP zircon dating (Kohút et al., 2009) in S-type granites of the Bratislava massif (**355 ± 5 Ma**) and I-type tonalites of the Modra massif (**347 ± 4 Ma**) in Malé Karpaty Mts pointed out a small age difference between two large groups of granitoids of W. Carpatians, however, I-type granitoids appear younger. Just like in the Malé Karpaty Mts (Kohút et al., 2009), also in Strážovské vrchy Mts, it is confirmed that S-types and I-types of granitoids were produced in the same collision event, but they represent different stages of decompression – shearing regime (S-types) until the opening of the space in the final, extensional phase of the orogenic cycle, which was associated with the output of higher thermal, deeper-based magmas of I-type, with manifestations of hybridism, with accompanying diorite magmas of small volumes.

According to the chemical dating of the monazite in the Strážovské vrchy, the age of I-type granites intrusion is older than the age of the monazite of the S-type granites associated with the shear-deformation regime. Geological relationships, however, indicate the opposite. I-type intrusives penetrate mainly in the E-W direction (ENE–WSW; i.e. at a small angle) through older deformation structures, which are associated with the emplacement of S-type granites in the NE-SW direction in a shear regime. Thus, I-type granodiorites can be considered late- to post-tectonic in relation to shear deformation associated with syntectonic intrusions of leucogranites.

Therefore, we assume that the intrusions of I-type granodiorites-tonalites and rarely diorites should be close in age to the formation of pegmatites, or follow them (within the Tournaisian / Visean interface). For this reason, it is necessary to carry out a geochronological investigation of zircon in I-type granitoids from this area.

The interpretation of the late emplacement of I-type granodiorites and small diorite bodies in the Strážovské vrchy is in agreement with the statement by Kohút & Larionov (2021): "The peak at ca 342–340 Ma, representing probably the main period of the collisional granites production / emplacement, was in part accompanied by intrusions of dioritic syn-plutonic dykes."

We determined the age of the change in deformation conditions in metamorphic complexes from ductile to semi-ductile and brittle conditions, based on monazite dating to approximately 345 Ma, which is the typical age of emplacement of aplite and pegmatite veins in brittle structures. Aplite and pegmatite veins are steeply dipping (mainly N–S dip) and their trend is generally oriented at a large angle to the main shear stress component (dominantly E–W direction), as was found in the eastern part of the Suchý massif. The mechanism of emplacement of granites in shear zones during the extensional regime has received more attention since the 1990s (Hutton et al., 1990). It is a mechanism when thickened continental crust is decompressed with the simultaneous ascent of granites in shear zones parallel to the axis of the orogen (orogen-parallel extension). Such placement mechanism is known e.g. in Caledonides (Braathen et al., 2000), Variscides (Oberc-Dziedic et al., 2015), or in "younger" ranges, e.g. from Greater Himalaya (Xu et al., 2013), or nearby Alpine Periadriatic líne with several intrusive complexes (Márton et al., 2006). In the environment of the Variscan shear zone, a transition from metatexites to diatexites accompanied by an increase in the volume of granite mobilizes up to the placement of peraluminous granodiorite in the shear zone was demonstrated (De Luca et al., 2023).

Later intrusions of I-type granitoids are evidence of the increase in thermality of the granitoid process at the end of the decompression granitogenic stage. A suitable mechanism for such a process is a model of the subsidence of a relict block of oceanic crust after a collision into the asthenosphere (slab breakoff), thermal ascent of mantle masses, acceleration of decompression of crustal parts, its melting associated with the ascent of deeper-seated intrusions. (napr. von Blanckenburg & Davies, 1995). For granitoids of the Low Tatra Mts, such a model is discussed by Maraszewska et al. (2022).

Orthogneisess represent a special phenomenon within the Suchý crystalline basement. Less significantly they occur also in the western part of the Magura massif. From the viewpoint of Variscan setting we consider them as the upper structural element. On the older geological map of Maheľ (1982) they were considered as migmatites. The presence of spindle-shaped polycrystalline glomeroblasts composed of feldspars and quartz, which are a manifestation of ductile deformation of older phenocrysts

and the absence of leukosome formation, testify against such interpretation. We assume that this crustal element (which, due to the monotonous character, composition and dating of the metamorphic reworking, we consider to be a pre-Varican granitoid; pre-VD0), within Variscan collision being obducted (VD1o) onto those parts of crystalline basement that primarily sedimented on the Paleozoic continental slope, or even on the ocean floor.

Orthogneiss lithologies were identified as a common component within the Western Carpathian crystalline basement. Several authors have investigated their age characteristics based on zircon dating. In the Western Tatras, they were dated from the upper and lower tectonic units using the method LA-MC-ICP-MS method by Burda & Klötzli (2011) to 534 Ma, which they considered to be the age of the protolith, while the age of 387 Ma they consider as the age of highly metamorphic Eo-Varican event. The age of the protolith of the Veporic orthogneisses from Muráň (Gaab et al., 2005) was determined to 464 ± 34 Ma (later redefined by Putiš et al., 2008 to Cadomian). Isochrone age of zircons from orthogneiss from the Low Tatra Mts (sample NTJ-1) was determined by Putiš et al. (2003) to 381 Ma, whereas model ages for different size fractions of zircons vary for isotopic system $^{207}Pb/^{235}U$ = 466.2–576.6 Ma and for isotopic system $^{206}Pb/^{238}U$ = 441.2–526.4 Ma. From this, it can also be concluded that the age of 381 Ma represents the high-temperature metamorphic overprint of the protolith. Later dating of orthogneisses, but also banded amphibolites from W. Carpathians (Putiš et al., 2008) provided wider Neo-Proterozoic-Cadomian age extent (640–530 Ma) at larger gruop of orthogneisses. Our chemical dating of monazite from orthogreisses with a distinct peak of 390 Ma can undoubtedly be considered as the metamorphic age of monazite, while ages in the range of 340–350 Ma represent the age of a subsequent thermal event associated with leucogranite intrusions.

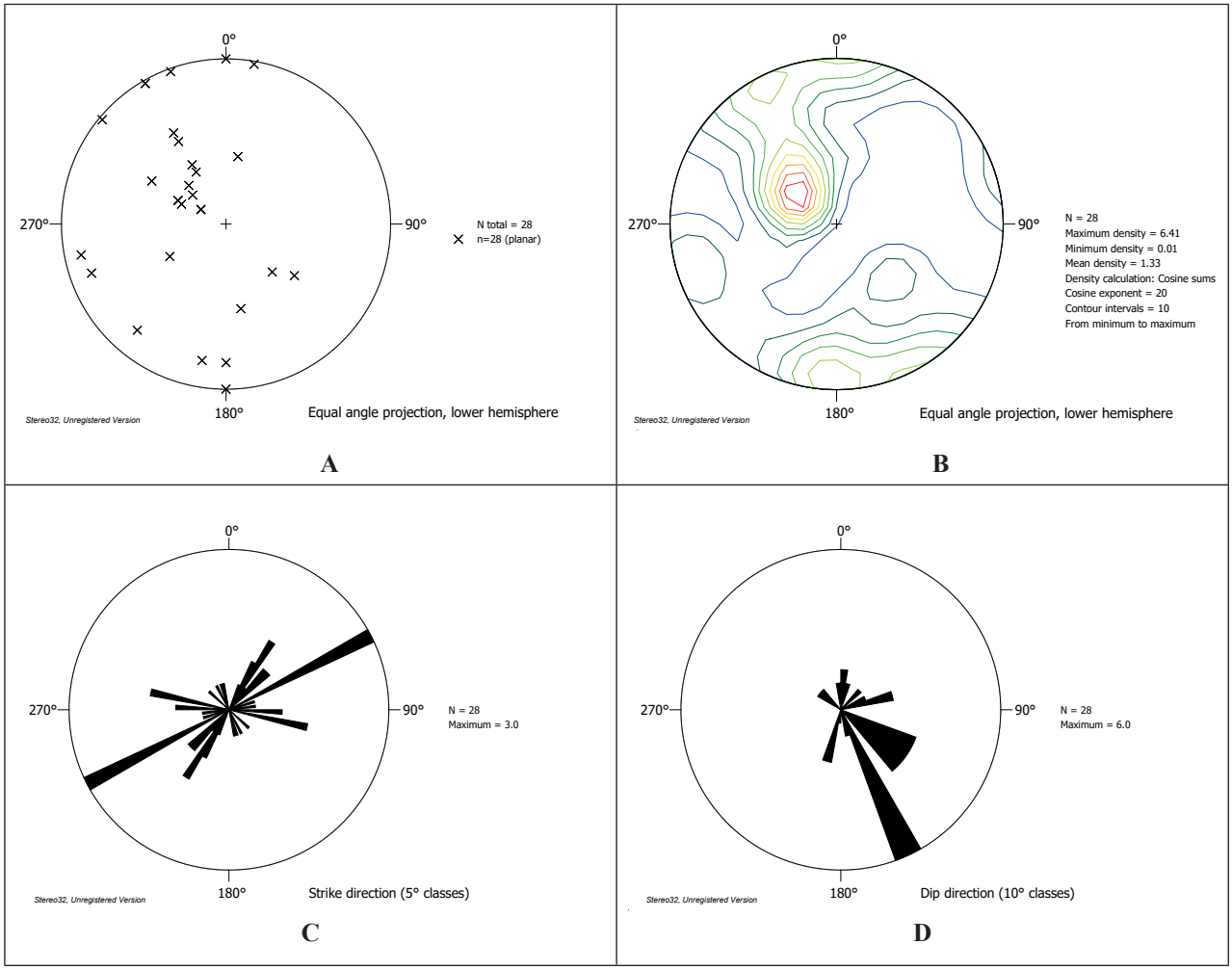

Fig. 52. Planar elements in orthogneisses (28 measurements): A – poles of plains, B – contourogram of poles of plains, C – prevailing trend of planes, D – dips of metamorphic schistosity of orthogneisses.

The metamorfnej schistosity of orthogneisses trending dominating ENE–WSW with steep to moderate dip to SSE–JJV. The field configuration indicates the shallow fan-like setting of orthogneiss body. The presence of distinct biotite lineations indicates a significant stress field acting at emplacement of orthogneisses in the Variscan setting. The more external (higher) position in the Variscan setting is emphasized by the absence, or the rarity of granitization manifestations, while transversal brittle structures in orthogneisses are filled only with aplitic and pegmatite veins (Figs. 24A and 39A).

When analyzing the structural elements of the crystalline basement in megascale, it is necessary to state that these very probably demonstrate Alpine-modified directions, which can be derived from the variable and often steep dips of the Mesozoic cover of Tatricum (Malá Magura cover succession) towards the NW. The Alpine tilting of the crystalline basement in the NW direction would indicate that the crystallinic structures were significantly more gently dipping to the NW in the pre-Alpine period.

Regarding the configuration of the entire structure of the Magura and Suchý massifs, it is necessary to point out again that the western part of the Strážovské vrchy crystalline basement – the Suchý massif represents more external and less granited part of Variscan setting, manifested mainly by sharp intrusive contacts of granitoids to metamorphites. In the western part of the Suchý massif, approximately from the Radiša valley, surfaces of metamorphic foliation have shallower dip, being accompanied with diaphtoresis of former metamorphic minerals from the greenschists facies. In microscale it is manifested by cataclasis of garnet phenocrysts, its new rotation, chloritization along cataclastic fractures, forming of actinolite at the expense of common amphibole in metabasites and replacement of original Al silicates in metapelites by glomeroblasts of fine-grained muscovite. We associate new metamorphic schistosity and retrograde mineral replacements with Late Variscan unroofing in shallow crustal levels.

Alpine metamorphic overprint

Alpine overprint (ApD, AnD) is not always reliably distinguishable from Late Variscan unroofing (VD2), however, there are some diagnostic signs that distinguish them. Fission-track dating of zircon from the Tatric crystalline basement (Marko et al., 2017) indicates that this basement during Alpine cycle was not overprinted by temperature higher than 320 °C (zircon closure temperature), which is valid also for sediments of the Malá Magura unit. Younger, Alpine low temperature metamorphism in the Magura massif (Čík & Petrík, 2014) was characterized by the presence of margarite and pumpellyite. Calculations of Alpine association in the Poruba area in migmatite provided values 480 °C at pressure 4.6 kbar (which we consider an unrealistically high value) and in paragneiss 300 °C at pressure 2.9 kbar. Radial arranged pumpellyite crystals can occasionally be found in granite fractures also in Suchý massif and often in thin sections from metabasites, mainly in W margin if the Suchý massif.

Planes of Alpine cleavage in crystalline basement have prevailing trends ENE–WSW VSV–ZJZ (55–65°) with dominant dip to SE, less to NW. The linear kinematic indicators show mainly to horizontal shifts (strike-slips) related to the Paleo-Alpine thrusts of higher units (ApD1c), mainly of the Fatricum, which was partially reflected also in the Tatric basement.

Thermal modelling (Marko et al., 2017) based on fission-track dating of zircon (ZFT ages, reflecting thermal transition between 230–250–max. 320 °C) indicated ages corresponding to gradual ascent of Paleozoic consilidated crystalline block, while the absence of Late Paleozoic sediments in Tatricum reflects denudation of Tatric segment down to the level of crystalline basement in the lowest Triassic. Younges ZFT ages (245, 239 and 222 Ma) reflect gradual, but irregular cooling of crystalline blocks in the Middle to Upper Triassic, possibly repeated uneven submergence of the crystalline basement during the Lower to Middle Jurassic (ages 198 and 168 Ma).

The distinguishing criterion for Late Variscan unroofing (VD2) and Alpine metamorphism (MAp) is mainly Alpine mineral metamorphism with the formation of pumpellyite facies minerals in metabasites, indicating lower temperature temperature metamorphic conditions in comparison with Late Variscan diaphtoresis. From the spatial view, the Alpine metamorphism is often bound with marginal parts of the massif in contact with sediments of Mesozoic Malá Magura unit, which are also strongly tektonically reduced. This is manifested by narrow mylonite zones parallel with the margins of the massif, which, in the case of binding to sediments with black schists (e.g. in the Čavoj area), are a source of metals remobilized into veins or stockworks in these narrow zones. During later Alpine updoming of crystalline basement after the completion of formation of the nappe setting, probably in the Upper Cretaceous or Paleogene, locally started in upper crustal conditions the origin of zones of low-temperature utracataclasis (kakiritization), demonstrated by origin of dark afanitic zones thick up to several cm. At a later stage, during the continuing structuring of the crystalline blocks, wider zones of ultracataclasis were formed in the granitoids and quartzites, which are mainly present in the area of the Radiša fault (more appropriate name – Radiša fault zone), Závadka fault, Šútovo fault, possibly also Diviaky fault (more appropriate name – Diviaky fault zone; Fig. 1). The final stage is the disintegration of the crystalline massif along the E-W oriented faults with the subsidence of the

southern blocks, as well as faults and fault zones in the N–S direction (e.g. Diviaky fault and Radiša fault; AnD4).

Acknowledgment

The authors appreciate the contribution of the research on the project *Geological map of the Strážovské vrchy Mts – Easten part* funded by the Ministry of Environment of the Slovak Republic. Results of petrological research by Rastislav Demko (State Geological Institute of Dionýz Štúr – ŠGÚDŠ Bratislava, Slovakia) are grealty appreciated. This paper is also a contribution of the State Geological Institute of Dionýz Štúr – ŠGÚDŠ, for the EC – CINEA HORIZON-CL5-2021-D3-D2 project 101075609 Geological Service for Europe (GSEU) within WP6 – Geological framework for the European geological data & information system and task T6.2.4 Lithotectonic units.

References

Bibikova, E. V., Korikovsky, S. P., Putiš, M., Broska, I., Golzman, Y. V. & Arakeliants, M. M., 1990: U/Pb, Rb/Sr and K/Ar dating of Sihla tonalites of Vepor Pluton (Western Carpathians). *Geologický zborník, Geologica Carpathica, 41, 427–436.*

Braathen, A., Nordgulen, Ø., Osmundsen, P. T., Andersen, T. B., Solli, A. & Roberts, D., 2000: Devonian, orogen-parallel, oposed extension in Central Norwegian Caledonides. *Geology, 28, 7, 615–618.*

Broska, I., Bibikova, E. V., Gracheva, T. V., Makarov, V. A. & Caňo, F., 1990: Zircon from granitoids rocks of the Tribeč-Zobor crystal-line complex: its typology, chemical and isotopic composition. *Geologický zborník, Geologica Carpathica, 41, 393–406.*

Broska, I. & Svojtka, M., 2020: Early Carboniferous successive I/S granite magmatism recorded in the Malá Fatra Mountains by LA-ICP-MS zircon dating (Western Carpathians). *Geologica Carpathica, 71, 5, 391–401.*

Burda, J. & Klötzli, U., 2011: Pre-Variscan evolution of the Western Tatra Mountains: new insight from U-Pb zircon dating. *Mineral. Petrol., 102, 99–115.*

De Luca, M., Ruberti, N., Oggiano. G., Rossi, Ph., Pascucci, V. & Casini, L., 2023: Structure of a Variscan migmatite-granite transition zone (N Sardinia, Italy). *Journal of Maps, 19, 1, 1–10.* DOI:10.1080/17445647.2023.2182721.

Dyda, M., 1988: Retrograde processes in paragneisses of the Suchy and Mala Magura Mts. *Geologický zborník, Geologica Carpathica, 39, 241–257.*

Dyda, M., 1990: Metamorphic processes in paragneisses from the Suchy and Mala Magura Mts. (The West Carpathians). *Geologický zborník, Geologica Carpathica, 41, 315–334.*

Gaab, A. S., Janák, M., Poller, U. & Todt, W., 2006: Alpine reworking of Ordovician protoliths in the Western Carpathians: Geochronological and geochemical data on the Muráň Gneiss Complex, Slovakia. *Lithos, 87, 261–275.*

Hovorka, D. & Fejdi, P., 1983: Garnets of peraluminious granites of the Suchý and the Malá Magura Mts. (The Western Carpathians) – their origin and geological significance. *Geologický zborník, Geologica Carpathica, 34, 1, 103–115.*

Hovorka, D. & Méres, Š., 1991: Pre-upper carboniferrous gneisses of the Strážovské vrchy uplandand the Malá Fatra Mts. (The Western Carpathians). *Acta geogr. geol. Univ. Comen., 46, 103–169.*

Hraško, Ľ., Pelech, O., Sentpetery, M. Olšavský, M., Kronome, B., Laurinc, D., Maglay, J., Németh, Z., Boorová, D., Žecová, K., Zlinská, A., Mikudíková, M., Fekete, K., Nagy, A., Demko, R. & Kováčik, M., 2020: Geologická mapa regiónu Strážovské vrchy – východná časť v mierke 1 : 25 000, listy 35-22-1 Pružina, 35-22-3 Valaská Belá, 35-24-1 Nitrianske Rudno a 35-24-3 Uhrovec. *Manuscript. Bratislava, archive ŠGÚDŠ, 289 p.*

Hraško, Ľ., Kováčik, M. (eds.), Olšavský, M., Sentpetery, M., Pelech, O., Laurinc, D., Maglay, J., Németh, Z., Kronome, B., Nagy, A., Kováčik, M.†, Vlačiky, M. & Dananaj, I., 2021: Geologická mapa Strážovských vrchov (východná časť) 1 : 50 000**,** *Bratislava, MŽP SR – ŠGÚDŠ.* https://www.geology.sk/wp-content/uploads/documents/foto/geol_mapy_50k/58_StrazovskeVrchy_final.jpg**.**

Hutton, D. H. W., Dempster, T. J., Brown, P. E. & Becker, S. D., 1990: A new mechanism of granite emplacement: intrusion in active extensional shear zones. *Nature, 343, 452–455.*

Ivan, P. & Méres, Š., 2015: Geochemistry of amphibolites and related graphitic gneisses from the Suchý and Malá Magura Mountains (central Western Carpathians) – evidence for relics of the Variscan ophiolite complex. *Geologica Carpathica, 66, 5, 347–360.*

Ivanov, M., 1957: Genéza a vzťah granitoidných intrúzií k super-krustálnym sériám kryštalinika Suchého a Malej Magury. *Geologické práce, Zošit, 47, 87–115.*

Kahan, Š., 1976: Štruktúrna charakteristika kryštalinika masívu Suchého a Malej Magury. *Manuscript. Bratislava, archive* Katedry geológie a paleontológie PFUK.

Kahan, Š., 1979: Čiastková správa o výskume kryštalinika Strážovských vrchov, riešenie v rokoch 1976–1978. *Manuscript. Bratislava, archive ŠGÚDŠ (arch. no. 45428), 81 p.*

Kahan, Š., 1980: Strukturelle und metamorphe Charakteristik des Gebirges Strážovské vrchy (Suchý und Malá Magura). *Geologický zborník, Geologica Carpathica, 31, 4, 577–602.*

Kahan, Š., Zelman, J. & Putiš, M., 1978: Správa o prácach vykonaných v rámci HZ 23/74 – VČ a HZ 36/76 VČ (Suchý – Malá Magura) v r. 1974–1976. *Manuscript. Bratislava, archive ŠGÚDŠ (arch. no. 50327), 134 p.*

Klinec, A., 1956: Zpráva o mapovaní kryštalinika pohoria Malá Magura. *Manuscript. Bratislava, archive ŠGÚDŠ.*

Klinec, A., 1958: Kryštalinikum severovýchodnej časti Malej Magury. *Geologické práce, Správy, 12, 93–101.*

Kohút, M., Uher, P., Putiš, M., Ondrejka, M., Sergeev, S., Larionov, A. & Paderin, I., 2009: SHRIMP U-Th-Pb zircon dating of the granitoid massifs in the Malé Karpaty Mountains (Western Carpathians): evidence of Meso-Hercynian successive S- to I-type granitic magmatism. *Geologica Carpathica, 60, 345–350.*

Kohút, M. & Larionov, A. N., 2021: From subduction to collision: Genesis of the Variscan granitic rocks from the Tatric Superunit (Western Carpatians, Slovakia). *Geologica Carpathica, 72, 2, 96–113.*

Konečný, P., Kusiak, M. A. & Dunkley, D. J., 2018: Improving U,Th,Pb electron microprobe dating using monazite age references. Invited review article. *Chemical Geology, 484, 22–35.*

Kráľ, J., Goltzman, Y. & Petrík, I., 1987: Rb-Sr whole-rock izochron data of granitic rocks from the Strážovské vrchy Mts: The preliminary report. *Geologický zborník, Geologica Carpathica, 38, 2, 171–179.*

Kráľ, J., Hess, C. Kober, B. & Lippolt, H. J., 1997: $^{207}Pb/^{206}Pb$ and $^{40}Ar/^{39}Ar$ age data from plutonic rocks of the Strážovské vrchy Mts. basement, Western Carpathians. In: Grecula, P., Hovorka, D. a Putiš, M. (eds.): Geological evolution of the Western Carpathians. *Mineralia Slovaca, Monogr., 253–260.*

Maheľ, M. & Gross, P., 1975: Vysvetlivky mapy 1 : 25 000 listy Kšinná, Nitrianske Rudno (sčasti i Nitrianske Sučany) – južná časť Strážovskej hornatiny, čiastková záverečná správa za rok: 1975. *Manuscript. Bratislava, archive ŠGÚDŠ, 1–39.*

Maheľ, M., 1983: Vysvetlivky ku geologickej mape Strážovských vrchov v mierke 1 : 50 000. *Bratislava, Geologický ústav Dionýza Štúra, 90 p.*

Maheľ, M., 1985: Geologická stavba Strážovských vrchov. *Bratislava, Geologický ústav Dionýza Štúra, 221 p.*

Maraszewska, M., Broska, I., Kohút, M., Yi , K., Konečný, P. & Kurylo, S., 2022: The Ďumbier-Prašivá high K-calc-alkaline granite suite (Low Tatra Mts., Western Carpathians): Insights into their evolution from geochemisty and geochronology. *Geologica Carpathica, 73, 4, 273–291.*

Marko, F., Andriessen P. A. M., Tomek, Č., Bezák, V., Fojtíková, L., Bošanský, M., Piovarči, M. & Reichwalder, P., 2017: Carpathian Shear Corridor – a strike-slip boundary of an extruded crustal segment. *Tectonophysics, 703–704, 119 – 134.*

Márton, E., Trojanova, M., Zupaničič, N. & Jelen, B., 2006: Formation, uplift and tectonic integration of a Periadriatic intrusive complex (Pohorje, Slovenia) as reflected in magnetic parameters and palaeomagnetic directions. *Geophys. Jour. Internat., 167, 3, 1148–1159.*

Mikoláš, S., Komora, J., Kandera, K., Sandanus, M., Šlepecký, T., Januš, J., Staňa, Š., Očenáš, D. & Stupák, J., 1995: Čavoj – Gápel – Ag, Pb, Zn rudy – vyhľadávací prieskum, stav k 31. 3. 1995. *Manuscript. Bratislava, archive ŠGÚDŠ (arch. no. 82971), 114 p., 44 príl.*

Montel, J. M., Foret, S., Veschambre, M., Nicollet, Ch. & Provost, A., 1996: Electron microprobe dating of monazite. *Chemical Geology, 131,1–4, 37–53.*

Németh, Z., Putiš, M. & Hraško, Ľ., 2016: The relation of metallogeny to geodynamic processes – the natural prerequisite for the origin of mineral deposits of public importance (MDoPOI: The case study in the Western Carpathians, Slovakia). *Mineralia Slovaca, 48, 2, 129–135.*

Németh, Z., 2021: Lithotectonic units of the Western Capathians: Suggestion of simple methodology for lithotectonic units defining, applicable for orogenic belts world-wide. *Mineralia Slovaca, 53, 81–90.*

Oberc-Dziedzic, T., Kryza, R. & Pin, Ch., 2015: Variscan granitods related to shear zones and faults: examples from Central Sudetes (Bohemian Massif) and the Middle Odra Fault Zone. *Int. Jour. of Earth Sci., 104,1139–1166.*

Putiš, M., Kotov, A. B., Petrík, I., Madarás, J., Salnikova, E. B., Yakovleva, S. Z., Berezhnaya, N. G., Plotkina, Y. V. Kovach, V. P., Lupták, B. & Majdán, M., 2003: Early- vs. Late orogenic granitoids relationships int the variscan basement of the Western Carpathians. *Geologica Carpathica, 54, 3, 163–174.*

Putiš, M., Sergeev, S., Ondrejka, M., Larionov, A., Siman, P., Spišiak, J., Uher, P. & Paderin, I., 2008: Cambrian-Ordovician metaigneous rocks associated with Cadomian fragments in the West-Carpathian basement dated by SHRIMP on zircons: a record from the Gondwana active margin setting. *Geologica Carpathica, 59, 1, 3–18.*

Vielzeuf, D. & Montel, J. M., 1994: Partial melting of metagreywackes: fluid-absent experiments and phase relationships. *Contrib. Mineral. Petrol., 117, 375–393.*

Vilinovičová, Ľ., 1988: Geochémia a petrogenéza granitoidných hornín Suchého a Malej Magury a ich vzťah k rulám. Kandidátska dizertačná práca. *Manuscript. Bratislava, archive ŠGÚDŠ (arch. no. 68031), 64 p.*

Vilinovičová, Ľ., 1990: Petrogenesis of gneisses and granitoids from the Strážovské vrchy Mts. *Geologický zborník, Geologica Carpathica, 41, 4, 335–376.*

White, R. W., Powel, R. & Johnson, T. E., 2014: The effect of Mn on mineral stability in metapelites revised: New a-x relations for manganese-bearing minerals. *Jour. Metamorphic. Geol., 32, 8, 809–828.*

Wu, Chun-Ming, Zhang, J. & Liu-Dong Ren, 2004: Empirical Garnet-Biotite-Plagioclase-Quartz (GBPQ) geobarometry in Medium- to High-Grade Metapelites. *?????, 45,1907–1921.*

Xu, Zh., Wang, Q., Pêcher, A., Liang, F., Qi, X., Cai, Zh., Li, H., Zeng, L. & Cao, H., 2013: Orogen-parallel ductile extension and extrusion of the Greater Himalaya in the late Oligocene and Miocene. *Tectonics, 32, 191–215.*

Von Blanckenburg, F. & Davies, J. H., 1995: Slab breakoff: A model for syncollisional magmatism and tectonics in the Alps. *Tectonics, 14, 1, 120–131.*

Variské litotektonické jednotky v masíve Suchého v Strážovských vrchoch, Západné Karpaty – výsledok sedimentárnych, tektonometamorfných a granitizačných procesov

V predalpínskej štruktúre západnej časti Strážovských vrchov (masív Suchého) boli vyčlenené tri litologicky odlišné variské litotektonické jednotky: 1. sedimenty, ktoré majú pôvod v hlbšom oceánskom bazéne (prevažne metapelity s rôznym obsahom organickej hmoty, metabazalty, metakarbonáty?); 2. sedimenty kontinentálneho svahu (flyšoidné sedimenty s prevahou drobových sedimentov); 3. jednotka kontinentálneho pôvodu blízka granitovému zloženiu (ortoruly), ktorá má pravdepodobne predvariský pôvod. Tieto komplexy rôznej geotektonickej provenience boli amalgamované a metamorfované pred granitizačným štádiom (štádium pre-VmD2 pred obdobím misisipu). Z pohľadu variskej polyorogénnej evolúcie variské procesy v tatriku reprezentujú mezovariskú evolúciu (VmD).

Maximálne P-T podmienky orogénnej (regionálnej) metamorfózy (do 610 °C a 7,5 – 8,5 kbar) neboli dostatočné na rozsiahlejšie prejavy anatexie. Z terénnych pozorovaní vyplýva, že k produkcii obmedzeného objemu granitoidných tavenín dochádzalo najmä pri kontaktoch amalgamovaných litotektonických jednotiek, pravdepodobne s prispením strižného tepla.

Pravdepodobne vplyvom dodatočného tepla produkovaného pod akrečným klinom spolu s dekompresným režimom nastala etapa tvorby a umiestňovania granitoidov v orogénnej fáze VmD2.

Etapa tvorby granitov počas misisipu (štádium VmD2) je spojená s umiestňovaním rôznych typov granitoidných magiem, pričom ako geologicky najstaršie vystupujú granodiority s častými šlírmi. Predstavujú málo diferencovanú a málo mobilnú kryštálovú kašu (jv. časť územia).

V hlavnom deformačnom štádiu súhlasne s deformačným plánom v metamorfovaných komplexoch intrudovali masy leukogranitov, ktoré interagovali s okolitými metamorfovanými horninami v plytších kôrových podmienkach a spôsobili kontaktnú premenu staršej metamorfnej asociácie (do 590 °C a 3 – 4 kbar). Syndeformačný charakter leukokratných granitov je daný usmernením lupeňov biotitu paralelne s deformačným plánom v okolitých metamorfitoch. Časť leukogranitov najmä v centrálnych častiach telies je všesmerná. Deformačné pole pôsobilo nielen počas intrúzie leukogranitovej magmy, ale aj v subsolidovom štádiu.

Záverečnou etapou tohto procesu bola tvorba veľkých telies pegmatitov v extenzných fraktúrach štádia VmD2, orientovaných pod veľkým uhlom k hlavnej zložke napätia. Textúra pegmatitov so sivým blokovým K-živcom a nedostatok minerálov obsahujúcich vodu poukazuje na pravdepodobnú pneumatolytickú frakturáciu v následne otvorenom prostredí štádia VmD2.

Záverečnou etapou **štádia** VmD2 sú intrúzie granodioritov typu I so znakmi miešania magiem (*mixing*, resp. *mingling*).

Chemické datovanie monazitu v granitoidoch umožňuje datovať jednotlivé fázy granitizačného procesu medzi 360 – 345 mil. rokov, pričom najmladšie veky korešpondujú so vznikom pegmatitov. Datovanie monazitu v metamorfovaných horninách poukazuje na termálne ovplyvnenie granitizačným procesom (360 – 350 mil. r.) a zároveň indikuje staršie regionálne metamorfné prepracovanie prevažne v období 370 – 380 mil. rokov. Staršie reliktné údaje, ktoré je problematické interpretovať, môžu byť sčasti odvodené od veku protolitu metamorfovaných hornín.

Scenár umiestňovania granitoidných intrúzií je súhlasný s dekompresným režimom (v štádiu VmD2) po závere kôrového zhrubnutia (v štádiu VmD1c) až po frakturáciu kôrového bloku s intrúziami magiem typu I hlbšieho pôvodu.

Po tomto období pokračovala exhumácia blokov kryštalinika, čiastočná diaftoréza a neskôr povrchová erózia až do spodného triasu.

Opätovné ponorenie kryštalinických komplexov je spojené s nízkym stupňom alpínskeho metamorfného prepracovania.

Doručené / Received: 30. 5. 2024
Prijaté na publikovanie / Accepted: 28. 6. 2024

Appendix

Table of sample basic field characteristic and coordinates

Sample	Field characteristics	WGS-84 coordinates		SJTSK coordinates	
		φ	λ	X	Y
LHS-42	Contact of Bt paragneiss and pegmatite with grey blocky Kfs. Metamorphic schistosity 320/85.	48.820 482	18.416 903	1 214 869.74	470 428.22
LHS-57	Metamorphically differentiated Bt paragneiss with small interbeds of granitic material, subvertical metamorphic schistosity in N–S direction.	48.816 606	18.441 510	1 215 450.29	468 663.70
LHS-73	Stock of the Ms-Bt massive granite.	48.838 813	18.433 411	1 212 940.00	469 050.00
LHS-94A	Medium-grained schlier granitoid with moderate preferred orientation of Bt-Plg, Kfs, contains planes rich in Bt.	48.839 33	18.448 381	1 212 974.39	467 950.35
LHS-94B	V LHS-94A small body of Plg-rich (up to 50 %) granodiorite with abundant Bt. Idiomorphic Plg large up to 1–2 mm. Interstices are filled with Bt.	48.839 33	18.448 381	1 212 974.39	467 950.35
LHS-114	Alternation of migmatites with predominant metamorphic schists with the direction of dip 300/85°. 2 generations of granites are present in them: 1. granite – ductile folded, parallel to the metamorphic schist. 2. In the fold cores there are coarse-grained Ms-Bt granites, with idiomorphic feldspars. This 2nd type is hybridized at the edges, finer-grained. The presence of Bt schists indicates low magma mobility. This 2nd type probably segregates into large volumes, so that granitoids predominate in the western flank of the outcrops.	48.837 475	18.464 977	1 213 281.35	466 753.53
LHS-131	Ductile folded migmatites with a ratio of melt to metatect of 1 : 1. In this, concordant positions of medium-grained leucogranites with inhomogeneously distributed Bt are placed, in them the Bt is parallel to that in the migmatites.	48.837 114	18.465 415	1 213 323.96	466 724.77
LHS-137	Stromatitic migmatite with 1 cm thick parallel granite positions.	48.831 848	18.467 765	1 213 921.89	466 601.54
LHS-153	Fine-grained amphibolitic rocks, containing positions of leucogranite veins parallel to the metamorphic foliation, a few cm thick, up to a younger generation of transversal granite veins, which branch intricately. Veins of pegmatitic granites are also present.	48.840 364	18.462 299	1 212 944.81	466 922.69
LHS-177-2	177-1 light-grey Bt paragneisses without foliation planes with Bt2, but Bt is lineated; 177-2 hybridic, 177-2 hybridic medium- to coarse-grained granodiorites with irregularly spatially and dimensionally arranged Bt (together with 177-1 light-grey Bt paragneisses without foliation planes with Bt2, Bt is lineated.	48.819 231	18.456 915	1 215 253.67	467 512.06
LHS-185	Schlier granitoids with xenoliths of fine-grained Bt paragneiss.	48.836 248	18.459 216	1 213 382.14	467 186.30
LHS-197	Grey, fine-grained paragneiss, schistose, which are affected by new thermal reworking, with the formation of larger Bt2 flakes. Metamorphic schistosity is subvertical in E–W direction.	48.836 381	18.397 549	1 212 988.88	471 695.77
LHS-200	Tectonized, partially diaphtorized? medium-grained Bt + Ms leucogranites without paragneisses.	48.842 981	18.400 166	1 212 273.72	471 442.73
LHS-204	Grey, metamorphically foliated fine–grained Bt paragneisses, with new thermal reworking, with 1–2 mm Bt2 flakes, parallel with new foliation surfaces.	48.828 532	18.389 932	1 213 811.65	472 326.31

Tab. – continue

Sample	Field characteristics	WGS-84 coordinates		SJTSK coordinates	
		φ	λ	X	Y
LHS-206	Medium- to coarse-grained pegmatite leucogranite with transition to pegmatite. Several hundred m thick vein, cropping out in N side of the valley, where large blocks fall down to the stream. Locally present tiny Grt and grey Kfs. Grt forms subparallel interbeds, which proves the zonality. Ms in larger flakes usually forms nests.	48.828 998	18.432 599	1 214 022.56	469 200.63
LHS-207	Banded gneisses with metamorphic differentiation with straight flat alternating of 1 mm thick light and dark bands. Foliation planes are covered with larger Bt flakes. Transversally to metamorphic foliation penetrating fine. to medium-grained veinlets of leucogranite.	48.826 465	18.402 749	1 214 119.71	471 407.99
LHS-255	Paragneiss to micaschist with the formation of chlorite, in contact with aplite with garnet, metamorphic shale in the direction of dip 320/15°.	48.829 517	18.378 054 5	1 213 629.24	473 186.11
LHS-261	Grey aphanitic omnidirectional rock originally supposed to be metaquartzite. Contains Hbl.	48.846 793	18.378 087 0	1 211 715.29	473 021.80
LHS-272	Porphyroblastic orthogneiss with 5 mm porphyroblasts of rotated feldspars.	48.849 538	18.385 927 0	1 211 459.60	472 422.79
LHS-273	Porphyroblastic orthogneiss.	48.853 505	18.387 930 0	1 211 032.43	472 239.20
LHS-329	Dark and light grey, fine-grained banded paragneiss.	48.858 451	18.342 786	1 210 204.72	475 493.36
LHS-350	Dark grey Bt paragneiss with graphitic admixture, associated with black graphitic schists, schistosity dip 50/35°.	48.860 370	18.344 089	1 210 000.00	475 380.00
LHS-356a	Micaceous Bt paragneiss, metamorphic foliated structure, micas approx. 1 mm large (metapelite), contact with aplite.	48.837 683	18.367 388	1 212 658.42	473 889.70
LHS-356b	Micaceous Bt paragneiss, metamorphic foliated structure, micas approx. 1 mm large (metapelite), contact with aplite.	48.837 683	18.367 388	1 212 658.42	473 889.70
LHS-415	Oriented Bt-rich orthogneiss on the road base, metamorphic foliation, oblique pegmatite vein with grey Kfs.	48.863 594	18.423 373	1 210 132.55	469 553.65
LHS-482A	Bt grey paragneisses with steep metamorphic schistosity. In foliation planes occur large Bt2, system is penetrated in shear regime by granites – leucocratic fine-grained with rare oriented Bt in magmatic flow, the same system is followed with coarse-grained to blocky pegmatites with grey blocky feldspars and rare Ms.	48.865 501	18.456 219	1 210 122.58	467 134.79
LHS-482B	Bt paragneisses with metamorphic schistosity, Bt2, interbeds of leucogranite with inhomogeneously distribued Bt. The weakly bordered pegmatite is present in them, being zonal, thick to 10 m, in the middle with grey Kfs and Ab at the margin.	48.865 812	18.455 568	1 210 084.14	467 179.50
LHS-557	Two-mica granite with prevailing Ms and pegmatite.	48.837647	18.421309	1 212 995.11	469 946.15
LHS-572	In environment of Bt paragneisses with Bt2, the grey to light-grey pegmatites frequently occur with sugar-type aplitic zone and often tiny Grt, central zone with Ms, Bt, Gtr, Kfs, Ab, Qtz.	48.849 571	18.407 010	1 211 585.96	470 880.79
LHS-599	Large blocks of pegmatites with blocky grey Kfs, aplites with garnet. Rock contains only Bt, Ms is missing. Vein crops our in the environment of two-mica granites.	48.830 616	18.434 235	1 213 853.53	469 066.00

Tab. – continue

Sample	Field characteristics	WGS-84 coordinates		SJTSK coordinates	
		φ	λ	X	Y
LHS-607	Two-mica leucogranite with irregularly distributed, oriented Bt, and omnidirectional Ms, present are not sharply bordered pegmatites.	48.842 982	18.423 083	1 212 414.87	469 766.75
LHS-611	Large blocks of pegmtites with grey blocky K-feldspar in environment of leucogranites with oriented Bt.	48.827 868	18.424 823	1 214 100.00	469 780.00
LHS-623	Light deformed granites in subsolidic regime, planar orientation in outcrop, Bt with preferred orientation.	48.849 214	18.441 503	1 211 837.30	468 361.74
LHS-626	Light leucogranite with oriented Bt and feldspars, Kfs is large up to 2–3 mm.	48.849 991	18.434 700	1 211 709.53	468 852.01
LHS-650	Migmatite with a predominance of felsic component.	48.847 407	18.476 226	1 212 249.59	465 839.11
LHS-711	Orthogneiss with oriented biotite.	48.862 027	18.370 590	1 209 981.00	473 427.10
SZN-24	Light fine-grained rock, omnidirectional keratophyre?	48.841 015	18.368 883	1 212 298.32	473 749.04
SZN-25	Black metamorphosed schist, folded.	48.840 181	18.381 699	1 212 469.97	472 819.50
SZN -32a	Alternation of grey to black metamorphosed shales and metasandstones.	48.844 398	18.365 499	1 211 902.50	473 964.71
SZN-34a	Dark metapelitic paragneiss with biotite, staurolite and garnet.	48.842 115	18.369 983	1 212 183.26	473 658.27
SZN-34b	Dark metapelitic paragneiss with biotite, staurolite and garnet.	48.842 115	18.369 983	1 212 183.26	473 658.27
SZN-34c	Dark metapelitic paragneiss with biotite, staurolite and garnet.	48.842 115	18.369 983	1 212 183.26	473 658.27
SZN-57	Dark-grey paragneiss with graphitic pigment.	48.861 108	18.354 930	1 209 985.55	474 580.53
SZN-66	Dark-grey to black paragneiss.	48.864 038	18.369 480	1 209 751.09	473 489.36
SZN-85	Fine-grained amphibolite.	48.845 178	18.374 989	1 211 874.84	473 263.40

Used abbreviations:

Minerals: Pl – plagioclase (Ab – albite, An – anortite), Kfs – K-feldspar, Hbl, Amf – hornblende, Cpx – clinopyroxene, Grt – garnet (Alm – almandine, Spess – spessartine, Pyr – pyrope, Gross – grossular), Qtz – quartz, Bt – biotite, Ms – muscovite, Sill – sillimanite, Stau, St – staurolite, Chl – chlorite, Ep – epidote, Ap – apatite, Zrn – zircon, Mnz – monazite, Mag – magnetite, Ilm – ilmenite

Mg # – ionic ratio $Mg/(Fe_{total} + Mg)$

BSEI – back scatterred electron images

TIMS – Thermal Ionization Mass Spectrometry

SHRIMP – Sensitive High Resolution Ion Micro-Probe

LA-ICP-MS – Laser Ablation Inductively Coupled Plasma Mass Spectrometry

Lithotectonic units – orogenic cycles, orogenic phases: VD – Variscan orogenic cycle, VmD0 – Meso-Variscan divergent orogenic phase, VmD1c – Meso-Variscan collisional phase, VmD2 – Meso-Variscan post-colllisional phase with thermal overheating over hot line, extensional and unrooging kinematics, AD – Alpine orogenic cycle, AnD3 – Neo-Alpine orogenic phase characteristic with subhorizontal shearing kinematics, AnD4 – Neo-Alpine orogenic phase characteristic with regional extension and origin of pure shear-type faults preferably of E–W and N–E course.

Mineralia Slovaca, Web ISSN 1338-3523, ISSN 0369-2086, https://doi.org/10.56623/ms.2024.56.1.2
56, 1 (2024), 51 – 70, © Authors 2024. CC BY 4.0

Structural evolution of the Selec Block in the Považský Inovec Mts. (Western Carpathians) and the Infratatric issue

ONDREJ PELECH[1] and JOZEF HÓK[2]

[1]State Geological Institute of Dionýz Štúr, Mlynská dolina 1, 817 04 Bratislava 1, Slovak Republic; ondrej.pelech@geology.sk
[2]Comenius University in Bratislava, Faculty of Natural Sciences, Department of Geology and Palaeontology, Ilkovičova 6, 842 15 Bratislava, Slovak Republic; hok@fns.uniba.sk

Abstract: In west-east direction, the Selec Block of the Považský Inovec Mts consists of three geologically and tectonically distinct segments of Tatricum.

1) Eastern segment is characterized by dominance of the Tatric crystalline basement rocks (mica schists), subautochthonous position and internally imbricated structure with thrust sheets of Permian, Triassic and Upper Cretaceous (Horné Belice Group) rocks. Rocks of the Fatricum and Hronicum are rudimentarily preserved along the eastern margin of the block.
2) Central segment represents deformed – folded and sheared structure, composed of the Tatric crystalline basement (orthogneiss) and sedimentary rocks of Carboniferous to Triassic age. This segment largely corresponds to lithology surrounding the Hôrka shear zone and the Selec thrust.
3) The western segment is represented by internally imbricated structure, containing Variscan (Lower Carboniferous) crystalline basement rocks (diapthorites of different types), Permian to Triassic rocks of the Tatricum and thin-skinned nappe complexes of Fatricum and Hronicum.

Key words: Tatricum, crystalline basement, Kálnica Group, Hôrka shear zone, Selec thrust

Graphical abstract

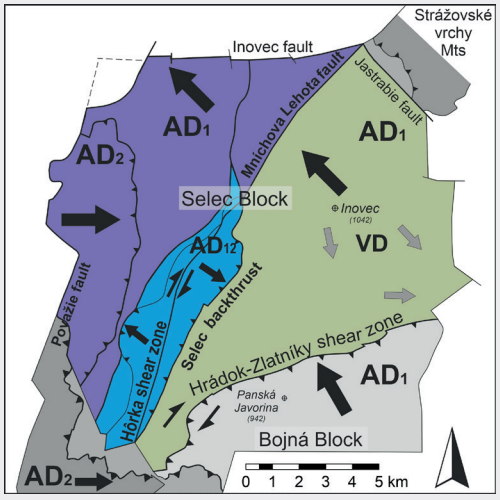

Highlights

The Selec Block in northern part of Považský Inovec Mts is divided into 3 distinct structural segments:

- Eastern segment (green in Graphical abstract) is composed mainly of Variscan (VD, Carboniferous) mica schists with Late Paleozoic to Mesozoic cover and locally preserved synclines filled by the Upper Cretaceous mélange. The whole sequence is imbricated by NW-vergent thrust sheets.
- Central segment (blue in GA) with thick Upper Paleozoic volcano-sedimentary sequence in dominant subvertical position, being strongly dextrally sheared due to the course of the Hôrka shear zone and Selec thrust.
- Western segment (violet in GA) consists of crystalline basement and its Upper Paleozoic to Mesozoic sedimentary cover, overlain by the Fatric and Hronic nappes. It shows signs of Paleogene to Early Miocene backthrusting and possible unroofing.

Introduction

The Považský Inovec Mts represents NNE-SSW trending elevated horst, belonging to the Western Carpathian Core mountains belt. It is composed dominantly of the subautochthonous Tatricum (Early Paleozoic crystalline basement and its Late Paleozoic / Mesozoic cover) and nappes of Fatricum and Hronicum (Late Paleozoic/ Mesozoic sequences). The geological structure of the Považský Inovec Mts is summarized in regional map at a scale 1 : 50 000 and accompanying explanatory notes (Ivanička et al., 2007, 2011). The Selec Block (Maheľ, 1986) represents the northern part of the mountain range, being separated from the south located Bojná Block by the Hrádok-Zlatníky dextral thrust shear zone (Pelech & Hók, 2017; Fig. 1). The substantial part of the Selec Block is represented by Tatricum, dominantly composed of Variscan mica schist to gneiss crystalline basement with locally occurring amphibolite bodies and sedimentary cover ranging from Late Carboniferous to Early Jurassic (Fig. 2;

Kamenický, 1956). These complexes are unevenly distributed. The crystalline basement prevails in the eastern side, while western and central part of the block is characterized by thicker Upper Paleozoic volcano-sedimentary rocks (Ivanička et al., 2007, 2011). The presence of thick Upper Paleozoic succession (Kálnica Group; see Štimmel et al., 1984; Miháľ, 2006; Olšavský, 2008) as well as Upper Cretaceous mélange (Horné Belice Group; Kullmanová & Gašpariková, 1982; Plašienka et al., 1994; Pelech et al., 2016, 2021) is unique within the Western Carpathian Core mountains and may be considered noticeable in the frame of other Tethyan regions, as well. The Hrádok-Zlatníky shear zone constitutes an important structure with respect to the structural position of investigated area. It is generally accepted that it represents the north-vergent Alpine (or Alpine rejuvenized) thrust of the Bojná Block on the Selec Block (Fig. 1; Putiš, 1980, 1991; Maheľ, 1986; Leško et al., 1988; Plašienka & Marko, 1993; Pelech & Hók, 2017).

The Bojná Block is generally considered as tectonic element of the Tatricum (e.g. Maheľ, 1986; Putiš, 1992; Plašienka & Marko, 1993; Plašienka, 1999) or so-called Carpathian Austroalpine (Leško et al., 1988). Due to tectonic position of the Selec Block in the footwall of the Tatric Bojná Block, Leško et al. (1988) considered the whole Selec Block as the Penninic Unit of the Western Carpathians. However, in this interpretation the sequences of Hronicum, Fatricum and both – Tatric crystalline basement and sedimentary cover (Inovec Unit) were also incorporated to this Western Carpathian Penninic Unit (l.c.). Later Putiš (1992) assigned the crystalline basement of the Selec Block as the Infratatricum, which seems to express the position below the Tatricum of the Bojná Block, and in the hanging wall of the Upper Cretaceous rocks which were called the "Perivahicum". However, the aforementioned reclassification was provided without any further comments or clear definitions (for further information see chapter *The question of Infratatricum*).

Plašienka et al. (1994) considered the rock complexes of the crystalline basement of the Selec Block (Inovec Unit) as the Tatricum, however emphasized its allochthonous position on the Upper Cretaceous sediments (Belice Succession), which are considered as equivalent of Penninic Unit of the Eastern Alps (in the W. Carpathians named the Vahic Unit). Later Plašienka (1995) designated the Inovec Unit as a nappe (Inovec nappe) of Tatric crystalline basement bearing autochthonous Upper Paleozoic (Kálnica Group) and rudimentary preserved Mesozoic sedimentary cover (Selec succession). Authors (Plašienka et al., 1994; Plašienka, 1995) in both cases underline that the Selec Block forms the northern – external part of the Tatricum. Such paleotectonic affiliation of the Selec Block (or Inovec nappe) resulted in new definition of Infratatricum (Plašienka et al., 1997; Plašienka, 1999), which was considered hierarchically as a sub-unit of Tatric superunit.

Ivanička et al. (2011) described the Selec Block of the Považský Inovec Mts as region composed of Hronicum, Fatricum and Tatricum or Infratatricum respectively, and included a separate Horné Belice Group. This study generally agrees with Ivanička et al. (2007, 2011) and considers rock complexes of Selec and Bojná blocks as integral part of Tatricum with complicated deformation history, including several smaller scale structures and superimposed Fatricum, Hronicum and the Horné Belice Group (Fig. 1).

One of the key points in the interpretation of the tectonic structure of the Selec Block is the position of the rock sequences of the Upper Cretaceous Horné Belice Group. The opinions on its structure and sedimentary sequence considerably vary and the discussion goes beyond the scope of this paper (Kullmanová & Gašpariková, 1982; Plašienka et al., 1994, 2017; Pelech et al., 2016, 2017a, b, c, 2021; Putiš et al., 2008, 2021). Some authors consider the Horné Belice Group as tectonic windows of the Váhicum (= Penninicum) or Infratatricum cropping out from beneath the Tatricum crystalline basement nappes. The stratigraphic range of the rocks of the Horné Belice Group is according to this interpretation Lower Jurassic to Upper Cretaceous (Plašienka et al., 1994; Putiš et al., 2008). However, the Horné Belice Group is a tectonic mélange formerly overlying the Tatric crystalline basement, now occurring in imbricated structure between the crystalline basement thrust sheets (Ivanička et al., 2007, 2011). It consists of the deep-water syn-orogenic sediments with olistoliths (block-in-matrix) of various rocks from the overlying Tatric crystalline basement as well as exotic blocks (Plašienka et al., 1994; Pelech et al., 2021).

Previous investigations have led to the definition of several tectonic structures. A brief characterization of them is necessary for the understanding of the following text. These are mainly:

The **Selec thrust** or **Selec backthrust** (Slovak: *selecký prešmyk*, defined formerly by Štimmel et al., 1984) represents NNE-SSW trending, WNW dipping brittle-ductile thrust and reverse fault zone along which Upper Paleozoic (mainly Permian) complexes are backthrust with top to ESE-vergence on to the Mesozoic and crystalline basement rocks in the east. It constitutes eastern margin of the Hôrka shear zone, located approx. between the Hôrčanská dolina valley and Klenkov vrch hill. The thrust is well marked by the borehole (Štimmel et al., 1984) and surface data. Most likely it represents reactivated normal fault which formerly played important role in the structure of the Late Paleozoic (Kálnica) rift basin, as the Upper Carboniferous complexes are not known east of this fault (Maheľ, 1986; Ivanička et al., 2007). However, Carboniferous

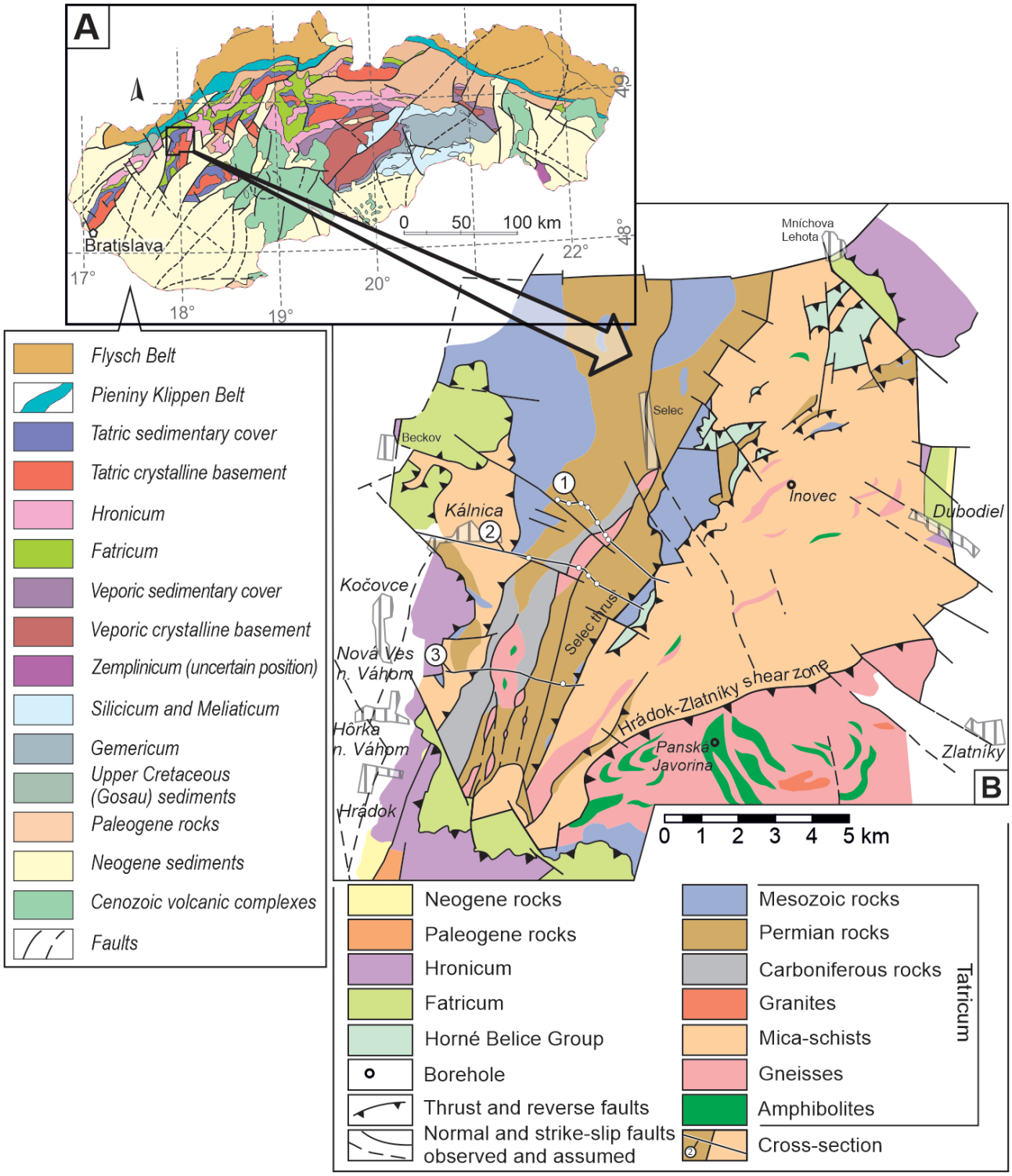

Fig. 1. A – Simplified tectonic map of Slovakia (based on Hók et al., 2019) with marked studied area. **B –** Simplified geological map of the northern Považský Inovec Mts (based on Elečko et al., 2008). E-W trending cross-sections in the map (1–3) show the relations among individual segments of the Selec Block in Fig. 11.

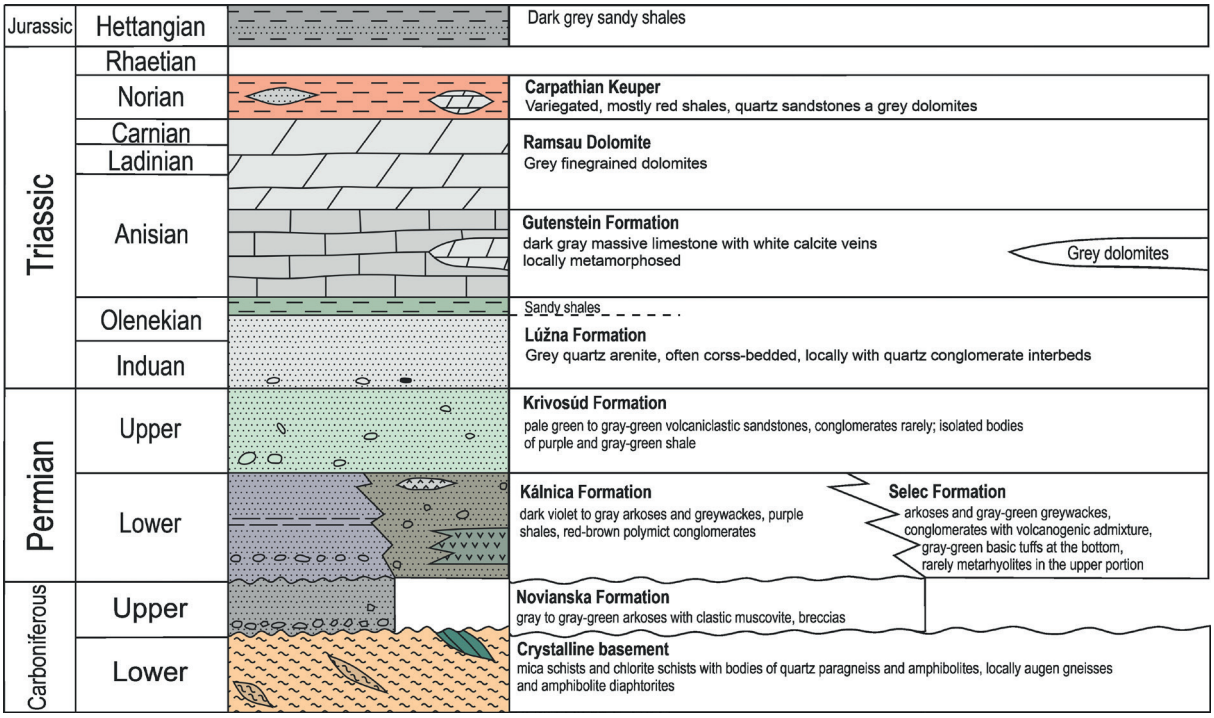

Fig. 2. Lithostratigraphic column of the Tatric cover sequence (Selec Unit) in the investigated area (based on Ivanička et al., 2011; Olšavský, 2008).

rocks are not exposed east of the Mníchova Lehota fault (described below), which is a younger structure bounding the Selec thrust from the west.

The **Hôrka shear zone** (Slovak: *hôrčanská strižná zóna*) was defined formerly by Maheľ (1986) as Hôrka [tectonic] slices belt (Slovak: *hôrčanské šupinové pásmo*) and later without further comments or clear definition renamed by Putiš (1991) as the Hrádok-Selec shear zone. However, we do not recommend using this term any longer due to the possibility of confusion with Hrádok-Zlatníky shear zone. The Hôrka shear zone represents N-S to NNE-SSW trending several 100 meters up to 2.5 km thick, dominantly dextral transpressional brittle-ductile shear zone marked by flower arrangement of strike-slip duplexes (Madarás et al., 2007). The shear zone is traceable in crystalline basement and Upper Paleozoic complexes between the Selec village and Hrádocká dolina valley, and is generally thickening to the south, where it is covered by thrust of the Hrádok-Zlatníky shear zone and Fatricum. The Hôrka shear zone is present west of Selec thrust and east of longitudinally irregular border, corresponding approximately to the westernmost occurrence of Upper Carboniferous Novianska Formation. It is characterized by the predominance of rocks of Kálnica Group and several isolated occurrences of crystalline basement rocks. Apart of typical Paleo-Alpine deformation also signs of older Albian (approx. 100 Ma) deformation are preserved (Štimmel et al., 1984; Putiš et al., 2008, 2009, 2019, 2021). However, it is not clear what particular events in terms of structural evolution have been dated by previous research. As detailed documentation and structural context of the dated samples are not available. Axial part of the shear zone is cut by the younger Mníchova Lehota fault zone.

The **Mníchova Lehota fault** (Slovak: *zlom Mníchovej Lehoty*), respectively the fault in direct continuation of the Strážov fault to the SW (*sensu* Elečko in Ivanička et al., 2011, Fig. 1) – this fault starts in the Mníchova Lehota and courses to the SW through the Selec village, where it deflects to the SSW and continues across the Prostredná and Krajná dolina valleys. In the area of Sevaldova kopanica it cuts the Hôrčanská dolina valley and is covered by the Fatricum south of Palkova kopanica settlement in the Hôrčanská dolina valley. This fault has not yet credited any important role. The NE segment of this fault was formerly interpreted as thrust of the mica schist basement of the eastern part of the block over the rocks of Kálnica Group (Ivanička et al., 2007). Despite the legitimacy of this interpretation, no signs of such contact are found in the area between the Selec and Mníchova Lehota villages (NE segment). This fault zone appears as an important structural boundary separating the crystalline basement and Carboniferous rocks from the Permian rocks of the Selec thrust (contact between the crystalline basement and so-called marginal succession of the Kálnica Group *sensu* Štimmel et al. (1984) in the region between Selec village and Hrádocká dolina valley. The fault is distinct as well in the DEM (Beták & Vojtko, 2009) and could be considered as relatively younger Neogene fault (AnD3-4).

Aims and methods

The main aim of this paper is to describe and define the kinematic character and timing of observed tectonic structures in the Selec Block of the Považský Inovec Mts. Study is based on the analysis and interpretation of the mesoscopic geological structures obtained during the fieldwork (Pelech, 2015). Classical methods of structural research were used to determine the kinematic character of deformation (e.g. Hanmer & Passchier, 1991; McClay, 1992; Pelech & Hók, 2017). Geological mapping was conducted at a scale 1 : 10 000, using standard GNSS instruments with an accuracy of +/– 5m. Location of important studied sites and boreholes is in the table 1. Most of the structural data were observed in the rocks of the Tatricum crystalline basement and autochthonous Upper Paleozoic and Mesozoic sedimentary cover as well as rocks of the Upper Cretaceous Horné Belice Group, Fatricum and Hronicum. Apart of the field data, the borehole data obtained by Uranium Exploration Comp. (Štimmel et al., 1984), the neotectonic analysis (Beták & Vojtko, 2009), and results of low temperature thermochronology (Kováč et al., 1994; Danišík et al., 2004; Králiková et al., 2016), as well as available geochronological data (Putiš et al., 2009, 2019, 2021; Kráľ et al., 2013) were integrated.

The deformation stages were designated according to their interpreted age and chronology as Variscan (VD) and Alpine (AD) as is standardly used in the Western Carpathians (eg., Plašienka & Marko, 1993; Madarás et al., 1994; Putiš et al., 2006, 2009; Vojtko & Kriváňová, 2024). XD labelling designation of orogenic cycles and their phases is based on method proposed by Németh (2021). This approach documents benefits from simultaneous use of both designation methodologies, allowing to reconstruct complicated multiphase orogenic & deformation evolution of studied regions.

The results and interpretation of structural research

The investigated area of the Selec Block could be divided into 3 main structural segments (Fig. 3) which differ in terms of quality and quantity of the structural record.

The **Eastern segment** (formerly the Železník unit *sensu* Maheľ, 1986); situated eastward of the Selec thrust and Mníchova Lehota fault) is characterized by dominance of the Tatric crystalline basement rocks and occurrence of the Upper Cretaceous flysch of the Horné Belice Group. The erosional remnants of Tatric sedimentary cover rocks, Fatricum and Hronicum complexes form only smaller part of the Eastern segment. The Eastern segment formerly represented the structurally higher unit relative to the Western and Central segment in the tectonic framework of the Selec Block.

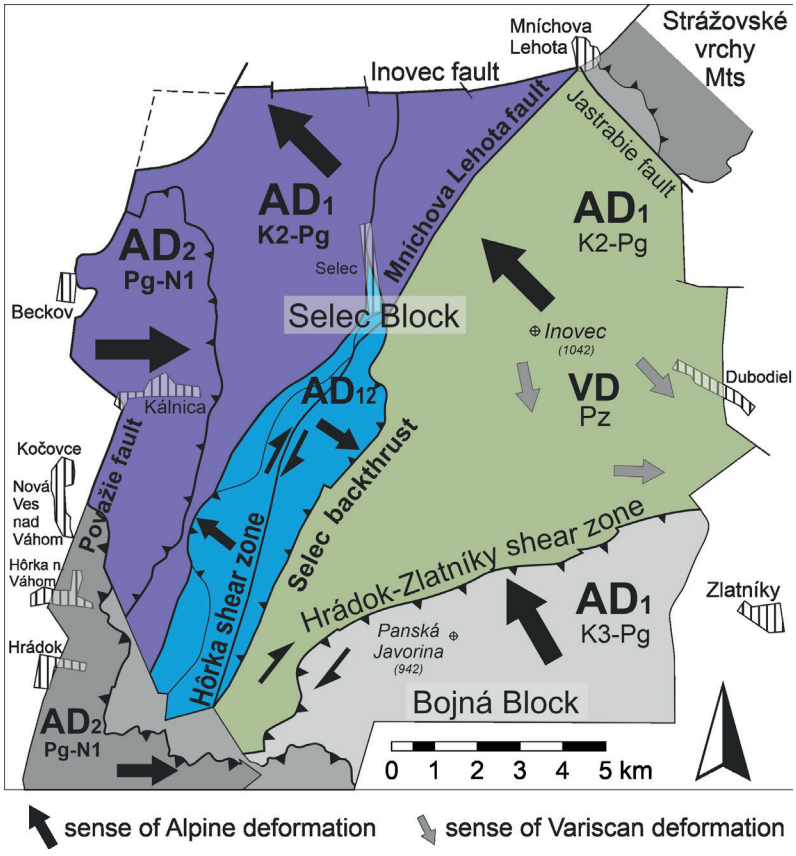

Fig. 3. Regional division of the Selec Block into 3 segments and naming of important regional tectonic features. Eastern segment is marked green, Central segment – blue and Western segment violet. The NW-vergent thrusts of Eastern and Western segments including their imbrication are interpreted to be Middle Cretaceous–Paleogene (in structural designation: AD_1 (or ApD1c sensu Németh, 2021). The dextral thrust of the Bojná Block (pale grey) along the Hrádok-Zlatníky shear zone on the Eastern segment is interpreted to be Late Cretaceous–Paleogene (AD1; ApD1c). East-vergent thrust (back-thrust) of westernmost zone within Western segment and units located more to the south (dark-grey colour), manifest relatively younger – Paleogene–Miocene thrusting and unroofing (AD_2; AnD1c, AnD2) are interpreted to be Neo-Alpine.

On contrary the **Western segment** (formerly the Drieňový vrch Monocline *sensu* Maheľ (1986); located west of the Selec thrust and Mníchova Lehota fault) is characterized by higher areal extent of Tatric sedimentary cover – the Upper Carboniferous and Permian rocks (Kálnica Group). The Tatric crystalline basement, Fatricum and Hronicum occur here as well, however are less frequent. So, the Western segment represents former Paleo-Alpine footwall structurally lower than Eastern segment.

The **Central segment** is represented by the Hôrka shear zone (formerly the Hôrka [tectonic] slices belt *sensu* Maheľ, 1986); located west of Selec thrust and east of longitudinaly irregular boundary approximately equivalent to westernmost occurrences of the Upper Carboniferous Novianska Formation. The zone is characterized by the predominance of Upper Paleozoic rocks of the Kálnica Group and several occurrences of crystalline basement, having similar structural record as the Western segment.

Bedding and metamorphic foliation

Eastern segment

The rock complexes of diaphtorites, mainly mica schists and gneisses, present in the eastern part of the Selec Block, show relatively uniform orientation of foliation, generally trending NE–SW, with dispersion between ENE–WSW to NNE–SSW, dipping generally to SE (Fig. 4). The diapthtoritic foliation generally copies the original bedding or schistosity of protolith. Current orientation of schistosity is a result of the Paleo-Alpine (Eoalpine) deformation (AD_1; ApD1c) which modified in various degrees the pre-existing Variscan diaphtoritic foliation.

Tab. 1

Location of important outcrops. Coordinates in S-JTSK system

Name	SJTSK X	SJTSK Y	Rocks	Structure or important notes	Figure
P40	–499580.5	–1213174.2	Sandstone, Krivosúd Fm.	Folded sandstone layer	Fig. 6E
P44	–501799.3	–1220204.4	Gneiss	Kink folds	Fig. 10A
P45	–502269.7	–1219604	Sandstones, Selec Fm.	Cleavage	Fig. 7A
P49	–507933.3	–1215981.7	Mica schist	Alpine folds in crystalline basement	Fig. 6D
P65	–500405.2	–1216243.5	Grey flysch, Rázová Fm.	Folded sandstone	Fig. 6G
P68	–499197.2	–1215900.4	Siliceous shales „Lazy Fm.“	Cleavage	Fig. 6F
P69	–497478.8	–1215464	Mica schists	Relics of separated hinges of folded quartz veins (Variscan)	Fig. 6C
P83	–508106	–1223528.6	Conglomerate, Novianska Fm.	Cleavage	Fig. 7D
P111	–499025.9	–1216822.1	Mica schists, gneiss	Alpine recumbent fold in the crystalline basement, Extensional kink bands, Character of mica schist and gneiss protolith	Fig. 6H, Fig. 10D
P124	–496388.1	–1218211.9	Mica schists, gneiss	Folded secretion quartz layers (Variscan)	
P133	–498421.9	–1222749.8	Mica schists	Folded secretion quartz layers (Variscan)	Fig. 6B
P143	–506843.1	–1224160.3	Sandstone, Selec Fm.	Compressional kink bands	Fig. 10C
P148	–504576.7	–1219262.6	Augen gneiss	Dextral sence of shear based on feldspar porphyroclasts, Hôrka shear zone	Fig. 7E
P310	–505487.6	–1218981.3	Conglomerates, Selec Fm.	Deformed conglomerate (dextral shear)	Fig. 7B
P313	–503012.1	–1220253.7	Sandstones, Selec Fm.	Folded quartz vein, mesocopic faults (slickensides)	Fig. 7C
P315	–502712.1	–1219927.1	Shales, Selec Fm.	Compressional kink bands	Fig. 10B
P403	–507716.9	–1224901.8	Augen gneiss	Dextral sence of shear based on feldspar porphyroclasts	Fig. 7F
P404	–507315.5	–1225012.6	Shales, Selec Fm.	Subvertical dip in the centre of the Hôrka shear zone	Fig. 7G
P406	–502040.7	–1216872.6	Mica schists	S/C structure	Fig. 7H

The Mesozoic and Upper Paleozoic rock complexes of the Tatric sedimentary cover unit located east of the block rest conformably with the strike of imbricated structures of crystalline basement and the Horné Belice Unit. Dip direction of olistholiths situated in the Horné Belice Group is conformal as well, whereby the dip to the SE dominates in all rock complexes (Fig. 4).

Western segment

The occurrences of crystalline basement rocks are less abundant in the western part of the Selec Block. They are composed mainly by augen gneisses, quartz paragneisses and lesser amount of mica schists. Here the trend of foliation is dominantly N–S to NW–SE, hence consistently with direction of the rock stripes (Fig. 5). Sedimentary and volcanic rocks of the Late Carboniferous and Permian age (Kálnica Group) are more abundant. The bedding planes are trending NNE–SSW and lesser in NNW–SSE direction. The bedding planes and metamorphic foliations are dipping to the west (Fig. 5). Important structural phenomenon is the flower-like arrangement with crystalline basement and Kálnica Group rocks located in the centre of the fan structure with nearly subvertical dip.

Western segment of the Selec Block is characterized with higher occurrence of Tatric Mesozoic rocks as well as the Mesozoic complexes of Fatricum and Hronicum. The Tatric sedimentary cover rocks are usually monoclinally dipping to the west. The Mesozoic rock sequence in the area between Beckov and Krivosúd-Bodovka villages is in overturned position (c.f. Ivanička et al., 2007). Overturned position is observed also in the Hronicum complexes of the Beckov castle rock (probably erosional remnant of larger overturned fold limb)

Folds and cleavage

The dispersion of the fold B-axis in the Selec Block is a result of polyphase deformation and interaction of Variscan and Alpine structures (Figs. 4 and 5). There is striking difference between the Eastern and Western segments.

The crystalline basement of the Eastern segment is dominated by E–W strike of B-axis and cleavage (Figs. 4 and 5A) which was pointed out as well by the previous studies (Putiš, 1983, 1986; Marko et al., 1990). E–W direction generally represents a result of Variscan deformation which was dominantly south-vergent (VD_1, Figs. 6A and C). Several localities (e.g. west of Inovec

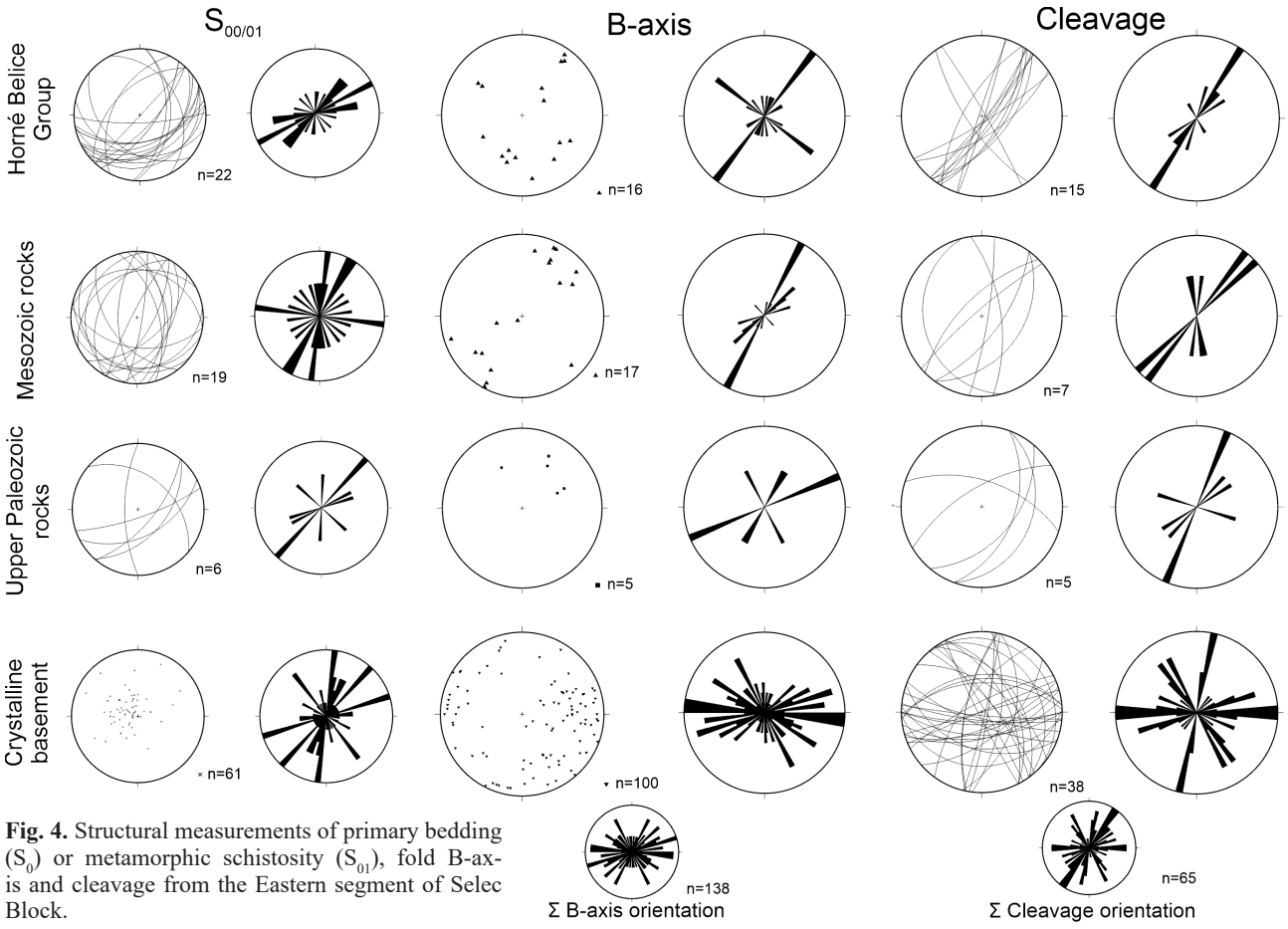

Fig. 4. Structural measurements of primary bedding (S_0) or metamorphic schistosity (S_{01}), fold B-axis and cleavage from the Eastern segment of Selec Block.

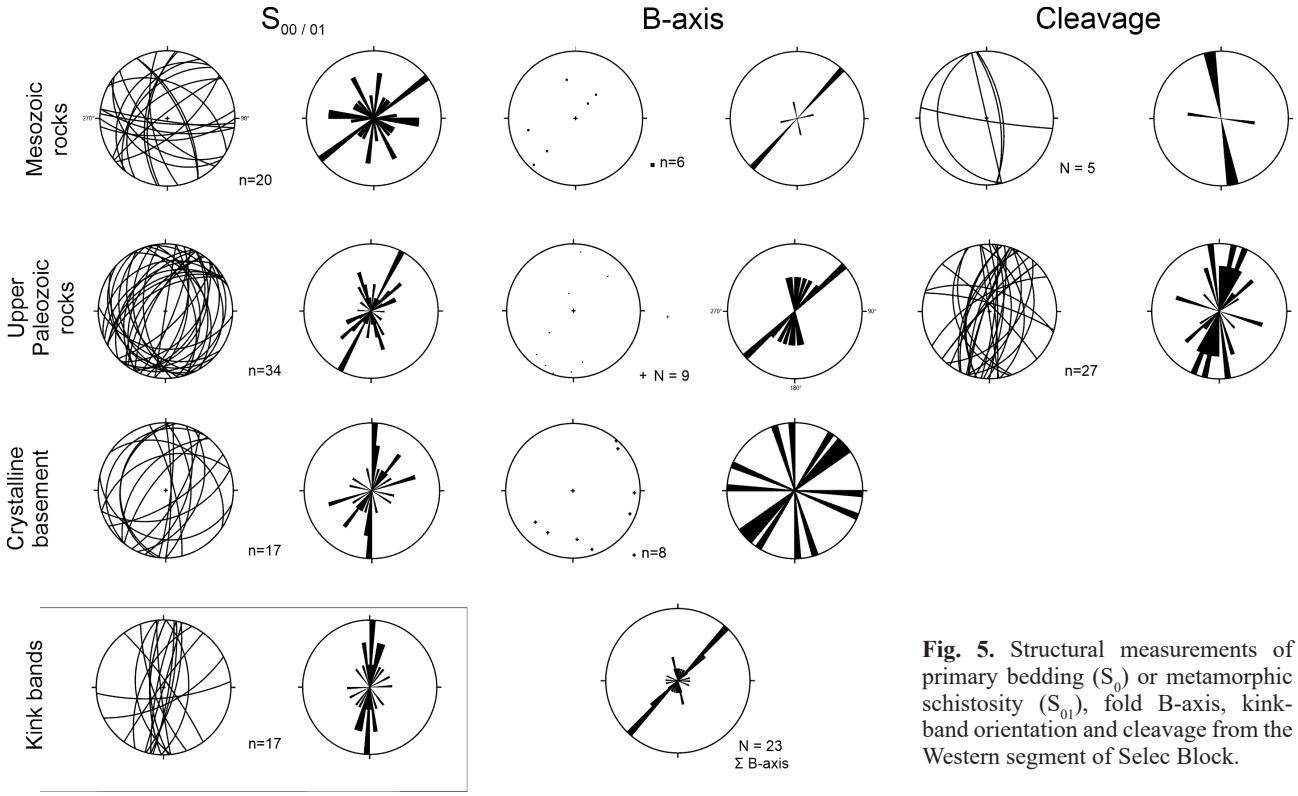

Fig. 5. Structural measurements of primary bedding (S_0) or metamorphic schistosity (S_{01}), fold B-axis, kink-band orientation and cleavage from the Western segment of Selec Block.

hill) within the crystalline basement outcrops show that E–W striking folds are affected by another deformation phase with E–W compression which resulted in restraining and formation of second generation of folds with N–S orientation of fold axis and vergence to the E (Fig. 6B). Such structures were not revealed in the Upper Paleozoic or Mesozoic complexes; and therefore, it is possible to regard them as Variscan. The N–S oriented structures related to E–W trending deformation, are missing in the other Western Carpathian areas, and therefore could be related to the VD_2 retrograde metamorphism dated to the period approx. 310.0 Ma (Kráľ et al., 2013).

The structural dataset from the Central and Western segment of the Selec Block is relatively small due to worse exposure conditions. It is especially true for the crystalline basement complexes where only few deformation structures were observed. The present observations so far show that the crystalline basement rocks were affected by Variscan deformation VD_1 responsible for E–W trending folds.

The whole Selec Block is characterized by the presence of the Alpine folds with NW-vergence and NE-SW orientation of fold axes (Figs. 4, 5, 6D-F and H). The fold B-axis in the Tatric sedimentary cover in the Eastern segment are oriented in NE–SW direction (Fig. 4).

The N-S trending folds axes and cleavage are dominating in the Central segment, present especially in the rocks of the Kálnica Group (Figs. 4, 7A, G, H). The N–S striking folds and cleavage are generally parallel to the elongated Kálnica Group occurrences and the N–S to NNE–SSW oriented branches of the Hôrka shear zone (Putiš, 1991; Madarás et al., 2007; Fig. 5). The region of the Hôrka shear zone is characterized for NNE–SSW orientation of metamorphic schistosity and primary sedimentary bedding (Fig. 8B). Orientation of the stretching lineation (Fig. 8A) as well as ductile kinematic indicators, primarily the sigmoidal deformed porphyroclasts, S-C structures and cleavage (Figs. 7B, D–H) indicate dextral (transpressional-transtensional) character of the shear zone. Prevailing structural record of Central and Western segment indicate presence of NW-vergent thrusting during the oldest deformation phase AD_1, occurring probably before the sedimentation of the Horné Belice Group (approx. 100 Ma, see Putiš et al., 2008, 2009, 2019, 2021), which is, however, missing in this region. Bivergent transpressional structures associated with the Hôrka shear zone probably occurred during this period as well.

The Selec thrust, as one of the most prominent tectonic structures in the Central segment, represents a brittle-ductile thrust with top to ESE-vergence which is very well marked by the borehole and surface data (Figs. 9 and 11; Štimmel et al., 1984). The thrust is located in the eastern margin of the shear zone, approx. between Hôrčanská dolina valley and Klenkov vrch hill, and represents the boundary between Eastern and Western segments of the Selec Block.

Fig. 6. A – South vergent (Variscan) parasitic folds within the limb of larger recumbent fold in the mica schists, NW of Inovec hill. **B** – Folded secretion quartz layers in mica schists with E vergence, Chotina valley. **C** – Relics of SE vergent secretion quartz veins in the mica schists, locality Vaškova chata (P124). **D** – NW-vergent folds in mica schists, brook SE of Beckov (P49). **E** – NW-vergent buckle fold in Permian sandstones of the Krivosúd Formation, Sedličiansky potok valley (P40). **F** – SE-dipping cleavage in the cherty shales ("Lazy Formation") olistolith in the Upper Cretaceous rocks of the Horné Belice Group, locality Lazy (P68). **G** – Non-cylindrical buckle fold in the Upper Cretaceous Rázová Formation of the Belice Unit, NNW of Hradisko hill (P65). **H** – NW vergent recumbent fold of crystalline basement in the hanging wall of the Upper Cretaceous Belice Unit, at the locality Hranty (P111).

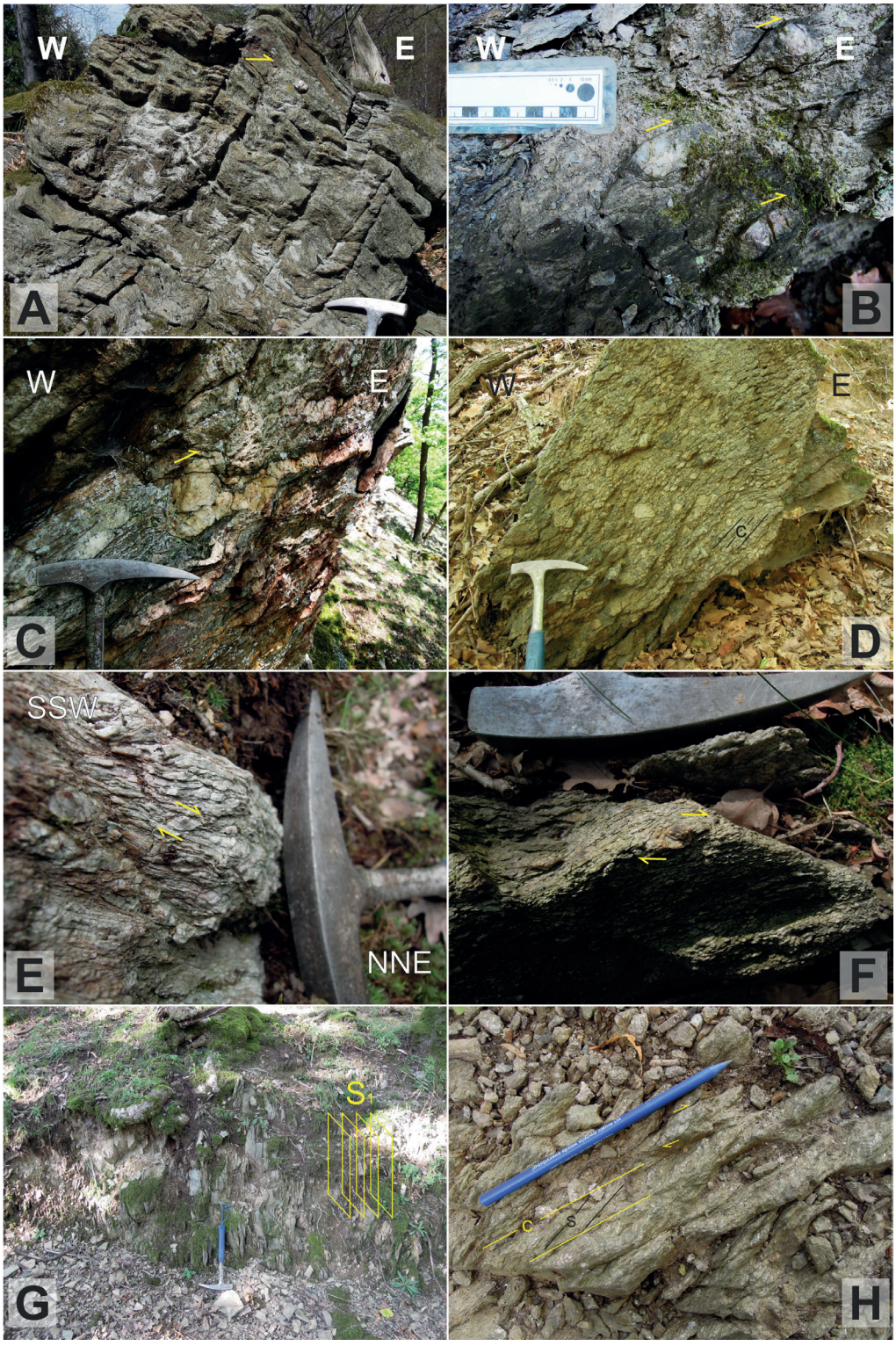

Fig. 7. A – W-dipping cleavage in Permian sandstones of Selec Formation, locality Nad Klenkovým vrchom (P45). **B** – Deformed quartz pebbles in sheared Permian conglomerate. Prostredná dolina valley (P310). **C** – Folded quartz vein with SE-vergence in the rocks of Permian Selec Formation, Prostredná dolina valley (P313). **D** – Cleavage in the conglomerates of the Novianska Fm., Hôrka valley (P83). **E** – Dextral shear in the pale augen paragneisses, Prostredná dolina valley (P148). **F** – Dextral shear in the pale augen paragneisses, locality Kopúnova kopanica, Hôrčanská dolina valley (P403). **G** – Subvertically dipping shales of Permian Selec Formation in the Hôrka shear zone, Holubací vrch hill (P404). **H** – S/C structures with apparent dextral shear sense in the mica schists, S of Selec (P406).

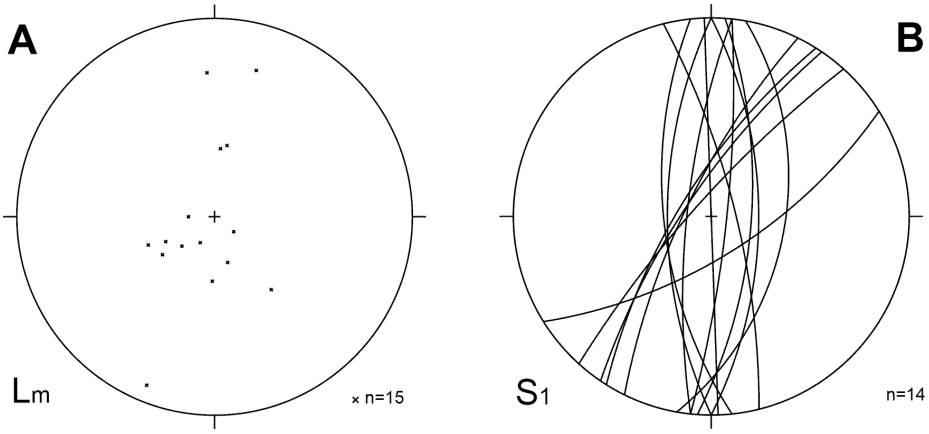

Fig. 8. Structural characteristics measured in the Hôrka shear zone. **A** – Orientation of mineral lineations collected in rocks of the Hôrka shear zone. **B** – Orientation of metamorphic foliation in the crystalline basement complexes and bedding of the Kálnica Group.

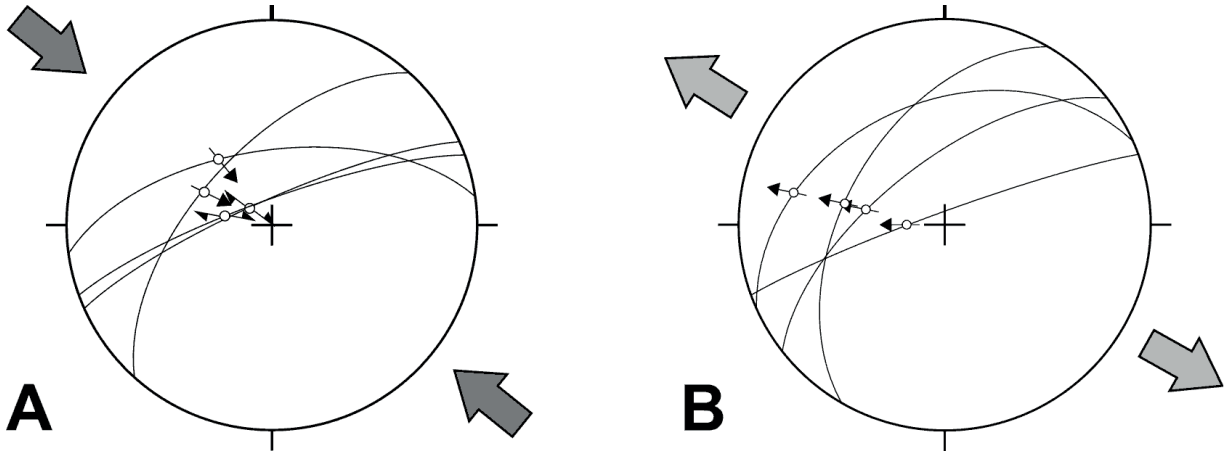

Fig. 9. A – Reverse faults of the Selec thrust related to AD_2 phase. **B** – Normal faults measured in the same area indicate unroofing. Measured at the Babia hora locality (P313).

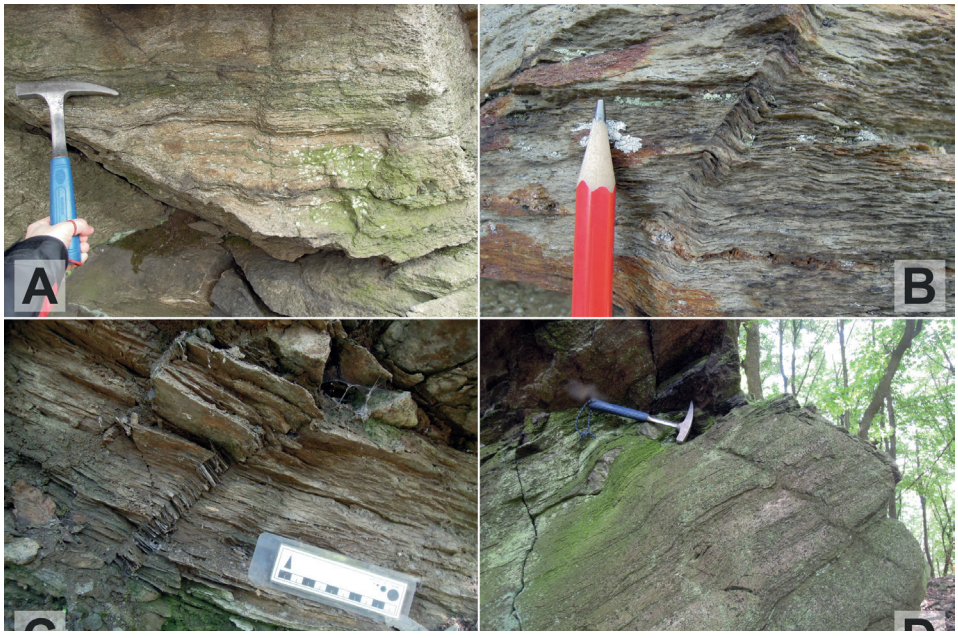

Fig. 10. A – Kink folds in the gneisses at the locality Pod Jakubovou (P44); **B** – Kink bands in the sandstones of the Selec Fm. (Lower Permian), Babia hora (P315); **C** – Kink bands in the sandstones and shales of the Selec Fm., Hôrčanská dolina valley (P143); **D** – Extensional kink bands related to Horné Belice Group exhumation, Hranty (P111).

Kink bands

Kink bands and kink folds, usually trending N–S or NNE–SSW, are very common in studied region (Fig. 5). Most of the previous studies (e.g. Putiš, 1986; Plašienka, 1995) associate them with the youngest deformation phases. The kink folds are found mainly in the strongly anisotropic Upper Paleozoic formations (Fig. 10) as well as foliated crystalline basement. Occurrences are scattered throughout the investigated area however strongly dominate in the Western segment.

Structural cross-sections

Cross-sections were constructed perpendicular to the observed structures in NW–SE or E–W directions applying our own structural data (Pelech, 2015), using issued official map (Ivanička et al., 2007) and with an important contribution of borehole data (summarized by Štimmel et al., 1984), to understand the complicated geological conditions west of the Selec thrust. Deformation is particularly expressive in the central part of the Selec Block affected by the Hôrka shear zone. Its manifestation in is the intense Paleo-Alpine ductile and brittle deformation of the crystalline rocks and the Kálnica Group, causing their subvertical to vertical arrangement (Figs. 7A and G). Evidence of the dextral shearing is provided mainly by the occurrences of crystalline basement rocks in the Hrádocká dolina valley (Kopúnova kopanica, Fig. 7E), Prostredná dolina valley (Pod Bielou hlinou, Fig. 7B) and in Selec village (Fig. 7H). The Paleo-Alpine structure is modified by younger Mníchova Lehota Fault.

Cross-section 1 follows the boreholes 814 (Kňažia Valley), 816, 812, 810, 806, enters the highest parts of Prostredná dolina Valley and ends at the locality Pod Jakubovou. The boreholes 816 and 812 demonstrate the structural position of the Novianska Formation and the adjacent crystalline basement complexes forming the recumbent overturned fold with northwestern vergence. Crystalline basement drilled by the borehole No. 810 represents core of the anticline, being dissected by the Mníchova Lehota fault and separated from the structurally higher complexes of the Selec thrust with eastern vergence (Fig. 7C). This segment of the Selec Thrust is built by 200 m thick body of Permian Selec and Krivosúd formations overlying the Triassic carbonates of Hradisko hill. Tectonic slice of the Upper Cretaceous Horné Belice Group cropping out from bellow the crystalline basement rocks is overlying the Triassic carbonates of the Hradisko hill in the upper part of the Prostredná dolina valley (Pelech et al., 2016).

Cross-section 2 starting in Kálnica, continuing parallel to the Prostredná dolina valley across the boreholes 811, 802, 724,742, 884, Kamenný krám ridge to the vicinity of Horné vápenice locality. The structure is dominated by the lower limb of an overturned north-vergent fold with rocks of the Novianska Formation and crystalline basement in its core, following the anticline documented in the cross-section 1. It is overlain from the west by two thick thrust sheets formed by carbonates of the Fatricum and, in particular, by a large body of diaphthorites exposed in the area south of Kálnica. The presence of east-vergent structures and the deformation of the hinge part of the anticline in the area of the mouth of the Prostredná dolina valley are documented by deformed conglomerate clasts and cleavage, visible in the rocks of the Selec Formation (Fig. 7B). The block of the Kálnica Group rocks in the hanging wall of the Selec thrust is thicker in the cross-section area and, according to borehole and surface information, deformed by west-vergent thrust faults that were formed during contraction after the backthrusts.

The southernmost **cross-section 3** passes through Novianska dolina valley, borehole No. 1110 to the Polámaný vrch hill. It demonstrates an imbricated structure with backthrust of crystalline basement rocks with rudimentarily preserved sedimentary cover over the Mesozoic, Permian and Carboniferous rocks of the Tatric sedimentary cover between the Babušina kopanica and Novianske kopanice localities. The central part of the section is dominated by an anticlinal fold structure of the Novianska Formation with crystalline basement rocks in its core, cut from the East by the Mníchova Lehota fault, which separates it from the body of Permian rocks in the hanging wall of the Selec thrust. The hanging wall of the Selec thrust is present in the borehole 1110 and is considerably thicker than in corss-sections 1 and 2. Surface and subsurface data do not confirm the presence of Mesozoic rocks of the Hradisko hill in the area.

Discussion

Transpression or two-phase deformation of Horné Belice Group

There are two views on the mode of formation of NW–SE trending "perpendicular" folds within the rocks of the Horné Belice Group (Fig. 3). Plašienka (1995) originally considered the perpendicular folds as kink folds and interpreted them as a result of the final stage of the closure of the former Belice Unit basin accompanied by transpression (AD_3 stage sensu Plašienka, l. c.). Later, Pešková (2011) considered folds of both directions as a single event resulting from inclined transpression (sensu Jones et al., 2004). According to the current knowledge, it cannot be clearly decided whether the transpression was ongoing throughout the AD_1 deformation event or represented only its final stage.

With respect to aforementioned, it is possible to distinguish 2 or 3 Alpine contractional tectonic events

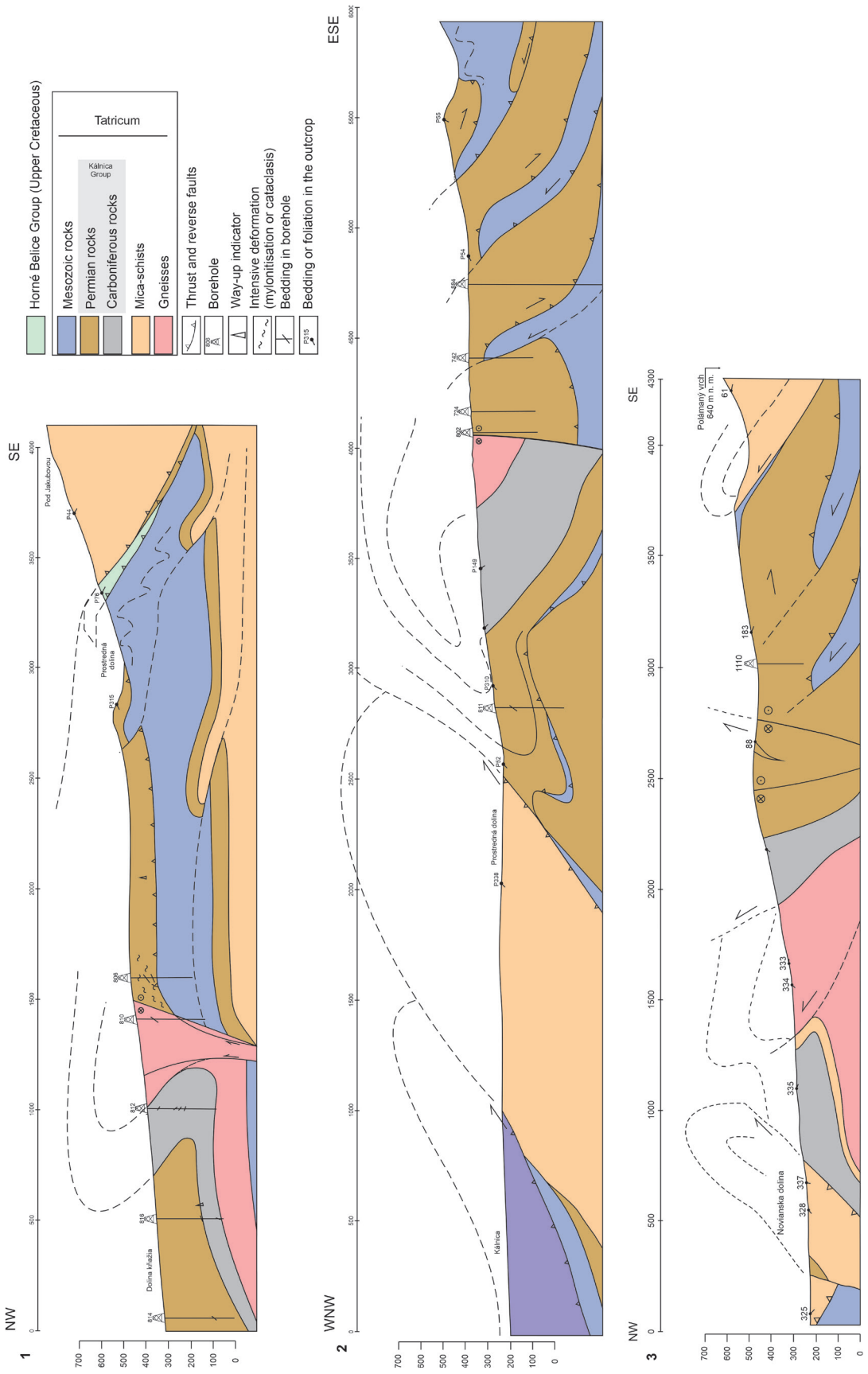

Fig. 11. Cross-sections 1, 2 and 3. For location see Fig. 1.

(ApD1c, AnD1c, AnD3) in the Selec Block. The presence of Cenomanian–Turonian Paleo-Alpine deformation (Hron phase *sensu* Plašienka, 2005), associated with the nappe emplacement of the Fatricum and Hronicum in this region, is not clear. Due to presence of Upper Cretaceous sequences of the Horné Belice Group as well as the occurrence of the Upper Cretaceous Hubina Formation in the Bojná Block (Pelech et al., 2017c), the nappe emplacement of the Fatricum and Hronicum occurred probably after Cretaceous/Paleocene boundary in the Považský Inovec Mts.

Kink folds

The kink folds are usually considered as generally low temperature deformation products (Anderson, 1964). Therefore, we consider their formation to be relatively younger and in shallower structural position within the Alpine deformation. Due to the increased presence of complexes with penetrative foliation within the rocks of the Selec Block, it is likely that the kink bands were formed in multiple stages of deformation. The compressional kink bads have predominantly N–S trend (Fig. 4) and are probably the result of the strong expression of second Alpine deformation AD_2 in the western part of the block and also the reorientation due to the activity of the Hôrka shear zone. At the same time, the similar orientation of the cleavage and kink bands indicates similar PT conditions and possible genetic relationship. The monoclinal and conjugate kink bands occurring in the rocks of the Kálnica Group represent an evidence of both – oblique and subhorizontal shortening. However, the genesis of kink folds within the basement rocks is apparently not uniform. Local kink bands are also associated with extensional structures in the overlying bodies of the Belice Unit showing signs of SE-vergent extension (ApD2) or possibly also Variscan.

The question of Infratatricum

The term *Infratatricum* was introduced by Putiš (1992) for the outer (northern in today's coordinates) margin of the Tatricum. However, it is important to remark, that no definition was provided in this paper. Only from the context and the Fig. 2 (ibid) one may get the message that the *Infratatricum* is represented by the crystalline basement of the Selec Block of the Považský Inovec Mts. The aim was to express the position of the Selec Block in the footwall of the typical Tatric Bojná Block; as well as the position above the Upper Cretaceous rock complexes (Horné Belice Group), which was designated as *Perivahicum* (no definition of this term was provided either). The definition or more precise spatial distribution of the aforementioned new terms was neither clearly expressed in the later works (cf. Korikovsky et al., 1995; Putiš et al., 2006, 2008, 2016 and 2021). The definition, however, appeared in the work of Plašienka et al. (1997, p. 141–145) as follows: *"The Infratatric units occur in the most external core mountains and include units as the Borinka and Orešany units in the Malé Karpaty Mts., Inovec nappe (Selec block) and*

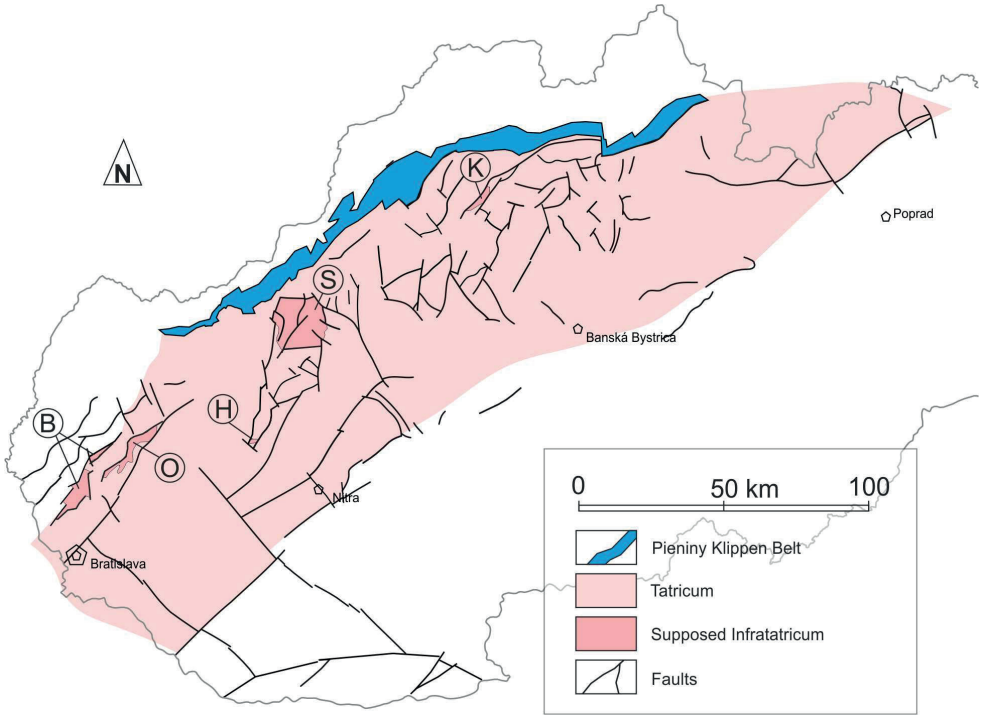

Fig. 12. Location of the Infratatricum occurrences within the Tatricum in the Western part of Slovakia: B – Borinka Unit, O – Orešany Unit, H – Hlohovec Unit, S – Selec Unit, K – Kozol Unit.

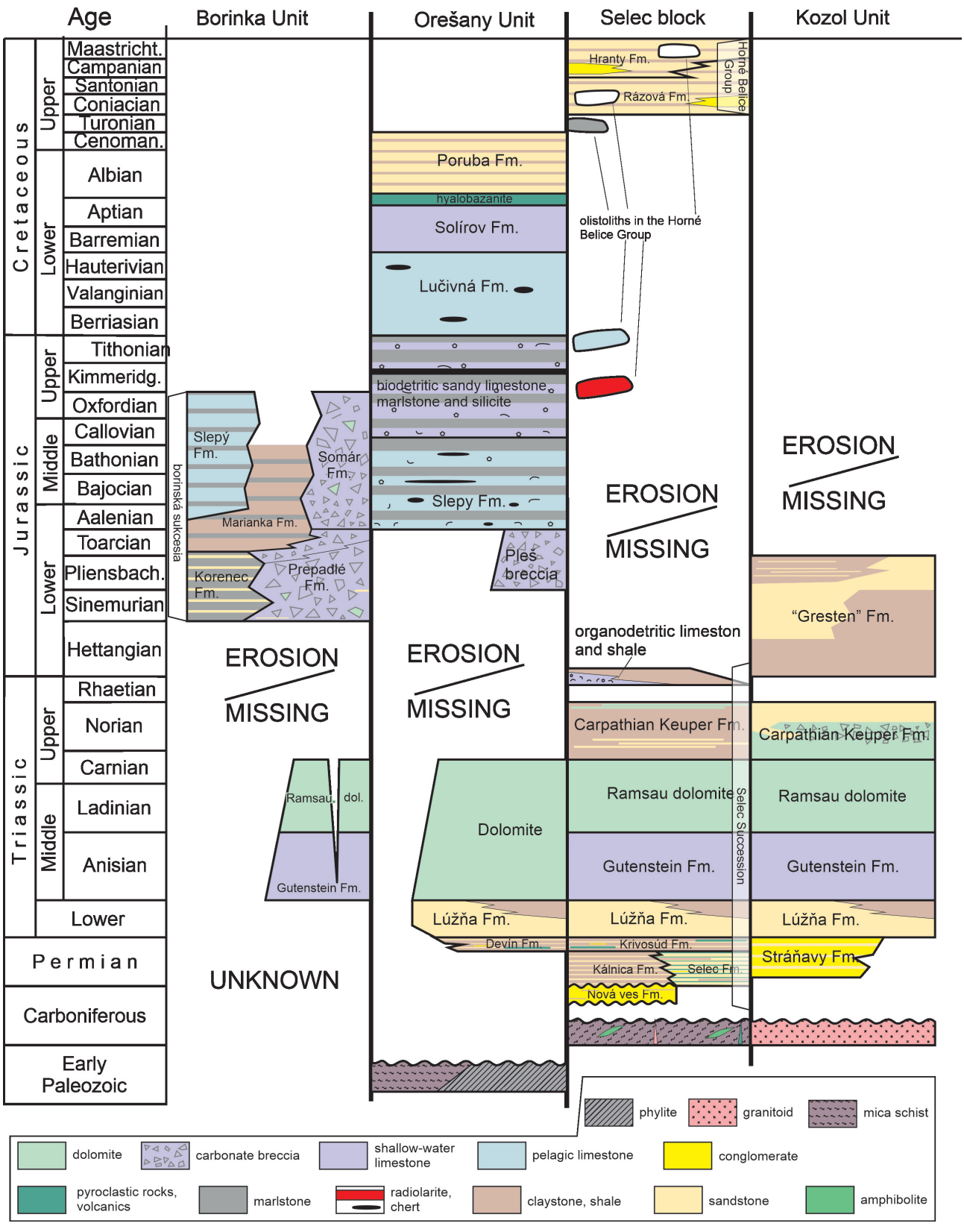

Fig. 13. Lithostratigraphic correlation scheme of supposed Infratatric units (based on Plašienka, 1987; Ivanička et al., 2011; Polák et al., 2012; Olšavský, 2007; Havrila & Olšavský, 2015).

Hlohovec nappe in the Považský Inovec Mts. and the Kozol unit in the Malá Fatra Mts." The characteristic features were: "*1) Pre-Alpine basement composed of low- to medium-grade metamorphics, less granitoids; 2) locally (Selec block, Kozol antiform) very thick Upper Paleozoic volcanosedimentary complexes are present; 3) deep erosion of the Triassic substratum during the two-phase Lower Jurassic rifting (Hettangian and Toarcian); 4) presence of syn-rift scarp breccias throughout the Jurassic, up to Lower Cretaceous (Borinka, Orešany and Inovec units); 5) the deepest structural position within the Tatric stack, below important regional thrust fault (Prepadlé shear zone between the Borinka unit and the Tatric Bratislava nappe, the Hrádok–Zlatniky thrust fault separating the Selec and Bojná blocks in the Považský Inovec Mts.); 6) regional low-grade metamorphism of cover sequences (Borinka unit, Selec block), complex internal structure either with dominating flattening and noncoaxial shearing (Borinka and Orešany units), or folding and imbrication (Selec block, Kozol unit); 7) partial resetting of K-Ar isotopic ages of pre-Alpine basement rocks within ductile-brittle shear zones (Malé Karpaty Mts.), which constrain the time of thrusting to the Late Cretaceous, confirmed by involvement of Senonian sediments and Krížna nappe rocks into the imbricated structure of the Selec block."* Later Plašienka (1999) excluded the Hlohovec block from the Infratatricum.

Recently, however, various authors have questioned the validity of the term Infratatricum for different regions (Pelech, 2015; Havrila & Olšavský, 2015; Hók et al., 2022). The common feature of Infratatricum is mainly the occurrence in the external Tatricum, intensive folding and presence in the footwall of the Tatric thrust sheets.

According to the latest study based on geological mapping in the Lúčanská zone of Malá Fatra Mts, the structure of so-called Kozol anticline was reinterpreted as an intensely imbricated Tatric monocline with overlying Fatricum and Hronicum (Havrila & Olšavský, 2015). There are no signs of overthrusting of Tatricum over the Kozol Unit. The Orešany Unit in the Malé Karpaty Mts is overthrust by Fatricum. The contact with the Modra Massif is usually interpreted as thrust of the crystalline basement of Tatric Modra Massif (Polák et al., 2011). However, the structural evidence is missing and contact could be interpreted alternatively as normal fault or backthrust.

Considering lithostratigraphic correlation of the studied sequences, the supposed Infratatricum does not show any material continuity (Figs. 12 and 13). The Jurassic olistostrome of the Borinka Unit (Plašienka, 1987; Polák et al., 2012) is not comparable with any other Tatric unit. Likewise, the correlation of the Orešany Unit (Michalík et al., 1991; Polák et al., 2012) with the the Selec or Kozol units is very difficult to impossible. There is also considerable difference between the Selec or Kozol units. Despite both contain the Upper Palaeozoic rocks, the thickness, stratigraphic range and lithologic variability is much higher in the Selec Unit (the Kálnica Group; Olšavský, 2008; Havrila & Olšavský, 2015). The presence of the Upper Cretaceous sequence is unique only for the Považský Inovec Mts. However, the occurrence was documented in all 3 blocks including supposed Infratatricum (Selec and Hlohovec blocks, Ivanička et al., 2007) as well in the Bojná Block (Pelech et al., 2017c), which is uniformly considered as Tatric (e.g. Plašienka, 1999; Ivanička et al., 2011). The unification of the all-aforementioned units into one tectonic unit, or sub-unit cannot be considered appropriate or necessary. The unique structure of the Selec Block points to fact that it undoubtedly represents the most external part of the Tatricum.

Conclusions

The paper gives a new insight into the structural evolution of the Selec Block of the Považský Inovec region, being documented by numerous structural measurements.

The Variscan deformation of the Selec Block was south-vergent and probably had several phases, the final one (ca. 310 Ma) of which was accompanied by extensive retrograde metamorphism (Kráľ et al., 2013). N–S compression VD_1 was dominant, generating numerous fold structures in the basement rocks (Figs. 6A and C). The Alpine deformation of the Selec Block occurred in 2 or 3 phases and was obviously bivergent in kinematics. The first was the Paleo-Alpine phase AD_1 (ApD1), when the Tatric basement complexes and their sedimentary cover, together with the rocks of the Horné Belice Group, were displaced towards the NW. Observations suggest that the NW-SE convergence was not perpendicular but also had elements of transpression. The nature of the deformation can be traced throughout the whole Selec Block area. However, on the basis of the present knowledge, it cannot be entirely excluded that the deformation during AD_1 was already of a bivergent character, and resulted in the formation of the Hôrka shear zone (in orogenic phase ApD3). Based on geochronological and stratigraphic evidence, especially the wedge-top provenance of the Horné Belice Group, the age of the AD_1 deformation phase is post Late Cretaceous, probably Paleogene (Maheľ & Kullmanová, 1975; Štimmel at al., 1984; Kováč et al., 1994; Putiš et al., 2009; Ivanička et al., 2007; Pelech et al., 2016, 2017b, c).

The second phase of deformation (AD_2) is represented by the km-scale E and SE-vergent backthrusts of the Tatric crystalline basement and sedimentary cover rocks as well as of the Hronic and Fatric rocks. Their presence is confirmed only in the western part of the mountain range, both within the Selec Block and in more southern areas (Pešková, 2011). The reverse thrusts, especially the Selec

thrust, are documented by both drilling (Štimmel et al., 1984, Fig. 13 ibid) and structural research (Figs. 7A–C). Their origin is probably related to the oblique collision of the Internal West Carpathian Block with the Bohemian Massif during the Oligocene to the Lower Miocene (Jiříček, 1979). The presence of the backthrusts is related to a broader zone extending from the Vienna Basin to Malá Fatra Mts (Sentpetery, 2011; Pešková et al., 2012; Pelech et al., 2018; Pelech & Olšavský, 2018; Olšavský & Pelech, 2021).

Significant exhumation that took place in the Selec Block in the area of the backtrust crystalline sheets and on the Mníchova Lehota Fault is documented by young AFT ages of 13–14 Ma (Danišík et al., 2004; Králiková et al., 2016). It indicates Neo-Alpine exhumation process (AnD2 to AnD4 *sensu* Németh, 2021).

Acknowledgements

Authors express their thanks to Ministry of Environment of the Slovak Republic for funding regional geological research projects, and simultaneously to Slovak Research and Development Agency (APVV) funding grant No. APVV-21-281 (*Alpine geodynamic evolution of the inner zones of the Western Carpathians*). Valuable comments of the reviewer Ľ. Gazdačko (ŠGÚDŠ) and another anonymous reviewer have improved the quality of the original manuscript. This paper is also a contribution of the State Geological Institute of Dionýz Štúr (ŠGÚDŠ), Slovakia, for the EC – CINEA HORIZON-CL5-2021-D3-D2 project 101075609 Geological Service for Europe (GSEU) within WP6 – Geological framework for the European geological data & information system.

References

Anderson, T. B., 1964: Kink-bands and related geological structures. *Nature, 202, 272–274.*

Beták, J. & Vojtko, R., 2009: Implementácia nástrojov tektonickej geomorfológie a v neotektonickom výskume (na príklade pohoria Považský Inovec). *Geografický časopis, 61, 29–47.*

Danišík, M., Dunkl, I., Putiš, M., Frisch, W. & Kráľ, J., 2004: Tertiary burial and exhumation history of basement highs along the NW margin of the Pannonian basin – an apatite fission track study. *Austrian Journal of Earth Sciences, 95/96, 60–70.*

Elečko, M. (ed.), Polák, M., Fordinál, K., Bezák, V., Ivanička, J., Mello, J., Konečný, V., Šimon, L., Nagy, A., Potfaj, M., Maglay, J., Broska, I., Buček, S., Gross, P., Havrila, M., Hók, J., Kohút, M., Kováčik, M., Madarás, J., Olšavský, M., Pristaš, J., Salaj, J. & Vozárová, A., 2008: Prehľadná geologická mapa Slovenskej republiky. List 35 Trnava 1 : 200 000. *Bratislava,* Š*GÚDŠ.*

Hanmer, S. & Passchier, C., 1991: Shear-sence indicators. A review. *Geological Survey of Canada Paper, 90-17, 1–72.*

Havrila, M. & Olšavský, M., 2015: Správa o geologickom mapovaní vrstvového sledu Kozla medzi Turskou dolinou a údolím Porubského potoka. *Geologické práce, Správy*, *127, 7–79.*

Hók, J., Pelech, O., Teťák, F., Németh, Z. & Nagy, A., 2019: Outline of the geology of Slovakia (W. Carpathians). *Mineralia Slovaca, 51, 1, 31–60.*

Hók, J., Schuster, R., Pelech, O., Vojtko, R. & Šamajová, L., 2022: Geological significance of Upper Cretaceous sediments in deciphering of the Alpine tectonic evolution at the contact of the Eastern Alps, Bohemian Massif and Western Carpathians. *International Journal of Earth Sciences (Geol. Rundschau), 111, 6, 1805–1822.* https://doi.org/10.1007/s00531-022-02201-5.

Ivanička, J., Havrila, M., Kohút, M. (eds.), Olšavský, M., Hók, J., Kováčik, M., Madarás, J., Polák, M., Rakús, M., Filo, I., Elečko, M., Fordinál, K., Maglay, J., Pristaš, J., Buček, S., Šimon, L., Kubeš, P., Scherer, S. & Zuberec, J., 2007: Geologická mapa Považského Inovca a jv. časti Trenčianskej kotliny, M = 1 : 50 000. *Bratislava, ŠGÚDŠ.*

Ivanička, J., Kohút, M. (eds.), Olšavský, M., Havrila, M., Hók, J., Kováčik, M., Madarás, J., Polák, M., Rakús, M., Filo, I., Elečko, M., Fordinál, K., Maglay, J., Pristaš, J., Buček, S., Šimon, L., Kubeš, P., Scherer, S. & Zuberec, J., 2011: Vysvetlivky ku Geologickej mape regiónu Považský Inovec a jv. časť Trenčianskej kotliny, M = 1 : 50 000. *Bratislava, ŠGÚDŠ, 389 p.*

Jiříček, R., 1979: Tektogenetický vývoj karpatského oblouku během oligocénu a neogénu. In: Maheľ, M.: Tektonické profily Západných Karpát. *Bratislava, GÚDŠ, 203–213.*

Jones, R. R., Holdsworth, R. E., Clegg, P., McCaffrey, K. & Tavarnelli, E., 2004: Inclined transpression. *Journal of Structural Geology, 26, 1531–1548.* https://doi.org/10.1016/j.jsg.2004.01.004.

Kamenický, J., 1956: Zpráva o geologickom výskume a mapovaní severnej časti kryštalinika Považského Inovca. *Geologické práce, Zpr*ávy, *8, 110–124.*

Korikovsky, S. P., Putiš, M., Plašienka, D., Jacko, S. & Ďurovič, V., 1997: Cretaceous very low-grade metamorphism of the InfraTatricum and SupraTatricum domains: an indicator of thin-skinned tectonics in the central Western Carpathians. In: Grecula, P., Hovorka, D. & Putiš, M. (eds.): Geological evolution of the Western Carpathians. *Bratislava, Mineralia Slovaca – Monograph., 89–106.*

Kováč, M., Kráľ, J., Márton, E., Plašienka, D. & Uher, P., 1994: Alpine uplift history of the Central Western Carpathians: geochronological, paleomagnetic, sedimentary and structural data. *Geologica Carpathica, 45, 2, 83–96.*

Kráľ, J., Hók, J., Bachliński, R. & Ivanička, J., 2013: Rb/Sr a ^{40}Ar/^{39}Ar údaje z kryštalinika Považského Inovca (Západné Karpaty). *Acta Geologica Slovaca, 5, 2, 195–210.*

Králiková, S., Vojtko, R., Hók, J., Fügenschuh, B. & Kováč, M., 2016: Low-temperature constraints on the Alpine thermal evolution of the Western Carpathian basement rock complexes. *Journal of Structural Geology, 91, 144–160.* https://doi.org/10.1016/j.jsg.2016.09.006.

Kullmanová, A. & Gašpariková, V., 1982: Vrchnokriedové sedimenty v severnej časti pohoria Považský Inovec. *Geologické práce, Spr*ávy, *78, 85–95.*

Leško, B., Šutora, A. & Putiš, M., 1988: Geology of the Považský Inovec Horst based on geophysical investigation. *Geologický zborník – Geologica Carpathica, 39, 2, 195–216.*

Madarás, J., Putiš, M. & Dubík, B., 1994: Štruktúrna charakteristika stredného úseku pohorelskej tektonickej zóny. *Mineralia Slovaca, 26, 177–191.*

Madarás, J., Olšavský, M., Siman, P. & Hók, J., 2007: Imbrikovaná stavba kryštalinika a sedimentárneho obalu sz. časti seleckého bloku Považského Inovca. In: Plašienka, D., Németh, Z., Šimon, L., Iglárová, Ľ. a Magálová, D. (eds.): 5. výročný predvianočný seminár Slovenskej geologickej spoločnosti. *Mineralia Slovaca, Geovestník, 14.*

Maheľ, M., 1986: Geológia Československých Karpát 1. Paleoalpínske jednotky. *Bratislava, Veda, 510 p.*

Marko, F., Hacura, A., Janták, V. & Plašienka, D., 1990: Geologická stavba a štruktúrne vzťahy v strednej časti Považského Inovca. Čiastková záverečná správa za úlohu II-4-5/01 ŠPZV Geologická stavba Malých Karpát, Považského Inovca a priľahlých území. *Manuscript. Bratislava, archive of Geological Inst. Slovak Acad. Sci., 85 p.*

McClay, K. R., 1992: The Mapping of Geological Structures. *Chichester, John Wiley, 161 p.*

Miháľ, F., 2003: Geologická stavba severnej časti Považského Inovca na základe výsledkov vyhľadávacieho prieskumu na rádioaktívne suroviny v rokoch 1972 – 1983. *Manuscript. Bratislava, archive of SGIDŠ (arch. n. 86922), 48 p.*

Michalík, J., Reháková, D. & Soták, J., 1994: Environments and setting of the Jurassic/Lower Cretaceous succession in the Tatri area, Malé Karpaty Mts. *Geologica Carpathica, 45, 1, 45–56.*

Németh, Z., 2021: Lithotectonic units of the Western Carpathians: Suggestion of simple methodology for lithotectonic units defining, applicable for orogenic belts world-wide. *Mineralia Slovaca, 53, 2, 81–90.*

Olšavský, M., 2008: Litostratigrafia a sedimentogenéza vrchnopaleozoických súvrství v severnej časti Považského Inovca. *Mineralia Slovaca, 40, 1–16.*

Olšavský, M. & Pelech, O., 2021: Nový výskyt brekcií a zlepencov asociujúcich so spätnými prešmykmi v oblasti Nitrických vrchov (juhovýchodná časť Strážovských vrchov). *Geologické práce, Správy, 137, 13–30.*

Pelech, O., 2015: Kinematická analýza tektonických jednotiek Považského Inovca. Dizertačná práca. *Manuscript. Bratislava, archive of Department of geology and paleontology, 166 p.* http://opac.crzp.sk/?fn=detailBiblioForm&sid=C2BA1884BE5254848992F6495C76

Pelech, O., Hók, J., Pešková, I. & Havrila, M., 2016: Structural position of the Upper Cretaceous sediments in the Považský Inovec Mts. (Western Carpathians). *Acta Geologica Slovaca, 8, 1, 43–58.*

Pelech, O. & Hók, J., 2017: Metodika mezoskopického štúdia strižných zón a jej aplikácia pri kinematickej analýze hrádocko-zlatníckej strižnej zóny v Považskom Inovci. *Geologické práce, Správy, 130, 47 – 67.*

Pelech, O., Hók, J., Havrila, M. & Pešková, I., 2017a: Reply to Comment on "Structural position of the Upper Cretaceous sediments in the Považský Inovec Mts. (Western Carpathians)". *Acta Geologica Slovaca, 9, 1, 39–43.*

Pelech, O., Kušnirák, D., Bošanský, M., Dostál, I., Putiška, R. & Hók, J., 2017b: The resistivity image of Upper Cretaceous Horné Belice Group, a case study from the Hranty area (Považský Inovec Mts., Western Carpahians). *Contributions Geophys. and Geodesy, 47, 1, 21–36.*

Pelech, O., Hók, J. & Józsa, Š., 2017c: Turonian-Santonian sediments in the Tatricum of the Považský Inovec Mts. (Internal Western Carpathians, Slovakia). *Austrian Journal of Earth Sciences, 110, 1, 19–33.*

Pelech, O. & Olšavský, M., 2018: Post-early Eocene backthrusting in the northeastern Strážovské vrchy Mts. (Western Carpathians). *Mineralia Slovaca, 50, 2, 147–156.*

Pelech, O., Józsa, Š. & Fajdek, P., 2018: Fold deformation of Fatricum – a case study from Banka section (Považský Inovec Mts., Slovakia). *Mineralia Slovaca, 50, 1, 25–36.*

Pelech, O., Boorová, D., Hók, J. & Rakús, M., 2021: Upper Cretaceous limestone olistoliths in the Rázová Formation (Horné Belice Group), Považský Inovec Mts (Slovakia). *Mineralia Slovaca, 53, 1, 39–48.*

Pešková, I., 2011: Tektonická interpretácia západného úseku kontaktnej zóny externíd a internid Západných Karpát. Dizertačná práca. *Manuscript. Bratislava, Archive of Department of geology and paleontology, 94 p.*

Pešková, I., Hók, J., Potfaj, M. & Vojtko, R., 2012: Štruktúrna interpretácia varínskeho a oravského úseku bradlového pásma. *Geologické práce, Správy, 120, 51–64.*

Plašienka, D., 1987: Litologicko-sedimentologický a paleotektonický charakter borinskej jednotky v Malých Karpatoch. *Mineralia Slovaca, 19, 3, 217–230.*

Plašienka, D., 1995: Pôvod a štruktúrna pozícia vrchnokriedových sedimentov v severnej časti Považského Inovca. Druhá časť: Štruktúrna geológia a paleotektonická rekonštrukcia. *Mineralia Slovaca, 27, 179–192.*

Plašienka, D., 1999: Tektochronológia a paleotektonický model jursko-kriedového vývoja centrálnych Západných Karpát. *Bratislava, Veda, 125 p.*

Plašienka, D., 2005: Tektonický vývoj Západných Karpát počas mezozoika. *Mineralia Slovaca, 37, 3, 179–184.*

Plašienka, D. & Marko, F., 1993: Geologická stavba strednej časti Považského Inovca. *Mineralia Slovaca, 25, 1, 11–25.*

Plašienka, D., Marschalko, R., Soták, J., Peterčáková, M. & Uher, P., 1994: Pôvod a štruktúrna pozícia vrchnokriedových sedimentov v severnej časti Považského Inovca. Prvá časť: Litostratigrafia a sedimentológia. *Mineralia Slovaca, 26, 311–334.*

Plašienka, D., Havrila, M., Michalík, J., Putiš, M. & Reháková, D., 1997: Nappe structure of the western part of the Central Carpathians. In: Plašienka, D., Hók, J., Vozár, J. & Elečko, M. (eds.): Alpine evolution of the Western Carpathians and related areas. Abstracts & Introductory Articles to the Excursion, Bratislava, Slovakia, September 11 – 14th. *Bratislava, Dionyz Stur Publishers, 139–161.*

Plašienka, D., Putiš, M., Soták, J. & Méres, Š., 2017: Are we still far from a reliable solution? *Acta Geologica Slovaca, 9, 1, 35–38.*

Polák, M. (ed.), Plašienka, D., Kohút, M., Putiš, M., Bezák, V., Filo, I., Olšavský, M., Havrila, M., Buček, S., Maglay, J., Elečko, M., Fordinál, K., Nagy, A., Hraško, Ľ., Németh, Z., Ivanička, J. & Broska, I., 2011: Geologická mapa Malých Karpát 1 : 50 000. *Bratislava, MŽP SR – ŠGÚDŠ.*

Polák, M. (ed.), Plašienka, D., Kohút, M., Putiš, M., Bezák, V., Maglay, J., Olšavský, M., Havrila, M., Buček, S., Elečko, M., Fordinál, K., Nagy, A., Hraško, Ľ., Németh Z., Malík, P., Liščák, P., Madarás, J., Slavkay, M., Kubeš, P., Kucharič, Ľ., Boorová, D., Zlinská, A., Siráňová, Z. & Žecová, K., 2012: Vysvetlivky ku geologickej mape regiónu Malé Karpaty 1 : 50 000. *Bratislava, ŠGÚDŠ, 287 p.*

Putiš, M., 1980: Succesion of tectonic structures in crystalline and envelope Paleozoic of the Považský Inovec Mts. *Geologický zborník – Geologica Carpathica, 31, 4, 619–625.*

Putiš, M., 1983: Outline of geological-structural development of the crystalline complex and envelope Paleozoic of the Považský Inovec Mts. *Geologický zborník – Geologica Carpathica, 34, 4, 457–482.*

Putiš, M., 1986: Príspevok k poznaniu mladšieho paleozoika Považského Inovca. *Geologické práce, Správy*, *84, 65–83.*

Putiš, M., 1991: Geology and petrotectonics of some shear zones in the Western Carpathian crystalline complexes. *Mineralia Slovaca, 23, 459–473.*

Putiš, M., 1992: Variscan and Alpidic nappe structures of the Western Carpathians crystalline complexes. *Geologica Carpathica, 43, 6, 369–380.*

Putiš, M., Gawlick, H. J., Frisch, W. & Sulák, M., 2008: Cretaceous transformation from passive to active continental margin in the Western Carpathians as indicated by the sedimentary record in the InfraTatricum unit. *Int. Journal of Earth Sciences (Geol. Rundsch.), 97, 4, 799–819.*

Putiš, M., Frank, W., Plašienka, D., Siman, D., Sulák, M. & Biroň, A., 2009: Progradation of the Alpidic Central Western Carpathians orogenic wedge related to two subduction: constrained by $^{40}Ar/^{39}Ar$ ages of white micas. *Geodyn. Acta, 22, 1–3, 31–56.*

Putiš, M., Danišík, M., Siman, P., Nemec, O., Tomek, Č. & Ružička, P., 2019: Cretaceous and Eocene tectono-thermal events determined in the Inner Western Carpathians orogenic front Infratatricum. *Geol. Quarterly, 63, 2, 1–47.*

Putiš, M., Nemec, O., Danišík, M., Jourdan, F., Soták, J., Tomek, Č., Ružička, P. & Molnárová, A., 2021: Formation of a Composite Albian-Eocene Orogenic Wedge in the Inner Western Carpathians: P-T Estimates and $^{40}Ar/^{39}Ar$ Geochronology from Structural Units. *Minerals, 11, 988.* https://doi.org/10.3390/min11090988.

Sentpetery, M., 2011: South-vergent structures observed in the western part of the Krivánska Fatra Mts. (Central Western Carpathians). *Acta Geologica Slovaca, 3, 2, 123–129.*

Štimmel, I., Máťuš, J., Novotný, L., Miháľ, F., Gluch, A., Gregorovič, J., Daniel, J., Cicmanová, S., Šimko, A. & Mlynarčík, L., 1984: Záverečná správa o geologicko-prieskumných prácach v oblasti Považského Inovca v rokoch 1965 – 1983. *Manuscript. Bratislava, archive of SGIDŠ (arch. no. 58751), 220 p.*

Vojtko, R. & Kriváňová, K., 2024: Cretaceous collision and thrusting of the Veporic Unit onto Tatric Unit in the Nízke Tatry Mts. revealed from structural analysis. *Acta Geologica Slovaca, 16, 1, 19–31.*

Štruktúrny vývoj seleckého bloku v Považskom Inovci a problematika infratatrika v Západných Karpatoch

Jadrové pohorie Považský Inovec je tradične rozdelené na tri bloky (Maheľ, 1986) líšiace sa nerovnomerným výskytom litotektonických jednotiek Vnútorných Západných Karpát. Objektom podrobného štruktúrneho výskumu bol selecký blok (obr. 1) situovaný na severe pohoria, ktorý sa vyznačuje najkomplexnejšou geologickou stavbou vrátane sedimentov mladšieho paleozoika (kálnická skupina *sensu* Štimmel et al., 1984; Miháľ, 2006; Olšavský, 2008) a vrchnej kriedy (hornobelická skupina *sensu* Rakús in Ivanička et al., 2011; Kullmanová a Gašpariková, 1982; Plašienka et al., 1994; Pelech et al., 2016, 2021), výnimočných v stavbe jadrových pohorí.

V rámci seleckého bloku boli definované variské a alpínske deformačné štruktúry. Variská deformácia (VD_1) sa vyznačuje kompresiou v smere S – J a vznikom juhovergentných štruktúr (obr. 6A a C). Štruktúrne pretvorenie bolo sprevádzané retrográdnou metamorfózou hornín kryštalinika (Kráľ et al., 2013).

Prvá fáza alpínskej deformácie (AD_1) postihla horninové komplexy tatrika vrátane sedimentov hornobelickej skupiny, ktoré boli presunuté smerom na SZ. Prvú fázu (AD_1) alpínskej deformácie je možné datovať do obdobia mástrichtu až paleocénu. Poukazujú na to biostratigrafické údaje vrchnokampánskeho veku z blokov (olistolitov) pelagických vápencov v sedimentoch tektonickej melanže hornobelickej skupiny (Pelech et al., 2021).

Druhú fázu alpínskej deformácie (AD_2) reprezentujú rozsiahle vrásy horninových súborov tatrika, fatrika a hronika s vergenciou na východ až severovýchod. Spätné presuny (najmä selecký spätný prešmyk) sú zdokumento-

vané výsledkami vrtných prác (Štimmel et al., 1984, obr. 13 ibid.), ako aj štruktúrnym výskumom (obr. 7A – C). Ich vznik pravdepodobne súvisí so šikmou kolíziou bloku Vnútorných Západných Karpát s Českým masívom počas oligocénu až spodného miocénu. Zároveň treba poznamenať, že spätné presuny mohli lokálne vznikať aj v transpresnom režime (AD_1), ako je to v prípade hôrčanskej strižnej zóny (obr. 3).

Posledná alpínska deformácia je spätá s neoalpínskou fázou, ktorá súvisí s výraznou exhumáciou seleckého bloku. Dokumentujú to AFT údaje o veku 13 – 14 Ma (Danišík et al., 2004; Králiková et al., 2016).

Na základe získaných údajov selecký blok v Považskom Inovci nie je možné považovať za súčasť infratatrika (*sensu* Putiš, 1992; Plašienka, 1997), podobne, ako je to v ostatných diskutovaných územiach (obr. 12 a 13).

Doručené / Received: 10. 5. 2024
Prijaté na publikovanie / Accepted: 28. 6. 2024

Mineralia Slovaca, Web ISSN 1338-3523, ISSN 0369-2086, https://doi.org/10.56623/ms.2024.56.1.3
56, 1 (2024), 71 – 88, © Authors 2024. CC BY 4.0

Geological structure of the Strelnica Massif (Muráň Plateau, Central Slovakia) based on new biostratigraphical data and geological mapping

BALÁZS KRONOME[1], DANIELA BOOROVÁ[1] and MÁRIO OLŠAVSKÝ[2]

[1]State Geological Institute of Dionýz Štúr, Mlynská dolina 1, SK-817 04 Bratislava, Slovak Republic; balazs.kronome@geology.sk
[2]State Geological Institute of Dionýz Štúr, Zelená 5, 974 04 Banská Bystrica, Slovak Republic

Abstract: The Strelnica Massif is a part of the Muráň Plateau near Tisovec town. The massif is of prolonged triangular shape and is sharply defined by fault lines from all sides: the Muráň line on the SE side, the Mýtna fault system from the SW side and a thrust/fault line with unclear character in the Martinová Valley on the N side. The massif was supposed to be built by Lower to Middle Triassic carbonate complexes, however our new biostratigraphic data had proven that in fact most of these light grey carbonates belong mostly to Upper Triassic, which makes necessary the reinterpretation of the structure of the whole massif. Despite of new and more complicated structural interpretation, our new age data are in better agreement with earlier works from the Tisovec quarry as it was in the former geological map (Klinec, 1976).
Our mapping works also confirmed, that the Strelnica Massif itself is built by two facially very different blocks: a deep-water type of succession with Reifling and Raming type limestones and a strongly tectonically reduced succesion from probably lower Carnian up to Liassic. These two blocks are in tectonic contact along a fault line and both are lying on the Lower Triassic shaley complex which forms the basal horizon of the Muráň Nappe. The Muráň Line is covered by Quaternary cover in the aera, but in addition we suppose also at least two newer fault systems: a NNW-SSE normal fault system, parallel with the Mýtna system in the Rimava Valley and a roughly WNW-ESE system with probable sinistral strike-slip character. Both systems were locally known from the Tisovec quarry, or the structural measurements from the Dielik cave in the NE part of the massif, however not mapped in the whole massif.

Key words: Strelnica massif, Muráň plateau, Triassic, biostratigraphy

Graphical abstract

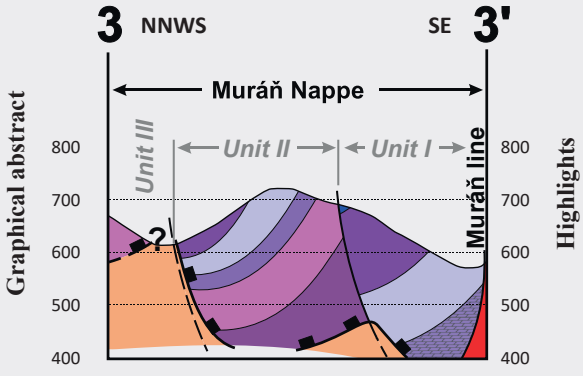

Highlights

- Based on new biostratigraphical data as well as geological mapping we suppose, that the Strelnica Massif is built by two lithologically different Triassic succesions, which are in tectonic contact with their underlying Lower Triassic basal formation. One of these sequences (unit I) is built by a reduced Upper Triassic carbonatic reef/lagunar strata (Tisovec and Dachstein limestones with rare Jurassic remnants), while the other (unit II) is of deep-water to slope facies (Reifling and Raming-type limestones). Unit III is the neighbouring Šarkanica Massif, which shows a typical Lower Triassic to Ladinian strata of a carbonate platform.
- The contact between these blocks is along thrust/shear zones subparallel with the Muráň Line. Moreover we also detected two younger fault system: one NNW-SSE normal fault system parallel with the Mýtna system and a roughly WNW-ESE slightly oblique, probably strike-slip fault system.

Introduction

The Strelnica Massif is located in the SW part of the Muráň Plateau, NE of town Tisovec. The massif forms a roughly elongated triangular mountain range sharply defined by faults from each side. From the SE it is the Muráň Line covered by Quaternary sediments of the Skalička Valley, from the N side the massif is cut by the Martinová Valley which separates the Strelnica massif from the Šarkanica massif and finally the valley of the Rimava river situated on the Mýtna fault zone (Fig. 1). Our geological mapping, biostratigraphical and structural evaluation of the Muráň Plateau was realized in the framework Projects of the Ministry of Environment of the Slovak Republic no. 16 06 and 17 13 (2010–2020): Updating the geological structure of problematic areas of the Slovak Republic at the scale 1 : 50 000 maps (Kronome et al., 2019).

In the area of the Muráň Plateau, the works of Foetterle (1867, 1868 in Bystrický, 1959b) were the only source on the geological structure until the works of Zoubek (1932) and Andrusov (1935a, b). After World War II, a collective led by Pouba mapped the central part of the Muráň Plateau (Pouba, 1951). Bystrický continued this work and found the modern comprehensive understanding of the geology of the Muráň Plateau. His geological maps from 1959 (Bystrický, 1959 a, b) summarized the results of mapping carried out between 1956 and 1958. These maps were later integrated in a slightly modified and simplified form into the 1 : 50 000 scale geological map of the Slovak Ore Mountains and the Low Tatras (Klinec, 1976), which is the only comprehensive geological map of the area to date. In this map, the Strelnica Massif appears as a relatively simple unit, composed mainly of Middle Triassic Gutenstein and Steinalm formations, with the exception of the Tisovec quarry, where Upper Triassic ages were already known at that time.

Another issue is the presence of two nappe structures – lower and upper – within the Muráň Nappe, where the "lower" is supposed to be deep-water and the "upper" is shallow-water carbonate platform in character (Havrila, 1997). Our geological mapping (Kronome et al., 2019) confirmed the existence of at least two thrust structures, but the tectonic structure of the Muráň Plateau is more complex and the "lower thrust – deep-water vs. upper thrust – shallow-water" scheme may not be valid everywhere. Most recently Hók and Olšavský (2023) assigned the lower Muráň Nappe into the Hronicum as its uppermost subunit – Vernaricum, but it should be noted, that the upper nappe also has numerous differences from the "classic" Silicicum, as well, as many similarities with the Hronicum, so its position is also unclear (Kronome et al., l.c.).

Problems of the Upper Triassic strata

Since one of our most important results is the presence of Carnian / Norian limestones in the massif of Strelnica, we need to look in detail at the issue of Upper Triassic limestones. Above the Wetterstein Fm. limestones / dolomites, or Hauptdolomites, respectively, in the Western

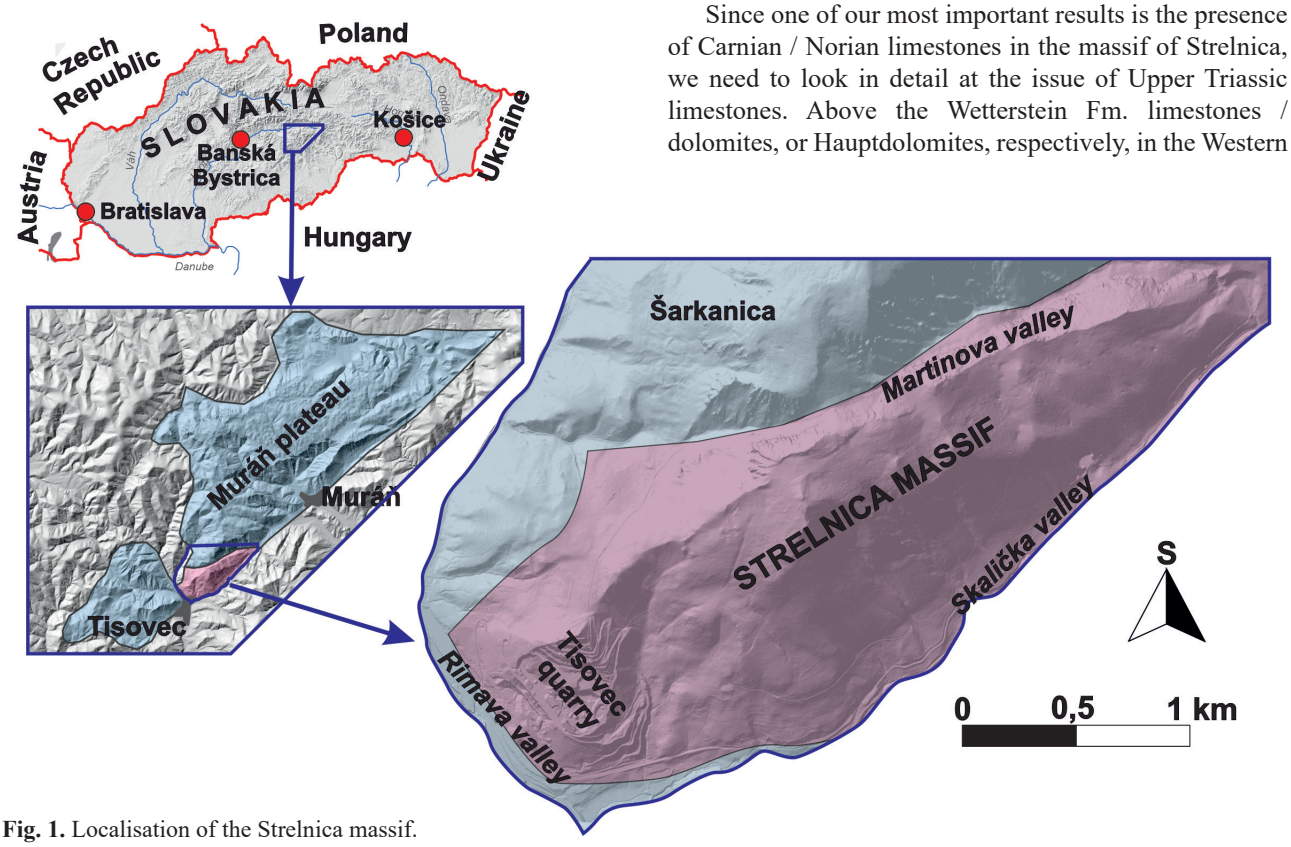

Fig. 1. Localisation of the Strelnica massif.

Carpathians an Upper Triassic complex of light to grey organodetritic limestones follows, the naming of which was (and is) problematic. It has long been known that both Carnian and Norian members are present in the strata, and distinguishing them during the field works is virtually impossible. The problem is, that these Carnian carbonates are of shallow-water to reef facies, where important leading fossils are rare, so although their age is clearly Carnian, their precise biostratigraphy is uncertain, without detailed zonation. Already in these first stratigraphic schemes, the authors encountered the problem of the Upper Triassic assemblages, which Pouba (1951) called "Carnian Wetterstein limestones", and Bystrický (1959a, b) describes them only as "light limestones", while he calls the similar Norian light limestones "light and grey thick bedded limestones with megalodonts (Dachstein limestones)". While in the Alps for the Carnian part of these Upper Triassic limestones the terms "Oponitz reef limestone" (Kristan-Tollmann, 1958 in Andrusovová et al., 1989) or "Carnian Dachstein limestone" (Lein and Zapfe, 1972 in Andrusovová et al., 1989) and for the Noriana to Rhaetian part the term "Dachstein limestones" (Krystyn et al., 1990) was used, in Slovakia for the Carnian limestones the term "Tisovec limestones" and for the Norian ones the term "Furmanec limestones" were introduced by Kollárová-Andrusovová (1960). However, as both Austrian and Slovak authors pointed out, the main differences are in the facies development: while the "Tisovec" limestones are rather lagoonal, the "Furmanec" limestones represent a reef environment, where both could have existed simultaneously.

The situation is moreover complicated by the fact that intensive mining in the last six decades removed parts of the quarry in which the "Tisovec" limestones were originally defined. Krystyn et al. (1990), when reinterpreting archival material taken by Bystrický during mapping in the late 1950s and published by Kollárová-Andrusová (1962) and comparing them with conodont samples found that the Carnian ages assigned to the Tisovec limestones are somewhat younger, however, today, after three more decades even the sampling localities of Krystyn and his colleagues are missing. Later, Slovak authors also agreed, that the term "Tisovec limestone" is unsatisfactory due to the lack of a precise lithological and lithofacies definition, while for the similar Norian they keep the term Furmanec limestones (Andrusovová et al., 1989). Krystyn et al. (1990) proposed the term "Waxeneck Limestone" for similar Carnian limestones because of its better defined type profile at the Kleine Waxeneck locality in Austria. On the other hand, Soták, on the basis of his study of the Tisovec quarry, expressed that the use of the term "Tisovec limestone" is well established and only its redefinition is needed, based on a new basic stratotype (Soták, 1990). We, aware of the aforementioned problems of nomenclature, will use in this paper the term "Tisovec limestones" for the Carnian and "Dachstein limestones" for the Norian part of this assemblage.

Lithological strata of the Strelnica Massif

The Strelnica Massif, as a part of the Muráň Nappe is overthrusted on the Veporic unit, even if this nappe contact is less visible along the Muráň line because of thick Quaternary cover. However along the Skalička Valley from the saddle Dielik to town Tisovec the Upper Triassic parts of the Muráň Nappe are lying directly on a Lower Triassic shaley complex, evidently belonging also to the Muráň Nappe – thus we see a large hiatus from Lower Triassic up to Lower Carnian. In the Martinová Valley the situation is similar. For our final geological map see Fig. 2 and 3.

Veporicum

The Veporic unit is of smaller importance from our point of view, it is represented by the usually tectonically reworked porphyric granitoides of the Kráľova hoľa unit in the western part of the area north of Tisovec town and exceptionally were also found in the lower part of the wide valley between the Strelnica and Čremošná massifs. They are followed by a Föderata-type cover sequence, built primarily by Lower Triassic quartzites. Higher parts of the cover sequence, as we know them in other places as the Strundžaník and Klátov grúň hills, Hrdzavá Valley etc. are preserved only as fragments incorporated in the thick complex of rauhwackes.

Rauhwackes

A massive range of rauhwackes, or rauhwackized members of both the Föderata unit and the Muráň nappe stretches along the western edge of the Šarkanica massif, i.e. in the zone where we assume normal nappe contact. In this rauhwacke belt we made a distinction between parts generated from only Föderata rocks and assigned them to Veporicum as its tectonically reworked cover, and the "real" rauhwackes indicating the overthrust of the Muráň Nappe, where Föderata-originated fragments are already missing.

The Muráň Nappe

The contact of the Muráň Nappe with the underlying Veporicum on the western side of the Muráň plateau is a nappe overthrust. In the area W of the Šarkanica massif this contact seems to be normal, and on the Lower Triassic strata the Gutenstein, Steinalm etc. formations follow. From a wide valley between the Čremošná and Strelnica massifs to the NE the situation gets more complicated, because there is a quite huge tectonic hiatus between

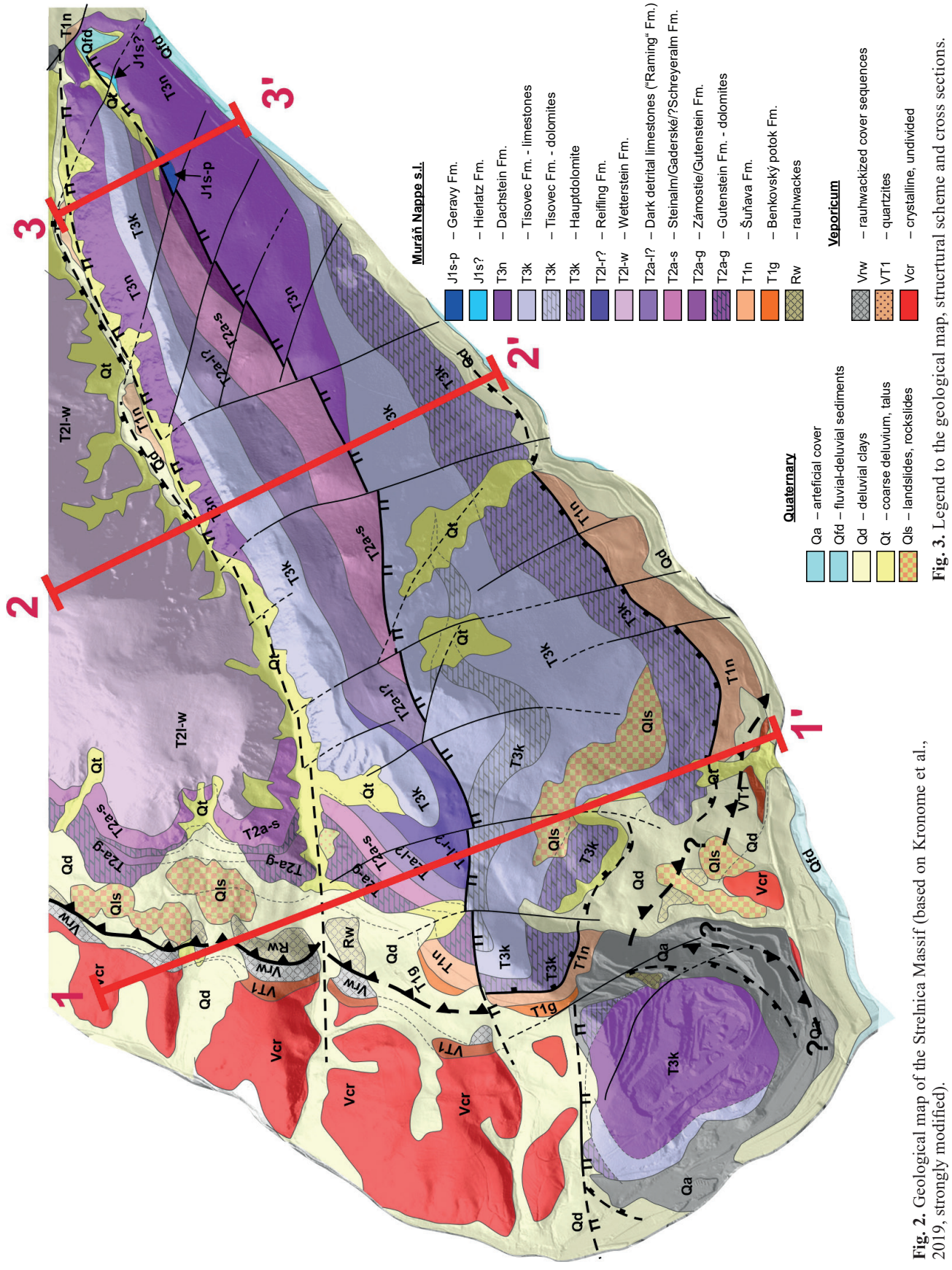

Fig. 3. Legend to the geological map, structural scheme and cross sections.

Fig. 2. Geological map of the Strelnica Massif (based on Kronome et al., 2019, strongly modified).

the Lower Triassic strata and its younger (mostly Upper Triassic) overlying sequence.

The internal structure of the Strelnica massif is composed of – at least – two lithologically very different elongated blocks with a thurst / shear(?) zone between them. We provisionally distinguished them as "unit I" and "unit II", where "unit III" is the part of the Muráň Plateau north of the Martinová Valley beginning with the Šarkanica massif, already out of our study area with a normal, tectonically not disturbed structure (Fig. 2). For the localisation of our biostratigraphic samples with added earlier data see the Fig. 4.

Benkovský potok and Šuňava Fm. – Lower Triassic

As we discussed already in the final report of our mapping project (Kronome et al., 2019) due to its lithological similarities with both the Hronic and Silicic nappe systems we suppose the Muráň Nappe a continuation of the Vernar Nappe / Vernaricum and thus according to Hók and Olšavský (2023) we consider at least its "lower nappe" a part of the Hronic nappe system, which in their structural concept comprises the uppermost subunit of the Hronicum. For that reason in the naming of the Lower Triassic formations we will use the "hronic terminology" (Benkovský potok and Šuňava fms.) instead of the usual "silicic" terms (Bódvaszilas and Szin fms.).

In the study area the lower Benkovský potok Fm. is relatively rarely preserved, mostly in the NW part of the nappe contact zone with the Veporicum and along the rauhwacke belt. In contrary the younger Šuňava Formation is present in huge volumes practically along the whole basal zone of the Muráň Nappe. The formation is built by the usual Lower Triassic rock types: reddish-yellowish to light greenish fine grained sandy shales.

Their contact to the underlying Veporicum – where it is visible at all – is clearly a nappe overthrust with a well developed rauhwacke belt, however the overlying Muráň Nappe sequences differs in all units. Interestingly, never was a rauhwacke horizon detected between the Lower Triassic basal part and the Upper Triassic strata above it, neither in the S slopes of the massif, nor in the Martinová Valley, so the character of their contact is not clear. Based on the mining report from the Tisovec quarry (Hruškovič et al., 1990) the situation there is similar: below Middle / Upper Triassic carbonates a tectonically reworked layer of

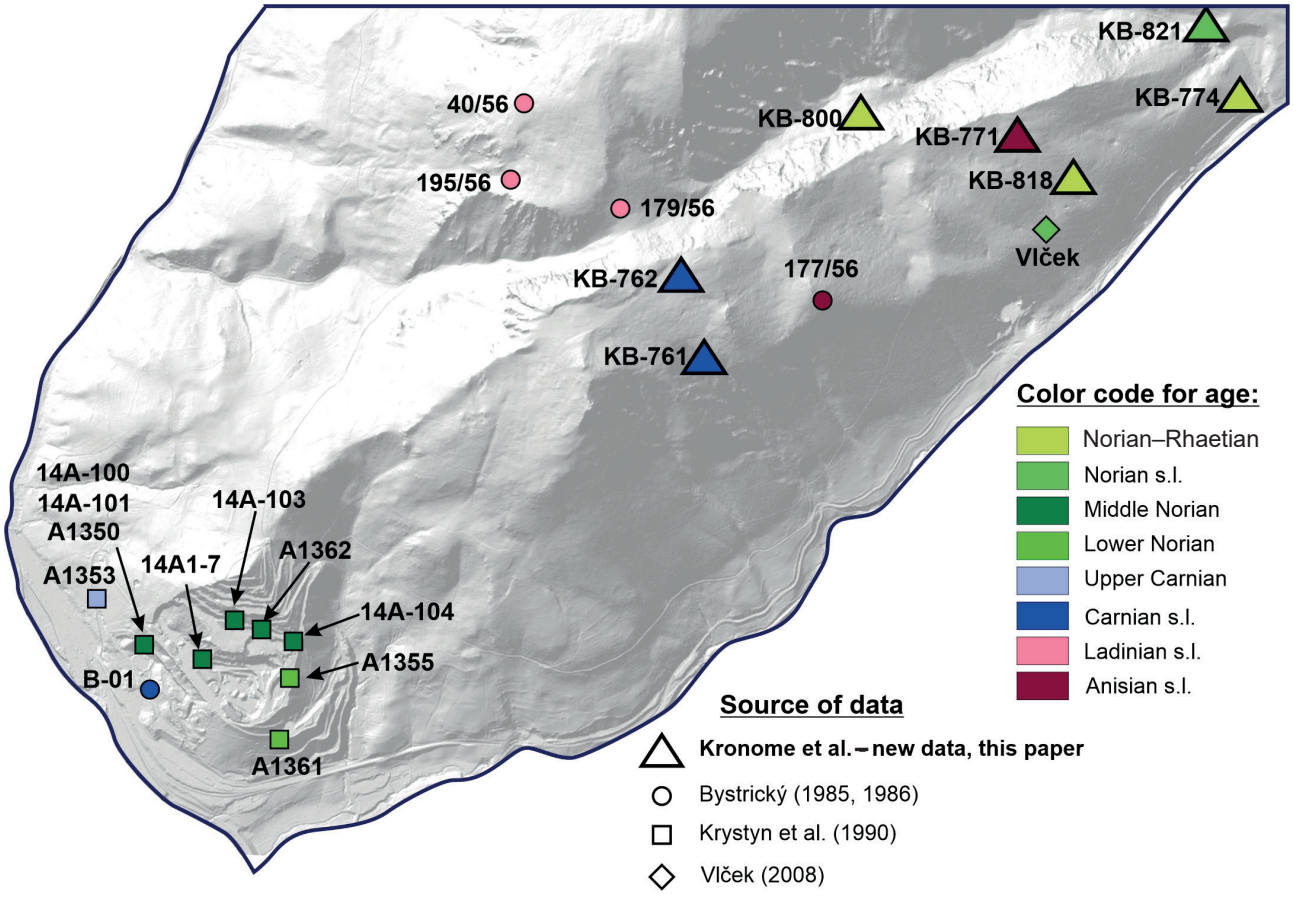

Fig. 4. Localization, source and age data of positive samples, compiled from our data (this paper), Krystyn et al. (1990) and Bystrický (1985, 1986).

Lower Triassic was proven by all drills, but the thickness of the formation is unknown. Based on the SW part of the Strelnica massif and the W slopes of the Šarkanica it is probably not thicker than 100 m, however the rheological character of that shaley complex enables high variability in its thickness, as we can see in other places in the Muráň Plateau (Hrdzavá Valley, Sitárka etc.).

Gutenstein Fm. – Anisian (Aegean–Bythinian)

The Gutenstein Formation is built by dark grey to black bituminose limestones and dolomites and is present in units II and III In the unit III they occur as a member of a normal stratigraphic sequence of the Muráň Nappe (Šarkanica and further to the north of it) where the dolomite types are unusually abundant for the Muráň Nappe. The second occurrence is in the unit II, in a narrow strip in the NE part of the massif. In this locality they are mixed with debris of other dark limestone types (Zámostie and Raming type detritic limestones), so the contours of that body and their relation to the underlying Lower Triassic are unclear.

Steinalm Fm. – Anisian (lower and middle Pelsonian)

The Steinalm limestones, as well as the Gutenstein Fm. occur in two units: the unit III on the W slopes of the Šarkanica and in the unit II in two positions: along with the strip of Gutenstein Fm. in the NW part of the Strelnica Massif, and as a stripe parallel with the Gutenstein limestones in the NE part of the massif, in both places as the formation overlying the Gutenstein Fm. In the second locality of the unit II the presence of the Steinalm limestones is proven by microfauna from our samples and also by dasycladal algae (Bystrický, 1985, 1986, doc. point 177/56, age: Pelsonian–Illyrian). The precise shape of the stripe is unclear for the same reason as in the case of the Gutenstein limestones: extensive talus cover of very different carbonates from both sides of the supposed thrust plane.

Zámostie / Raming?Fm. – Anisian (upper Pelsonian) to lower Carnian

From the upper Pelsonian stage the stratigraphical sequences of the III and II units begin strongly differ (the unit I begins as late as in the Carnian with no preserved Middle Triassic members). While the unit III strata (Šarkanica and further to the north) represents the "classical" evolution of the Wetterstein carbonate platform, in the unit II the deep water / slope environment sedimentation is alternating the Wetterstein platform facies. This type of strata is usually taken as typical for the "lower Muráň Nappe" (sensu Havrila, 1997) and is usually corralated with the Vernaricum.

In the unit II this type of sedimentation is starting with dark detrital limestones above the Steinalm Fm., which we can correlate with the Zámostie Fm. defined in the Choč Nappe (Kochanová & Michalík, 1986) as an upper Pelsonian to Illyrian formation built by dark grey biomicritic limestones with abundant fossil relics (lower member – Jasenie Beds) and by thick layered dark grey calcarenites and crinoidal limestones (upper member, Ráztoka Beds). These beds are considered the product of the so-called "Reifling event" ("Reiflinger wende" sensu Schlager & Schöllnberger, 1974) which signalizes the beginning of tectonic unrest in the area, corresponding with the opening of the Meliatic basin. This event is manifested even in the parts of the carbonate platform with no significant tectonic disturbances in the form of breccia layers and neptunic dykes in the Steinalm Fm.

Among our samples the black organodetritic limestone (KB-771, see Kronome et al., 2019, app. 3 and 4, for the localisation of the sample see Fig. 4) can be ranged into that formation containing the following Anisian foraminifera assemblage:

foto_01, foto_02 Grey, dark grey to black organodetritic and detrital limestones from the Strelnica Massif

Frondicularia woodwardi Howchin

Nodosaria sp.

Meandrospira sp. (Meandrospira deformata Salaj, *?Meandrospira cf. cheni* Ho*)*

Agathammina austroalpina Kristan–Tollmann et Tollmann

These rocks were formerly mapped as Gutenstein Fm. limestones, but based our new age data this interpretation is incorrect.

Reifling Fm. – Ladinian to Lower Carnian

In the western part of the Strelnica Massif, near to the saddle between the Strelnica and Čremošná massifs smaller cliffs and rocky outcrops of grey cherty limestones were found in an oblique strip in the unit II in tectonic contact with light dolomites of the I unit. Bedding planes show that the bed forms an assymetrical synclinal structure, eastward these limestones are gradually changing into the mentioned dark detrital limestones, however the problem with talus cover is remaining, so the precise contours of the body are unclear. At the moment we had no biostratigraphic data for the age of these beds, but because of their stratigraphic position between the underlying dark biodetritic limestones and overlying light grey shallow water to reefal limestones (Waxeneck Fm. – see below) we correlate this strata with the Reifling Fm. In the geological map of Klinec, 1976 these limestones were also assigned to Gutenstein Fm.

Wetterstein Fm. – Ladinian

Despite the fact, that the Wetterstein limestones are the most common lithotype in the whole Muráň Plateau they are not present neither in unit I (the succession begins with lower Carnian), nor in the unit II, where they are subtituted by detrital and deep-water limestones. They build a thick strata in the unit III (Šarkanica) which is already out of the strictly taken Strelnica Massif and represents a "normal" carbonate platform type of succesion typical for the upper Muráň Nappe. In the neighbouring Šarkanica massif

foto_03, foto_04 Dark grey cherty limestones

foto_05 Loferitic dolomite of the Wetterstein / Hauptdolomite Fm., small quarry in the Dielik saddle

foto_06 Dark grey dolomite to dolomitic limestone, small quarry in the Dielik saddle

Bystrický had proven their Ladinian age (1985, 1986, samples 179/56, 195/56 a 40/56, see Fig. 4) by dasycladal algae.

Wetterstein dolomite / Hauptdolomite Fm. – upper Ladinian to lower Carnian (Julian)

The thick dolomitic part of the Wetterstein Fm. in other localities of the Muráň Plateau is continuing into the Carnian, however rarely a bed of shales and fine grained sandstones can be preserved correlated with the Rheingraben / Lunz Fm. Dolomites above that horizon should be ranged already into the Hauptdolomite Fm., but when the shaley horizon is not present – and usually is not – we can not distinguish the lower Wetterstein part from the upper Hauptdolomite part of the strata.

Loferitic light to darker grey dolomites build a massive bed in the SE slopes of the Strelnica Massif, e.g. in the unit I. Since this dolomitic horizon is situated below the horizon of Tisovec Lmst. with proven age, we suppose, that in the SE and S slopes of the Strelnica Massif they should belong to the Wetterstein / Hauptdolomite Fm., however their upper Ladinian / lower Carnian age was not documented yet. Probably the same horizon is proven by several drills in the Tisovec quarry (Hruškovič et al., 1990).

Tisovec („Waxeneck") Fm. – Carnian

The most dominant rocks of the Strelnica Massif are light grey organodetritic limestones and dolomites forming the steep ridge on the northern side of the massif as well as supposedly most of its southern slopes (see Fig. 2). Since between these two belts the above mentioned Anisian and Ladinian formations are located, these two belts must be different, belonging to different tectonic blocks.

The northern belt forms a narrow ridge along the northern edge of the massif in the form of very steep cliffs to the Martinová Valley on the north, but also shows a sudden morphological elevation from the southern side to the neighbouring Middle Triassic to lower Carnian formations. A sample of dark grey to black organodetritic nodular limestones with already Lower Carnian age (KB-762, see Kronome et al., 2019, app. 3 and 4) represents a transitional type to the deep-water Reifling type or detrital Raming / Zámostie-type limestones (see below):

incertae sedis: *Thaumatoporella parvovesiculifera* Raineri

foraminifera: *Trochammina almtalensis* Koehn-Zaninetti

Agathammina austroalpina Kristan–Tollmann et Tollmann

Bispiranella ovata Samuel, Salaj et Borza

Frondicularia woodwardi Howchin

Endothyra kuepperi Oberhauser

This Lower Carnian age at the stratigraphic boundary between detrital dark limestones and the overlying Tisovec limestones implies, that in the unit II the deep water / slope environment limestones were most probably formed during the whole Ladinian.

We obtained biostratigraphical data also from the southern belt, which in general does not form as impressive rock walls but builds almost the whole S and most of the SE slope of the massif.

KB 761 – light grey – grey organodetritic limestone – Carnian

foraminifera: *Bispiranella ovata* Samuel, Salaj et Borza

Aulotortus sinuosus Weynschenk

Duostomina sp.

The southern slope of the massif built by the Tisovec Fm. contains also a significant and roughly continous

foto_07 foto_08 Light grey organodetritic reefal limestones of the Tisovec Fm., southern edge of the Strelnica Massif

stripe of light grey dolomites exposed from the saddle near the tectonic with the Reifling Fm. further in the S-SE slopes. Good outcrops of dolomites can be found between the first cliffs on the southern edge of the massif. Since at this southern slope the bulk thickness of the Tisovec Fm. limestones and dolomites strongly exceeds their average thickness in other places, we can not exclude some hidden tectonic complications in this area. In this case the mentioned dolomitic belt in fact could belong to the stratigraphically underlying Wetterstein / Hauptdolomite strata and its presence can signify a smaller "hidden" overthurst plane, however without further age data we cannot prove this idea.

Dachstein („Furmanec") Fm. – Norian

Bystrický presented only one sample of Anisian age (Bystrický, 1985, 1986, sample 177/56) from the Strelnica Massif. This only sample was probably the reason, why was the massif interpreted in former geological maps (Bystrický, 1959; Klinec, 1976) as built by Anisian limestones (the concept of former maps was roughly: light grey – Steinalm Fm., darker to black – Gutenstein Fm.).

Since Bystrický's mapping and sampling until now only one biostratigraphical age was proven by Vlček (2004) from the cave Dielik and its surroundings, who identified megalodont bivalves:

Neomegalodon complanatus Gümb.

Neomegalodon triqueter dolomiticus Frech, resp. *Neomegalodon* cf. *triqeter dolomiticus* Frech

Our samples confirmed Vlček's findings and in several localities offered Norian or Norian to Rhaetian ages (see Fig. 4).

KB 774 – light grey organodetritic limestones – Norian (Salaj et al., 1983) or Norian–Rhaetian (Gale et al., 2013)

incertae sedis: *Thaumatoporella parvovesiculifera* (Raineri)

foraminifera: *Agathammina austroalpina* Kristan–Tollmann et Tollmann

?Decapoalina schaeferae Zaninetti, Altiner, Dager et Ducret

Opthalmidium sp.,

Ostracoda div. sp.,

Tubiphytes sp.

KB 800 – light grey organodetritic limestones – Norian–Rhaetian

incertae sedis: *Thaumatoporella parvovesiculifera* (Raineri)

foraminifera: *Frondicularia woodwardi* Howchin

Aulotortus sinuosus Weynschenk

Decapoalina schaeferae Zaninetti, Altiner, Dager et Ducret

Angulodiscus sp.

Trochammina sp.

Duostomina sp.

Planiinvoluta sp.

Tubiphytes ?obscurus Maslov, resp. *Tubiphytes* sp.

KB 818 – light grey organodetritic limestones – Norian–Rhaetian

foraminifera: *Galeanella panticae* Zaninetti et Brönnimann, resp.

Opthalmidium sp.

Duostomina sp.

?Decapoalina sp.

KB 821 – light grey organodetritic limestones – probably Norian

Spiroloculina cf. *praecursor* Oberhauser

Miliopora cuvillieri Broennimann et Zaninetti

Trochammina sp.

foto_09 Light grey reef limestone of the Dachstein Fm., SE slope of the Strelnica Massif

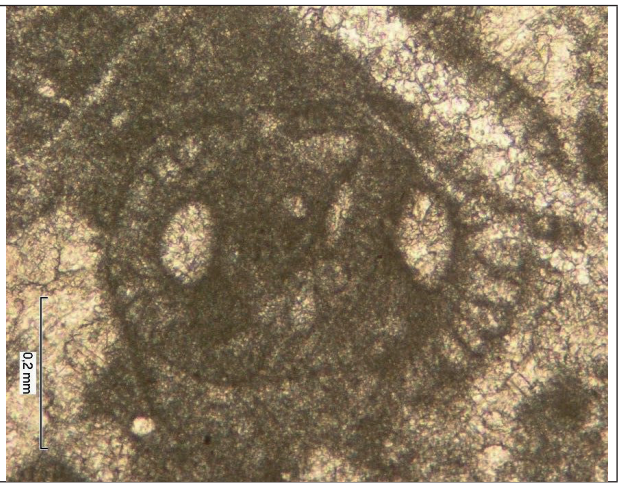

foto_10 Microphoto of foraminifer *Galeanella panticae*, SE slope of the Strelnica Massif (sample KB-818)

?Hierlatz Fm. – Jurassic, ?Hettangian

foto_11 Pinkish crinoidal limestones, NE end of the Strelnica Massif, entry of the Martinová Valley

foto_12 Iron ore from the shear zone between units I and II, entry of the Martinová Valley

At the entry of the Martinová Valley in the near vicinity of the belt of Dachstein limestones we found pinkish crinoidal limestones without identifiable fauna or flora, which we correlate with the lowermost Jurassic Hierlatz type limestones because of their lithological character and superposition above the Dachstein limestones. Rakús and Sýkora (2001) found similar limestones at the Tesná skala massif, and however the rare and crushed fauna did not provide age data, Rakús and Sýkora (l.c.) supposed Sinemurian age for them.

In that place the thrust/shear plane between the units I and II is located which is bound with iron ore mineralization which was also mined in the past. We can find here remnants of former mining activities as a small spoil tip and an entry of probably collapsed mining / exploration shaft.

Geravy Fm. – Jurassic, Pliensbachian?

The youngest lithological member of the succession of the unit I are grey marly limestones and marls which were not mentioned by former authors. Their occurrence is very limited, and similarly as the supposedly Jurassic Hierlatz Fm. limestones nearby, they occur in the close vicinity with the Dachstein Fm. limestones. Based on dating in other places, where the age of this formation was established as Pliensbachian (Rakús & Sýkora, 2001) we must propose a stratigraphic hiatus between the Dachstein and Geravy formations.

Similar Jurassic rocks are very rarely preserved in the Muráň Nappe, they were observed only in the axis of the narrow synclinal structure from Javorina saddle to Mokrá Poľana valley in the Tesná skala massif, in some enigmatic blocks at a highly situated small plane in the

foto_13, foto_14 Dark grey – grey marly limestones of the Geravy Fm. from the NE part of the Strelnica Massif

slopes of the Hrdzavá Valley and a little different type (detritic limestones in neptunic dykes) at the Goštanová hill, north of Tisovec (Vojtko, 1999). All these occurrences are rather small and almost always bound to tectonically complicated zones, often in the vicinity of the Muráň Line.

The Tisovec quarry

For its importance we need to summarize the published data about geological structure and age data of the Tisovec quarry, which are in good agreement with our results. The most important works on stratigraphy of the quarry were carried out by Kollárová-Andrusovová (1960, 1961, 1962), Soták (1990) and Krystyn et al. (1990), very valuable data about the structure of the massif were provided in the mining exploration report of Hruškovič et al. (1990) (Fig. 5).

However most of the biostratigraphical data originate from the Tisovec quarry, there are problems with their exact localisation, mostly because of the continuing mining removed the original sampling places. Kollárová-Andrusovová identified samples collected by Bystrický in the late 50-ties, and also the places sampled by Soták and Krystyn in the latest 80-ties were extracted since then. The place where Kollárová-Andrusovová (1962) defined the "Tisovec Formation" existed in 1990, when Krystyn et al. (1990) based mostly on conodonts determined their ages a little younger and thus shifting the boundary already into Norian – into the Dachstein / Furmanec Fm. In the same year Soták (1990) objected, that their samples were also not from those exact places as Kollárová-Andrusovová studied, the quarry is most probably built by both Carnian and Norian limestones, and rather than reject the term "Tisovec Fm." and substitute it with the term "Waxeneck Fm." it would be better to find a proper stratotype.

The excellent exploration report (Hruškovič et al., 1990) was not focusing on stratigraphy, rather on quality of the carbonates, the purity of limestones and the limestone / dolomite ratio, but its number of boreholes and cross sections show a structure which is in very good agreement with our results (Fig. 5). According to these cross sections below the massive limestone complex a dolomitic horizon

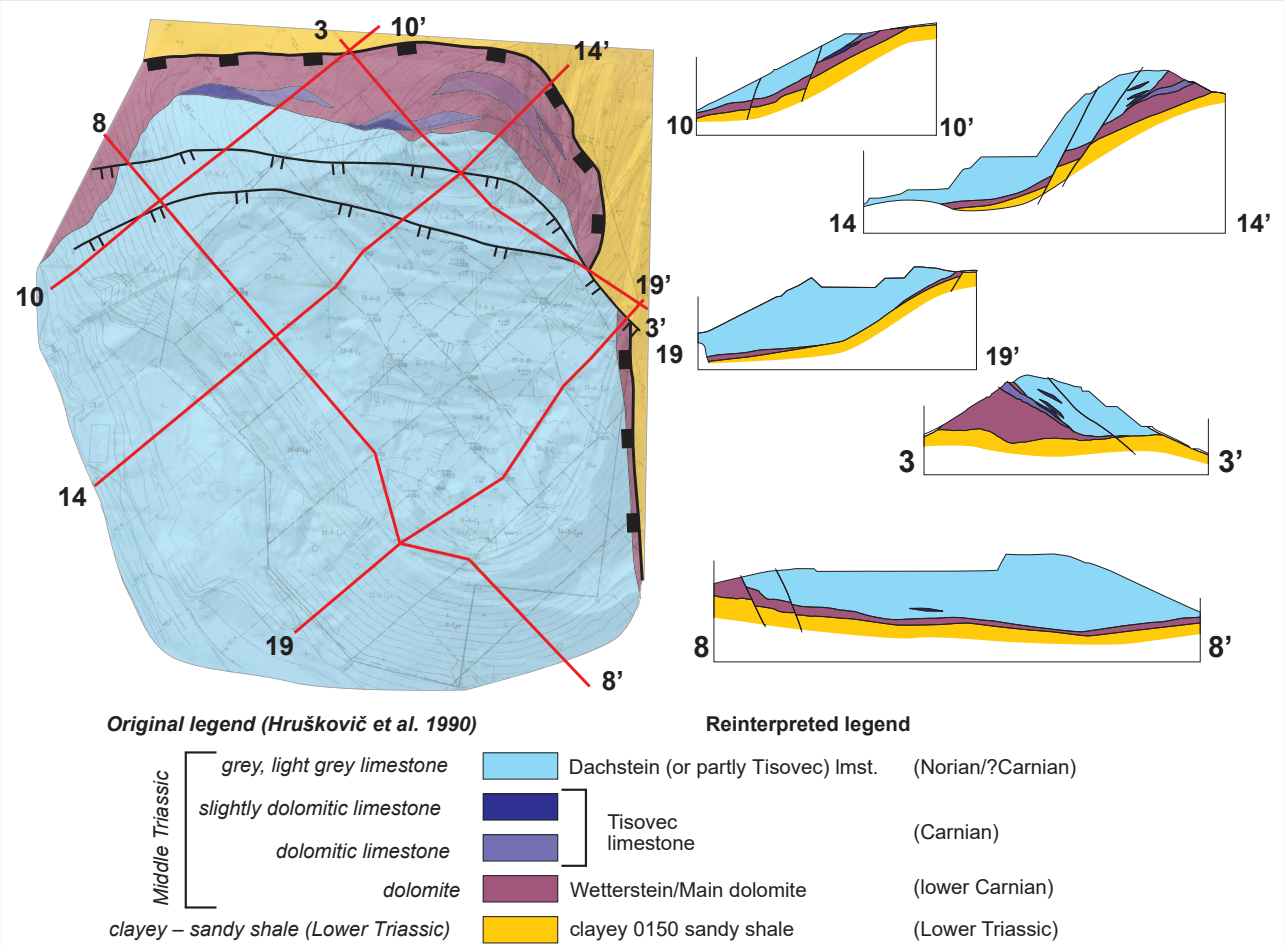

Fig. 5. Attempt to reinterpretate the exploration geological maps and cross sections of the Tisovec quarry – based on Hruškovič et al. (1990), edited.

is present in the eastern part of the massif, thinning but not missing westward. Soták (1990) correlates these dolomites with the Wetterstein Fm., however they also can be already Carnian – e.g. belonging already to the Haputdolomit Fm. which in other localities of the Muráň Plateau are immediately undelying the Tisovec limestones (see Kronome & Boorová, 2014; Kronome et al., 2019).

Below these dolomites the same Lower Triassic shaley sequence is developed as we saw it in the SE slopes of the Strelnica Massif, probably also after a tectonic hiatus (Hruškovič et al., 1990).

Structural results of the geological mapping

According to the above summarized age data together with the structural results of our mapping we suppose, that the Strelnica Massif is built by (at least) two tectonically defined units with different stratigraphic succesions. As a third unit we can define the massif of Šarkanica, which is already out of the strictly taken Strelnica massif and represents a normal succession of the Muráň Nappe.

The Lower Triassic "base" of all three units has a special function probably because of its ability for ductile behavior. This ductile behavior is documented in the final report on our mapping works during years 2010–2019 (Kronome et al., 2019) and is manifested by formation of duplexes, partial nappe bodies, folding and thus shows extreme variability of the thickness of the Lower Triassic strata in the whole Muráň Nappe. In the W slopes of unit III (Šarkanica and further to the north) it seems to be in a stratigraphically normal position. In the Martinová Valley the Wetterstein limestones of unit III as well, as Dachstein lmst. of unit II are both directly in contact with Lower Triassic shales and sandstones, so here the character of their contact is unclear. In the unit II the character of the relatively short contact of Lower and Middle Triassic strata in the western segment is also unclear (partly because of the talus and other deluvial sediments). In the case of unit I the contact is clearly tectonic in its entire perimeter. Similar situation was documented in the Tisovec quarry (Hruškovič et al., 1990) which we suppose to be the continuation of unit I.

We can characterize in short the three blocks or units as follows (Fig. 7 and 8):

- Unit I is built by a strongly tectonically reduced Upper Triassic to lowermost Jurassic strata which lies discordantly directly on Lower Triassic complexes of the Muráň Nappe, so the whole Middle Triassic is missing. The unit is in a long tectonic contact with the Muráň Line in the NE part and further to the west it is lying together with the Lower Triassic in nappe position on the Veporic unit's crystalline and thin cover complexes. The

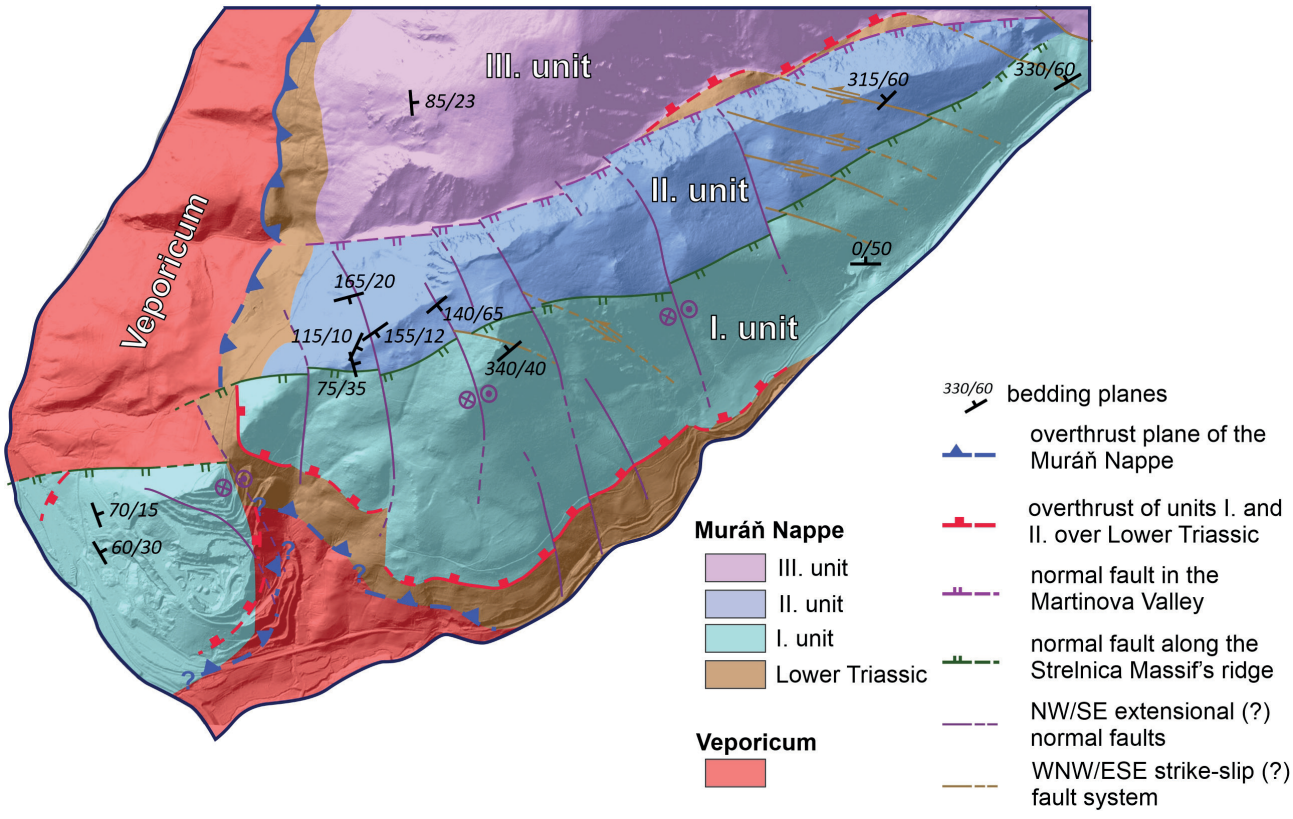

Fig. 6. Schematic structural map of main tectonic units and features.

unit is also with sharp and probably steep fault contact with the unit II stretching along the ridge of the Strelnica Massif subparalelly with the Muráň Line. Based on both the stratigraphical composition and structural buildup, the Čremošná Massif (e.g. Tisovec quarry) is an extension of this unit, cut from it by a roughly NW-SE normal fault and internally blocked with a set of smaller faults of the same sense, parallel with the Mýtna fault zone.

- Unit II stratigraphically represents a sequence with slope / deep water facies during the Middle Triassic and a "classic" carbonate platform facies during the Upper Triassic. This succession is very different from both I and III units, however on the western side near the W end of the Martinová Valley the Middle to Upper Triassic succession seems to be in normal position without overthrusting on the Lower Triassic. In the NE part of the Strelnica Massif also older Middle Triassic rocks (e.g. Gutenstein and Steinalm Fm.) are preserved, so the unit probably contains the whole Triassic strata. Moreover, in the western part a clear, but probably not too extensive synclinal structure was discovered.
- Unit III is already out of the Strelnica Massif, is contrasting with the unit II and represents a typical evolution of the upper Muráň Nappe from Lower Triassic basal horizon through Gutenstein and Steinalm Fm. up to Wetterstein Fm. limestones, but no younger members are known in the area.

In addition to these main units, we have identified several structural zones with different character.

1. Overtrust planes:
   a) The main nappe overthrust plane of the Muráň Nappe over the Veporicum, which is visible only in the western part of the area.
   b) A partial overthrust zone between the Lower Triassic strata and its overlying complexes, affecting unit I, at least partially also unit II.
2. Steep NE-SW faults:
   a) The most important fault structure in the area is the Muráň Line, even it is not manifested on the surface because of the Quaternary deluvial and fluvial cover. Analogically from other segments of this line, we suppose its steep normal fault character dipping to the NW. The huge sinkhole in the Dielik saddle, which is roughly on the Muráň Line can signalize, that deeper below an unknown limestone horizon can be present.

   Probably steep antitethic normal faults with dipping supposedly to the SE:
   b) Along the ridge of the Strelnica Massif – between units I and II.
   c) In the Martinová Valley – between units II and III.

All three normal fault zones were already mapped by Bystrický (1959a, b, also in Klinec, 1976) but without biostratigraphic data incorrectly interpreted.

3. Younger faults with different character:
   a) An extensional, slightly oblique normal fault set of roughly NW-SE direction is developed in the Strelnica Massif, most significantly evident

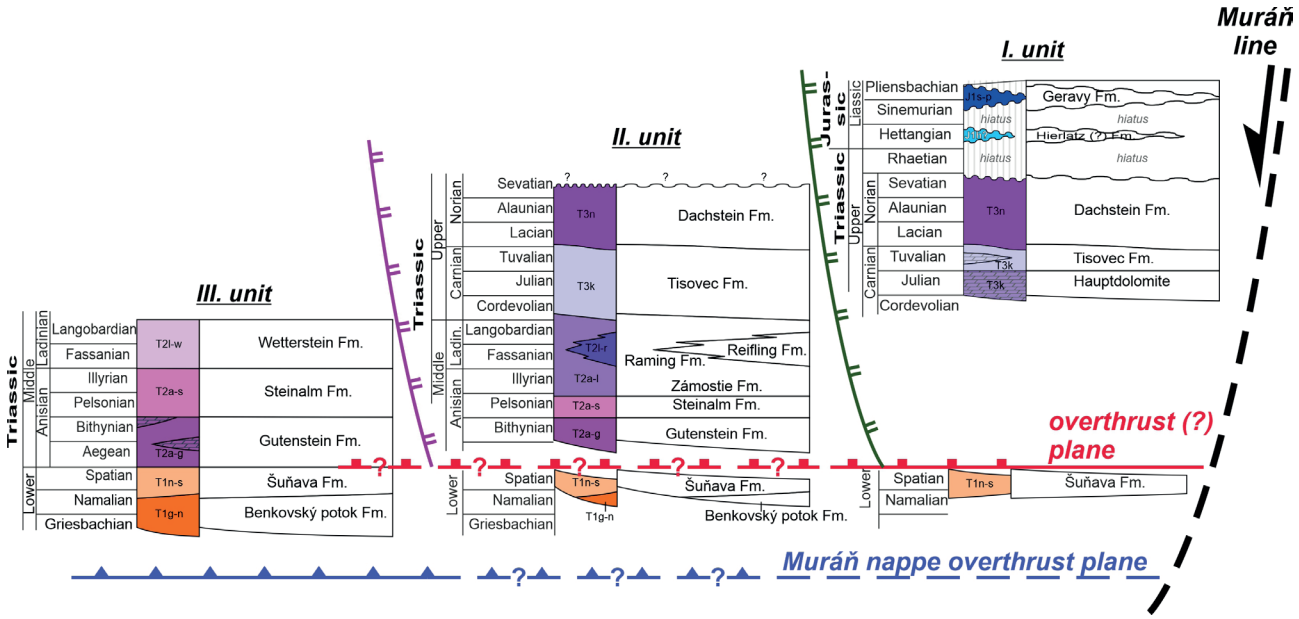

Fig. 7. Stratigraphic and tectonic scheme of the Strelnica Massif.

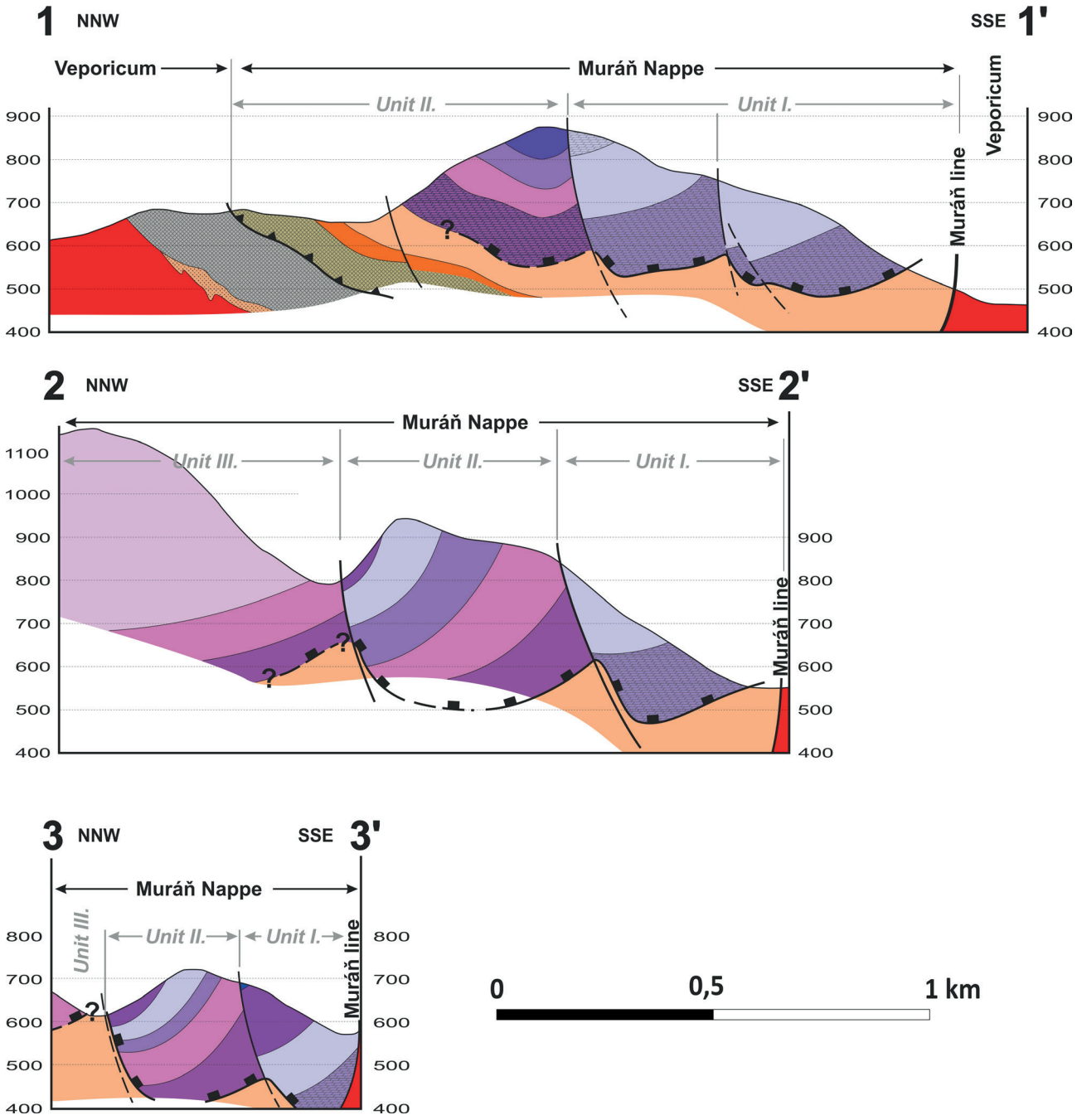

Fig. 8. Hypothetical geological cross section, for the localization of the profiles see Fig. 2 or Fig. 6.

between the Strelnica and Čremošná massifs, but with weakening intensity towards NE present in the whole massif. This fault set is parallel with the Mýtna fault system.

b) Mostly in the NE part of the Strelnica Massif a set of smaller WNW-ESE faults can be mapped, its character is probably a sinistral strike-slip. On the ridge of the Strelnica Massif this fault set is accompanied with a set of usually smaller sinkholes mostly in the Dachstein Fm. and is in accordance with fault measurements in the Dielik cave (Vlček, 2008).

Conclusions

During the geological mapping in the years 2010–2020 we found, that most of the Strelnica Massif is built by Upper Triassic carbonates in contrary to the former opinion, where the massif was supposed to be built by lower Middle Triassic rocks (Gutenstein and Steinalm Fms.). Similar age data were already known from the neighbouring Čremošná Massif, in which the Tisovec quarry is situated, thus this massif is far better known, than the rest of the Strelnica Massif. The spatial distribution of our new and other authors' already published age data indicate a very complicated tectonic structure of the massif composed of (at least) three facially different units, which we provisionally called units I, II and III respectively. All three lie directly on the Lower Triassic shaley complexes, sometimes clearly in tectonic position, in other places their relation to the Lower Triassic is unclear – it can be a normal sedimentary continuation as well as a hidden tectonic contact.

Unit I is above the Muráň Line and is built by a strongly tectonically reduced uppermost Middle to Upper Triassic strata of carbonate platform development with remnants of the lowermost Jurassic in tectonic contact with the Lower Triassic, the unit II shows a very different lower Anisian to lower Carnian succession with deep water / slope facies carbonates in the Middle Triassic (detrital limestones, Reifling lmst.) where the character with the Lower Triassic is unclear, and finally the unit III is building the Massif of Šarkanica already out of the strictly taken Strelnica Massif which shows the "typical" developement of the Muráň Nappe with Gutenstein, Steinalm and Wetterstein platform-type limestones and dolomites seemingly in normal stratigraphic contact with the Lower Triassic.

All three units are in tectonic contact along dip-slip normal fault zones subparallel (but not exactly parallel) to the Muráň Line: such is the fault along the ridge of the Strelnica Massif (between units I and II) and in the Martinova Valley (between unit II and III).

We were able to distinguish two dominant younger fault directions: an extensional, in the map oblique dip-slip fault set of NW-SE direction and a probably strike-slip system developed mostly in the NE part of the Strelnica Massif.

Acknowledgement

The Authors express their thanks to Ministry of Environment of the Slovak Republic for funding the Projects of the Ministry of Environment of the Slovak Republic no. 16 06 and 17 13 (2010–2020): *Updating the geological structure of problematic areas of the Slovak Republic at the scale 1:50000 maps*, based on which the geological mapping, and biostratigraphic and other data collecting and evaluation were performed. Comments of reviewers Ján Soták (Slovak Academy of Sciences) and Rastislav Vojtko (Comenius University) contributed much to improvement of primary manuscript. This paper is also a contribution of the State Geological Institute of Dionýz Štúr (ŠGÚDŠ), Slovakia, for the EC – CINEA HORIZON-CL5-2021- D3-D2 project 101075609 Geological Service for Europe (GSEU) within WP6 – Geological framework for the European geological data & information system.

References

Andrusov, D., 1935a: Stratigrafie triasu slovenských Karpat. *Věst. SGÚ, 11, 3–4, 54–56.*

Andrusov, D., 1935b: Subtatranské příkrovy západních Karpat. *Práce geologicko-paleontologického ústavu Karlovy university v Praze, 1935, 1–50.*

Andrusovová, V., Jendrejáková, O., Mello, J., Siblík, M. & Soták, J., 1989: Biostratigrafické a biofaciálne členenie a postavenie karnických tisovských vápencov. *Mineralia Slovaca, 21, 480.*

Bystrický, J., 1959a: Mezozoikum Muránskej plošiny. *Manuscript. Bratislava, archive ŠGÚDŠ, 1–45.*

Bystrický, J., 1959b: Príspevok k stratigrafii muránskeho mezozoika (Muránska plošina). *Geologické Práce, Zošit, 56, 5–53.*

Bystrický, J., 1985: Dokumentácia výbrusov z lokalít Muránskej plošiny za roky 1956–1976 (Documentation of thin sections from the localities of the Muráň Plateau, years 1956–1976 – in Slovak). *Manuscript. Bratislava, archive Ústav vied o Zemi SAV, K-512.*

Bystrický, J., 1986: Stratigraphic Ranging and Zonation of Dasycladal Algae in the West Carpathians Mts., Triassic. *Mineralia Slovaca, Bratislava, 18, 4, 289–321.*

Gale, L., Rettori, R., Martini, R. & Rožič, B., 2013: Decapoalina n. gen. (Miliolata, Milioliporidae; Late Triassic), a new foraminiferal genus for "Sigmoilina" schaeferae Zaninetti, Altiner, Dager & Ducret, 1982. *Bollettino della Societa Paleontologica Italiana 52, 2, 81–93.*

Havrila, M., 1997: Vzťah hronika a silicika (Relationship of the Hronicum and Silicicum – in Slovak). *Manuscript. Bratislava, archive ŠGÚDŠ, 1–31.*

Hók, J. & Olšavský, M., 2023: Vernaricum – regional distribution, lithostratigraphy, tectonics and paleogeography. *Mineralia Slovaca, 55, 1, 3–12.*

Hruškovič, P., Hrnčár, A. & Sýkorová, E., 1990: Tisovec – vápence, podrobný prieskum; Záverečná správa a výpočet zásob. *Manuscript. Bratislava, archive ŠGÚDŠ (arch. no. 76190), 1–72.*

Klinec, A., 1976: Geologická mapa Slovenského rudohoria a Nízkych Tatier 1 : 50 000. *Bratislava, GÚDŠ.*

Kochanová, M. & Michalík, J., 1986: Stratigraphy and macrofauna of the Zámostie limestones (Upper Pelsonian – Lower Illyrian) of the Choč Nappe at the southern slopes of the Nízke Tatry Mts. (West Carpathians). *Geologický Zborník Geologica Carpathica, 37, 4, 501–531.*

Kollárová-Andrusovová, V., 1960: Récentes trouvailles d'Ammonoides dans le Trias des Karpates occidentales. *Geol. sbor. Slov. Akad. Vied, 11/1, 105–110.*

Kollárová-Andrusovová, V., 1961: Amonoidné hlavonožce z triasu Slovenska (Ammonoid cephalopoda from the Triassic

of Slovakia – in Slovak), I. Všeobecná časť. *Geologický sborník SAV, 203–260.*

Kollárová-Andrusovová, V., 1962: Amonoidné hlavonožce z triasu Slovenska (Ammonoid cephalopoda from the Triassic of Slovakia – in Slovak), I. Systematická časť. *Geologický sborník SAV, 13–80.*

Kronome, B. & Boorová, D., 2014: Geologická stavba masívu Tesnej skaly (Muránska planina, centrálne Západné Karpaty) – výsledky geologického mapovania a biostratigrafického štúdia. *Geologické práce, Správy, 123, 7–29.*

Kronome, B., Boorová, D., Buček, P., Olšavský, M., Sentpetery, M., Maglay, J. & Vlačiky, M., 2019: Geologická stavba Muránskej planiny. In: Hraško, Ľ. (ed.): Výskum geologickej stavby a zostavenie geologických máp v problematických územiach Slovenskej republiky. Čiastková záverečná správa. *Manuscript. Bratislava, archive ŠGÚDŠ, 1–156.*

Kronome, B., Boorová, D., Buček, P., Olšavský, M., Sentpetery, M., Maglay, J. & Vlačiky, M., 2017: Geologická stavba Muránskej planiny. In: Hraško, Ľ. (ed.): Výskum geologickej stavby a zostavenie geologických máp v problematických územiach Slovenskej republiky. Čiastková záverečná správa. *Manuscript. Bratislava, archive ŠGÚDŠ.*

Krystyn, L., Lein, R., Mello, J., Riedel, P. & Piller, W., 1990: "Tisovec limestone" – an example of the problems of lithostratigraphic correlation between the Northern Calcareous Alps and the Central Western Carpathianp. In: Minaříková, D. a Lobitzer, H. (eds.): Thirty years of geological cooperation between Austria and Czechoslovakia. *Vienna, Geological Survey – Prague, Federal Geological Survey, 125–136.*

Pouba, Z., 1951: Geologie střední části Muráňské plošiny. *Sbor. Ústř. Úst. geol., 18, 273–300.*

Rakús, M. & Sýkora, M., 2001: Jurassic of Silicicum. *Slovak Geological Magazine, 7, 1, 53–84.*

Salaj, J., Borza, K. & Samuel, O., 1983: Triassic Foraminifera of the West Carpathians. *Bratislava, GÚDŠ, 1–213.*

Schlager, W. & Schöllnberger, W., 1974: Das Prinzip der stratigraphischen Wenden in der Schichtfolge der Nördlichen Kalkalpen. *Mitteilungen der Geologischen Gesellschaft in Wien, 66–67, 165–193.*

Soták, J., 1990: Stratigrafia a litológia vápencového komplexu ložiska Tisovec (Stratigraphy and lithology of the limestone complex of the Tisovec deposit – in Slovak). In: Hruškovič, P., Hrnčár, A. & Sýkorová, E., 1990: Tisovec – vápence, podrobný prieskum. Záverečná správa a výpočet zásob. *Manuscript. Bratislava, archive ŠGÚDŠ, 43.*

Vlček, L., 2004: Predbežná správa o náleze fosílnej fauny Megalodontaceae v jaskyni Dielik na Muránskej planine (Preliminary report on the finding of fossil Megalodontaceae in the Dielik Cave in the Muráň karstic plateau). *Aragonit, 9, 21–23.*

Vlček, L., 2008: Geologická charakteristika jaskyne Dielik na Muránskej planine (Geological characteristics of the Dielik Cave, Muránska Plateau – in Slovak). *Aragonit, 13, 2, 10–16.*

Vojtko, R., 1999: Geológia a tektonika Tisovského krasu (Geology and tectonics of the Tisovec Karst). *Manuscript. Bratislava, archive PriF UK, 1–77 (in Slovak).*

Zoubek, V., 1932: Předběžná zpráva o mapování na listu Velká Revúca. *Věst. SGÚ, 8, 3, 136–145.*

Geologická stavba masívu Strelnice (Muránska planina, stredné Slovensko) na základe nových biostratigrafických údajov a geologického mapovania

Masív Strelnice sa nachádza pri meste Tisovec na Muránskej planine. Zo všetkých strán je ostro ohraničený zlomami: muránskou líniou z JV, mýtňansko-tisoveckým zlomovým systémom z JZ a zlomom nejasného charakteru v doline Martinová na S od masívu. V doterajších prácach sa predpokladalo, že masív budujú najmä gutensteinské a steinalmské vápence a aniské súvrstvia, pričom takáto interpretácia sa zakladala iba na nedostatočnom počte biostratigrafických údajov. V stavbe Muránskej planiny sú známe dva typy sukcesií: vývoj karbonátovej platformy reprezentovaný wettersteinskými vápencami a dolomitmi v ladine a hlbokovodný/svahový vývoj, kde ladinské horizonty sú zastúpené detritickými a rohovcovými vápencami. Na základe týchto odlišných vývojov sa uvažovalo o spodnom príkrove s hlbokovodným vývojom a vrchnom príkrove s platformovým vývojom. Spodný príkrov sa považuje za súčasť najvyššieho čiastkového príkrovu hronika (vernárika) a vrchný za silicikum.

Naše biostratigrafické údaje preukázali, že stavba masívu Strelnice je omnoho zložitejšia a skladá sa z troch čiastkových jednotiek, oddelených od seba zlomami. Zlomy sú zhruba, ale nie presne paralelné s muránskym zlomom – pracovne sme ich nazvali jednotka I, II a III. Spodnotriasové súbory majú na Strelnici osobitný význam. Všade tvoria podložie nadložných súborov, niekedy so značným hiátom. Ich styk s nadložím je teda aspoň v časti jednotiek určite tektonický. Jednotka I je najbližšie k muránskemu zlomu. Predstavuje silne tektonicky redukovaný sled začínajúci sa až vrchnokarnskými tisoveckými vápencami a pokračujúci cez dachsteinské

vápence až do spodnej jury. Jednotka II je po „klasickom“ začiatku s gutensteinskými a steinalmskými vápencami budovaná svahovým až hlbokovodným sledom, kde sú od najvyššieho pelsónu až do spodného karnu zastúpené tmavé detritické vápence rôzneho veku (anis – zámostské, karn, ladin/karn – raminské?), v západnej časti aj rohovcové reiflinské vápence, po ktorých sedimentovali opäť svetlé vrchnotriasové vápence dachsteinského typu. Ako jednotku III sme vyčlenili masív Šarkanice. Tá je už síce mimo orograficky vzatého masívu Strelnice, predstavuje však tretí typ sukcesie, ktorý sa bez viditeľných znakov diskordancií vyvíja zo spodnotriasových súvrství cez gutensteinské a steinalmské vápence do wettersteinských vápencov – ide teda o „klasický“ vývoj muránskeho príkrovu. Podľa publikovaných vekových údajov a prieskumnej správy z kameňolomu v Tisovci masív Čremošnej, v ktorom je lokalizovaný samotný kameňolom, patrí do jednotky I.

V masíve Strelnice môžeme rozlíšiť niekoľko tektonických zón odlišného charakteru. Masív Strelnice ako celok leží jednoznačne príkrovovo na veporskom kryštaliniku, niekedy aj na obale föderatského typu. Na tejto násunovej ploche býva často vyvinutý rauvakový horizont. Na báze všetkých čiastkových jednotiek všade nachádzame spodnotriasové bridličnaté súbory, ktoré vďaka svojej náchylnosti na duktilné správanie mohli plniť úlohu akéhosi „mazadla“ na báze. Nad týmto horizontom, v prípade jednotky I určite a v prípade jednotky II čiastočne, predpokladáme ďalší násunový horizont. Vyššie triasové súbory jednotlivých jednotiek oddeľujú pravdepodobne strmé zlomové zóny: prvou je samotný muránsky zlom a medzi jednotkami I a II prebieha zlom po hrebeni masívu Strelnice, pozdĺž ktorého nachádzame najmladšie členy jednotky I a najstaršie členy jednotky II. Ďalší výrazný zlom oddeľujúci dachsteinské vápence jednotky II a wettersteinské vápence jednotky III prebieha v doline Martinová, pričom aj v tejto doline sú odkryté a dokumentované výskyty spodnotriasových súborov. Sklon vrstiev vo všetkých troch jednotkách je generálne na SZ, v jednotka II s pravdepodobnou menšou vrásovou štruktúrou vyvinutou v reiflinských vápencoch. Za mladšie zlomové systémy považujeme pravdepodobne extenzné zlomy zhruba sz.-jv. smeru paralelné s mýtňansko-tisoveckým zlomom, najsilnejšie vyvinuté v západnej časti masívu, a zlomy zhruba zsz.-vjv. smeru v sv. časti masívu, ktoré majú pravdepodobne *strike-slipový* charakter.

Doručené / Received: 10. 6. 2024
Prijaté na publikovanie / Accepted: 28. 6. 2024

Mineralia Slovaca, Web ISSN 1338-3523, ISSN 0369-2086, https://doi.org/10.56623/ms.2024.56.1.4
56, 1 (2024), 89 – 104, © Authors 2024. CC BY 4.0

Research, assessing and water quality change trends in the Holocene and Pleistocene layers to meet water supply requirements for the coastal area of Binh Thuan province, Vietnam

HUYNH PHU[1*], HUYNH THI NGOC HAN[2] and TRAN THI MINH HA[3]

[1]HUTECH University; 475A Điện Biên Phu Street, Ward 25, Binh Thanh District, Ho Chi Minh City, Vietnam; h.phu@hutech.edu.vn

[2]Ho Chi Minh University of Natural Resources and Environment; 236B Le Van Sy Street, Ward 1, Tan Binh District, Ho Chi Minh City, Vietnam; htnhan_ctn@hcmunre.edu.vn

[3]Tay Nguyen University; Dak Lak province, Vietnam; ttmha@ttn.edu.vn;

[*]E-mail: h.phu@hutech.edu.vn; htnhan_ctn@hcmunre.edu.vn

Abstract: The study conducted water sampling at 30 well locations in 3 aquifers with different water depths (X15 m, X24 m, X36 m) in the Holocene and Pleistocene aquifers in the coastal area of Binh Thuan province, Vietnam. Water quality index calculation methods, correlation analysis, and principal component analysis were applied. The results showed that the Groundwater Quality Index fluctuated at "Excellent", accounting for 18.61 %; "Good" accounts for 38.05 %; "Poor" accounts for 20.55 %, the remaining "Very Poor" and "Inappropriate" account for 22.79 %. The most "inappropriate" part is in Ham Thuan, Phan Thiet. Some well sites are not suitable for water supply. In the coastal area of Phan Thiet, the average chloride content during the year is higher than the allowed standard. During 3 years of monitoring, in the dry season, the highest chloride content was 478 mg.L^{-1} at sites GWBT16, GWBT20, and 521 mg.L^{-1} at GWBT24. The results of the principal component correlation analysis of water quality in the X15 m aquifer show a tendency to be more severely affected by high tides during the rainy season.

Key words: Binh Thuan Province, Correlation analysis, GWQI, Holocene Aquifer, Pleistocene Aquifer

Graphical abstract

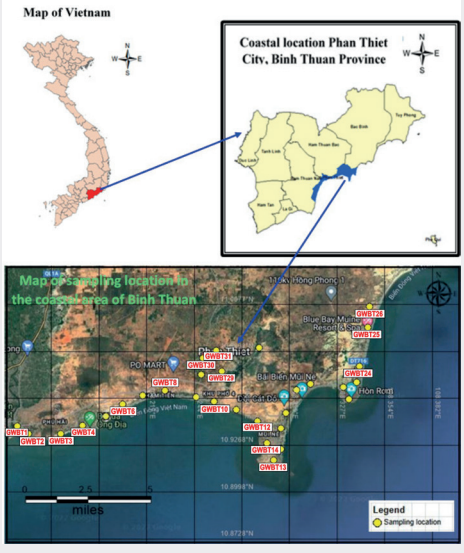

Highlights

- People in the coastal area of Binh Thuan province, Vietnam mainly use drilled well water, but due to prolonged heat and increased damage caused by climate change, the groundwater level in deep aquifers has decreased.
- There were 30 well locations in 3 aquifers with different depths (X15 m, X24 m, X36 m) sampled at the coastal area of Binh Thuan, Vietnam to conduct research.

1 Introduction

Most people in the coastal area of Binh Thuan Province use drilled well water, but due to prolonged heat and increased damage from climate change, groundwater levels have decreased in deep aquifers. In addition, deeper wells contain a lot of salty water due to the influence of sedimentary history, craft village activities, the tradition of processing anchovies, and the fish sauce of residents over the years. Binh Thuan Province's groundwater resources are divided into two porous aquifers, four aquifers,

and fissure aquifer zones, geological formations that are very poor in water or contain no water. The results of assessing exploitable reserves of groundwater in Binh Thuan Province have shown that the distribution area of freshwater aquifers is about 4,080.7 km^2, with exploitable reserves of 652,290 m^3.day^{-1} (DOWR, 2017).

Currently, the exploitation of groundwater sources in the province has 29 projects, with a total flow of 14,210 m^3.day^{-1}.

In Binh Thuan, domestic water demand in the province is met by only 40 % from surface water; the rest is mostly exploited from groundwater sources, especially by hotels serving coastal tourists of the province (DOWR, 2021). Vietnam's geological structure is characterized by aquifers mainly found in tectonic rupture zones and karst, basalt, or sedimentary rocks. Groundwater in coastal areas is mainly exploited in porous and fractured aquifers (Thang, 1999). The porous aquifers of the Binh Thuan coastal area are formed in Quaternary unconsolidated sediments. These aquifers have the characteristics of laminar groundwater flow, changing with seasons and coastal dynamics. The source of additional water reserves for this aquifer is mainly water seepage from rainwater and runoff water from mountains and from other aquifers along the coast. The water reservoir thickness in these sediments can reach 5–10 m, even up to 25–30 m in some places, with hydraulic gradient usually small, about 0.005 to 0.01. The common thickness of aquifers is usually about 5–10 m (Viet, 2023). Fractured aquifers consist mainly of fractured rock masses of Basalt formations and terrigenous sediments. The hydraulic characteristics of water flow in this aquifer are turbulent flow. One of the widely used and effective methods of assessing groundwater quality is the Groundwater Quality Index (GWQI).

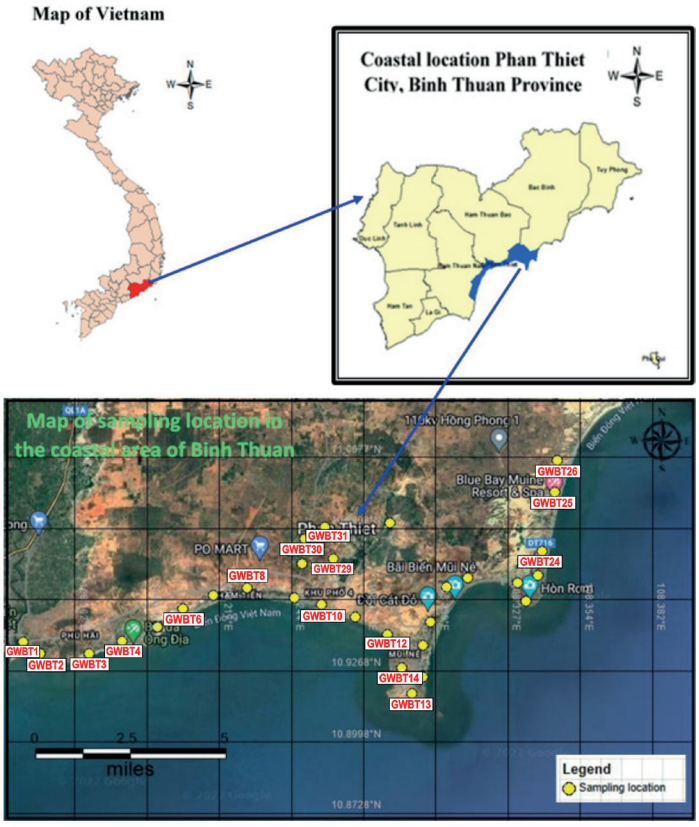

Fig. 1. Sampling area in Binh Thuan province.

GWQI is a quantitative assessment method of groundwater quality expressed through a scale, which is an important parameter for zoning groundwater quality. The GWQI is widely used worldwide, calculation formula was developed to evaluate groundwater quality in Al Najaf City, Iraq (Brown et al., 1972). These authors used the World Health Organization's domestic allowable limit values to calculate the weights. The GWQI index is also widely used in the environmental field, such as for studying groundwater quality developments and evaluating environmental quality parameters in Bangladesh (Doza et al., 2016), Turkey (Varol et al., 2015), Egypt (Masoud et al., 2018), and Japan (Shrestha et al., 2007).

In Vietnam, the GWQI is still widely used in research to evaluate groundwater quality depending on use purposes and regions. A study of the GWQI index in groundwater in Ba Ria-Vung Tau used weighted values based on the importance of the indicators and showed that in the dry season, it fluctuates in the range of 10–271, respectively, with water quality declining from "Good" to "Very Poor". For the rainy season, the GWQI index value is higher than in the dry season and ranges from 15–403, corresponding to a decline in water quality from "Good" to "Unsuitable" (Au et al., 2020). However, currently, there is no research using this method to evaluate groundwater quality in Holocene and Pleistocene sedimentary aquifers for coastal areas for tourism exploitation in Binh Thuan province, Vietnam. In addition, the correlation and relationship between the evolution of groundwater quality in these aquifers over time (rainy season, dry season) and space (high tide, low tide) have not been given due attention in this field, considering the current climate change situation.

The purpose of this study is to evaluate the current status of groundwater quality and consider its correlation in space and time to predict future developments. Based on the results, the study proposes timely solutions to ensure quality water supply to serve the province's coastal tourism development needs and the strategy to protect the water resources of the entire region.

Tab. 1

Site coordinates of studied wells

No.	Sampling site name	Coordinates		Water depth [m]	Aquifer	Stratigraphic characteristics
1	GWBT-1	N 10° 56′ 20.1″	E 108° 08′ 33.0″	10.120	X15 m	From the ground to a depth of 15 m, it contains mainly Holocene sediments, easily affecting the environment of recharge water sources. It is a shallow vascular layer, almost pressureless. The main composition of this aquifer includes small to medium-grained sand of white-gray color, containing Imenite, the lower part contains grit, gravel, pebbles and a little clay powder.
2	GWBT-2	N 10° 56′ 00.7″	E 108° 08′ 54.5″	11.200		
3	GWBT-3	N 10° 55′ 58.0″	E 108° 10′ 01.7″	10.291		
4	GWBT-4	N 10° 56′ 14.8″	E 108° 10′ 46.0″	10.213		
5	GWBT-5	N 10° 56′ 34.4″	E 108° 11′ 36.4″	10.102		
6	GWBT-6	N 10° 56′ 51.1″	E 108° 12′ 05.5″	11.322		
7	GWBT-7	N 10° 57′ 20.2″	E 108° 12′ 52.3″	10.218		
8	GWBT-8	N 10° 57′ 31.5″	E 108° 13′ 37.8″	11.234		
9	GWBT-9	N 10° 57′ 16.1″	E 108° 14′ 42.4″	10.109		
10	GWBT-10	N 10° 57′ 07.0″	E 108° 15′ 19.9″	10.200		
11	GWBT-11	N 10° 56′ 49.1″	E 108° 16′ 07.0″	17.172	X24 m	From the ground to a depth of 24 m, it consists of Holocene sediments and Pleistocene sediments. The stratigraphy of this aquifer mainly consists of white-gray and yellow-gray sand, fine sand grains mixed with Holocene clay silt.
12	GWBT-12	N 10° 56′ 25.5″	E 108° 16′ 50.5″	18.968		
13	GWBT-13	N 10° 56′ 09.6″	E 108° 17′ 12.6″	17.110		
14	GWBT-14	N 10° 55′ 40.2″	E 108° 17′ 10.0″	18.218		
15	GWBT-15	N 10° 55′ 06.2″	E 108° 17′ 24.6″	17.549		
16	GWBT-16	N 10° 55′ 27.7″	E 108° 17′ 38.1″	17.222		
17	GWBT-17	N 10° 56′ 17.6″	E 108° 17′ 38.3″	17.306		
18	GWBT-18	N 10° 56′ 43.0″	E 108° 17′ 49.4″	18.813		
19	GWBT-19	N 10° 57′ 30.7″	E 108° 18′ 12.1″	18.109		
20	GWBT-20	N 10° 57′ 42.1″	E 108° 18′ 39.0″	18.287		
21	GWBT-21	N 10° 57′ 36.1″	E 108° 19′ 49.0″	24.251	X36 m	From the ground to a depth of 36 m, it is mainly Pleistocene sediments. The main stratigraphy of this aquifer consists of yellow-brown and red-brown sand, fine sand grains mixed with Pleistocene clay silt.
22	GWBT-22	N 10° 57′ 40.1″	E 108°20′06.2″	24.199		
23	GWBT-23	N 10° 57′ 47.6″	E 108° 20′ 16.0″	24.197		
24	GWBT-24	N 10° 58′ 16.5″	E 108° 20′ 23.9″	24.233		
25	GWBT-25	N 10° 59′ 33.6″	E 108° 20′ 39.7″	24.000		
26	GWBT-26	N 11° 00′ 09.1″	E 108° 20′ 50.2″	24.292		
27	GWBT-27	N 10° 58′ 58.7″	E 108° 16′ 54.6″	24.310		
28	GWBT-28	N 10° 58′ 06.8″	E 108° 15′ 35.6″	24.111		
29	GWBT-29	N 10° 58′ 00.9″	E 108° 14′ 53.8″	24.219		
30	GWBT-30	N 10° 58′ 34.8″	E 108° 14′ 56.6″	24.202		

2 Materials and Methods

2.1 Study area and investigative surveys

Holocene aquifers are shallow, close-to-ground aquifers that are easily contaminated directly from discharge sources. They are unpressurized aquifers, with a shallow water level that fluctuates seasonally and tidally, rising and falling twice a day with an amplitude ranging from 0.5–0.7 m. The aquifer in Holocene sediments (qh) of the entire Binh Thuan province is quite widely distributed, covering an area of about 710.5 km^2. The total thickness of Holocene sediments varies greatly from 5–50 m and include many different sources of replenishment. The main sources of additional water supply for these sediments are rainwater and permeable surface water. These sediments is composed of small to medium-grained quartz sand, white gray in color, containing Imenite. The lower part has gravel, and pebbles mixed with a little clay silt, with a thickness of 10–15 m (Phu et al., 2020a). This is the first aquifer to receive direct rainwater and discharge from residential areas and industrial zones.

Pleistocene sediments are mainly composed of marine, river-sea, and sediments. These sediments typically do not have a separate waterproof layer. The thickness of the Pleistocene sediment layer ranges from 2 to 25 m, commonly from 8 to 12 m. Their main composition includes sand mixed with silt-clay, silt-clay mixed with yellow sand, and white quartz sand, and the lower part has a thin layer of pebbles and gravel. The additional supply source for these sedimentary layers is direct rainwater infiltration (Phu et al., 2022a).

2.2 Sampling site and analysis method

Samples were taken at hotels and motels that had private wells drilled to serve tourists, along the coast of Binh Thuan province (Fig. 1). Coordinates and names of coded wells and different water extraction depths are presented in Tab. 1.

The study surveyed and took samples at 30 wells in both the rainy and dry seasons in three years 2021, 2022, and 2023. Using specialized machines, pH, dissolved oxygen (DO), electrical conductivity (EC), and oxidation-reduction potential (Eh) are measured on-site to determine the basic physicochemical characteristics of groundwater samples taken from drilling wells at various elevations that serve as domestic water sources for hotels. The depth of the wells surveyed in the study ranges from a minimum water level of 0.5 m to a maximum water level of 40 m. A total of 2 samples are required to be collected at each site. Sampling was conducted every 6 months, both during the dry and rainy season throughout the year. In Binh Thuan province, the rainy season extends from May to December, while the dry season lasts from January to April. The sampling work has been carried out during the period of 2019–2021. The groundwater sampling process follows the requirements specified in TCVN 6663 (ISO 5667) (Tab. 2).

Tab. 2

Analytical parameters and standards

No.	Parameter	Units	Standard and methods
1	pH	–	TCVN 6492:2011
2	TH	mg/L	TCVN 6224:1996
3	TDS	mg/L	TCVN 9462:2012 ASTM D5284-09
4	SO_4^{2-}	mg/L	SMEWW 5220C:2012
5	Cl^-	mg/L	TCVN 6194:1996
6	$N–NH_4^+$	mg/L	SMEWW 4500-NH_3.B&F:2012
7	$N–NO_3^-$	mg/L	SMEWW 4500-NO_3^-.E:2012
8	Cu^{2+}	mg/L	SMEWW 3113B:2012
9	Fe^{2+}	mg/L	SMEWW 3113B:2012
10	F^-	mg/L	SMEWW 3113B:2012
11	Coliforms	CFU/100 ml	TCVN 6187-2: 1996

A total of 360 water samples from the Holocene and Pleistocene aquifers in Binh Thuan coastal area were analyzed for physicochemical parameters. The water sample was quickly analyzed for 5 parameters at the sampling scene including temperature (°C), pH, desolved oxygen (DO), electrical conductivity (EC), oxygen reduction potential (ORP), whereas 10 parameters at the national lab and the Southern Institute of Environment and Circular Economy (IECES) including total hardness (TH), total dissolved solids (TDS), sulphate (SO_4^{2-}), ammonium as N (NH_4^+), nitrate as N (NO_3^-), iron (Fe^{2+}), chloride (Cl^-), copper (Cu^{2+}), fluoride (F^-) and coliform parameters.

2.3 GWQI calculation method

The Ground Water Quality Index (GWQI) is a useful tool for establishing water quality and indicating the overall impact of chemical composition on water quality. GWQI is a quantitative description method of water quality and usability, expressed through a scale, and is an important parameter for zoning groundwater quality (Varol et al., 2015). This study used Brown's (1972) basic arithmetic equations (Brown et al., 1972) to calculate the GWQI index. Limit values of water quality indicators are given in QCVN 09:2023/MONRE (National technical regulation on ground water quality in Vietnam). The groundwater quality assessment scale is shown in Tab. 3.

Tab. 3
Water quality assessment scale using GWQI value

GWQI value	Rating of water quality
< 25	Excellent
25–50	Good
51–75	Poor
76–100	Very poor
> 100	Unsuitable

The calculation steps are as follows:

i) Weight distribution (ωi) for each parameter based on their importance to groundwater quality,
ii) Calculate relative weight (Wi) using equation (1),
iii) Calculate the quality assessment scale (qi) for each indicator according to equation (2),
iv) Determine SIi for each indicator according to equation (3),
v) Each survey sample is calculated GWQI using equation (4).

$$W_i = \frac{\omega_i}{\sum_{i=1}^{n} \omega_i} \quad (1)$$

$$q_i = \frac{C_i}{S_i} \text{ x } 100 \quad (2)$$

$$SI_i = W_i \, x \, qi \quad (3)$$

$$GWQI = \sum_{i=1}^{n} SI_i \quad (4)$$

Where: ω_i is the weight of each indicator and n is the number of survey indicators; W_i is the relative weight of each indicator; q_i is used to evaluate quality based on each specific indicator; C_i is the concentration of each indicator in the water sample (mg.L^{-1}); and Si is the standard of each indicator (mg.L^{-1}), taken according to QCVN 09:2023/MONRE. After calculating, the study used the GWQI value table corresponding to the water quality assessment level to compare and evaluate as shown in Tab. 3.

2.4 Multivariate correlation analysis

The study conducted correlation analysis, correlation matrix, and r value to evaluate the significance of correlation between water quality parameters in two seasons. The correlation coefficient (r) is a statistical index that measures the correlation between two variables. The correlation coefficient ranges from –1 to 1. A correlation coefficient of 0 (or close to 0) means that the two variables are not related. On the contrary, if the coefficient is –1 or 1, it means the two variables have an absolute relationship. If the value of the correlation coefficient is negative (r < 0), it means that when value x increases, value y decreases (and vice versa, when value x decreases, value y increases); If the value of the correlation coefficient is positive (r > 0), it means that when value x increases, value y also increases, and when value x decreases, value y also decreases, respectively. The correlation coefficient (r) is only meaningful if and only if the observed significance level is < 0.05 (Tuan, 2014).

2.5 Principal Component Analysis (PCA)

The PCA method represents high-dimensional data on a space with orthogonal bases, meaning if we consider each basis in the new space as a variable then the image of the original data in this new space is represented. expressed through independent (linear) variables. The PCA method finds a new space with the criterion of trying to reflect as much of the original information as possible. This allows consideration of using only a small number of variables to explain the data (Tuan, 2014).

Finding PCs that are a function of original variables:

$$PC_k = \delta_{1k}X_1 + \delta_{2k}X_2 + \cdots + \delta_{pk}X_p \quad (5)$$

We have p correlated variables: X1, X2, …, Xp obtained from n subjects. We want to find a method of transformation of X (n x p) matrix such that:

$$Y=\delta_1 X_1 + \delta_2 X_2 + \cdots + \delta_p X_p \quad (6)$$

Where, Y (vector of k) is called "principal components"; δ (δ1, δ2, …, δp): vector of weights such that:

$$\delta_1^2 + \delta_2^2 + \cdots + \delta_p^2 = 1 \quad (7)$$

→ Maximize the variance of data (X).
Find δ so that:

$$var(\delta^T X)=\delta^T \, var(X)\delta \quad (8)$$

The matric C = var(X) is actually covariance of X_i
The variance of Y (PC) is called the eigenvalue. According to the Kaiser criterion, PCs with eigenvalues > 1 and the number of PCs with total variance explained between 50 % and 70 % were kept constant (Tuan, 2014).

2.6 Representation of analytical data

The calculation and statistical results were performed using Microsoft Excel software, and the results of correlation analysis and PCA analysis were processed using R4.2.0 programming language (http://cran.r- project.org).

3 Research results and discussion

3.1 Results of analyzing coastal groundwater quality according to the GWQI index

The monitoring data of the two sampling periods were statistically calculated and shown in Tab. 4. Measurement results of some water quality parameters at the sampling sites; They are including temperature, pH, DO, EC, and

ORP reflected the basic physicochemical properties of the water sample at the time of sampling (Tab. 4).

Monitoring results have shown that the pH value of groundwater in the study area during sampling periods in the dry and rainy seasons in 2021, 2022, and 2023 are all within the allowable limits of QCVN 09:2023/MONRE (National technical regulation on groundwater quality in Vietnam). The difference and balance in the pH value of groundwater inside the aquifers is due to the composition of soil and rock or the water supplement environment.

In general, over the years surveyed, the pH in the rainy season is lower than in the dry season. Low pH values cause corrosion to plumbing systems and equipment, making them susceptible to wear and tear, causing waste of clean water. In addition, corrosive substances released from equipment and metal pipes such as lead, copper, iron, and zinc enter the water supply, affecting the health of water users in the area.

The water temperature also did not have a big difference between the two sampling periods, the smallest average temperature value was 25.5 °C and the largest was 28.3 °C. The redox potential (ORP) in the study area is mostly negative and ranges from –54 mV to –107 mV in the dry season, and from –38 to –123.5 mV in the rainy season. Thus, at most well sites, the water contains many antioxidants. The average EC conductivity represents a high amount of ions present in the water, indicating high salinity, in the dry season especially with quite high values from 306.7 $\mu S.cm^{-1}$ to 401.9 $\mu S.cm^{-1}$.

Based on the survey results at the sites of drilled and dug wells in the Holocene aquifer, it has been shown that the water has no pressure, the shallow water level varies

Tab. 4

Summary of average measurement results of some water quality parameters at the sampling sites

Quick measurement results of some water quality parameters in 2021										
Value	**Dry-season**					**Rainy-season**				
	Temper [°C]	**pH**	**DO [mg.L^{-1}]**	**ORP [mV]**	**EC [µS.cm^{-1}]**	**Temper [°C]**	**pH**	**DO [mg.L^{-1}]**	**ORP (mV)**	**EC [µS.cm^{-1}]**
QCVN 09:2023/ MONRE	–	5.5–8.5	–	–	–	–	5.5–8.5	–	–	–
Minimum	25.5	5.5	3.2	–330	7.5	20.4	4.9	3.3	–349	5.1
Maximun	27.8	7.6	5.2	116	673	25.6	7.2	3.9	102	73
Mean	26.7	6.5	4.2	–107	340.3	23.0	6.0	3.6	–123.5	39.1
Quick measurement results of some water quality parameters in 2022										
Value	**Dry-season**					**Rainy-season**				
	Temper [°C]	**pH**	**DO [mg.L^{-1}]**	**ORP [mV]**	**EC [µS.cm^{-1}]**	**Temper [°C]**	**pH**	**DO [mg.L^{-1}]**	**ORP [mV]**	**EC [µS.cm^{-1}]**
QCVN 09:2023/ MONRE	–	5.5–8.5	–	–	–	–	5.5–8.5	–	–	–
Minimum	27.1	5.2	2.6	–300	7.8	21.6	5.7	3.5	–309	5.6
Maximun	28.5	7.6	5.2	156	796	29.3	7.0	4.2	115	93
Mean	27.8	6.4	3.9	–72	401.9	25.5	5.8	3.9	–38	49.3
Quick measurement results of some water quality parameters in 2023										
Value	**Dry-season**					**Rainy-season**				
	Temper [°C]	**pH**	**DO [mg.L^{-1}]**	**ORP [mV]**	**EC [µS.cm^{-1}]**	**Temper [°C]**	**pH**	**DO [mg.L^{-1}]**	**ORP [mV]**	**EC [µS.cm^{-1}]**
QCVN 09:2023/ MONRE	–	5.5–8.5	–	–	–	–	5.5–8.5	–	–	–
Minimum	27.4	5.3	1.7	–250	6.7	24.3	5.4	2.5	–359	7.6
Maximun	29.2	7.7	4.1	142	606	28.3	7.8	4.0	176	113
Mean	28.3	6.5	2.9	–54	306.7	26.5	6.7	3.5	–91.5	60.3

Notes:"–": Not regulated; "Temper": temperature

from m to 5.0 m. The flow rate at exposed points is Q_0 = 0.01–0.3 L.s^{-1}. The chemical composition in the Holocene sedimentary aquifer is a mixture of bicarbonate chloride and bicarbonate sodium chloride. Chloride (Cl^-) content varies greatly: 3.0–478.0 mg.L^{-1}. Particularly in Phan Thiet, total chloride salt varies from 4.0–478 mg.L^{-1}. In particular, in the coastal of Phan Thiet, the average chloride salt content of the well during the year is very high compared to standards such as GWBT16, GWBT17, GWBT18, GWBT19, GWBT20 in all 3 years, and it is high in the dry season (Specifically, in the dry season at low tide, in 2022 and 2023, the chloride content has a maximum value of 478 mg.L^{-1} (GWBT16 and GWBT20) and 521 mg.L^{-1} (GWBT24), respectively).

Monitoring data showed that groundwater parameters are affected by geochemical and geological conditions such as average TH and TDS in groundwater in the rainy season is lower than in the dry season. This result can be explained by dilution from precipitation water infiltration; In particular, it shows a sharp decrease in concentration between two seasons in open wells. The main source of supply for the Holocene aquifer is rainwater. The two-season water level fluctuation according to monitoring documents is AH = 0.3–0.4 m. Therefore, the water quality in this sediment is susceptible to external environmental influences and has a high possibility of salinity. If used for daily life and tourism needs, the study suggests it is necessary to water from deeper aquifers.

The proportionality constant K is 0.295, it is determined based on QCVN 09:2023/MONRE for physicochemical parameters. The study has determined the influence weights of physicochemical parameters, the results are shown in Tab. 5.

Tab. 5

Weight of water quality patermeters according to QCVN 09:2023/MONRE

Number	Parameter	Units	Weight
1	pH	–	0.0347
2	TH	mg.L^{-1}	0.0006
3	TDS	mg.L^{-1}	0.0002
4	SO_4^{2-}	mg.L^{-1}	0.0007
5	Cl^-	mg.L^{-1}	0.0012
6	$N–NH_4^+$	mg.L^{-1}	0.2950
7	$N–NO_3^-$	mg.L^{-1}	0.0197
8	Cu^{2+}	mg.L^{-1}	0.2950
9	Fe^{2+}	mg.L^{-1}	0.0590
10	F^-	mg.L^{-1}	0.2950
Total			1.0000

The average value for all three water depths and color spectrum according to the value scale of the GWQI index at coastal sampling sites in Binh Thuan in 2021, 2022 and 2023 is shown in Tab. 6.

According to the water quality assessment color scale of Tab. 3 and the average GWQI values of the 3 aquifers in Tab. 6, it shows that the coastal area of Binh Thuan province mostly has groundwater quality reaching "Excellent" to "Good". Of these, sites that reached levels of excellent, good, poor, very poor, and unsuitable are 18.61 %, 38.05 %, 20.55 %, 10.83 %, and 11.96 %, respectively. Visualization of groundwater quality rates on a rating scale using GWQI values is shown in Fig. 2.

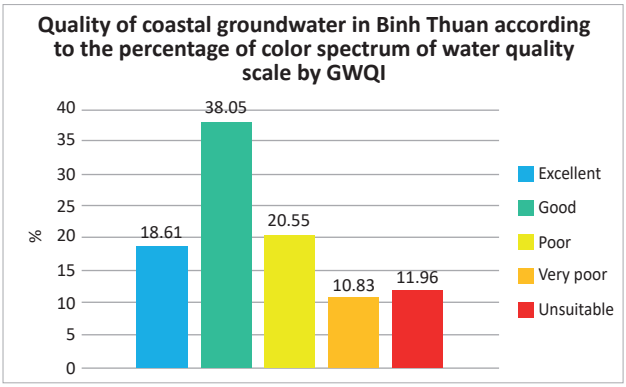

Fig. 2. Coastal groundwater quality in Binh Thuan, Vietnam according to the percentage of color spectrum of water quality scale by GWQI index.

In general, the majority of water quality at points meets the requirements for water supply. However, it should be noted the decrease in the number of wells reaching the "Excellent" color scale in 2021, and the transition to the majority of the "Good" color scale in the following two years, 2022 and 2023. This shows that groundwater quality is deteriorating and decreasing in quality year by year. In addition, water quality that cannot be used to serve hotels, motels, or local activities ("Unsuitable" corresponds to the red color in the scale of Tab. 3) is concentrated at well sites: GWBT20, GWBT21, GWBT22, GWBT23, GWBT24, GWBT25, GWBT26, GWBT27, and GWBT28. These sites are located at the bay in the territory of Ham Tien and Phan Thiet of Binh Thuan province. Heterogeneity with increased permeability in aquifers is quite favorable for water flow replenishment in aquifers. However, these cracks are also favorable for saline intrusion and pollution from additional sources.

During the years surveyed, the water quality in the aquifers of Holocene and Pleistocene sediments was found to be contaminated by organic substances and high levels of Ammonium. This was attributed to the problem of

Tab. 6

Average GWQI index values and color spectra for all 3 water depths at groundwater sampling sites in the study area in 2022–2023

Site	2021				2022				2023			
	Dry season		Rainy season		Dry season		Rainy season		Dry season		Rainy season	
	LT	HT	LT	HT	LT	HT	LT	HT	LT	HT	LT	HT
GWBT1	29	50	28	39	19	68	37	24	41	33	67	18
GWBT2	8	46	14	3	22	44	53	44	22	46	28	39
GWBT3	3	32	73	17	76	55	43	60	37	36	60	18
GWBT4	72	64	95	4	42	45	32	31	76	33	73	34
GWBT5	13	12	47	10	40	56	35	22	35	88	51	38
GWBT6	15	55	56	6	141	68	36	210	50	37	53	28
GWBT7	30	9	17	8	41	30	56	25	60	26	48	43
GWBT8	8	46	66	3	44	32	42	29	31	37	75	28
GWBT9 38 17			73	125	50	55	52	207	33	44	48	66
GWBT10	37	7	23	29	85	28	42	102	44	45	36	47
GWBT11	26	11	24	8	68	50	60	43	50	29	42	43
GWBT12	30	38	72	23	78	70	40	26	28	37	31	53
GWBT13	3	23	38	8	59	73	41	56	39	38	73	46
GWBT14	5	30	97	39	67	56	33	42	9	52	79	51
GWBT15	29	10	50	89	74	65	30	24	40	34	41	51
GWBT16	23	28	28	24	76	90	71	59	29	26	38	23
GWBT17	19	16	29	4	60	39	88	45	23	30	86	62
GWBT18	8	11	127	52	45	80	56	59	51	39	67	106
GWBT19	28	40	96	5	98	59	91	28	81	64	98	39
GWBT20	133	116	115	8	90	152	79	68	102	57	71	58
GWBT21	35	55	72	127	115	107	89	24	79	83	106	127
GWBT22	158	127	110	3	75	70	80	35	146	114	117	54
GWBT23	159	94	158	5	111	113	119	34	106	122	125	60
GWBT24	72	38	27	275	36	62	138	62	87	80	76	145
GWBT25	13	23	125	23	87	97	106	48	50	93	153	69
GWBT26	13	30	125	30	105	60	68	245	50	64	126	41
GWBT27	12	34	72	39	54	76	119	43	46	77	87	32
GWBT28	8	28	38	39	81	43	68	30	54	45	101	33
GWBT29	24	16	98	17	58	59	97	25	45	43	80	37
GWBT30	3	6	13	25	25	41	45	35	11	40	77	60

Note: LT-Low tide; HT-High tide

concentrated residential and tourist activities. According to Tab. 5, this factor has an influence weight of 0.2950. Besides, the location of Ham Tien Beach has the shape of a bay, easily concentrating pollutants, salt, and other substances that follow the ocean waves, creating layers of residue and sediment over time.

Results of correlation analysis between GWQI values at 30 well sites in space (high tide and low tide), and over time (dry season and rainy season) at 3 aquifers X15 m, X24 m, X36 m in 3 survey years 2021, 2022, and 2023 are shown in Fig. 3. Results indicate GWQI values at 30 well sites in space and time over 3 years surveyed at 3 levels. containing X15 m, X24 m, and X36 m are all correlated with each other; In particular, in 2021 and 2022, the water quality of the X24 m aquifer and the X36 m aquifer is quite strongly correlated (correlation coefficient r reaches 0.69).

3.2 Analyze the main components and trends of coastal groundwater quality in the province in the coming years

All monitoring sites with GWQI values in the three aquifers of Holocene and Pleistocene sediments surveyed, X15 m, X24 m, and X36 m have seasonal and tidal changes in sea level. To predict the evolution of the GWQI value of groundwater in these three aquifers and combine it with the results of correlation analysis in Fig. 4. The study performed principal component analysis. The results of data mining and extraction are shown in Fig. 4.

a)

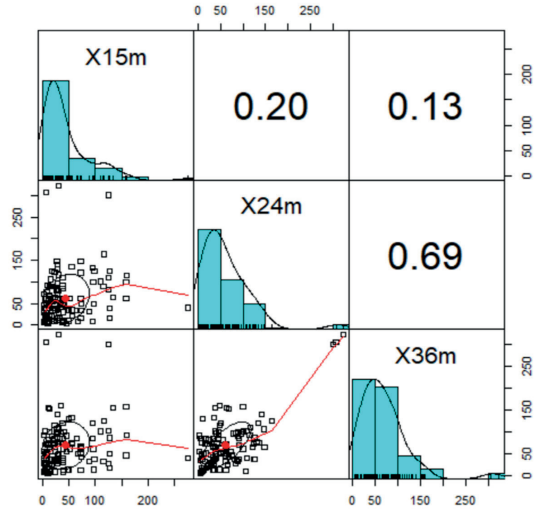

b)

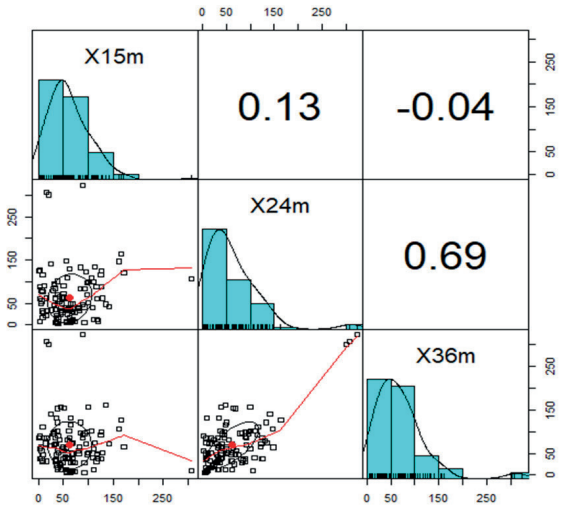

c)

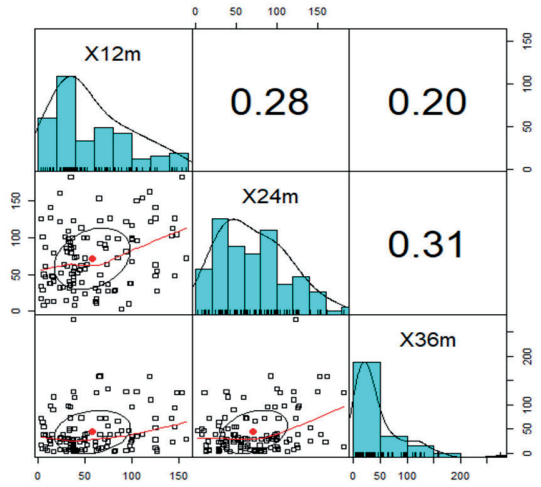

Fig. 3. Correlation matrix between GWQI values at 30 well sites in space and time over 3 years of survey:
a) 2021; b) 2022; c) 2023.

a)

```
> print(pc)
Standard deviations (1, .., p=3):
[1] 1.3273287 0.9656780 0.5528692

Rotation (n x k) = (3 x 3):
             PC1         PC2         PC3
X15m 0.2939663  0.9523077 -0.08181639
X24m 0.6835184 -0.1496143  0.71443556
X36m 0.6681215 -0.2659430 -0.69490137
> summary(pc)
Importance of components:
                          PC1    PC2    PC3
Standard deviation     1.3273 0.9657 0.5529
Proportion of Variance 0.5873 0.3108 0.1019
Cumulative Proportion  0.5873 0.8981 1.0000
```

b)

```
> print(pc)
Standard deviations (1, .., p=3):
[1] 1.3021491 1.0071162 0.5386321

Rotation (n x k) = (3 x 3):
             PC1         PC2         PC3
X15m -0.0905821 -0.98201401 -0.1656604
X24m -0.7096697 -0.05305294  0.7025342
X36m -0.6986872  0.18120118 -0.6920999
> summary(pc)
Importance of components:
                          PC1    PC2    PC3
Standard deviation     1.3021 1.0071 0.53863
Proportion of Variance 0.5652 0.3381 0.09671
Cumulative Proportion  0.5652 0.9033 1.00000
```

c)

```
> print(pc)
Standard deviations (1, .., p=3):
[1] 1.2357593 0.8968225 0.8176847

Rotation (n x k) = (3 x 3):
             PC1         PC2         PC3
X12m 0.5419293  0.76431805  0.3494718
X24m 0.6204177 -0.08333367 -0.7798316
X36m 0.5669166 -0.63943210  0.5193574
> summary(pc)
Importance of components:
                          PC1    PC2    PC3
Standard deviation     1.236 0.8968 0.8177
Proportion of Variance 0.509 0.2681 0.2229
Cumulative Proportion  0.509 0.7771 1.0000
```

d)

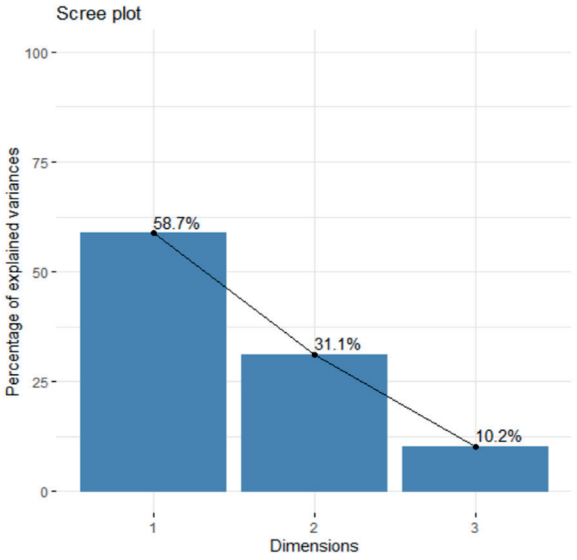

e)

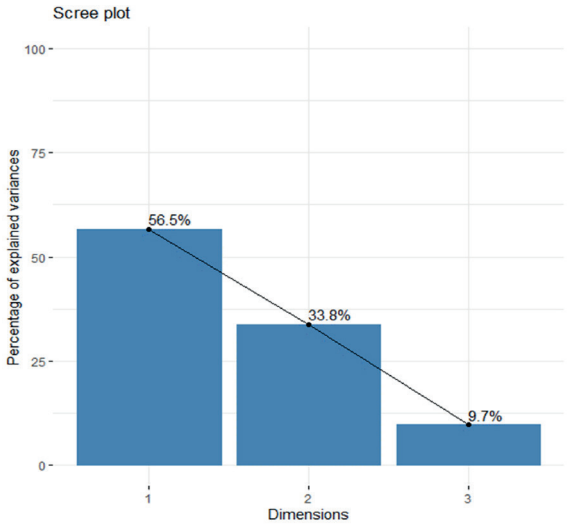

f)

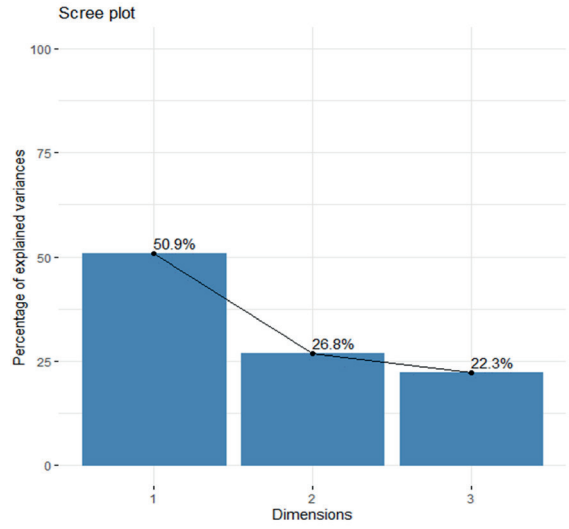

Fig. 4. Results of mining and extracting data of GWQI values at 30 well sites in space and time over the 3 years surveyed:
a) Principal component extraction results of GWQI values in 2021;
b) Principal component extraction results of GWQI values in 2022;
c) Principal component extraction results of GWQI values in 2023;
c) Sreen plot chart in 2021;
d) Sreen plot chart in 2022;
f) Sreen plot chart in 2023.

The results of mining and extracting principal components of GWQI values at 30 well sites in space and time during the 3 survey years 2021, 2022 and 2023 show:

i) In 2021 (Fig. 4a and 4d), the research has identified 3 main components including PC1 explains 58.7 % of the data variance, PC2 explains 31.1 % of the data variance and PC3 explains 10.2 % data variance. However, the study only selected PC1 and PC2 to analyze for forecasting because both of these components explained almost all of the data (reaching 89.81 %);

ii) In 2022 (Fig. 4b and 4e), the research has identified 3 main components including PC1 explains 56.5 % of data variance, PC2 explains 33.8 % of data variance and PC3 explains 9.7 % data variance. However, the study only selected PC1 and PC2 to analyze for forecasting because both of these components explained almost all of the data (reaching 77.71 %);

iii) In 2023, similarly (Fig. 4c and 4f), the study has identified 3 main components including PC1 explains 50.9 % of data variance, PC2 explains 26.8 % of data variance and PC3 explains covers 22.3 % of the data variance. However, the study only selected PC1 and PC2 to analyze for forecasting because both of these components explained almost all of the data (reaching 90.33 %).

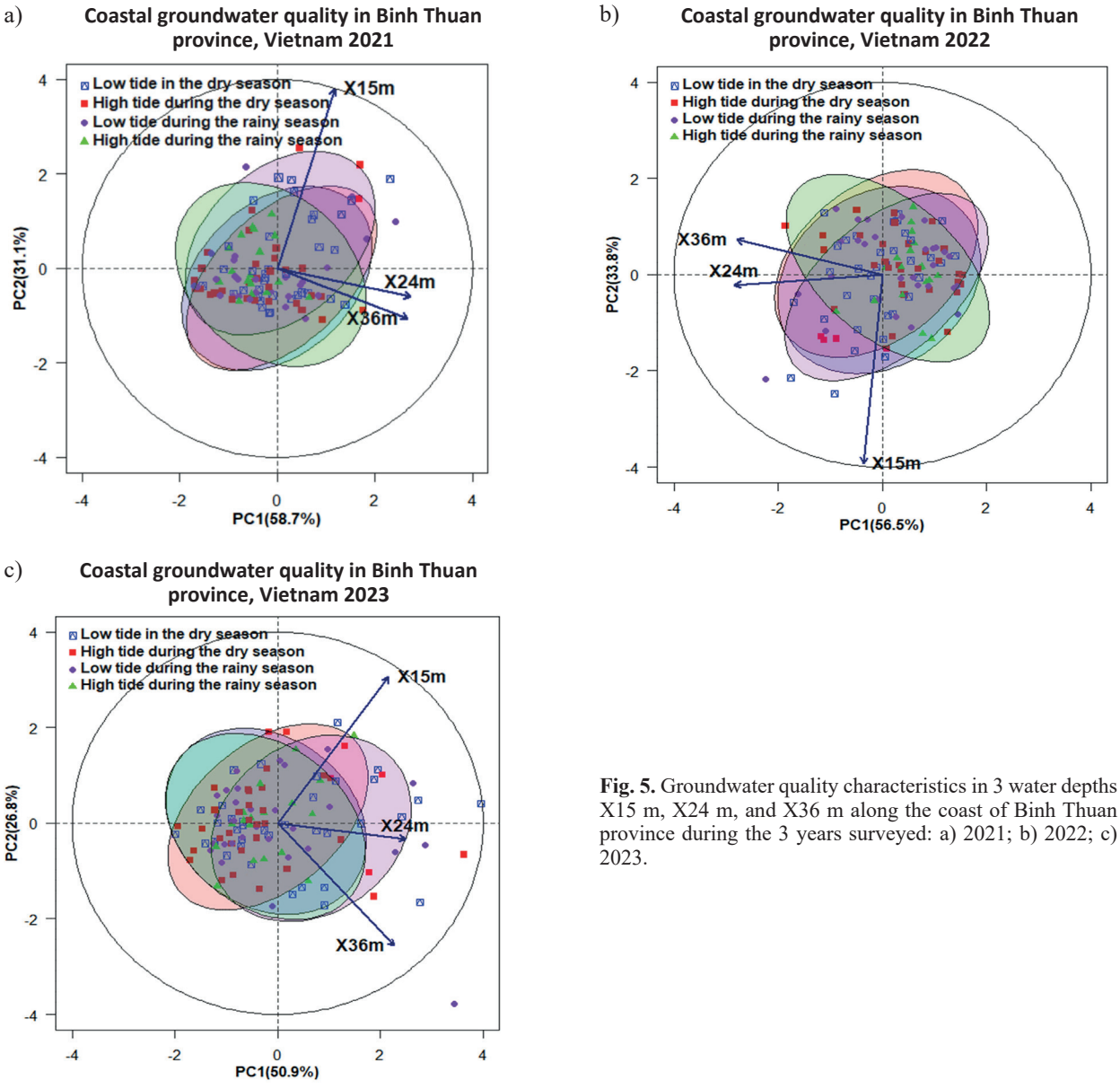

Fig. 5. Groundwater quality characteristics in 3 water depths X15 m, X24 m, and X36 m along the coast of Binh Thuan province during the 3 years surveyed: a) 2021; b) 2022; c) 2023.

The regression equation for the two components PC1 and PC2 according to the three water levels surveyed in 2021, 2022, and 2023 is presented in Tab. 7.

Tab. 7

Regression equation and regression coefficients for main components PC1 and PC2 in the 3 years surveyed

Year	Regression equation for two main components PC1 and PC2	
	PC1	PC2
2021	PC1 = 0.68*X24 m + 0.67*X36 m	PC2 = 0.95*X15 m
2022	PC1 = –0.7*X24 m – 0.69*X36 m	PC2 = –0.98*X15 m
2023	PC1 = 0.62*X24 m + 0.56*X36 m	PC2 = 0.76*X15 m

Notes:
– X15 m: GWQI value at 15m water depth,
– X24 m: GWQI value at 24m water depth,
– X36 m: GWQI value at 36m water depth.

Results of analyzing groundwater quality characteristics in 3 water depths X15 m, X24 m, and X36 m coastal Binh Thuan province during 3 years of survey are shown in Figure Fig. 5.

The results of data analysis from Fig.4 and Fig. 5 give the following conclusions: in 2021, the GWQI value of groundwater at the X15 m aquifer is greatly affected at high tide and in the rainy season (PC2) and the remaining 2 layers are both dependent on tide and season. For 2022, similar to the characteristics of 2021, the GWQI value of groundwater at the X15 m aquifer has been greatly affected by high Thuan province during 3 years of survey are shown in Fig. 5 tides, it all depends on the tide and the season. And in 2023, the GWQI value of groundwater at the high tide in the dry season.

3.3 Proposing solutions to prevent and develop coastal groundwater resources in Phan Thiet City, Binh Thuan Province

3.3.1 Build water storage, do not allow water flows into the sea

This is a model that has been successfully applied in the world (Phu et al., 2024). When the rainy season comes, many areas of Binh Thuan province are flooded (Ham Thuan Bac district, Tanh Linh district). We have studied geology, geomorphology, hydrogeology, structure of aquifers to come up with a plan to build water storage (on the face and under the ground).

3.3.2 Water replenishment for aquifers

Areas were selected based on the following conditions:

i) Determine the permeability coefficient of the soil cover on the topographic surface in the selected areas for water storage;

ii) Check the wetting ability of the unsaturated zone and check for the existence of tarnished areas in the unsaturated zone that may adversely affect the water quality;

iii) Check the water transmission capacity of aquifers;

iv) Field investigation of geology, hydrogeology, geochemistry to select the distribution areas of surface sediments with high permeability coefficient in Binh Thuan. The results of field investigations on geology and hydrogeology of the coastal sand strip distributed from Phan Ri to Ham Tan – Binh Thuan have satisfied the above conditions. These are the suitable areas

The water replenishment for aquifers has been developed in several countries around the world. In Vietnam, water replenishment for aquifers has been applied some provinces in the Tay Nguyen area (Phu et al., 2022b). The reference to the literature and the combination of our research results are the basis for us to choose the appropriate positions. Water replenishment was rainwater. for the arrangement of construction systems that add rainwater to the Holocene sediments (qh).

Rainwater is added to underground aquifers in the following manner:

Create a rainwater reservoir at a site with a permeability coefficient of 2–7m/day, rainwater will seep through the sand layers to the Holocene sediments (qh).

Collect rainwater in the drainage ditch and put it in a suitable location to add rainwater for the underground aquifer. Build underground storage tanks under buildings for rainwater collection and add rainwater to the aquifer with wells. We recommend that it is necessary to design boreholes and an additional water pump to the Holocene sediments (qh) (Fig. 6).

3.3.3 The subsurface dam method

This method has been applied in some countries around the world such as India, and Japan (https://sswm.info/es/sswm-solutions-bop-markets/). In Vietnam, the subsurface dam model in the sand, the anti-water loss has been successfully built in My Thanh (Binh Thuan). The subsurface dam with soil cement – Bentonite is 370 m long, from 5 m to 9.5 m deep forming a cobblestone tank with a capacity of 200,000 m^3, guaranteeing My Thanh water factory 3 months of operation in the dry season (Dung et al., 2022).

From this model, it is possible to extend to similar areas in the territory of Vietnam. In addition, it is possible to build a sand barrier dam at the foot of the coastwise dunes of Binh Thuan province. This sand barrier dam will keep rainwater contained in the sand layer and prevent the infiltration of sea water into the land. In the dry season, Binh Thuan province is very short of water. The sand dam

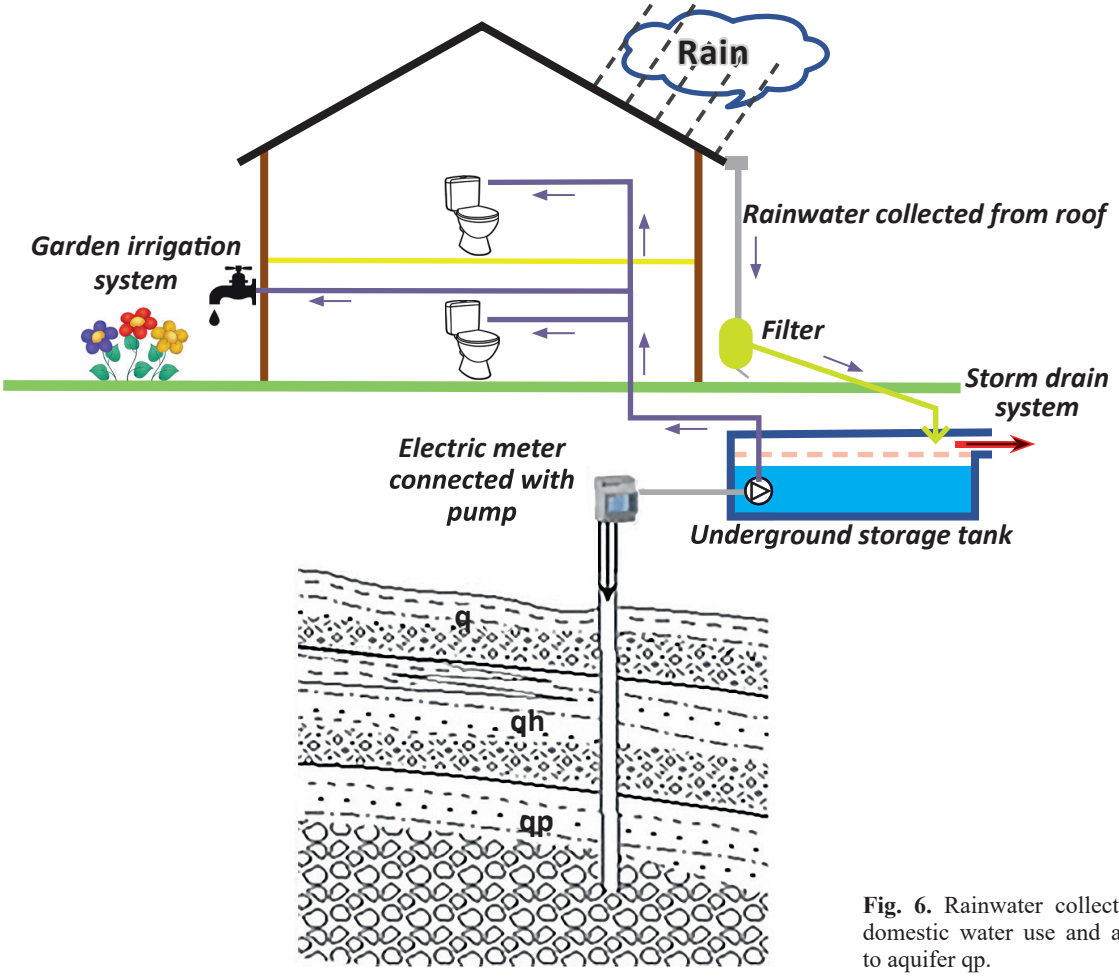

Fig. 6. Rainwater collection for domestic water use and addition to aquifer qp.

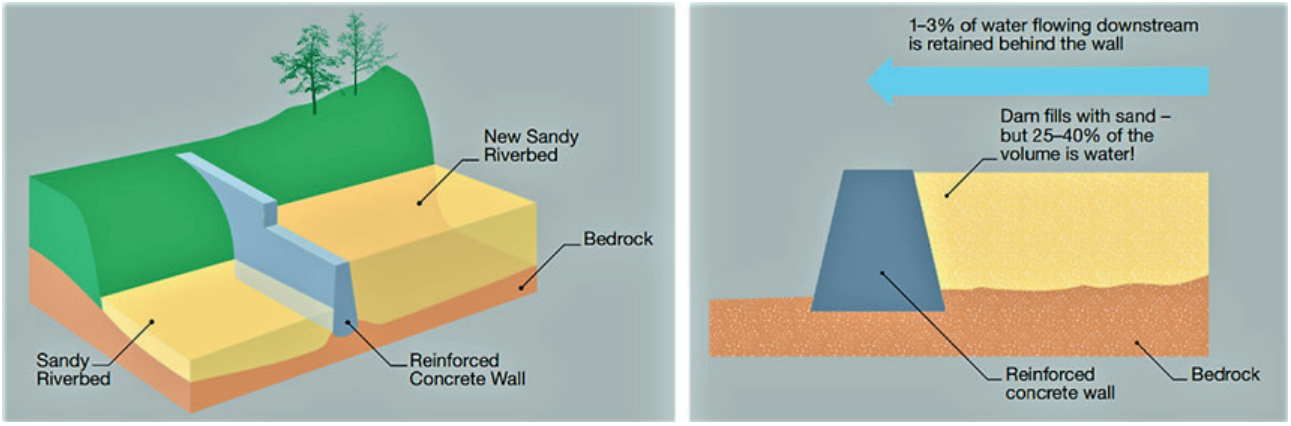

Fig. 7. Left: Schematic cross-section of a sand dam. Right: Sand accumulates until the dam is completely full of sand up to the spillway. Water is stored within the sand, protected and filtered, making up to 40 % of the total volume (Ryan et al., 2016).

Fig. 8. Rainwater addition to aquifer qp.

can be built for water storage. This model has been present in many countries around the world such as India, South Africa, and Kenya (Fig. 7).

3.3.4 Manufacturing seawater purifier

Vietnam has successfully made seawater purifier into freshwater with power reached 91 million liters of fresh water per day, named "Made in Vietnam". Vietnam has exported seawater purifiers to Saudi Arabia. We also made this device with power from 400 to 600m3/day (Phu et al., 2020b) (Fig. 8). Seawater purifier has been installed in Binh Thuan, Ben Tre, and Can Tho provinces. The defect of this device is the high price.

Binh Thuan province has 7 groundwater aquifers. The authors' suggestions for minimizing water shortage have been applied in Binh Thuan province. The solutions are the use of a catchment area, at the same time, simultaneously pumping rainwater into the qp aquifer, building underground dams, embanking sand dams and storing water, building a rainwater drainage system in the Northwest-Southeast direction, increasing the movement of water have also been applied. Solutions for sustainable development of groundwater resources are not only beneficial for Binh Thuan province but also can be applied well to other provinces in the territory of Vietnam. The authors' suggestions for minimizing water shortage have been applied in Binh Thuan province. The solutions are the use of a catchment area, at the same time, simultaneously pumping rainwater into the qp aquifer, building underground dams, embanking sand dams and storing water, building a rainwater drainage system in the Northwest-Southeast direction, increasing the movement of water have also been applied. Solutions for sustainable development of groundwater resources are not only beneficial for Binh Thuan province but also can be applied well to other provinces in the territory of Vietnam.

4 Conclusion

Research results have identified water quality trends in aquifers of Holocene and Pleistocene sediments along the coast of Binh Thuan province. The results of calculating the GWQI index and correlation analysis as well as principal component extraction analysis have shown changes in water quality in aquifers. This study also showed the decline in groundwater quality along Binh Thuan's coast in aquifers. In particular, wells in the Ham Tien area are declining more and more seriously, with some sites not meeting the requirements for water supply for domestic use or tourism in the area. Therefore, to supply water to this area, it is necessary to supplement or replace it with other water sources such as surface water, rainwater, treated seawater, or drill deep wells inland, which must have a safe radius of protection and a good drilling depth that meets the requirements of QCVN 09:2023/MONRE. The study has proposed a number of solutions to develop water resources to meet the daily living needs of the people and serve coastal tourists in Binh Thuan province, Vietnam.

References

Ahmad, A. B., 2014: Evaluation of Groundwater Quality Index for Drinking Purpose from some Villages Around Darbandikhan District. *Kurdistan Region-Science*, *7, 9, 34–41*. https://doi.org/10.9790/2380-07913441.

Au, N. H., Nhi, P. T. T., Vy, T. M. H., Hien, T. T., Hiep, T. N., Linh, L. K., Minh, T. B. & Ha, L. T. H., 2020: Application of Groundwater Quality Index (GWQI) and GIS in Groundwater Quality Zoning in the Pleistocene Aquifer in Phu My Town, Ba Ria-Vung Tau Province. *Science and Technology Development Journal – Science of the Earth & Environment, 4, 1, 149–161*. https://doi.org/10.32508/stdjsee.v4i1.525 (in Vietnamese).

Brown, R. M., Mcclelland, N. I., Deininger, R. A. & O'Connor, M. F, 1972: A Water Quality Index crashing the

Physiological Barrier. *Environmental Science Research*, *1, 173–182.*

DOWR, 2017: Department of Water Resources Management, http://dwrm.gov.vn/index.php?language=vi&nv=news&op=Hoat-dong-cua-dia-phuong/Binh-Thuan-se-duoc-quy-hoach-ve-tai-nguyen-nuoc-6511 (accessed August 9, 2023).

DOWR, 2021: Department of Water Resources, http://www.tongcucthuyloi.gov.vn/tin-tuc-su-kien/dam-bao-an-ninh-nguon-nuoc-kinh-6079 (accessed August 9, 2023).

Doza, M. B., Islam, A. R. M. T., Ahmed, F., Das, S., Saha, N. & Rahman, M. S., 2016: Characterization of groundwater quality using water evaluation indices, multivariate statistics and geostatistics in central Bangladesh. *Water Science, 30, 1, 19–40.* DOI:10.1016/j.wsj.2016.05.001.

Masoud, A. A., Horiny, M. M. E., Atwia, M. G., Gemail, K. S. & Koike, K., 2018: Assessment of groundwater and soil quality degradation using multivariate and geostatistical analyses, Dakhla Oasis, Egypt. *Journal of African Earth Sciences, 142, 64–81.* DOI:10.1016/j.jafrearsci.2018.03.009.

Phu, H. & Thao, H. T. P., 2020: Project report: "Planning for allocation and protection of groundwater resources in coastal sandy areas of Binh Thuan province". *Department of Natural Resources and Environment of Binh Thuan Province.*

Phu, H., Do, N. T., Han, H. T. N. & Ha, T. T. M., 2022: Assessing surface water quality of main rivers in Binh Thuan province by WQI index and proposing solutions to protect water resources. *VN J. Hydrometeorol*., 13, 118–133. doi:10.36335/VNJHM.2022(13).

Shrestha, S. & Kazama, F., 2007: Assessment of surface water quality using multivariate statistical techniques: A case study of the Fuji river basin, Japan. *Environmental Modelling & Software, 22, 464–475.* DOI: 10.1016/j.envsoft.2006.02.001.

Thang, N. D., 1999: Geology and minerals in Phan Thiet and Gia Ray – Ba Ria newspaper groups. Explanation of geological maps at 1/200,000 scale. *Hanoi, Vietnam Department of Investigation and Inspection.*

Tuan, N. V., 2014: Data analysis with R. Publishing House General TP. *HCM, 145–148.*

Varol, S. & Davraz, A., 2015: Evaluation of the groundwater quality with WQI (Water Quality Index) and multivariate analysis: a case study of the Tefenni plain (Burdur/Turkey). *Environmental Earth Sciences, 73, 4, 1725–1744.*

Viet, B. H., Binh, H. V. & Thanh, P. V., 2023: Hydrogeochemical characteristics and water quality in coastal areas of Binh Thuan province. Link: http://www.idm.gov.vn/nguon_luc/Xuat_ban/2006/A297/a38.htm (accessed August 9, 2023).

Výskum, hodnotenie a zmena trendov kvality vody v holocénnych a pleistocénnych vrstvách na splnenie požiadaviek na zásobovanie vodou v pobrežnej oblasti provincie Binh Thuan, Vietnam

V rámci výskumu na zabezpečenie zásobovania vodou v pobrežnej oblasti provincie Binh Thuan vo Vietname bol zrealizovaný odber vzoriek vody pomocou vrtov situovaných na 30 miestach a prestupujúcich 3 zvodnené vrstvy s rôznymi úrovňami vodonosných vrstiev (generálne X15 m, X24 m, X36 m) v holocénnych a pleistocénnych vodonosných vrstvách.

Na spracovanie získaných údajov boli aplikované metódy výpočtu indexu kvality vody, korelačná analýza a analýza hlavných zložiek. Výsledky ukázali, že index kvality podzemnej vody sa pohyboval na úrovni „vynikajúca", čo predstavuje 18,61 %, „dobrá" 38,05 %, „zlá" 20,55 %, pričom kategórie „veľmi zlá" a „nevhodná" podzemná voda tvoria spolu 22,79 %. Najviac „nevhodná" podzemná voda je v oblastiach Ham Thuan a Phan Thiet, takže miestne studne nie sú vhodné na zásobovanie vodou. V pobrežnej oblasti Phan Thiet je priemerný obsah chloridov počas roka vyšší než povolený štandard. Počas 3 rokov sledovania bol v období sucha najvyšší obsah chloridov 478 mg . l^{-1} v oblasti vrtov GWBT16 a GWBT20 a 521 mg . l^{-1} vo vrte GWBT24. Výsledky korelačnej analýzy kvality vody vo vodonosnej vrstve X15 m ukazujú tendenciu k výraznejšiemu ovplyvneniu kvality vysokým prílivom a odlivom počas obdobia dažďov.

Doručené / Received: 10. 5. 2024
Prijaté na publikovanie / Accepted: 28. 6. 2024

Inštrukcie autorom

Etika publikovania, záväzná pri publikovaní v časopise Mineralia Slovaca: *www.geology.sk/mineralia položka* ***Publikačná etika***

1. Geovedný časopis Mineralia Slovaca publikuje scientometricky hodnotné recenzované pôvodné vedecké články s vysokým citačným potenciálom. V úvode príspevku musí autor jasne deklarovať, čím konkrétnym je jeho príspevok prínosný pre rozvoj geovied. Rešeršné štúdie sa publikujú len ojedinele.

2. Články na publikovanie (manuskripty) sa do redakcie zasielajú poštou (dva vytlačené exempláre a CD so všetkými súbormi v editovateľnej podobe) alebo e-mailom (editovateľné súbory a kompletná verzia vo formáte PDF).

3. Súčasne s článkom je potrebné redakcii poslať autorské vyhlásenie o originalite textu a obrázkov. Kópie obrázkov z iných publikácií musia byť legalizované získaním práva na publikovanie. Vyhlásenie musí obsahovať meno autora (autorov), akademický titul a trvalé bydlisko.

4. Rozsah manuskriptu na publikovanie je najviac 25 rukopisných strán (MS Word, Times New Roman, veľkosť písmen 12 bodov, riadkovanie 1,5) vrátane literatúry, obrázkov a vysvetliviek. V prípade veľkého odborného prínosu sú v ojedinelých prípadoch povolené aj dlhšie články.

5. Články sú publikované v angličtine so slovenským resumé v závere článku (za zoznamom citovanej literatúry).

Text

1. Abstrakt stručne sumarizuje článok. Môže mať najviac 200 slov a nemá obsahovať citácie. Počet kľúčových slov je maximálne 6. Text má mať úvod, charakteristiku (stav) skúmaného problému, použitú metodiku, nové zistenia, ich interpretáciu, diskusiu, záver a zoznam literatúry. Východiskové údaje musia byť zreteľne odlíšené od interpretácií. V texte musia byť odvolávky na všetky použité obrázky a tabuľky.

2. Hierarchiu nadpisov v texte je potrebné vyznačiť ceruzkou na ľavom okraji strany manuskriptu: 1 – najvyššia, 2 – nižšia, 3 – najnižšia.

3. V texte sa uprednostňuje citácia v zátvorke, napr. (Dubčák, 1987; Hrubý et al., 1988), pred formou ... podľa Dubčáka (1987).

4. Pozícia obrázkov a tabuliek v texte sa označí. Nie je vhodné, aby text v editore MS Word obsahoval vložené obrázky, ale náhľadová verzia v pdf ich má obsahovať.

5. Grécke písmená treba identifikovať na ľavom okraji slovom (napr. sigma). Potrebné je odlišovať pomlčku od spojovníka. Symboly, matematické značky, názvy skamenelín a pod., ktoré sa majú vysádzať kurzívou, autor v rukopise podčiarkne vlnovkou.

Obrázky a tabuľky

1. Ilustrácie a tabuľky vysokej kvality bývajú publikované buď **na šírku stĺpca (81 mm), alebo strany (170 mm).** Optimálna veľkosť písma a čísiel v publikovaných obrázkoch je 2 mm. Všetky texty v obrázkoch a tabuľkách, rovnako ako popisy k nim musia byť v angličtine. **Maximálny rozmer ilustrácie a tabuľky vytlačený v časopise je 170 x 230 mm.** Väčšie (skladané) ilustrácie sú publikované len v ojedinelých prípadoch.

2. Pri počítačovej tvorbe obrázkov odporúčame používať programy s vektorovým zobrazením (Corel Draw, Adobe Illustrator a pod.). Čiary tzv. vlasovej hrúbky, softvérová alebo rastrová výplň plôch (napr. v Corel Draw) nie sú prípustné. Výplne v obrázkoch musia pozostávať zo samostatne vysádzaných objektov.

3. Ilustrácie vrátane fotografií musia obsahovať **grafickú mierku** v centimetrovej či metrovej škále, prípadne sa rozmer zobrazených objektov vyjadrí v popise obrázka. Mapy a profily musia mať aj **azimutálnu orientáciu** a jednotné vysvetlivky, ktoré sa uvedú pri prvom obrázku. Zoskupené obrázky, napr. fotografie a diagramy, sa uvádzajú ako jeden obrázok s jednotlivými časťami označenými písmenami (a, b, c atď.).

4. Pri zasielaní fotografií vo forme počítačových súborov (formáty JPG alebo TIF) sa požaduje rozlíšenie minimálne 600 DPI. Publikovanie farebných ilustrácií môže byť spoplatnené.

Literatúra

1. Minimálne 50 % citácií musí reprezentovať publikácie od roku 2000. V zozname literatúry sa v abecednom poradí uvádza len literatúra citovaná v danom článku.

2. Spôsob uvádzania literatúry v zozname literatúry

Knižná publikácia: Gazda, L. & Čech, M., 1988: Paleozoikum medzevského príkrovu. *Bratislava, Alfa, 155 s.*

Článok v časopise: Vrba, P., 1989: Strižné zóny v metapelitoch. *Miner. Slov., 21, 135 – 142.*

Zborník: Návesný, D., 1987: Vysokodraselné ryolity. *In: Romanov, V. (ed.): Stratiformné ložiská gemerika. Špec. publ. Košice, Slov. geol. spol., 203 – 215.*

Manuskript: Radvanský, F., Slivka, B., Viktor, J. & Srnka, T., 1985: Žilné ložiská jedľoveckého príkrovu gemerika. Záverečná správa z úlohy SGR--geofyzika. *Manuskript. Spišská Nová Ves, archív Št. Geol. Úst. D. Štúra, 28 s.*

3. Pri článku viac ako dvoch autorov sa v texte cituje iba prvý autor s dodatkom et al., ale v zozname literatúry sa uvádzajú všetci.

Instructions to authors

Publication ethics, being obligatory for publishing in the journal Mineralia Slovaca: *www.geology.sk/mineralia item* ***Publication ethics***

1. Geoscientific journal Mineralia Slovaca publishes scientometrically valuable original peer-reviewed scientific articles with a high citation potential. In the introduction of each article the author(s) must clearly declare, which innovative data the paper brings for the development of geosciences. The retrieval studies are published only exceptionally.

2. The articles for publishing (manuscripts) must be sent to Editorial Office by post (two printed copies and CD with editable files), or by e-mail (editable files plus complete preview version in PDF format).

3. Simultaneously with the article the Editorial Office must receive the author´s proclamation that no part of the manuscript was already published and figures and tables are original as well. Copied illustrations from other publications must contain a copyright.

4. The extent of the manuscript for publishing is limited to 25 manuscript pages (MS Word, 12 points Times New Roman, line spacing 1.5) including figures, tables, explanations and references. In the case of contribution with a high scientific value, the longer manuscripts for publishing are exceptionally permitted.

5. Articles are published in English, with Slovak summary at their end. In a case of foreign authors not able to submit the article summary in Slovak, the Editorial Office translates their English summary to Slovak version.

Text

1. Abstract briefly summarizing the article is limited to 200 words, no references are allowed. The maximum number of key words is 6. Text of the article has to contain the introduction, characterization (state) of investigated problem, applied methodology, presented new data, discussion, conclusion and references. The obtained data must be distinctly separated from interpretations. All applied figures and tables must be referred in the text.

2. The hierarchy of headings in the manuscript must be clearly indicated.

3. The references in the text prefer parentheses, e.g. (Dubčák, 1987; Hrubý et al., 1988). The form “according to Dubčák (1987)” should be used only exceptionally.

4. Position of figures and tables must be indicated in the manuscript. Editable text of manuscript sent to editorial office must be without figures and tables, though the preview PDF has to contain them in a correct position.

5. Greek letter in the text must be identified at the left margin of the text (e.g. sigma). The text should strictly distinguish the dash from hyphen. Symbols, mathematic signs, names of fossils, etc., which should be printed in italics, must be underlined in the manuscript.

Figures and tables

1. The high quality figures and tables can be published either in **maximum width of column (81 mm) or page (170 mm).** The optimum size of letters and numbers in the camera-ready figure is 2 mm. All texts in figures and tables, as well as descriptions and notes to figures and tables must be in English. **Maximum dimension of figures and tables in the journal is 170 x 230 mm. Larger (fanfolded)** illustrations are published only exceptionally.

2. For figures drawing the editorial office recommends the vector graphics editors (Corel Draw, Adobe Illustrator, etc.). The very thin lines (hair lines), the pre-defined software or raster fillings of polygons (e.g. in Corel Draw) are not allowed. The filling must consist from separately set objects.

3. Each illustration including photographs must contain graphic (metric) scale, eventually the dimensions of visualized objects have to be stated in the describing text to figure. Maps and profiles must contain also the azimuth orientation, their detail explanations are stated at the first figure. Grouped figures, e.g. photographs and diagrams, are compiled as one figure with separate parts designated by letters (a, b, c, etc.).

4. The photographs sent as JPG of TIF files are required for having minimum 600 DPI resolution. Publishing of colour illustrations can be charged by a fee.

References

1. Minimum 50 % of referred works must represent contemporary publications after 2000. The references in alphanumeric order encompass only literature cited in the article.

2. Examples of referring:

Book: Gazda, L. & Čech, M., 1988: Paleozoic of the Medzev nappe. *Bratislava, Alfa, 155 p.*

Article in journal: Vrba, P., 1989: Shear zones in the metapelite complexes. *Miner. Slov., 21, 135–142.*

Anniversary volume: Návesný, D., 1987: High-potassium rhyolites. *In: Romanov, V. (ed.): Stratiform deposits of Gemericum. Spec. publ. Košice, Slov. geol. soc., 203–215.*

Manuscript: Radvanský, F., Slivka, B., Viktor, J. & Srnka, T., 1985: Vein deposits of the Jedľovec nappe of Gemericum. Final report from the project SGR-geophysics. *Manuscript. Spišská Nová Ves, Archive Št. Geol. Úst. D. Štúra, 28 p.*

3. The article with more than two authors is referred by the name of the first author with the amendment et al., but the list of references contains names of all authors.

Ďalšie informácie / Further information: mineralia.slovaca@geology.sk; zoltan.nemeth@geology.sk

OBSAH – CONTENT

PÔVODNÉ ČLÁNKY – ORIGINAL PAPERS

Indexed / Abstracted / Accessed by SCOPUS, WEB OF SCIENCE and EBSCO
Indexované / abstraktované / sprístupňované databázami SCOPUS, WEB OF SCIENCE a EBSCO

www.geology.sk/mineralia